

BULLETIN OF THE RESEARCH COUNCIL OF ISRAEL

Section G GEO - SCIENCES

Bull. Res. Council. of Israel. Geo-Sciences

*This volume is dedicated to
PROFESSOR LEO PICARD
on the occasion of his sixtieth birthday*

BULLETIN OF THE RESEARCH COUNCIL OF ISRAEL

Section G GEO - SCIENCES

Bull. Res. Coun. of Israel. Geo-Sciences

Page

- I-V Appreciation of Leo Picard — on the occasion of his sixtieth birthday *M. Avnimelech*
- VI-X Bibliography *L. Picard*
- 1 Records No. 3-8 of the Hebrew University Geological Museum *M. Avnimelech*
- 17 Petrographical outline of the Precambrian in Israel *Y. K. Bendor*
- 64 The geology of Mount Gilboa *A. Flexer*
- 79 Distribution of Lower Turonian ammonites in Israel and the neighbouring countries *R. Freund*
- 115 On the Cenomanian-Turonian lithostratigraphy of central Galilee *U. Golani*
- 147 Neogene gas prospects in the Central Coastal Plain, Israel
P. Grader and G. Gvirtzman
- 173 The Plio-Pleistocene geology of the Ashdod area *A. Issar*
- 183 Airborne salts — the major source of the salinity of waters in Israel *S. Loewengart*
- 207 A Lower Cretaceous volcano in Machtesh Ramon (Southern Israel) *E. Mazor*
- 216 On the occurrence of *Pseudopygurus* Lambert in Southern Israel *A. Parnes*
- 223 Lower Cretaceous microfacies and microfossils from Galilee *Z. Reiss*
- 247 Weathering phenomena in the crystalline of the Sinai in the light of current notions *I. Schattner*
- 267 New data on the artesian aquifers of the southern Dead Sea basin and their geological evolution *Z. Shifan*
- 292 Nodules cuprifères du Neguev Méridional (Israel) *A. Slatkine*
- 302 Iraq-el-Baroud: Nouvelle grotte préhistorique au Mont Carmel *M. Stekelis*
- 321 On the Red Sea rift problem *A. Vroman*
- REVIEW AND COMMENTS
- 339 Soils of Israel and their classification *D. H. Yaalon*

**BULLETIN
OF THE RESEARCH COUNCIL
OF ISRAEL**

MIRIAM BALABAN

Editor

GENERAL EDITORIAL BOARD

S. ADLER
E. D. BERGMANN
M. EVENARI
A. KATCHALSKY
L. PICARD
G. RACAH
M. REINER
S. SAMBURSKY

EDITORIAL BOARDS

**SECTION A
CHEMISTRY**

Y. AVIDOR
E. D. BERGMANN
M. R. BLOCH
H. BERNSTEIN,
E. KATCHALSKI
A. KATZIR (KATCHALSKY)
G. STEIN
(Chairman,
Israel Chemical Society)

**SECTION B
ZOOLOGY**

H. MENDELSON
K. REICH
L. SACHS
A. YASHOUV

**SECTION C
TECHNOLOGY**

A. DANIEL
J. BRAVERMAN
A. DE LEEUW
M. LEWIN
M. REINER
A. TALMI
E. GOLDBERG, Technion
Publications Language Editor

**SECTION D
BOTANY**

N. FEINBRUN
N. LANDAU
H. OPPENHEIMER
T. RAYSS
I. REICHERT
M. ZOHARY

**SECTION E
EXPERIMENTAL MEDICINE**

S. ADLER
A. DE VRIES
A. FEIGENBAUM
M. RACHMILEWITZ
B. ZONDEK

**SECTION F
MATHEMATICS and PHYSICS**

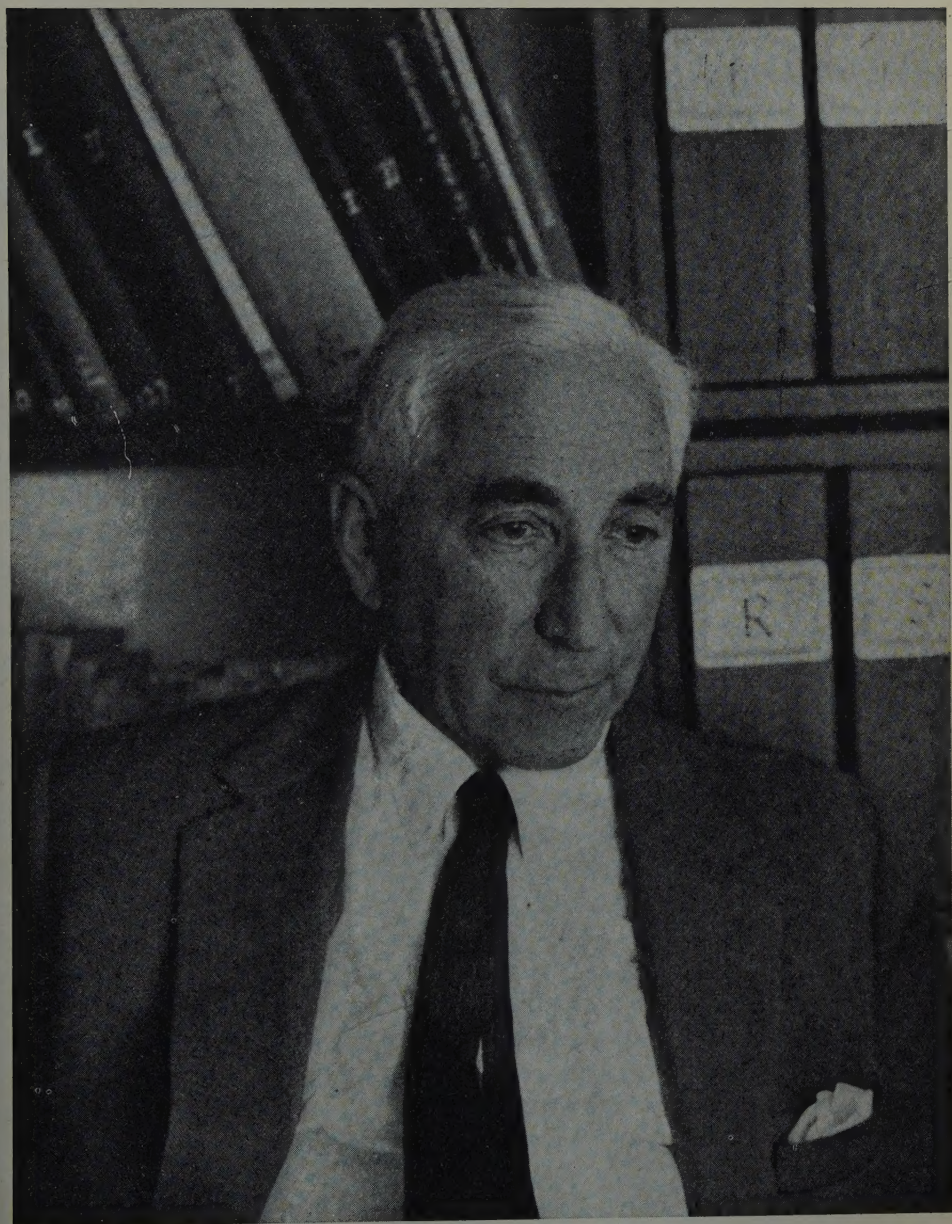
A. DVORETZKY
J. GILLIS
F. OLLENDORFF
G. RACAH

**SECTION G
GEO-SCIENCES**

G. DESSAU
J. NEUMANN
L. PICARD

This issue is published with the editorial assistance of D.H. YAALON, Y.K. BENTOR and M. AVNIMELECH, for the Israel Geological Society, the Geological Survey of Israel and the Department of Geology, The Hebrew University of Jerusalem.

Orders in America should be addressed to The Weizmann Science Press, P.O.B. 801, Jerusalem, or through booksellers, and in England and Europe to Wm. Dawson and Sons, Ltd., Cannon House, Macklin Street, London, W. C. 2, directly or through booksellers.—Annual subscription per section (four issues): IL. 6.000 (£6.00, £2.20). Single copy: IL. 1.500 (\$1.50, 12s.)—Manuscripts should be addressed: The Editor, The Weizmann Science Press of Israel, P.O.B. 801, Jerusalem, 33 King George Ave, Telephone 26345



LEO PICARD

LEO PICARD — ON THE OCCASION OF HIS SIXTIETH BIRTHDAY

A survey of the rich and varied scientific achievements of Prof. L. Picard is not only of personal but also of general interest since the activities of Leo Picard are closely connected with the history of Science in Israel which has developed and matured from the necessity of dealing with the vital problems of a new nation.

Prof. Picard was born in Germany in 1900 and came to Eretz Israel in 1924, shortly after the opening of the Hebrew University on Mt. Scopus. At first he gave lectures in crystallography and mineralogy to first year students of chemistry. He could also start almost immediately with his geological research since he was familiar with the literature on this region and had brought with him his private library which contained the necessary geological and paleontological publications.

Much of Picard's first geological work was linked with colonization enterprises. His pioneering work closely accompanied the development of new settlements. In the courses of his practical work, he also studied phenomena of mainly geological interest. For instance, in prospecting in connection with the construction of the Nesher Portland Cement Plant, near Haifa, Picard investigated the structure of the north eastern slopes of Mt. Carmel adjacent to the Kishon Valley. The results of this research (3,7)* provide to-day the basic data for the determination of the age and sequence of strata of Mt. Carmel.

The beginning of colonization of the Esdraelon and Beit-Shean Valleys gave Picard an excellent opportunity to pursue a detailed survey of these areas and of the neighbouring mountain area (8,10). This research allowed for the study of the geological formations of this area, their origin and structure as evidenced by the folding and faulting pattern (15). As a logical corollary of this study, new problems arose concerning the inter-relationships between the local faults and the extensively developed system of faults which crosses East Africa and branches off to enter our regions (18,19). In works published at that time the emphasis was laid on factors of economic importance, particularly on aspects of water research. Hence the chronological and spatial succession of the water bearing strata was determined. Also the particular importance of fault lines was clarified. Along these fault lines, springs are often found, and through bore-holes the subsurface waters are easily obtainable in the vicinity of the faulted areas (5,26,30,43).

The construction of Rutenberg's hydroelectric power plant brought Picard to the Jordan Valley and the Sea of Galilee. The study of this region, placed in juxtaposition to the regions previously explored, completed the survey of a continuous area extending from Mount Carmel and Haifa Bay to the Jordan River and Sea of

* Numbers refer to bibliography pp. VI-IX

Galilee. Investigation of the strata exposed in the Jordan Valley in Lower Galilee evoked a number of challenging and important questions as to the younger geological history of the valley which is at present in a state of subsidence. The research on the origin and succession of various geological beds resulted in a detailed history of the region from Miocene time (21,22,23,24). Here scientists had again encountered the problem of the origin and evolution of that immense depression which crosses almost the entire length of East Africa and ramifies into the Circum-Mediterranean region approaching Asia Minor.

New economic projects called for Picard's presence in the central parts of the country: Judean Desert, Jericho Plains and the Dead Sea. This work resulted in publications on the Cretaceous stratigraphy and palaeontology of the district (11,13,14). At the same time oil prospects on the eastern and western coasts of the Dead Sea were investigated.

The Dead Sea also presented other problems for investigation. Near the southern shores of this sea and along the borders of the Araba Valley southwards to the Gulf of Eilat (Aqaba), exposures of the oldest sedimentary rocks are found. These are rocks of Cambrian age which were deposited approximately 500 million years ago, and in which rare fossils are found. Still older metamorphic and magmatic Precambrian rocks bearing on the enigma of unknown eras crop out in this part of the country. Picard proceeded with research on trilobites and other fossils characteristic of the Cambrian (46), as well as on the distribution of Precambrian metamorphic and plutonic rocks exposed in the vicinity of Eilat, extending from there into the Sinai Peninsula and the Red Sea coasts of Africa (44,45).

Thus, step by step, Picard expanded the scope of his research until he went beyond the narrower bounds of the problems bearing on local geology. In all his work the scientific method of research prevails. He carefully analyses all the details which are to serve as a basis for a broader synthesis, precisely delineating the problem and providing a thorough theoretical analysis. Picard has always proceeded from the study of particular problems to the synthesis of general ones. In 1936 he presented a synopsis on the Palestinian-Syrian Pleistocene history at the INQUA meeting in Vienna (32,34). At the 17th International Geological Congress, in 1937, in Moscow, Picard delivered a lecture on the geological structure of the Arabian Peninsula (35). This lecture, which appeared under this title a few years later, provided the necessary stimulus for starting a wider research on the outline of the tectonics of the Earth with special emphasis on Africa (42). This work, treating some of the basic problems of the structure of the Earth, has been noted with considerable interest by geologists not only because of the subject matter but also because of the way problems are presented. The paper also demonstrates the tutorial method of Picard; emphasis on points of principle and basic importance from which the reader can derive his own conclusions.

Structure and Evolution of Palestine with Comparative Notes on Neighbouring Countries, published in 1943 (47) constitutes another step taken by Picard on his

way of synthesis in geology. This book presents a summary of knowledge on the geological development of this country from the most ancient until recent times. The facts have been meticulously selected and arranged anew in order to delineate an explicit and informative picture. The book was greatly appreciated by many geologists, and to Israel geologists it became a handbook for everyday reference.

Picard's engagement in petroleum prospecting enabled him to review the geology of Israel in regard to the possible location of petroleum sources as inferred from the evolutionary history and geological structure of the country (48,49). A synopsis on this subject was presented to the 5th World Petroleum Congress held in New York in 1959 (72).

As already mentioned, Picard's scientific work was frequently closely connected with the economy, colonization and development of the country. Foremost among his problems was that of water supply to agricultural settlements. Picard's rich experience in subsurface water research rendered him an authoritative "water geologist" and took him as an adviser and instructor to other countries, as well as a contributor to several international institutions (55,57,65,71). His acquaintance with oil prospecting resulted in a concept that a certain similarity exists between the behaviour of oil and water in depth (57). Picard has passed on his knowledge and methods to his students, some of whom now occupy authoritative posts in water prospecting and engineering companies, and others have been engaged in similar work abroad.

Other aspects of applied geology have also attracted his attention. Among these may be mentioned the gypsum deposits of Gesher-Menahamiya, raw materials for the Portland cement industry, phosphates, and others. After the establishment of the State of Israel, Picard founded the Geological Survey and was its first director. In later years he devoted much of his time to oil prospecting, while continuing to head the Department of Geology at the Hebrew University.

Picard's teaching is dominated by the spirit of his researches. He never teaches from a book but conveys to his students the ideas drawn from original investigations, after having carefully analyzed and summarized the data from his particular point of view. Having a strong feeling for the fine arts, he illustrates his lectures with colourful sections and sketches.

Leo Picard can be proud of his many-sided achievements. As a research worker, he has reached the status of a distinguished scientist; as a geologist in the field of applied science he has contributed greatly to the development of the country and its economy; as a teacher he has guided hundreds of students, many of whom are following his ideas and theories in pure and applied geology.

M. AVNIMELECH

BIBLIOGRAPHY OF SCIENTIFIC PUBLICATIONS OF

LEO PICARD

UP TO 1960

Compiled by M. A.

- 1923: 1. Die fränkische Alb von Weissenburg i.B. und Umgebung, *Inaugural-Dissertation*, Freiburg, Konstanz, 80 pp.
- 1926: 2. Report on the local geology, in An expedition to Southern Palestine, *Hebrew Univ.*, Jerusalem.
3. Sur le Cénomanien du Carmel (S. E. de Haifa), *Acad. sci. [Paris] Comptes rendus*, **183** (20), 895-898.
- 1927: 4. (avec R. Soyer), Sur la présence du Jurassique, du Crétacé inférieur et moyen sur le versant ouest de l'Antiliban, *Acad. sci. [Paris] Comptes rendus*, **185**, 656-658.
5. Springs and groundwater in Esdraelon Valley and the Coastal Plain, *Bull. Assoc. Architects*, "Construction and Industry", no. 5-6, 8-10 ill., (also in Hebrew), Tel-Aviv.
- 1928: 6. Recherches nouvelles en Palestine, *Soc. géol. France Bull.*, ser. 4, **28**, 79-83.
7. Zur Geologie der Kishonebene, *Deutsche Palästina Ver. Zeitschr.*, **51**, 5-72, map, ill.
8. Ueber die Verbreitung des Pliocäns im nördlichen Palästina, *Centralbl. f. Min. etc.*, Abt. B, No. 5, 326-335, ill.
9. Ein Eocänprofil des Gilboas in Palästina, *Centralbl. f. Min. etc.*, Abt. B, 578-582.
- 1929: 10. Zur Geologie der Besanebene, *Deutsche Palästina Ver. Zeitschr.*, **52**, 1-73, map, ill.
11. On Upper Cretaceous (chiefly Maestrichtian) Ammonoidea from Palestine, *Annals and Mag. Nat. Hist.*, ser. 10, **3**, 433-456, ill.
- 1930: 12. Bücherbesprechung: A. Reifenberg, Die Entstehung der mediterranen Roterde, *Deutsche Palästina Ver. Zeitschr.*, **53**, 90-91.
13. Upper Cretaceous (chiefly Campanian and Maestrichtian) Gastropoda and Pelecypoda from Palestine, *Annals and Mag. Nat. Hist.*, ser. 10, **5**, 513-543.
- 1931: 14. *Geological researches in the Judean Desert*, Jerusalem, 108 pp., map, ill.
15. Tektonische Entwicklungsphasen im nördlichen Palästina, *Deutsche geol. Gesell. Zeitschr.*, **83**, 164-184, ill.
16. Chapters on the geology of Eretz Israel, *Hateva ve Haaretz*, **1** (2, 4, 5), 73-78, 280-284, 315-319, ill. (in Hebrew), Tel-Aviv.
- 1932: 17. Géologie de la Grotte d'Oumm-Qatafa, *Palestine Orient. Soc. Jour.*, **11**, 164-171, ill.
18. Grabenstrukturen im Jordantal, *Fortschr. Geolog. Palaeont. Berlin*, **11** (33), "Deecke Festschrift", 88-98, ill.
19. The hypothetical ramp-faults in Palestine, in Bailey Willis and L. Picard, The Jordan Valley and Judean Highlands, *Geol. Mag.*, **69**, 103-107.
20. Geologische Probleme am Südrand des Tiberiassees, *Palestine Orient. Soc. Jour.*, **72**, 1-6.
21. Zur Geologie des mittleren Jordantales, *Deutsche Palästina Ver. Zeitschr.*, **55**, 169-237 map, pls., ill.
- 1933: 22. Zur postmiocänen Entwicklung des Kontinentalbeckens Nord-Palästinas, *Neues Jahrb. Min. etc.*, Beil. Bd. **10**, Abt. B, 93-115, pl.

- 1934: 23. Zur Geologie des Gebietes zwischen Gilboa und Wadi Fara, *Centralbl. f. Min. etc.*, Abt. B, 27–33, ill.
24. Mollusken der levantinischen Stufe Nordpalästinas (Jordantal), *Archiv Molluskenkunde*, 66, 105–139, ill.
25. Les dépôts de minéraux et d'eaux souterraines en Palestine, *La Bourse Egyptienne*, edit. spéc.
- 1935: 26. Das Wasserproblem Palästinas, "Palästina" Wien, 1935, pp. 1–16 (also in Hebrew in "Hassadeh", 15).
27. Geology of Tel-Aviv, *Jubilee Book of Tel-Aviv*, 1, 3–15, ill. (in Hebrew).
28. "The site, its history and remains", in Sukenik, E. L., *The ancient synagogue of El-Hammeh (Hammath-by-Gadara)*, Jerusalem, Chapter 1, pp. 13–18.
- 1936: 29. (with M. Stekelis), Jisr Banât Yaqūb, in Excavations in Palestine 1935–36, *Quart. Dept. of Antiq. Palestine*, 6 (3–4), 214–215.
30. Conditions of underground water in the Western Emek, *Geol. Dept. Hebrew Univ. Bull.*, 1, 1–23 (also in Hebrew).
31. (with P. Solomonica), On the geology of the Gaza-Beersheba district, *Palestine Orient. Soc. Jour.*, 16, 180–223, map. ill., and *Geol. Dept., Hebrew Univ. Bull.*, 2, 1–44.
32. Ueber Fauna, Flora und Klima des Pleistocäns Palästina-Syriens, *III Internat. Quart. Konfer. Verh.*, Wien, 2, 1–4.
33. (with M. Avnimelech and L. Doncieux), Sur la découverte d'une série nummulitique au SE du Mont Carmel en Palestine, *Soc. géol. France Comptes rendus*, 41–43.
- 1937: 34. Inferences on the problem of the Pleistocene climate of Palestine and Syria drawn from flora, fauna and stratigraphy, *Prehist. Soc. Proc.*, Paper no. 5, 58–70.
35. On the structure of the Arabian Peninsula, 17e Congr. Internat. Géol., Moscow 1937, 2, 415–423, and *Geol. Dept. Hebrew Univ. Bull.*, 3.
36. (with M. Avnimelech), On the geology of the Central Coastal Plain, *Palestine Orient. Soc. Jour.*, 17, 255–299 and *Geol. Dept. Hebrew Univ. Bull.*, 4.
37. (with L. Doncieux), Sur la présence de l'Eocene supérieur – Oligocene inférieur avec *Nummulites incrassatus* de la Harpe en Palestine, *Soc. géol. France Comptes rendus*, 62–63.
38. (with L. Doncieux and M. Avnimelech), Sur l'existence d'un étage Libyen dans les environs de Maan (Transjordanie), *Soc. géol. France Comptes Rendus*, no. 6, 74–75.
- 1938: 39. The geology of New Jerusalem, *Geol. Dept. Hebrew Univ. Bull.*, 2 (1), 1–12 (also in Hebrew).
40. Synopsis of stratigraphic terms in Palestinian geology, *Geol. Dept. Hebrew Univ. Bull.*, 2 (2), 1–24.
41. Economic minerals and groundwater in Palestine, *Technika ve'Mada*, 2 (6), 1–2 (in Hebrew).
- 1939: 42. Outline on the tectonics of the Earth, with special emphasis upon Africa, *Geol. Dept. Hebrew Univ. Bull.*, 2 (3–4), 1–66.
43. Groundwater in Palestine, *Geol. Dept. Hebrew Univ. Bull.*, 3 (1), 1–24 (also in Hebrew) *Jewish Palestine Expl. Soc. Bull.*, 7 (2).
- 1940: 44. Sur l'orogénese de l'Algonkien supérieur en Arabo-Afrique septentrionale, *Soc. géol. France Bull.*, sér. 5, 10, 49–58.
- 1941: 45. The Precambrian of the North Arabian-Nubian Massif, *Geol. Dept. Hebrew Univ. Bull.*, 3 (3–4), 1–30.
46. New Cambrian fossils and Paleozoic Problematica from the Dead Sea and Arabia, *Geol. Dept. Hebrew Univ. Bull.*, 4 (1), 1–18, ill.
- 1943: 47. Structure and evolution of Palestine, with comparative notes on neighbouring countries, *Geol. Dept. Hebrew Univ. Bull.*, 4 (2–3–4), 1–134.

- 1947: 48. Palestine: search and conception, in *Review of Petroleum Geology*, 1946, *Colorado School of Mines Quart.*, **42** (3), 122 (reprinted in 1958 and 1960).
- 1948: 49. Le pétrole en Palestine, *Moniteur de Petrole Roumain*, no. 1-2, 13-14, ill.
 50. La structure du Nord-Ouest de l'Argentine avec quelques réflexions sur la structure des Andes, *Soc. géol. France Bull.*, sér. 5, **18**, 765-846, ill.
 51. Sur l'âge de la "Formacion Petrolifera" en Amérique du Sud, *Soc. géol. France Bull.*, sér. 5, **18**, 215-218.
- 1951: 52. Geomorphogeny of Israel: The Negev, *Bull. Research Council of Israel*, **1** (1-2), 5-32, map.
- 1952: 53. The Pleistocene peat of Lake Hula, *Bull. Research Council of Israel*, **2** (2), 147-156.
 54. Geology of Kfar Giladi, *Hebrew Soc. Expl. Palestine, Eretz-Israel-Book*, **2**, 73-77 (in Hebrew).
- 1953: 55. The history of groundwater exploration in Palestine, *Desert Research, Research Council of Israel Spec. pub. no. 2*, 583-591 (also in *Geol. Inst., Jerusalem, Pub. 4*, and in *Israel Econ. Forum*, 1954, **6** (3), 102-107, with Addendum: 107, 151).
 56. Silurian in the Negev (Israel), 19e *Congr. Géol. Internat. Alger* 1952, sec. 2, fasc. 2, 179-182 (also in *Bull. Research Council of Israel*).
 57. Outline of groundwater geology in arid regions, in *Proc. Ankara Symp. on Arid Zone Hydrology, Arid Zone Programme*, **2**, 165-176, *Unesco* (also in 19e *Congr. Géol. Intern., Alger* 1952, *Comptes rendus*, sec. 8, 117-136, ill., and in *Bull. Research Council of Israel*, **2**, no. 4, 358-371).
 58. Disharmonic faulting, a tectonic concept, *Bull. Research Council of Israel*, **3**, nos. 1-2, 132-135.
- 1954: 59. Disharmonic faulting in the Jordan-Araba graben. 19e *Congr. Géol. Internat., Alger* 1952, fasc. 21, 213-214.
 60. The structural pattern of Palestine (Israel and Cis-Jordan), 19e *Congr. Géol. Internat., Alger* 1952, fasc. 16, 301-305, also in *Bull. Research Council of Israel*, **4**, no. 1, 48-50.
 61. Geological reasoning for Pontiac's drilling on Israel Continental's South Carmel area. Pamphlet issued by *Maine Investment Co. Montreal*. (also in *Israel Expl. Soc. Bull.*, 1956, **20** (3-4), 121-128 (in Hebrew), and as Geological background on petroleum drilling in Zikhron Yaacov (S. Carmel), *Bull. Research Council of Israel*, 1958, **7G**, no. 1, 20-26.
- 1955: 62. History of mineral research in Israel, *Israel Econ. Forum*, **6** (3), 1-38.
 63. Literature relating to the history of mineral research in Israel, *Israel Econ. Forum.*, **6** (3), 146-150.
 64. Geology (of Palestine), in *Encyclopaedia Mikrayit* (Biblical Encyclopaedia), **1**, 616-633, geol. map. (in Hebrew).
- 1956: 65. Development of underground water resources in Greece, *Report of U.N. Techn. Assist. Programme*, File No. TAA 173/25/Oil, Rep. No. TAA/Gre/5.
 66. Geological situation of Jerusalem, *Jerusalem Book*, **1**, 33-44, ill. (in Hebrew).
- 1957: 67. Book review: Seismicity of the Earth (and associated phenomena) by Gutenberg and Richter, *Bull. Research Council of Israel*, **6B**, nos. 3-4, 257-2.
 38. The geological map of Israel, scale 1:100,000 *Geol. Survey of Israel*, Jerusalem:

Sheet 1 — Metulla
 Sheet 2 — Haifa
 Sheet 3 — Safed
 Sheet 4 — Zikhron Yaacov
 Sheet 5 — Nazareth
 Sheet 6 — Tel-Aviv

LEO PICARD

Sheet 8 — Yebna
Sheet 9 — Ramle
Sheet 10 — Jerusalem
Sheet 11 — Gaza

- 1958: 69. (with E. Kashai), Lithostratigraphy and tectonics of the Carmél, *Bull. Research Council of Israel*, 7G, no. 1, 1-19.
70. Book review: Introduction to physical geology by C. R. Longwell and R. Foster Flint (1955), *Bull. Research Council of Israel*, 7G, no. 4, 207-208.
- 1959: 71. The water problem in arid areas, *Mada*, 3 (3-4), 14-15 (in Hebrew).
72. Geology and oil exploration of Israel, 1959 *Fifth World Petroleum Congress*, New York, sec. 1, pap. 13, 1-22, ill. (also in *Bull. Research Council of Israel*, 8G, no. 1, 1-30, pls., map).
73. Geological map of Israel and adjoining territories, at the scale 1:500,000, *Survey of Israel*, Tel-Aviv.
77. Geological observations of Aharon Aronson, *Mada*, 4 (1) (in Hebrew).

CENOMANOCARCINUS, A DECAPOD CRAB FROM THE UPPER CENOMANIAN OF JERUSALEM

(RECORD NO. 3 OF THE HEBREW UNIVERSITY GEOLOGICAL MUSEUM)

M. AVNIMELECH

Department of Geology, The Hebrew University of Jerusalem

Several years ago J.M. Remy and M. Avnimelech (1955) published a short account on two fossil decapods, one originating from Senonian, the other from the Cenomanian rocks of Israel. The second one was recognized as *Cenomanocarcinus* cf. *vanstraeleni* Stenzel [Ord. *Decapoda*: subord. *Reptantia*: tribe *Brachyura*: subtribe *Oxystomata*: fam. *Calappidae*: gen. *Cenomanocarcinus* (Van Straelen 1936) in Stenzel, 1945]. Its remnant was found in the Upper Cenomanian *Neolobites* horizon in the west of Jerusalem; it consisted of an incomplete, by weathering slightly obliterated, cephalothorax, with well preserved rostrum, orbital margin and tuberculate ridges. Recently, another similar decapod was discovered among unclassified material in the collections of the Department of Geology of the Hebrew University. This material belonged previously to the Agricultural Museum of the Zionist Organization, which existed in Jerusalem for several years up to 1928. The specimen was accompanied by *Neolobites vibrayeana* (d'Orb). The attached label indicates that the fossils were found in a place near the Holy Cross Monastery in the west of Jerusalem, in Upper Cenomanian limestone beds, viz. stratigraphically equal to the former finding.

The specimen of the *Cenomanocarcinus* sp. is represented by a fragment of a completely decorticated carapace, consisting of a part of mesogastric, gastro-cardiac, cardiac and intestinal areas, as well as of epi- and meso-metabranial areas. The three longitudinal, medial, cardiac-intestinal and the two meso-metabranial ridges, with their characteristic tubercles, are well preserved; also well visible is the right epibranial ridge, ending with epibranial spine. A small portion of the postero-lateral margin and, in fragments, the antero-lateral and anterior margins are preserved, so that their general outline can be easily traced. Due to its general character, but especially to its three tuberculate longitudinal ridges and to the epibranial ridge, the carapace is perfectly comparable with *Cenomanocarcinus inflatus* (A. Milne-Edwards) Van Straelen from the Cenomanian of Le Mans and from the Lower Turonian of Gard (France), as well as with *C. vanstraeleni* Stenzel from the Lower Turonian Britton formation and from the Cenomanian Woodbine formation of Texas. However, our specimen differs from both species by having the two meso-metabranial ridges posteriorly clearly divergent, forming an angle

of about 30°, while in *C. vanstraeleni* these ridges are almost parallel, and in *C. inflatus* only slightly oblique. Moreover, in our specimen the meso-metabranthial area forms a broader angle with the epibranchial ridge. Consequently, the entire carapace is broader and shorter, the width exceeding the length by nearly 50% while in *C. inflatus*, as well as in *C. vanstraeleni*, it is not greater than 25%. Our specimen is also much smaller, being half as big as the figured specimen of *C. inflatus*, but this fact does not present any specific significance. However, in spite of the general resemblance, the Jerusalem specimen seems to present a different species to which herewith the name of *C. hierosolymitanus* is given. Possibly the former specimen, determined by J. Remy and deposited in the palaeontological collections of the Muséum National d'Histoire Naturelle in Paris (No. DE 207), belongs also to this species. The present specimen, which is the holotype of the new species, is numbered 20989 in the palaeontological collections of the Hebrew University Geological Department.

The genus *Cenomanocarcinus* as a whole, ranges, according to Stenzel, from Upper Albian to Lower Turonian. Its type-species is the already quoted *C. inflatus* of Upper Cenomanian–Lower Turonian age. The other Cenomano–Turonian species are *C. vanstraeleni* and *C. hierosolymitanus*. The Upper Albian species are *C. oklahomensis* (Rathbun) and *C. armatus* (Rathbun), the latter possibly belonging according to Stenzel, to the related genus *Necrocarcinus* Bell.

The wide geographical dispersion of this genus over the Tethian spaces, from Texas up to the Eastern Mediterranean, and its quite limited stratigraphical range make these decapod species especially interesting.

REFERENCES

1. BOULE, M. AND PIVETAU, J., 1935, *Les Fossiles*, Paris, p. 392, Fig. 670: *Necrocarcinus inflatus*.
2. GUILLIER, A., 1886, Géologie du Département de la Sarthe, Paris et Mans, p. 244: *Necrocarcinus inflatus* A. Milne-Edwards MS.
3. REMY, JEAN-M. AND AVNIMELECH, MOCHÉ, 1955, *Eryon yehoachi* n.sp. et *Cenomanocarcinus* cf. *vanstraeleni* Stenzel, crustacés décapodes du Cretacé supérieur de l'Etat d'Israël, *Bull. Soc. Géol. France*, (6) 5, 311–314.
4. STENZEL, H.B., 1945, Decapod Crustaceans from the Cretaceous of Texas, *Univ. Texas Publ.* 4401: 401–476, p. 447: *C. vanstraeleni*.
5. STENZEL, H.B., 1952, Decapod Crustaceans from the Woodbine formation of Texas, in: Stephenson, L.W., Larger Invertebrate fossils of the Woodbine Formation, *U.S. Geol. Surv. Professional Pap.*, 242, 212–217.
6. VAN STRAELEN, VICTOR, 1936, Crustacés décapodes nouveaux ou peu connus de l'époque crétacique, *Bull. Mus. roy. Hist. nat. Belgique*, 12, 45, p. 36: *C. inflatus*.

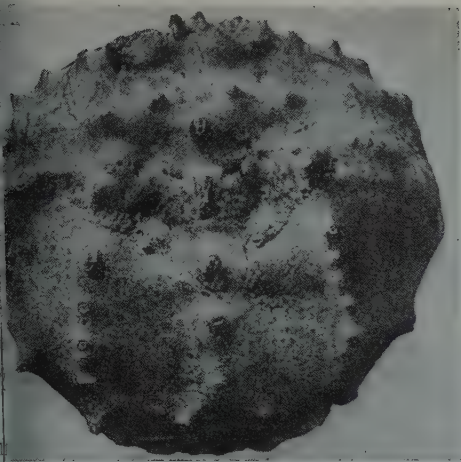


Figure 1. *Cenomanocarcinus inflatus* (Milne-Edwards) Van Straelen, Upper Cenomanian, Le Mans (After Van Straelen, 1936, Pl. IV, fig. 8).



Figure 2. *Cenomanocarcinus vanstraeleni* Stenzel (After Stenzel, 1945, Pl. XLIV, fig. 1).

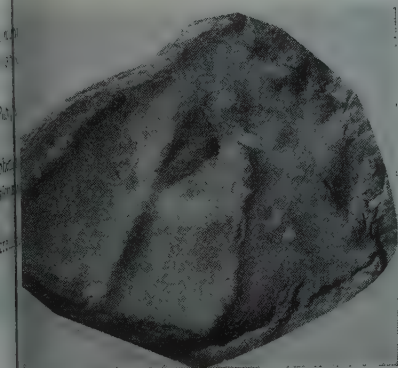


Figure 3. *Cenomanocarcinus hierosolymitanus* Avnimelech, Upper Cenomanian, Jerusalem, Israel.



Figure 4. The same, analysis of the carapace.

ISOCRINID FRAGMENT FROM UPPER GALILEE OF ASSUMED MIDDLE CRETACEOUS AGE

(RECORD NO. 4 OF THE HEBREW UNIVERSITY GEOLOGICAL MUSEUM)

M. AVNIMELECH

Department of Geology, The Hebrew University of Jerusalem

A piece of brown chert with an impression of a pentagonal crinoid stem was presented to the collections of the Department of Geology of the Hebrew University (registration No. 20987) by Mr. Eliahu Hurwitz from the "Beth Ussishkin" Natural History Museum in the Dan settlement, Upper Galilee. The specimen was found isolated in the vicinity of the small town of Qiryat-Shemoneh, at the foot of the north-eastern marge of the Upper Galilee mountains.

The impression shows three pentasterid columnals of a stem, 8 mm in diameter. The impression of the basal surface of a columnal bears five quite prominent radial ridges corresponding to the original furrows. Between the branches of the pentasterid each columnal bears—at its junction with the other columnal—four symmetrically disposed cirri, the presence of which is witnessed to by relatively deep sockets. The cross-section of the stem is thus not exactly pentagonal, being rather bilateral, as shown by the present figure.



The limited preservation of the crinoid fragment prevents exact determination; only tentatively could it be ascribed to *Isocrinus* or to some allied genus. This determination, often generalized, gives of course no direct information about its age, and only the geological relations of the region and the character of the chert may give some hint. The chert is similar to that occurring in Albion or Lower Cenomanian beds, and possibly the crinoid is of this age. As up to now no crinoid occurrence was noted in the Middle Cretaceous of Israel or of the neighbouring countries, it is worthwhile to report its occurrence in view of future findings and investigation.

LOWER EOCENE STARFISH REMNANT FROM LOWER GALILEE

RECORD NO. 5 OF THE HEBREW UNIVERSITY GEOLOGICAL MUSEUM

M. AVNIMELECH

Department of Geology, The Hebrew University of Jerusalem

Mr. Eviatar Nevo from the Oranim Teachers College, near Haifa, has kindly submitted to the Department of Geology of the Hebrew University a piece of chert with a quite well preserved negative impression of a fragment of starfish arm (reg. No. 20988). The fossil was found at Sha'ar Ha'amaqim, SE of Haifa, of undoubtedly Lower Eocene age. The chert is of creamy-greyish colour, of natural flat shape, showing that it originated in a thin layer of chert within a chalky formation; it includes numerous alveolar cavities and is covered with brown limonitic film.

The impression discloses an oral surface of a slightly arched arm, nearly 45 mm long and approximately 15 mm broad. It shows a well visible ambulacral channel with radial canal and ambulacral groove, framed on both sides by rows of adambulacrals. The depth of ambulacral channel in comparison to that of adambulacrals is appr. 3 mm. The ad- and inframarginals are preserved only on one side of the arm. The inframarginals bear broad axial ridge with three spinal tubercles. The



Figure 1

Astropecten (Archastropecten ?) sp., Sha'ar Ha'amaqim, near Haifa, Lower Eocene.
Original negative impression.



Figure 2

The same — plasticene (positive) mould.

details of the surface — as far as they are visible — might be slightly distorted by the processes of silification, as well as by the presence of the alveoles.

Despite the fragmentary preservation, the general character is well exposed and allows to recognize the fossil as an asteroid (it was already recognized as such by Mr. Nevo), belonging to the family *Astropectinidae* (ordo *Phanerozonida*, subordo *Paxillosa*), probably of the genus *Archastropecten* H. Hess 1955.

It is the first time that a fossil asteroid is discovered in the Eocene of Israel or of the neighbouring countries, although Ophiuroids are common in the Upper Cretaceous, especially in the famous Upper Cenomanian outcrop of Hakel and Upper Senonian of Sahel Alma, both near Beirut in Lebanon. Therefore, the finding of the Eocene *Astropecten* is of particular interest.

REFERENCES

1. DURHAM, J. WYATT AND ROBERTS, WAYNE, A., 1948, Cretaceous asteroids from California *Journ. Paleontol.*, **22**, 432.
2. FORBES, EDWARD, 1852, Monograph of the Echinodermata of the British Tertiary, *Palaeontograph. Soc.*
3. HESS, HANS, 1955, Die fossilen Astropectiniden (Asteroidea), *Schweizerische Palaeontologische Abhandlungen*, **71**.
4. UBAGHS, G., 1953, Classe des Stelléroïdes (Stelleroidea), *Traité de Paléontologie*, ed. J. Piveteau, **3**, 774.

PACHYDISCID AMMONITE (Cephalopoda: Ammonoidea: Ammonitina:
Desmoceratacea: Pachydiscida) FROM CAMPANIAN CHERT OF ISRAEL

(RECORD NO. 6 OF THE HEBREW UNIVERSITY GEOLOGICAL MUSEUM)

M. AVNIMELECH

Department of Geology, The Hebrew University of Jerusalem

Among non-classified material in the collection of the Hebrew University Geology Department, was found a piece of brown chert, of undoubted Upper Senonian (Campanian) age. A fragment of small, juvenile ammonite was preserved in this chert (reg. No. 21410). The locality of the fossil finding was not indicated, but most likely it is the area of Jerusalem, either Mt. Scopus (around the former University Campus grounds) or the south of the town, near the Talpioth quarter.

The fragment shows a part of an inner whorl, appr. 13 mm in diam., embraced by the following whorl, nearly 30 mm in diam., which is partly open. Three last septa are preserved in this latter whorl, and about a quarter of volution is occupied by body chamber. The fossil is completely silicified, being partly cherty, partly opaline, and incrustated inside with dense cluster of tiny quartz crystals. Inside the body chamber, attached to the wall, is visible a worm-like callus, made of opal and microcrystalline quartz, which doubtless has no connection with the structure of the shell itself, but which is related to the process of silification.

The preservation of the fossil is so poor that any attempt of a detailed and exact determination is useless. Nevertheless, the scarcity of ammonite species in the Upper Senonian of Palestine and of the neighbouring countries, calls our attention to this fragment, as it reveals a different shape from that of the commonly occurring species of this age. Its main character is its broad, almost perfectly rounded, semi-circular ventrum. The shell, in its juvenile whorls, is almost smooth, while in the following volution it seems to be ornamented with low spaced ribs. On the basis of the known data we do not have many alternatives for determining to what genus this particular ammonite may belong.

The characteristically rounded, semi-circular ventrum, points to the pachydiscid group, such as the genera *Eupachydiscus* or *Anapachydiscus*. The shape of the inner whorl corresponds to the s.c. "ganesa stage" (Collignon 1935) of the quoted genera.

Pachydiscids were reported from Palestine by H. Taubenhaus (1920), but his determinations were already doubted by Blanckenhorn (1927). Examination of his material (deposited now in the collections of the Hebrew University Geology Department) fully justifies this criticism.

Taubenhaus quotes and discusses three following species: (1) *P. arrialorrensis*

Stoliczka (mistake: should be "*arrialoorensis*"); (2) *P. cf. vaju* Stol.; (3) *P. sp. aff. P. neubergicus* v. Hauer em. Schlüter.

The general shape and ornamentation of *P. arrialoorensis* Taubenhaus, found in the Upper Senonian (Campanian) in the south of Jerusalem (our collection No. 2139), has aroused Collignon's doubts (1955, p. 50) as to the correctness of this determination. The true *P. arrialoorensis* is ascribed to the genus *Anapachydiscus* Yabe & Shimizu, while Taubenhaus' specimen has rather the character of *Eupachydiscus* Spath. As far as a reliable determination could be done without knowing the suture line, it seems that Taubenhaus' specimen is identical, or at least very near, to *E. isculensis* (Redtenbach), a well known species occurring in the Upper Santonian — Lower Campanian of Western and Southern Europe, of East Africa and of Madagascar.

The second species, discussed by Taubenhaus, *Pachydiscus cf. vaju* (Stol.) (our collection No. 2189), is correctly determined, although its illustration gives only a very vague idea about its characteristics. In his description the author surprisingly affirms that the Palestinian specimen is ten times (!) bigger than the Indian, as described and figured by Kossmat (1895, p. 90[154], Pl. XIV[XX], figs. 4a, b); in reality, the Palestinian specimen is a little more than twice as big, the diameters being 150 mm and 63 mm respectively. The stratigraphical horizon of the Indian specimen is the Lower Trichinopoly group, which is equivalent to the standard Santonian, in good correlation with the stratigraphical level of the Palestinian specimen. The species, according to the modern standards, belongs now to the genus *Lewesiceras* Spath.

The third species, *Pachydiscus aff. neubergicus* (our collection No. 2140), is wrongly determined and, unfortunately, the geographical and stratigraphical informations are also incorrectly given. The specimen was found by Blanckenhorn on the way from the Mezra'a locality, on the eastern shores of Dead Sea, to Kerak; Blanckenhorn

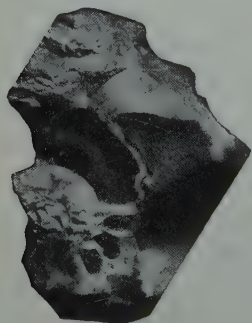


Figure 1
Eupachydiscus sp., Campanian, Jerusalem,
lateral view (Department of Geology, Hebrew University, Collection No. 21410).

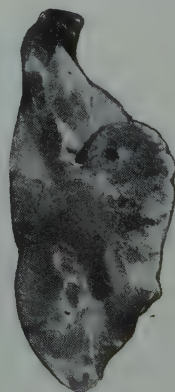


Figure 2
The same: natural cross-section of a whorl.

has ascribed it to Cenomanian. *P. neubergicus* is a species of Maestrichtian age. Probably because of this determination, Taubenhaus has chosen a "middle way", attributing this ammonite to an Emscherian (Lower Senonian) age.

Although unsatisfactorily preserved, this ammonite can be classified without hesitation as belonging to Pachydiscidae. Most probably it is *Lewesiceras* and, possibly, *L. peramplum* of Lower Turonian age. An ammonite, tentatively identified as *Pachydiscus peramplus*, was reported by E. Basse (1937, p. 191) from Lower Turonian of Ain Tineh, in the North Alaouite Mountains (NW Syria). It thus seems that pachydiscids are more common in the Palestino-Syrian region than it has been known up to now.

REFERENCES

1. ARKELL, W.J., KUMMEL, B. AND WRIGHT, C.W., 1957, Mesozoic Ammonoidea, in: *Treatise on Invertebrate Paleontology* (Moore, R.C.), L4: Cephalopoda, Ammonoidea, 80-465.
2. BASSE, E., 1937, Les Céphalopodes crétacés des massifs côtiers syriens, *Notes et Mémoires* (L. Dubertret), *Haut Comm. Rep. Franc., Syrie-Liban*, II, 165-200.
3. BLANCKENHORN, M., 1927, Einige kritische Bemerkungen zu der Beschreibung der syrisch-palästinischen Cephalopoden durch H. Taubenhaus, in: *Die fossilen Gastropoden etc., Palaeontographica*, **69**, 185-186.
4. COLLIGNON, M., 1955, Ammonites néocrétacés du Menabe (Madagascar), II: Les Pachydiscidae, *Madagascar Ann. Géol. Serv.*, **21**.
5. KOSSMAT, F., 1895, Untersuchungen über die südindische Kreideformation, *Beitr. Paläont. Oesterr.—Ung.*, **9**, 3-4, 97-203.
6. TAUBENHAUS, H., 1920, Die Ammoneen der Kreideformation Palästinas und Syriens, *Zeitschr. deutsch. Palästina-Ver.*, **43**, 1-2, 1-57.

PLACENTICERATID AMMONITE (Ammonoidea: Ammonitina: Hoplitacea:
Placenticeratidae) FROM THE CAMPANIAN PHOSPHATE LIMESTONE
OF PALESTINE

(RECORD NO. 7 OF THE HEBREW UNIVERSITY GEOLOGICAL MUSEUM)

M. AVNIMELECH

Department of Geology, The Hebrew University of Jerusalem

A small piece of phosphate limestone, with a remarkably well preserved ammonite, was recently discovered among specimens of unsorted material recovered from the collections of the Department of Geology of the Hebrew University, which, because of political circumstances during the past twelve years, were stored in the former premises of the University on Mt. Scopus. During this period there was no free approach to these collections, and, therefore, it was impossible either to take proper care or study them. Consequently, much damage was done, and many valuable specimens were irreparably lost.

The unusual shape (for the Palestinian Senonian) of this ammonite, as well as its excellent preservation, have attracted our attention. The rock-piece which includes it, measures no more than 40 per 35 mm. It is extremely fossiliferous and of the kind of phosphatic "bone-bed" which commonly occurs in the Judean Desert, in the north-eastern Negev and in the Amman district of Transjordan. No informative label was attached to the specimen except a small paper-square with the letter "D" glued on it. Specimens marked in this way were often received for examination by the Department of Geology from a geologically-minded cleric, Père Cogniant, living in the Holy Piscine cloister in the Old City of Jerusalem. The monk left Jerusalem in 1946 on a mission to one of the tropical countries of Africa; thus, a part of his material remained in the Department of Geology collections. It seems that the phosphate specimen, with its beautiful ammonite, most likely originated from some place in the Judean Desert, as this region was of great interest for the pious clericals and their disciples. Its age is well attested by the lithology, as well as by the tiny fossils crowded on the surface of the rock-piece. Among them it was possible to recognize as follows:

Astarte undulosa Conrad

Corbula cf. *paracrassa* Wade

? *Meretrix* (*Dosiniopsis*) *Judaica* L. Picard

? *Crassatella* sp.

Natica (*Ampullina*) *farafrensis* Wanner

Dentalium aff. *inornatum* Wade

Bone and teeth fragments of fishes and reptiles

Coprolithes

This association indicates Campanian age.

The ammonite, (reg. No. 21378) disclosing appr. $2\frac{1}{2}$ volutions, is not more than 17 mm of max. diam. and 13 mm of min. diam. It is compressed, nearly involute; its umbilicus has $3\frac{1}{2}$ mm in max. diam., and, in relation to the umbilical margin, is appr. $1\frac{1}{2}$ mm deep. The shell surface is beautifully preserved, displaying opalescent lustre. In the youngest volutions it is ornamented by sinuous, bifurcating and relatively broad ribs, which gradually pass into flat, sinuous and finely fasciculate plicae; these plicae radiate at the umbilical margin from curved elongated knots. The ventrum is grooved, and its width, in the disclosed part of our specimen is 1-2 mm; it is bordered on both sides by characteristically finely denticulated clavi, which terminate the ribs, resp. the plicae; in the youngest portion of volutions these clavi are symmetrically arranged, but later become probably alternating as a result of the not perfect regularity of the plicae.

Although the suture lines are not disclosed, the excellent preservation of the external features leaves no doubt as to its attribution to the genus *Placenticeras* Meek. As a rule, a juvenile shell restricts the exactness of determination, but, in this case, the perfect similarity of our ammonite to *Placentiras intercalare* Meek (*Pl. placenta* var. *intercalare* Meek, 1876, p. 468, Pl. 23; figs. la,b,c, and especially as described and figured by Hyatt, 1903, p. 207, Pls. 35-38), from the Upper Cretaceous Fort Pierre formation (Upper Senonian) of the U.S.A., allows us to ascribe it to this species. It is for the first time that *Pl. intercalare* is recorded from our region.

Very few placenticeratids were reported from Israel or from the neighbouring countries. Taubenhaus (1920) names two species. One of them, *Placenticeras subplanum*, was described as new; it is represented by two specimens, each of different locality in Transjordan (not from one, as wrongly stated by Taubenhaus). Already Blanckenhorn (1927, p. 186), in his critique on Taubenhaus' paper, corrected the determination of one of the specimens (deposited in our collections, No. 2206), stating that it is not a *Placenticeras* but a *Hoplitoides*, cf. *H. mirabilis* Pervinquière. Similar *Hoplitoides* was reported and figured by E. Basse from the Turonian of Lebanon, considered as new species and named *H. baalbeckensis* (Basse, 1937, p. 189, Pl. VIII; figs. 4a, b). The specimen which represents it, is very imperfect, its sutures being deeply abraded. In size and in shape it is very similar to the above quoted *H. cf. mirabilis* from Transjordan and, possibly, it is identical with it; Basse poses it near *H. ingens* (Koenen) Solger.

The second specimen of "*Placenticeras subplanum* Taubenhaus" (No. 2158) in our collections was later determined by L.S. Spath as *Hoplitoides* cf. *ingens* (Koenen) Solger, a Lower Turonian to Lower Coniacian species. It seems, therefore, that both

specimens, reported under the name of "*Placenticerias subplanum*", are not *Placenticerias* at all. Anyhow, they point to Turonian age, correcting the conclusions of Taubenhause (Senonian), as well as those of Blanckenhorn (Cenomanian).

The second species quoted by Taubenhause is *Placenticerias* cf. *pseudoplacenta* Hyatt from the Emscherian (Lower Senonian) of Jerusalem. This specimen is deposited in the Natural History Museum of Stuttgart. It is described in a very general way and no figure is given. The author emphasizes its bad preservation.

E. Basse (1937, p. 191) reported on a *Hoplitoplacenticerias* aff. *H. plasticus* Paulcke from the probable Campanian of Lebanon. The specimen, according to the author and to the given figure, is too poorly preserved for any additional discussion.

The nearest to our species is that reported by A. Chavan (1947, p. 129) under the name of *Hoplitoplacentirias vari* (Schlüter) (determined by E. Basse de Menorval),

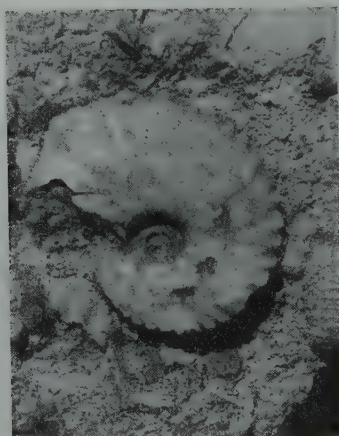


Figure 1
Placenticerias intercalare Meek, Campanian, Judean Desert.

found in the Campanian "Leda-beds" of Mount of Olives in Jerusalem. In our specimen of *Placenticerias intercalare* the sides are slightly convex, the width of the flat, narrow ventrum widens very slowly, the ribs are faint, falcoid. On the contrary, the *Hoplitoplacenticerias vari* has a trapezoidal, almost inflated cross-section; the flat ventrum of this species widens quite quickly and its ribs are coarse and broad, with prominent umbilical and ventro-lateral tubercles.

Chavan also notes — according to unpublished information of E. Basse — that *Hoplitoplacenticerias vari* occurs in Syria (? Lebanon, locality unspecified). It seems then, that placenticeratids are represented among the Senonian ammonites of the Levant by the two quoted species at least.

REFERENCES

1. ARKELL, W.J., KUMMEL, B. and WRIGHT, C.W., 1957, Mesozoic Ammonoidea, in: *Treatise on Invertebrate Paleontology, L4: Ctephalopoda: Ammonoidea*, 80-465.
2. BASSE, E., 1937, Les Céphalopodes crétaçés des massifs côtiers syriens, *Notes et Mémoires, Syrie-Liban*, **2**, 165.
3. BLANCKENHORN, M., 1927, Einige kritische Bermerkungen zu der Beschreibung der syrisch-palästinischen Cephalopoden durch H. Taubenhaus, in: Die fossilen Gastropoden etc. *Palaeontographica*, **69**, 185-186.
4. CHAVAN, A., 1947, La faune campanienne du Mont des Olives d'après les matériaux Vignal-Massé, *Journ. Conchyliologie*, **87**, 129. Pl. II, fig.
5. HYATT, A., 1903, Pseudoceratites of the Cretaceous, *U.S. Geol. Surv.*
6. MEEK, F.B., 1876, A report on the invertebrate Cretaceous and Tertiary fossils, *U.S. Geol. Surv. of the Territories*.
7. PERVINQUIERE, L., 1907, Etudes de Paléontologie tunisienne, I: Céphalopodes des terrains secondaires, *Tunis, Dir. Gen. Trav. Publ.*

OCCURRENCE OF THE ECHINOID GENUS ANORTHOPYGUS
(Echinoidea Irregularia: Holectypoida: Holectypidae) IN THE CENOMANIAN
OF PALESTINE

(RECORD NO. 8 OF THE HEBREW UNIVERSITY GEOLOGICAL MUSEUM)

M. AVNIMELECH

Department of Geology, The Hebrew University of Jerusalem

The echinoid fossil fauna of the Levant countries (Lebanon-Syria, Palestine, Egypt), had been studied by G. Cotteau, P. de Loriol, R. Fourtau and later by M. Blanckenhorn (1925), who summarized the data on the Cretaceous echinoids of Palestine. One of the species discussed in Blanckenhorn's monograph is *Holectypus portentosus* Coquand (1: p. 89, Pl. VII, fig. 8a, b); the specimens of this species, accompanied by *Heterodiadema libycum* (Desor), were found in a Cenomanian horizon at Ain-Homar, east of es-Salt (Transjordan). They were also found, according to Blanckenhorn, together with *Orthopsis miliaris* (d'Archiac), at Ain Jalo, near Jerusalem. It is also mentioned that according to Fourtau this species occurs in a probable Albian horizon at Der-el-Qamar in Lebanon. However, the figured specimen of *H. portentosus*, is not one of those mentioned in the text, but a different one, from a collection of Germer-Durant, a clerical scholar in Jerusalem. The provenance of this specimen is designated, in a general way, as "Lebanon".

The species, *Holectypus portentosus*, originates from Djebel Bou Thaleb (Sétif) in Algeria, from a horizon designated as Lower Aptian (4, p. 30, Pl. II, fig. 9-11). As a typical *Holectypus*, it has a submarginal periproct, and its apical system contains five genital plates, the posterior of which remains unperforated. The occurrence of this species was known up till now in Aptian-Albian only. Therefore, its occurrence in the Cenomanian (more exactly: in Upper Cenomanian) of Palestine, as reported by Blanckenhorn, arouses some distrust as to the exactness of the information or the correctness of the determination.

Blanckenhorn's collections are in the possession of the Hebrew University Geological Department, and they include the Lebanon specimen of Germer-Durand (No. 1845), as well as three specimens (No. 1846) from Ain Homar in Transjordan.

The Lebanon specimen, drawn but not quoted in Blanckenhorn's text, is not perfectly preserved. Its posterior margin has been damaged and consequently, the periproct is not preserved although its submarginal position is clearly indicated. Its apical system and the character of ambulacra clearly prove its identity with *H. portentosus*, as described and drawn by Cotteau (4, l.c.) and by Fourtau

(6, p. 46, Pl. XII, fig. 6). Mechanical deformation has caused a forward shifting of the apex from its central position, and thus the specimen appears slightly asymmetric in its antero-postero section. There could be no doubt as to the Albian age of this Lebanon echinoid.

The examination of the three specimens from Ain Homar in Transjordan have given quite different results. Two of them are of approximately 40 mm diameter, of which one is almost completely decorticated, disclosing innercast; the third, 30 mm in diameter, has preserved its test, although corroded. Blanckenhorn has evidently overlooked (probably because of their imperfect preservation) the fact that all three specimens have an oblique, supramarginal periproct, and the small specimen shows very clearly an ethmolytic apex in which the posterior ocular and genitals are separated by elongated madreporite. These characters prove, without any doubt, that all three specimens from Ain Homar belong to the genus *Anorthopygus* Cotteau and not to that of *Hoelectypus*.

Of the known *Anorthopygus* species, one, *atavus* Fourtau, occurs in Upper Albian; four — *orbicularis* (Grateloup), *excisus* Lambert, *zumoffeni* Loriol and *texanus* W. Cooke — in Cenomanian; one — *micHELINI* Cotteau — in Turonian and one — *paradoxus* Hawkins — in Senonian (?). All but one — the North American *Anorthopygus texanus* — are from the circum-mediterranean region.

The species of *Anorthopygus* are distinguished from each other chiefly by the shape of their supramarginal periproct, the shape of their ethmolytic apex and, especially, the shape of madreporite and by the general proportions of the test.

Due to their diagnostic features, the samples (No. 1846) from Ain Homar are identical with the *Anorthopygus orbicularis* (Grateloup). The strongly oblique periproct of this species, descending from right to left, distinguishes it from all the other, which have a less oblique periproct or are even situated almost vertically in the posterior inter-ambulacral suture. In its usual, apparently mature size, it is nearly 50% larger than the *An. excisus*, and about 50% smaller than that of *An. zumoffeni* which was reported to occur in the Cenomanian at Ghazir, Lebanon. The Turonian *An. micHELINI* is relatively much higher, and the madreporite of the apical system extends very broadly, attaining a rather round outline. The nearest species to *An. orbicularis* seems to be *An. atavus* Fourtau from the Upper Albian of Egypt, which chiefly differs by the less oblique situation of the periproct.

The original collection of Blanckenhorn also includes two poorly preserved echinoid fragments (our No. 1832) from Ain Yalu, west of Jerusalem, labelled as *Orthopsis miliaris* (d'Archiac) and as such quoted and discussed in his memoir (p. 87 and 89).

However, examination proves that one of the fragments represents the well known Cenomanian species, *Diplopodia (Tetragramma) variolare* (Brongniart); the other is *Anorthopygus* sp., possibly *orbicularis* Cott. or *excisus* Lamb.

These findings suggest that the genus *Anorthopygus*, is probably one of the common elements of the echinoid fauna of the Palestino-Syrian Cenomanian. This fact was probably overlooked because of the external resemblance of this genus to *Hoelectypus*.

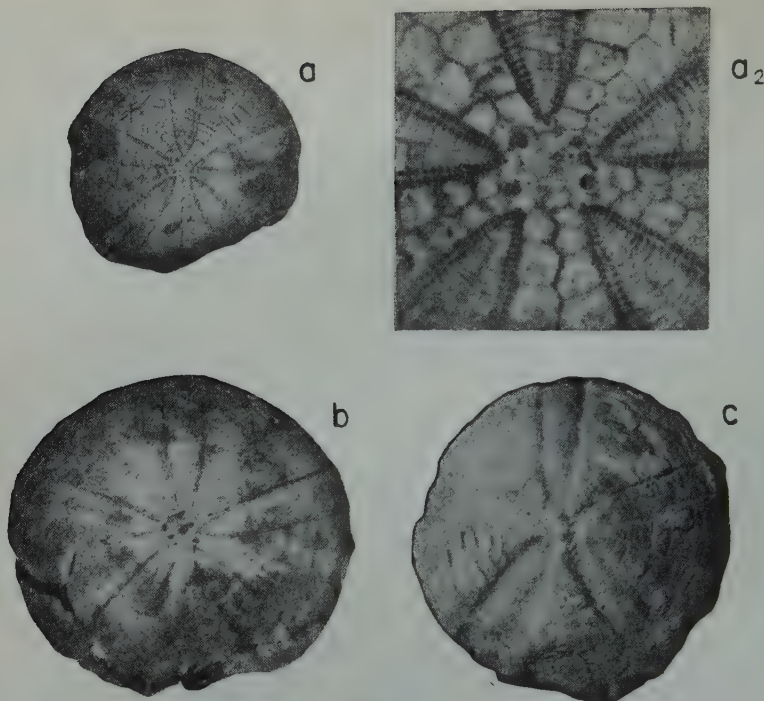


Figure 1

Anorthopygus orbicularis (Grat.), Ain Homar. Upper Cenomanian. a) smaller specimen, nat. size. a2) same apical region, X5. b) the bigger species in cu. c) decorticated specimen.

REFERENCES

1. BLANCKENHORN, M., 1925, Die Seeigelfauna der Kreide Palästinas, *Palaeontographica*, **67**, p. 89, Pl. VII, fig. 8 (*Holectypus portentosus*).
2. COOKE, C. WYTHE, 1946, Comanche Echinoids, *Journ. Paleontology*, **20** (3), 193-237 (p. 219, Pl. XXXIV, fig. 9-12: *Anorthopygus texanus*).
3. COTTEAU, G., 1862-1867, Echinides, in: *Paléontologie Française*, Terrain Crétacé, 7E, (p. 63, Pl. 1019: *An. orbicularis*; p. 67, Pl. 1020: *An. michelini*).
4. COTTEAU, PERON & GAUTHIER, 1876, Echinides fossiles de l'Algérie: Terrains secondaires, **1** (p. 30, Pl. II, fig. 9-11: *Holactypus portentosus*).
5. COTTEAU & TRIGER, 1855-1869, Echinides du Département de la Sarthe, Paris (p. 177, Pl. XXXI, fig. 1-9: *An. orbicularis*).
6. FOURTAU, R., 1911, Contribution à l'étude des Echinides fossiles de la Syrie, *Mem. Inst. Egyptien*, **7**, fasc. II (p. 46, Pl. XII (I), fig. 6: *Hol. portentosus*).
7. FOURTAU, R., 1921, Catalogue des Invertébrés fossiles de l'Egypte Terrains Crétacés, 3^e partie: Echinodermes (Supplement), *Egypt. Geol. Surv., Paleont. Ser.*, **5** (p. 53, Pl. II, fig. 5: *An. atavus*).
8. HAWKINS, H.L., 1935, Cretaceous Echinoidea, in: *Geology and Palaeontology of British Somalilands*, II (p. 51, Pl. VII, fig. 1: *An. paradoxus*).
9. LAMBERT, J., 1919, Echinides fossiles des environs de Santander, *Mem. Soc. Linnéenne de Lyon* (p. 10: *Anorth. orbicularis*, p. 11, Pl. I, fig. 18: *An. excisus* Lamb).
10. LAMBERT, J. AND THIERY, P., 1909-1925, Essai de nomenclature raisonnée des Echinides. Chaumont, p. 278 & 575: *Anorthopygus* p. 279 & 575: *Holactypus*.
11. LORJOL, P. de, 1901, Notes pour servir à l'étude des Echinodermes, fasc. IX, Genève, p. 30, Pl. II, fig. 23 (*Pseudopileus zumoffeni* Loriol).
12. MORTENSEN, TH., 1948, A Monograph of the Echinoidea, **1**: Holactypoida, Cassiduloida. Copenhagen, 1948.

PETROGRAPHICAL OUTLINE OF THE PRECAMBRIAN IN ISRAEL

TABLE OF CONTENTS

Abstract

Introduction

Petrography

I. The Metamorphic Complex

- (a) Mica-schists
- (b) Taba Gneiss
- (c) Chlorite-schists
- (d) Amphibolites
- (e) Injection-gneiss
- (f) Quartzites
- (g) Phyllites
- (h) Epidote-schists
- (i) Summary and conclusions

II. The Intrusive Complex

A. Major Intrusions

- (a) Eilat Gabbro and related rock types, including pegmatitic hornblendite
- (b) Timna Gabbro
- (c) The monzonites and related rocks of Timna
- (d) Roded Quartz-diorite and its xenoliths
- (e) Rehav'am Quartz-diorite
- (f) Timna Granite-porphyry
- (g) Timna Granite
- (h) Eilat Granite
- (i) Shahmon Granite
- (k) Order of emplacement and relationships

B. The Older Dike Group

- (a) Dike rocks closely connected with the major intrusions
- (b) Pegmatites and aplites
- (c) Pyritic quartz-porphyries
- (d) "Schist dikes"

III. The Volcano-Conglomeratic Complex

A. Plutonic Masses

- (a) Timna Syenite
- (b) Yehoshaphat Granite
- (c) Amram Granite-porphyry

B. Lavas, agglomerates and tuffs

- (a) Amram Quartz-porphyry and related tuffs and agglomerates
- (b) Spilites, basalts and associated rocks

C. The Young Dike Group

- (a) Albite-diabase
- (b) Intermediate rocks
- (c) Quartz-porphyries

D. Eilat Conglomerate

E. Chronology of the Volcano-Conglomeratic Complex

Appendix: Dikes of doubtful (Precambrian) age

- (a) Olivine-dolerite
- (b) Trachy-andesite
- (c) Biotite-hornblende-meladiorite
- (d) Lamprophyre (?)

Remarks on the Fault History of the Precambrian Area in the Southern Neguev

The Magmatic History of the Israel Precambrian

References



PETROGRAPHICAL OUTLINE OF THE PRECAMBRIAN IN ISRAEL

YAAKOV K. BENTOR

The Hebrew University of Jerusalem and Geological Survey of Israel

ABSTRACT

The Precambrian of Israel, outcropping in the south of the country, near the gulf of Eilat, is composed of three petrographic complexes. The oldest of them, the Metamorphic Complex, consists of a very thick sequence, mainly of mica-schists and gneisses. These rocks are derived by metamorphism from geosynclinal sediments originally mainly composed of shales and graywacke. Ultrabasic magmatic rocks, emplaced early in the geosynclinal cycle, have been transformed into amphibolites. These rocks were intruded by the second rock group, the Intrusive Complex, composed of several major intrusions comprising basic, intermediate, and acid rock types. The Intrusive Complex also comprises a large number of dike rocks, the Older Dike Group, mainly of abyssal to hypabyssal, but also of volcanic, facies. The third rock group, the Volcano-Conglomeratic Complex, overlies the former two along a major unconformity. It comprises intermediate to acid intrusions, basic and acid lavas and tephra, basic, intermediate and acid dikes (Younger Dike Group), as well as a thick conglomerate sequence cemented by viscous lava. The Intrusive Complex was emplaced late in the orogenic cycle, while the magmatic rocks of the Volcano-Conglomeratic Complex are post-kinematic and connected with large-scale faulting. The Intrusive Complex is calco-alkaline, the igneous rocks of the Volcano-Conglomeratic Complex are alkaline to hyperalkaline in character.

INTRODUCTION

Outcrops of Precambrian rocks are found in Israel only in the southern Negev near the Gulf of Eilat (Red Sea) (Figure 1). The Precambrian rock sequence exposed forms part of what has been called by L. Picard (1941) the Arabo-Nubian massif. These outcrops are continuous with those in the Sinai Peninsula, the southern third of which is built by Precambrian rocks. Owing to the tectonic "weld" along both sides of both the Suez and Eilat grabens the Precambrian outcrops of the Sinai Peninsula continue in a narrow strip along the western and eastern coasts. The eastern Precambrian coastal strip of the Sinai links up with the Precambrian outcrops in Israel, while that along the western coast of the peninsula can be followed north until the region of Abu Zuneima. Precambrian outcrops extend over large areas on the African side of the Suez graben in Upper Egypt, where they were recently investigated by H.M.E. Schürmann (1949, 1954, 1956, 1957). East of the Arava-Eilat Gulf — Red Sea graben, the outcrops of Precambrian rocks continue northward to the latitude of Ein Hatzeva and they crop out again farther north, near the south-east corner of the Dead Sea.

Received January 2, 1961

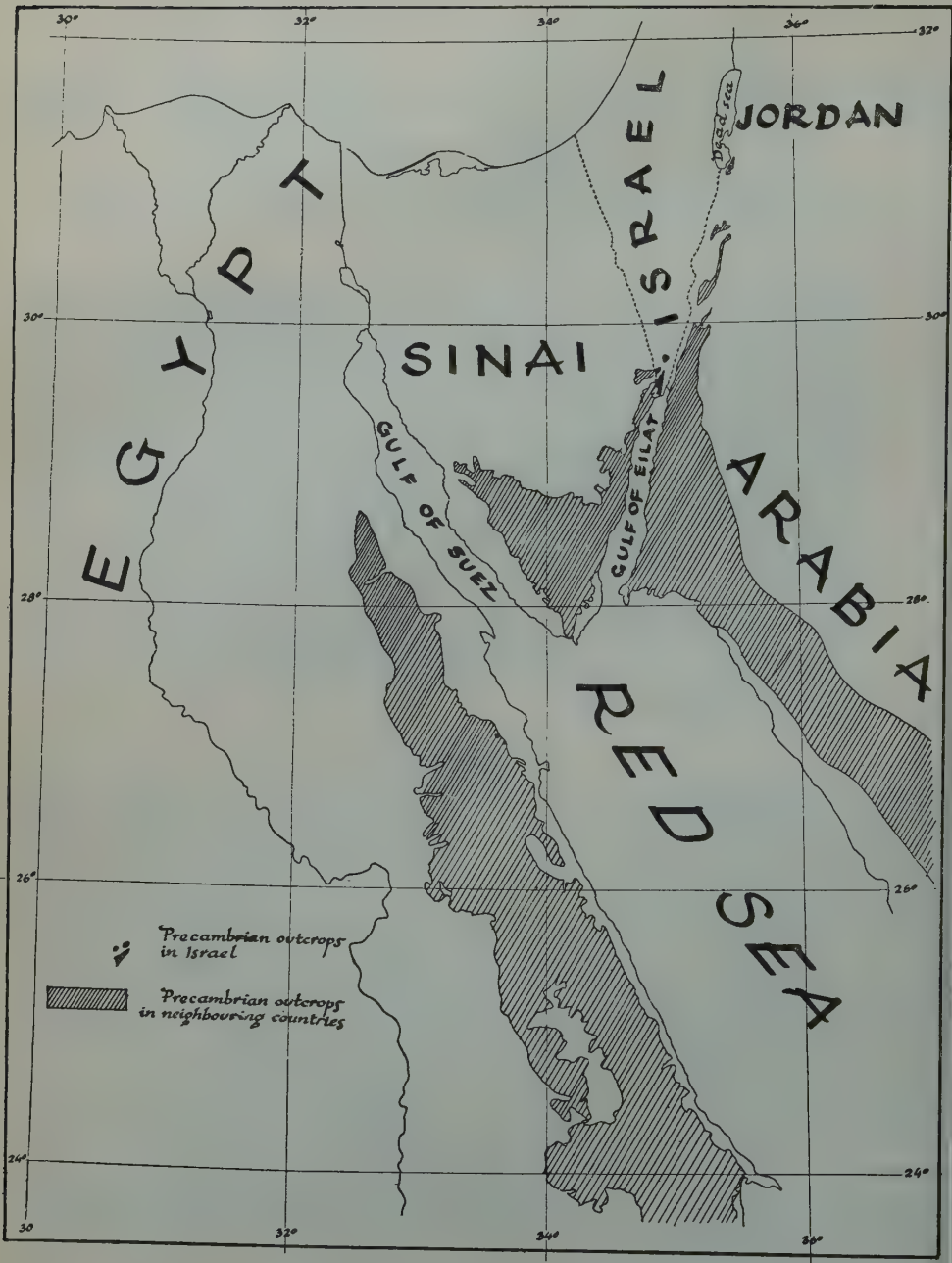


Figure 1
Precambrian outcrops in the Red Sea area

The Precambrian rocks now comprised within Israel's borders are first mentioned by L. Lartet (1869). They were studied by E. Hull (1886-9) who divided them into two complexes: an older, mainly metamorphic one, comprising hornblende-, chlorite- and talc-schists with subordinate gneisses and granites; and a younger one composed mainly of porphyries passing into granites with associated agglomerates and tuffs. Some of these rocks are described by F. W. Hudler (in E. Hull, 1886). Hull was uncertain as to the age of these rocks and considered the older complex to be Archaean, Laurentian or Cambro-Silurian and the upper complex Lower or Upper Silurian in age. The Precambrian rock complex was later dealt with by M. Blanckenhorn (1914) and G.S. Blake (1935), who also published a number of analyses. A short description of the area is also given in a paper on the Arabo-Nubian massif by L. Picard (1941).

A detailed investigation of the Precambrian in Israel was first undertaken in 1949 by the author and A. Vroman during the mapping of the Negev on the 1:100,000 scale. They divided the rock sequence into 14 units, and these were shown on the geological map of the Negev, Sheet 24: Eilat (Y.K. Bentor and A. Vroman 1955). Since 1955 the whole area, with the exception of Mount Shelomo, was mapped on the 1:20,000 scale and a considerable amount of petrographic work was done (Eyal 1959, Backler 1960, Posner 1954, Shiloni 1959, Weissbrod 1960, Wurtzburger 1959, Stalkine and Wurtzburger 1957). The results of this detailed study showed that some of the rock units, which were previously considered to be homogeneous, are in fact composed of a number of different rock types. The following table correlates the classification of the rock units shown in the geological map of Eilat (Bentor and Vroman, 1955) with that used in the present paper.

The total area of Precambrian outcrops in Israel is only about 70 km². Nevertheless, a surprisingly large variety of rock types — metamorphic, plutonic, volcanic and sedimentary — are present. This heterogeneity is only partly original; essentially it is a consequence of extensive tectonic disturbances of large magnitude, which caused different levels of the Precambrian crust to be exposed now in close geographical vicinity. It is noteworthy that almost all the Precambrian rock types exposed in the Sinai can be matched by similar rocks in Israel. Although the outcrops in the Sinai peninsula are about 170 times larger, they are considerably less affected by faulting.

In addition to the intense tectonic dissection the study of the Israel Precambrian rock sequence is made difficult by the fact that its outcrops are not continuous. Most of the Precambrian basement was already buried in early Paleozoic time under a thick sequence of sediments. This cover was increased considerably by marine sedimentation which in this area lasted at least from Cenomanian to early Eocene times. Only in consequence of the strong faulting movements of the Rift Valley, which took place during the Tertiary and continued possibly into the Pleistocene, were parts of the old Precambrian basement exposed again; in the low-lying tectonic

TABLE I
Subdivisions of Israel Precambrian Rock Sequence
(Excluding Dike Rocks)

Bentor-Vroman: Geological Map of Eilat, 1955	Present Paper ¹
Eilat conglomerate	Eilat Conglomerate
Acid volcanic rocks	Amram Quartz-porphyry
Volcanic tuffs	Not divided from corresponding lava flows
—	Spilites
Dike country	—
Eilat granite	{ Eilat Granite (s.str.) Rehav'am Quartz-diorite Yehoshaphat Granite
Roded granite	{ Roded Quartz-diorite Shahmon Granite
Timna granite	Timna Granite
Timna granite-porphyry	Timna Granite-porphyry
Amram granite-porphyry	Amram Granite-porphyry
Syenite	Timna Syenite
Diorite, gabbro	{ Eilat Gabbro Timna Gabbro Monzonites and related rocks of Timna
Eilat schist	Metamorphic Complex including Taba
Roded Schist	Gneiss (subdivided on petrographic basis)
Gneiss	{ Eilat Granite-gneiss Roded Quartz-diorite-gneiss

1 The type localities of the Precambrian formations are shown in Figure 2.

blocks, however, the Paleozoic to Eocene sedimentary strata, masking the Precambrian basement, are still preserved.

As a result of both the tectonic movements and the discontinuity of outcrops, the Precambrian basement complex of Israel is divided into a number of massifs (Figure 2), each with its distinctive rock types. These massifs are:

I. *The Eilat massif* which is divided into two parts by the Yotam graben. The eastern part extends from beyond the southern border near Taba to the Shehoret Hill in the north. It is bordered on the west by the Yotam graben, and on the east by the western border faults of the Arava Rift Valley. North of the Shehoert Hill these two fault zones meet, leading to a northern wedge-like ending of this part of the Eilat massif. The western part of the Eilat massif, west of the Yotam graben, is bordered in the south by the important Yehoshafat fault, on the west by the very large Netafim fault, and joins the Shahmon massif toward the north, near the southern slope of Mount Shelomo.

II. *The Shahmon (Roded) massif* which comprises the major part of Mount Shelomo, as well as the Shahmon and Shehoret Mountains. It is bordered to the east

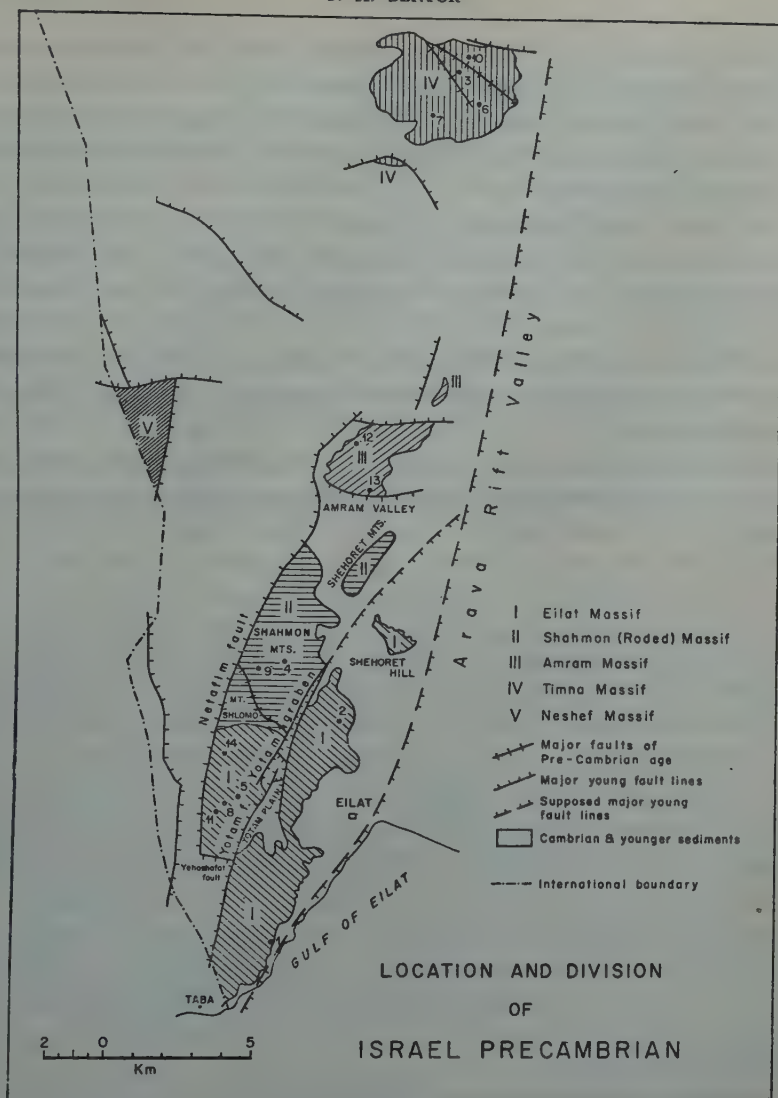


fig. 2

Drawing: Dev B.

Formation

Formation	Type Locality
1. Taba Gneiss	1418/8803 south of Shelomo Valley
2. Eilat Gabbro	1440/8878 south of Roded Valley
3. Timna Gabbro	1477/9094 central block of Timna massif
4. Roded Quartz-diorite	1420/8900 upper Roded Valley
5. Rehav'am Quartz-diorite	1409/8855 west of Yotam Plain
6. Timna Granite-porphyr	1485/9087 central block of Timna massif
7. Timna Granite	1470/9085 western block of Timna massif
8. Eilat Granite	1403/8850 west of Yotam Plain
9. Shahmon Granite	1412/8894 Netafim Valley
10. Timna Syenite	1482/9103 eastern block of Timna massif
11. Yehoshaphat Granite	1402/8846 Mount Yehoshaphat
12. Amram Granite-porphyr	1445/8973 south of Avrona Valley
13. Amram Quartz-porphyr	1450/8956 north of Amram Valley
14. Eilat Conglomerate	1401/8868 east of Shelomo Valley

by the Yotam graben, to the west by the Netafim fault, and disappears toward the north under the sedimentary cover of the Amram Valley.

III. *The Amram massif*, bordered to the south, west and north by fault zones along which the sedimentary strata are down-thrown against the massif, and to the east by the Arava border fault.

IV. *The Timna massif*, exposed in the core of the Timna dome. This massif disappears to the south, west and north under the sedimentary cover dipping away from the Precambrian core, and is cut off toward the east by the Arava border fault.

V. *The Neshef massif*, situated mainly in the Sinai but extends a few kilometers into Israel; it is here bordered to the north and east by very large fault zones down-throwing the sediments.

The aim of this paper is to review the known basic data and to outline a first interpretation. A more detailed petrographic and petrologic study is at present in preparation.

PETROGRAPHY

According to field relationships the Precambrian rock sequence of southern Israel can be divided into three units: the oldest of these is composed of a variety of metamorphic rocks and is termed here the *Metamorphic Complex*. The next one, the *Intrusive Complex*, consists essentially of igneous rocks ranging in composition from ultrabasic to acid. This group comprises also orthogneisses clearly derived from granites, granodiorites and quartz-diorites, and dike rocks of various ages, but older than the third rock group. Although probably more than one age of dike formation is present, all are included in the term the "*Older Dike Group*". Wherever contact relationships can be observed, the various rocks of the *Intrusive Complex* can be shown to be either intrusive into each other or into rocks of the *Metamorphic Complex*. It can therefore be concluded that all the rocks of the second group, intrusive country rocks, dike intrusions and their metamorphic derivatives, are younger than the *Metamorphic Complex*.

The third rock group is composed of volcanic rocks, lavas and associated agglomerates, tuffs and subvolcanic intrusions, their hypabyssal dike equivalent — the "*Younger Dike Group*" — as well as by a thick conglomerate sequence. This group, designated as the *Volcano Conglomeratic Complex*, overlies rocks of the two older complexes along a major unconformity. It is in turn overlain unconformably by "Nubian" sandstones of early Cambrian age.

The Metamorphic Complex

Rocks of the *Metamorphic Complex* are confined to the two southern massifs — those of Eilat and Shahmon (Roded). On the geological map of Eilat (Bentor and Vroman, 1955) two different rock formations, the Eilat schists and the Roded schists,

were distinguished. More recent research by M. Eyal (1959) and T. Weissbrod (1960) has shown, however, that certain rock types are found in both sequences, although they are not equally frequent in both massifs. The two sequences may, therefore, have a common origin and are therefore here dealt with together. A short petrographic description of the various rocks composing the Metamorphic Complex is given in the following, in the order of decreasing frequency.

(a) *Mica-schists*. This group comprises several rock types of varying mineralogical composition. All contain quartz, sodic plagioclase, which is sometimes albite and sometimes oligoclase, and one or two micas. The most widespread rock type is a *biotite-schist* containing 20–35% quartz; the amount of plagioclase varies from 10–40% in the Eilat massif to about 50% in the more northerly Shahmon massif. The amount of biotite varies from 9–20%; orthoclase is usually present in small amounts, augite is occasionally found in the Eilat massif and sphene, apatite, ore minerals and green hornblende occur as accessories. The average grain size of these rocks is about 0.5 mm. Foliation is fine, persistent and very pronounced. In the Eilat massif two structurally different rock types can be distinguished, each occurring in a separate area: the first, and more widespread rock shows planar foliation with fine layers of quartz-feldspar and biotite alternating in planes perpendicular to the c-axis. The other type shows pronounced linear foliation with quartz-feldspar and biotite segregated along the a-axis, but alternating in the plane perpendicular to it.

Through the appearance of muscovite these rocks pass into *two-mica-schists* in which muscovite is commonly porphyroblastic. Another frequent mineral is a garnet of the pyrope-almandite group; in most *garnet-mica-schists* this mineral also forms porphyroblasts which may reach a diameter of 4 mm. In the southern part of the Shahmon massif a very quartz-rich garnet-two-mica-schist occurs in which quartz forms about 70% and biotite, muscovite and garnet about 10% each. Finally, *staurolite-mica-schists* and *staurolite-garnet-mica-schists* occur in a small area in the Eilat massif north of the Yotam Plain.

The chemical analysis of a *garnet-mica-schist* from the Shelomo Valley is given in Table II, No. 1. This is the composition of a normal shale; the predominance of sodium over potassium, however, is unusual.

(b) *Taba Gneiss*. This rock has a wide distribution in both the Eilat and Shahmon massifs. Its major constituent minerals are quartz, plagioclase and biotite. The amount of quartz varies from 10–35%; plagioclase is highly variable in amount as well as composition. In most cases it is oligoclase, sometimes andesine, but in some areas in the southern Eilat massif almost pure anorthite has been found. The amount of plagioclase increases, just as in the case of the associated mica-schists, from 25–50% in the south to 50–70% in the north. Biotite is present in amounts varying from 5–20%. In the Eilat massif small amounts of augite can occasionally be observed; potash-feldspar, either orthoclase or microcline, is frequently present but its amount rarely exceeds 6%. Accessory minerals are muscovite (rare and always very sparse),

green hornblende (up to about 1%), apatite, zircon, sphene and ore minerals. In comparison with the mica-schists the Taba Gneiss is much coarser grained with an average grain size of about 2.5 mm, and less schistose. Its dominant texture is gneissose, but occasionally the rock passes into a nearly non-oriented and massive variety of almost igneous habit. The degree of metamorphism is stronger than in the mica-schists, but seems to decrease toward the north.

Three analyses of Taba gneisses, from the northern and southern Eilat massif and the Shahmon massif, are given in Table II, Nos. 2 to 4. There are considerable differences, particularly in the parameters *calk* and *k*. While granites to granodiorites could have a similar composition, the balance of the chemical evidence, and especially the extremely high value of $T(= al-alk)$ of analysis 2, favours the interpretation of the Taba Gneiss as a metasediment.

(c) *Chlorite-schists*. Chlorite-schist is a rare rock type found only in the northern part of the Shahmon massif. The chlorite, seldom more than 6% of the rock mass, is clearly an alteration product of biotite, the latter mineral sometimes being totally replaced by it. In all other respects the rock is similar to the biotite-schists, and therefore best explained as a product of their retrograde metamorphism.

(d) *Amphibolites*. Amphibolitic rock masses occur in two restricted areas: one in the southern, the other in the northern part of the Shahmon massif. They show sharp cross-cutting contacts toward the surrounding mica-schists, and there can be little doubt that they result from the metamorphism of basic intrusives.

The southern and northern rock types are different in mineralogical composition and in texture. Both contain as major constituents green hornblende and plagioclase. The latter is oligoclase in the northern, but andesine in the southern outcrops. A second mafic mineral is always present; it is biotite in the northern, but diopsidic augite in the southern rocks. Accessory minerals, present in very small amounts, are in both cases; sphene, zircon, apatite, ores, sometimes epidote and secondary calcite. The quantitative mineralogical composition determined by the Rosival method is as follows:

	Northern type	Southern type
oligoclase	38%	—
andesine	—	27%
green hornblende	38%	37%
biotite	22%	—
diopsidic augite	—	35%
accessories	2%	1%

The northern type is thus a *biotite-amphibolite*, the southern one an *augite-amphibolite*.

These rocks are dense, hard and dark green to black. The hornblende of the northern type is prismatic and the rock has a pronounced linear schistosity. The hornblende of the southern type is equidimensional and surrounds cores of augite; it is, at least

in part, uraltic. The structure is massive-granular and non-schistose. The chemical composition of the southern amphibolite type is given in Table II, No. 5. These rocks are very basic and show unusually low percentages of SiO_2 and Al_2O_3 . Accordingly, the colour-index of the amphibolites is frequently more than 70. The magma type is typically ultrabasic: hornblenditic to issitic.

(e) *Injection-gneiss*. Injection-gneisses are found in various places in the southern part of the Shahmon massif. They occur always within the Metamorphic Complex in the vicinity of intrusive quartz-diorite masses and consist of alternating bands of schist and quartz-feldspar aggregate.

(f) *Quartzites*. Thin bands of quartzites are common, alternating with mica-schists, particularly in the Eilat massif. They are composed mainly of quartz with subordinate amounts of biotite and muscovite. These rocks exhibit a very low degree of metamorphism and should properly be classified as micaceous sandstones, derived from argillaceous sandy sediments.

(g) *Phyllites*. Phyllites have a very limited distribution and occur only in small outcrops in the Eilat massif east of the Yotam Plain, where they form the roof of one of the granite intrusions. These rocks are dense, dark gray to black in colour, show an extremely well developed planar schistosity, are poorly crystallized and contain frequently a high percentage of tiny scales of sericite.

(h) *Epidote-schists*. In the northern part of the schist belt of the Eilat massif occur some small bands of a fine grained dark-gray rock composed of about 70% epidote, 20–25% quartz and small amounts of plagioclase, apatite, sphene and secondary calcite. These rocks are, therefore, *epidote-schists* and may represent thin bands of argillaceous limestone in the original sedimentary sequence.

(i) *Summary and conclusions*. The Metamorphic Complex consists in its major part of metasediments, transformed by regional metamorphism into phyllites and mica-schists. The schistosity of these rocks is generally parallel to the original bedding, although in some cases more than one direction of schistosity can be observed. Many depositional features of the original sediments, such as concretionary structures, pebbles and bedding, can still be recognized. There can be little doubt that this part of the Metamorphic Complex represents a geosynclinal sequence of sediments composed originally mainly of shales and graywacke, with subordinate amounts of pure and argillaceous sandstones and some limestones. Because of the intense tectonic disturbances the exposed original thickness of this sequence is difficult to estimate. It certainly exceeded 1,000 m and may well have reached several thousand.

These sediments were affected by two kinds of metamorphism; regional metamorphism is the dominant type and a regular arrangement of metamorphic zones can be recognized. The rocks most highly metamorphosed belong to the garnet-staurolite zone. These are encountered mainly to the north-east of the Yotam Plain. Farther outward from this centre garnet-schists dominate (Shelomo Valley, southern part of Shahmon massif), which grade toward the periphery into two-mica-schists. These latter types are best developed in the northern part of the Shahmon massif.

Much slighter is the metamorphic influence of the later magmatic intrusions which, moreover, is generally confined to a zone a few hundred metres wide along the intrusive margins. In the immediate vicinity of the intrusive contacts extensive exchange of material led to the formation of migmatites (Eilat massif, west of Eilat) which grade into typical injection-gneisses farther away from the contact. These rock types are particularly well exposed west of Eilat and in the southern part of the Shahmon massif.

The interpretation of the Taba Gneiss and its related rock types is more difficult. No significative minerals have so far been found in these rocks, but on the basis of their chemical composition it is more likely that they represent metasediments different in original composition from those which were metamorphosed into the various mica-schists, than dynamically metamorphosed igneous rocks. The origin of the amphibolites, on the other hand, is clear. They are metamorphosed basic intrusives originating early in the geosynclinal stage.

The Intrusive Complex

Rocks of the Intrusive Complex are more widely distributed than those of the two other complexes. They form about half of the Eilat massif, the major part of the Shahmon massif, almost the entire Timna massif, but are absent from the Amram and Neshef massifs.

The Intrusive Complex contains a large variety of rock types. These are here briefly described, starting with the major intrusive rock masses in order of increasing acidity, and ending with the associated dike rocks of the Older Dike Group.

A. Major Intrusions

(a) *Eilat Gabbro and related rock types, including pegmatitic hornblendite.* A series of basic to ultrabasic intrusive rocks are found in various places within the Metamorphic Complex of the Eilat massif, but never outside it. These rocks are generally medium grained, mostly equigranular, but occasionally porphyritic, and have a dark-gray to black colour. They are composed mainly of plagioclase, varying in composition from andesine to labradorite and green hornblende. Biotite is frequent and small amounts of quartz are occasionally present. Accessory minerals are orthoclase, apatite, sphene and ore minerals; in some instances the latter form up to 7% of the rock. The relative amounts of these minerals are subject to large variations, as shown in the following:

plagioclase	20-60 %
green amphibole	20-40 %
biotite	0-30 %
quartz	0-15 %

Accordingly, a number of different rocks can be distinguished which grade, however, continuously into each other. These are: *amphibole-gabbro*, *biotite-amphibole-*

gabbro, *biotite-amphibole-meladiorite*, *biotite-amphibole-diorite*, *amphibole-diorite*, *hornblende-quartz-diorite*. This group of rocks, and particularly the *biotite-amphibole-gabbro*, may be related to the *biotite-amphibolite* of the Shahmon massif.

One particular rock of this group remains to be mentioned. It is dark green, very coarse grained and ultrabasic, its average grain size is about 1 cm, but individual crystals often reach 5 cm. The rock consists of 90 % green hornblende, 7 % ore minerals and 3 % labradorite, and accordingly should be classified as a *pegmatitic hornblendite*. This rock, which is known only from two small outcrops, grades laterally into the associated basic rocks and can be interpreted as a *pegmatitic marginal facies* of the Eilat gabbro rock group.

(b) *Timna Gabbro**. The Timna gabbro builds a large part of the central block of the Timna massif. In its fresh outcrops, which are extremely limited in area, it is black, compact and very hard. Its mineralogical composition is: labradorite with An_{54} , olivine, enstatite, lamprobolite, common hornblende and biotite. Accessory minerals are: apatite, magnetite.

This is the only Precambrian rock containing fresh olivine which, moreover, is here very abundant. It is occasionally altered to iddingsite, antigorite and magnetite.

The chemical analysis of this rock is given in Table II, No. 6.

The magma type is hornblenditic to hornblende-peridotitic, a composition very basic for a member of the gabbro group. The occurrence of small amounts of biotite in the rock is surprising, in view of the exceedingly small alk- and k- values. The rock should be termed *biotitiferous noritic olivine-melagabbro*. Chemically it is clearly distinct from the amphibolites, as shown by the large differences in the fm- and c-values.

Over most of its area this rock is deeply altered into a dark green loose soil-like material composed mainly of well crystallized corrensite, vermiculite, chlorite and palygorskite. In view of the good crystallinity of the clay minerals and in the general absence of chemically formed soils in the highly arid southern Negev, the formation of this material is attributed to hydrothermal alteration.

(c) *The monzonites and related rocks of Timna*. A closely related, but variable, group of rocks ranging from gabbrodiorites through diorites and monzonites to quartz-diorites and granodiorites occurs in the Timna massif. The various rock types grade continuously into each other and generally cannot be mapped separately. The outcrops of this rock sequence form an envelope around the southern margin of the central Timna massif, but also penetrate into its interior on the central and eastern blocks.

The rocks are medium to fine grained, and most of them show a pronounced porphyritic texture. Their colour varies from dark gray and green-black at the basic end through greenish gray to reddish for the more acid types. The constituent minerals are: plagioclase, which is always present and varies from labradorite with An_{60}

* The microscopic description of the Timna rocks is based on Slatkine and Wurzbürger (1957)

in the basic rocks to oligoclase with An_{20} in the acid rocks; potash-feldspar, which is present practically throughout the whole range, and is an accessory mineral in the basic rocks, but the dominant one in the acid ones; for the most part, it is perthitic microcline, but in the monzonitic types orthoclase is the dominant potash-feldspar; quartz, present throughout almost the whole range, rare and only interstitial in the basic rock types, but among the phenocrysts in the acid rocks; in some of the more basic gabbrodiorites, which have negative quartz numbers, quartz is absent. Amphiboles are present in all rock types: they are dominant in the gabbrodiorites where basaltic, green hornblende and urallite occur side by side; in the intermediate and acid rocks only common hornblende is found. In these rocks biotite is the dominant mafic mineral, but it persists in small amounts also in the basic rocks. In the latter, small amounts of greenish augite appear occasionally. Accessory minerals are widespread and sometimes relatively abundant. They include sphene, apatite, magnetite and — in the basic rocks — also ilmenite which is sometimes transformed into rutile.

According to mineral composition and texture, the following rock types can be distinguished: *amphibole-gabbro-diorite*, *amphibole-biotite-(quartz)-diorite*, *amphibole-biotite-(quartz)-monzonite*, *amphibole-biotite-granodiorite*. The chemical composition of this rock sequence is given in Table II, Nos. 7–24. Chemically as mineralogically, this is a continuous series, ranging from moderately basic to moderately acid. The major trend is from the normalgabbrodioritic magma type to normaldioritic, normalquartzdioritic, normalgranodioritic to josemitgranitic and, finally, engadinitgranitic.

This rock sequence has been explained by Slatkine and Wurzbürger (1957) as hybrid and formed by the action of a gabbroidic magma on preexisting granites. A mechanism of this kind would explain that the chemical development is not a thoroughly straight one, and occasionally orbitic, leucomiharaitic, lamprodioritic, si-monzonitic, larvikitic (?) and natronrapakivitic magma types are encountered. Hybridization of a granitic rock necessitates differential melting, the degree of which will depend on the amount of super-heat present in the hybridizing magma, and this amount is certainly subject to local variations.

At its acid end the monzonite rock sequence links up with granites of the Timna massif, and particularly well with the Timna Granite-porphyry, as shown by the moderate k -values which characterize the majority of rocks in the monzonite sequence as well as the Timna Granite-porphyry, while the k -values of the Timna Granite are much higher. At its basic end the monzonite sequence is separated by a gap from the only basic rock found in the Timna massif: the Timna Gabbro. As the magma, from which the Timna Gabbro crystallized, may well be the one responsible for the formation of the monzonite sequence, it may be concluded that the Timna Gabbro itself already represents a basic differentiate of this gabbroidic magma. Altogether, the chemical evidence lends support to the hybridization theory which was formulated by Slatkine and Wurzbürger mainly on the basis of field evidence.

(d) *Roded Quartz-diorite and its xenoliths.* The very characteristic rocks included in the name Roded Quartz-diorite are clearly intrusive into the Metamorphic Complex. They form the major part of the Shahmon (Roded) massif and of the Shehoret Mountains. The rock is medium to coarse grained with an average grain size of about 2 mm. Its colour varies from dark green to dark red. The texture is hypidiomorphic to xenomorphic-granular. High amounts of mafic minerals are typical of most of these rocks. The most common type consists of 50 to 70% oligoclase with An_{20} , with very subordinate amounts, not exceeding 2–6%, of microcline. Quartz is always present, but in amounts varying from 8–22%. Among the mafic minerals, biotite is a constant constituent forming 8–15% of the rock. Green hornblende is generally present, and sometimes forms up to 20% of the rock mass. Accessory minerals are apatite, zircon, muscovite and ore minerals. Thus, this rock is sometimes an *amphibole-biotite-quartzdiorite* and sometimes a *biotite-amphibole-quartzdiorite*.

Chemical analyses of these rocks are given in Table II, Nos. 25–27. The dominant magma type is quartz-dioritic, with a tendency toward farsunditic and occasionally toward opdalitic.

Notwithstanding the large amount of mafic constituents, this rock passes occasionally into a leucocratic variety in which biotite forms less than 2.5% of the rock. Very small amounts of green hornblende may also be present. This rock should be classified as *leuco-quartzdiorite*.

The Roded Quartz-diorite is very rich in xenoliths, some of which reach large sizes. These xenoliths are darker and much more fine grained than the enclosing rocks with an average grain size of about 0.5 mm. Several rock types are present which however, grade into each other. They range in composition from quartz-free diorite to a granite rich in mafic constituents. The mineralogical composition of the extreme rock types (Rosival modal measurements) is as follows:

Diorite		Melanocratic granite	
andesine	57	quartz	14
green hornblende	31	albite with An_{08}	63
biotite	8	biotite	14
accessories, mainly		green hornblende	9
magnetite	4	accessories	tr

The chemical composition of the acid member of this rock sequence is given in Table II, No. 28. Notwithstanding the high proportion of albite in the rock, the magma-type is normalquartzdioritic, most of the calcium being contained in the hornblende.

There can be little doubt that these xenoliths represent an earlier magmatic intrusion similar to the Roded Quartz-diorite, but slightly less differentiated.

(e) *Rehav'am Quartz-diorite.* On the geological map of Eilat (Bentor and Vroman, 1955) this rock was not separated from the Eilat Granite. In the meantime S. Shiloni (1959) has shown this rock to be different from the Eilat Granite and to belong to a separate and probably earlier intrusion. The Rehav'am Quartz-diorite occurs

in relatively small outcrops in the Eilat massif between the Yotam Plain and the Shelomo Valley. Macroscopically the rock is gray, medium grained and equigranular. Under the microscope, the texture is hypidiomorphic-granular. The average rock is composed of 43 % quartz, 34 % oligoclase, 10 % orthoclase, 5 % biotite, 4 % muscovite and 4 % accessories. It is thus a *two-mica-quartz-diorite* with high amounts of quartz and very low ones of mafic minerals. Its chemical composition is given in Table II, No. 29. The magma type is leucoquartzdioritic; the alk-value is relatively low as compared with other rocks of the area of similar acidity.

(f) *Timna Granite-porphyry* (= Porphyroid granite of Slatkine and Wurzburger 1957). This very characteristic rock type occurs mainly in the central block of the Timna massif and possibly also in the northern part of the Shahmon massif. The rock is gray to reddish or orange in colour, highly porphyritic with large phenocrysts of pink perthitic microcline up to 3 cm in size, and sometimes of gray quartz, up to 1 cm in size. Phenocrysts of oligoclase, generally rimmed by microcline, are rare. The groundmass shows a granular texture, is frequently cataclastic, and consists mainly of quartz and oligoclase. Some chloritized biotite is generally, and microcline sometimes, present; rare accessory minerals are sphene, apatite, magnetite and rutile.

The chemical analyses, given in Table II, Nos. 30–34, show that these rocks belong to the calc-alkaline series, but are somewhat variable in composition. Granosyenitic, leucoquartzdioritic, natronrapakivitic, engadinitgranitic, and even aplitgranitic magma types are represented. The parameter fm is considerable and almost always above 10; k-values are low and rarely exceed 0.4.

At a few places an acid marginal facies of this *leucocratic biotite-granite-porphyry* is found. It is a fine grained leucocratic rock consisting of two crystal generations, each composed of perthitic microcline and quartz with some rare biotite in the groundmass. Plagioclase is absent. According to the analysis given in Table II, No. 35, this rock belongs to the alkaligranitaplitic magma type. It is noteworthy that many acid rock groups of the area show a sudden increase in the parameter alk in their most acid members which brings them into the alkaline sequence.

(g) *Timna Granite* (= Aplitic granite of Slatkine and Wurzburger 1957). The Timna Granite is the most widespread rock of the Timna massif and builds approximately half of its total mass. It is the dominant rock type of both the western and eastern block of the central massif, as well as of the smaller outlying outcrops.

The rock is medium grained, dark red and shows frequently small miarolitic cavities; it is very homogeneous in its different outcrops, but in some places, such as the north-eastern corner of the central massif it is finer grained and shows a microgranitic texture. Under the microscope the texture is generally equigranular and graphic intergrowth of quartz and feldspar is common. The two major constituent minerals are quartz and perthitic microcline. Some crystals of the latter contain cores of plagioclase with An₁₀. The only mafic mineral present is rare biotite which is normally chloritized. Accessory minerals are rare and include zircon and magnetite. The rock is, therefore, a leucocratic *biotite-granite*.

Chemical analyses are given in Table II, Nos. 36-41. This rock group is much more homogeneous than the Timna Granite-porphyry, although the parameter *si* varies from 267 to 525. Except in the most basic and most acid varieties the magma type is aplitgranitic throughout. *k*-values are much higher than in the granite-porphyry; they are always above 0.4 and frequently above 0.6. *mg*-values are low and the Timna granites appear in the upper left corner of the *k*-*mg*-diagram. The parameter *fm* is significantly lower than in the granite-porphyry. Again, the most acid variety of this group (analysis 41) is alkali-granitaplitic.

(h) *Eilat Granite*. The term Eilat Granite is used here in a more restricted sense than in the geological map of Eilat. The Rehavam Quartz-diorite and the Yehoshaphat Granite were included there, but are here excluded from the term. Even in this restricted sense the Eilat Granite is still the dominant igneous rock type in the Eilat massif, but does not occur outside it. Its colour varies from gray to reddish. The rock is medium to coarse grained with an average grain size of 2 to 3 mm, but individual crystals frequently reach 1 cm and more. A porphyritic texture is sometimes pronounced. The rock is very homogeneous throughout its various outcrops and weathers easily to a loose arkose, a type of weathering typical for this particular rock type. Under the microscope its texture is xenomorphic-inequigranular. Its mineralogical composition is as follows:

albite with An_{06}	40-50%	} 65-70%
orthoclase	10-25%	
microcline	5%	
quartz	20-35%	
biotite	3- 5%	
muscovite	0- 2%	
accessories (apatite, sphene, ores and secondary calcite)	tr	

Accordingly, the rock is a *leucocratic albite-two-mica-granite*.

Its chemical composition is given in Table II, No. 42. Its leucocratic character is well shown by the analysis, the magma type being natrongranitaplitic to normal-engadinitic. Chemically and mineralogically the Eilat Granite is closely related to the microcline-albite type of the Shahmon Granite, although the latter is markedly richer in silica and poorer in sodium.

(i) *Shahmon Granite*. The Shahmon Granite is the most acid rock of the Intrusive Complex. It appears in relatively small intrusions, some of them almost dike-like, within the Roded Granodiorite. The Shahmon Granite is more resistant to erosion and therefore forms most of the higher peaks of the massif. The rock is dark red and fine grained, with an average grain size of about 1 mm.

TABLE III

	microcline- albite-granite	oligoclase- microcline- quartz-monzonite	oligoclase- microcline- granite
quartz	34%	39%	33%
microcline	20%	31%	51%
albite	46%	—	—
oligoclase	—	30%	15%
accessories, incl. biotite and muscovite	tr	tr	1%

Its mineralogical composition is somewhat variable. The dominant rock type is a *microcline-albite-granite* (Table III, column 1). Its chemical composition, as given in Table II, No. 43, leads to a natronengadinitic to engadinitgranitic magma type. The value of $T = 17.4$ is very high because of the exceptionally low alkali content.

At some places the plagioclase of the rock becomes slightly more basic and is near oligoclase. At the same time, potash-feldspar increases until both plagioclase and potash-feldspar appear in about equal amounts. The mineralogical composition of this variant is given in the second column of Table III, and its chemical composition in Table II, No. 44. Mineralogically this rock is an *oligoclase-microcline-quartz-monzonite*. Its magma type, however, is aplitgranitic. As compared with the dominant rock type, si has decreased, alk and particularly k have increased; as the amount of sodium has not decreased a larger proportion of it must have entered the microcline.

Occasionally this tendency is still more pronounced until microcline largely dominates over oligoclase and the rock turns into an *oligoclase-microcline-granite*. The quantitative composition of this rock type is given in the third column of Table III.

(k) *Order of emplacement and relationships.* The Intrusive Complex contains a large variety of igneous rocks, ranging from ultrabasic to highly acid. There can be little doubt that all these rocks were emplaced during one long period of igneous intrusions, but the exact succession of their emplacement is not easily determined. Contact relationships can be observed only between rocks appearing in the same massif, and even here this evidence is frequently inconclusive. None of the major rock types has so far been found in more than one of the separate massifs, a surprising fact in view of the small size of the area. Inference on the age relationships between the rocks of the different massifs must therefore rely upon indirect evidence and general considerations, and is thus at best tentative.

The following age relationships seem to be established: in the *Eilat massif* intrusive contacts can be observed only between the Rehavam and Eilat Granites and the latter seems to be the older rock. The Eilat Gabbro and its associated ultrabasic rocks occur only as intrusive bodies within the Metamorphic Complex. For this reason, and owing to the fact that these rocks are still frequently affected by the regional metamorphism, they are likely to be the oldest igneous rocks of the Eilat massif.

In the *Shahmon massif* the Roded Quartz-diorite and its predecessor, the fine grained diorite, is clearly older than the Shahmon Granite which is intrusive into them.

In the case of the *Timna massif* relationships are more complicated. The Timna Gabbro is clearly intrusive into the granite-porphyry, and the monzonitic rock sequence is definitely younger than all the granitic rocks of Timna. This last statement is proved by the fact that the monzonitic rocks are already unaffected by Precambrian faults which dislocate all other intrusive rocks of Timna. No direct evidence is available as to the age relationship between the granite-porphyry and the Timna Granite, as these rock types come only into contact along Precambrian faults. It is, however, remarkable that the granite-porphyry is cut by many more dikes than the Timna Granite, and, while many dikes are found in both rocks, certain dike rocks, such as the pyritic quartz-porphyrates, are definitely confined to the granite-porphyry. The relative density of dikes is certainly not a criterion for the relative age of intrusive rock masses, since regional variations in the number of dikes per square unit may well have existed. If, however, as in the Timna massif, one rock type — i.e. the Granite-porphyry — comes into direct fault contact with another rock, the Timna Granite, and the former contains many times as many dikes per square unit as the granite, and moreover most of them peculiar to it, the conclusion is almost inescapable that the granite-porphyry is the older rock.

The olivine-gabbro is clearly connected with the monzonite rock sequence, which can be shown to obliterate faults of Precambrian age. If the monzonites are hybrid, they are certainly the result of the action of this gabbro magma on one of the granite rock types. But even if they result from a separate intrusion, this was closely connected with that of the gabbro magma. Olivine-gabbro and monzonites are therefore practically of the same age and thus among the youngest rocks of the Timna massif.

The age relationship between the intrusive rocks of the different massifs is obviously still less certain. On the basis of general petrological considerations the following order from older to younger rock types is suggested: Eilat Gabbro → Roded Quartz-diorite, Rehav'am Quartz-diorite → Timna Granite-porphyry → Timna Granite, Eilat Granite, Shahmon Granite → Timna Gabbro, monzonites of Timna.

B. The Older Dike Group

Dikes play an important role in the Precambrian of the Negev. Their distribution is very irregular; certain areas are almost devoid of them, while in others they appear in such numbers as almost to obliterate the country rocks.

The petrography of the dike rocks has been much less studied than that of the major intrusions. It is, however, evident that at least two major phases of dike formation must be distinguished; the first, the so-called *Older Dike Group*, is connected with the Intrusive Complex, and these dikes were formed either contemporaneously with, or immediately following, the emplacement of the various larger intrusive rock masses. The second, the so-called *Younger Dike Group*, is

connected with the Volcano-Conglomeratic Complex. A large number of dikes cannot at present be attributed with certainty to the first or second of these groups; they are classified here as *dikes of unknown (Precambrian) age*.

The dikes of the older group are frequently very irregular in form, disappear abruptly, and can rarely be followed over long distances. Those of the second group are generally straight and continue frequently over distances of several kilometers. It may be assumed that the older dikes were intruded at greater depth and possibly still under the effect of the folding movements, while the outcrops of the younger dikes correspond to a much higher level of the crust. Correspondingly, rocks of the older dikes show generally abyssal, those of the second group hypabyssal to volcanic textures. Only part of the irregularities in form exhibited by the older dikes, however, is original. These dikes were affected by two periods of tectonic dislocation, the older of which, occurring in late Precambrian time, was very intensive. The younger dikes, on the other hand, have only been affected by the Tertiary-Pleistocene taphrogenesis.

(a) *Dike rocks closely connected with the major intrusions*. Most of the rocks forming the major intrusive masses can also be found as dikes. These dike rocks are either identical with those of the major intrusions, or differ from them only by a more pronounced porphyritic texture. The following rock groups are represented among these dike rocks: *gabbro, quartz-monzonite, quartz-diorite, granodiorite, granite*. The last rock type is the most common one, particularly in the Eilat massif, where it appears in great numbers, mainly in the metamorphic schist belt near the intrusive border of the Eilat Granite. There can be no doubt that these latter dikes are genetically connected with the intrusion of the Eilat Granite; some of the dike rocks are almost indistinguishable from it, but others differ somewhat in mineralogy and chemical composition. They are richer in quartz and mica, particularly muscovite, and often carry garnet. Two analyses of these *garnet-two-mica-granites*, as given in Table II, Nos. 45-46, show the magma type to be (natron-) rapakivitic. As compared with the Eilat Granite (analysis 42), the dike rocks are richer in silica, have much higher *al*- and *fm*-values and considerably lower values of *c* and *alk*, although the parameter *k* is slightly higher. The value of $T = \text{al-alk}$ is 23.5, i.e. extremely high. For mineralogical, as well as chemical reasons, it may therefore be assumed that the magma of these dike rocks has assimilated a certain amount of schist material.

A different type of acid dike rock is represented by fine grained microgranites which are particularly abundant at Mount Yehoyahin (Eilat massif). Their chemical analysis is given in Table II, No. 47. These rocks are probably connected with the Rehav'am Quartz-diorite, from which they are chemically distinguished only by somewhat higher values of the parameter *fm*.

(b) *Pegmatites and aplites*. Two of the major intrusions, the Eilat Gabbro and the Eilat Granite, are accompanied by pegmatite dikes. The *gabbro-pegmatites* show a composition similar to the gabbro itself, but their crystals frequently reach a size of 5 cm. Of all the different granitic and related intrusions only that of the Eilat Granite

has produced pegmatites in large numbers. Individual pegmatite dikes are widely scattered, but most of them are centred in two swarms: the southern one occurs in the Metamorphic Complex south of the Shelomo Valley near the intrusive contacts of the Eilat Granite; the northern one near the northern edge of the Eilat massif. In this area the pegmatites occur partly in the surrounding mica-schists and partly within the Granite itself. Everywhere the pegmatite dikes are conspicuously concentrated within the contact zone between the Eilat Granite and the intruded Metamorphic Complex, and decrease sharply in number in both directions away from the contact. It is thus certain that the *granite-pegmatites* are genetically connected with the intrusion of the Eilat Granite. However, the occurrence of many well defined dikes within this granite itself, shows that their formation post-dates slightly its solidification.

As to their mineralogical composition, three different types of pegmatites can be distinguished:

(1) pegmatites of syenitic composition, built essentially of K-feldspar with very minor amounts of quartz;

(2) K-feldspar-quartz-pegmatites in which these two minerals occur either in large separate crystals or in graphic intergrowth; some of these pegmatites carry also considerable amounts of oligoclase;

(3) quartz-K-feldspar-mica pegmatites. This is by far the most widespread type and carries, apart from quartz and orthoclase, mainly muscovite with or without biotite. These pegmatites show a marked zonal structure with mica concentrated on the margin and quartz in the core.

Accessory minerals are rare in all pegmatites and comprise mainly hornblende, green apatite, garnet, zircon, tourmaline, rutile, columbite and beryl.

Many granitic pegmatites are closely associated with *granite-aplites*. These rocks are fine grained, with grain sizes of less than 0.5 mm, dark red in colour and composed of about 25 % quartz, 50 % oligoclase, 20 % K-feldspar and minor amounts of garnet, zircon and ore minerals. They occur frequently along the margin of the pegmatite dikes, but form also independent bodies and small veinlets cutting the Eilat Granite.

A different type of aplite is found in lenticular bodies within the Eilat Granite, mainly in the Shelomo Valley area. It is a white, sugary rock composed of quartz, orthoclase, albitic plagioclase, garnet and abundant muscovite.

(c) *Pyritic quartz-porphyrries*. These dikes occur in very large numbers cutting the Timna Granite-porphyry, but have not been found in any other country rock. They are easily recognized by their orange-red colour and by the constant presence of pyrite and other sulphides. The rock is porphyritic and carries phenocrysts of corroded perthitic microcline and quartz in a micrograined groundmass of sodium-microcline (optical determination) and quartz. Accessory minerals are abundant sulphides and rare sphene.

The chemical analysis of these rocks, given in Table II, No. 48, shows a close relationship to the Timna Granite-porphry, although the dike rocks are considerably richer in silica. The medium k-value is particularly characteristic. These dikes were therefore emplaced following the intrusion of the Timna Granite-porphry, but antedate the Timna Granite.

(d) "*Schist dikes*". A curious feature of the Precambrian in Israel is dikes of schists. These appear in large numbers in the Eilat massif and, though more rarely, in the southern part of the Shahmon massif. The rock of these dikes is greenish gray and fine grained, and shows a pronounced fine foliation. It is composed of quartz, basic plagioclase and biotite, the latter often transformed into chlorite. Schistosity is well developed and always parallel to the dike walls. The dikes vary in thickness from a few centimetres to several metres, are very straight and can often be followed for several hundred metres. They occur mainly in granite, but many of them extend from the granite into the surrounding schists of the Metamorphic Complex. The explanation of the schists as xenoliths is excluded by the form of these bodies which are always dike-like, and by the fact that they transgress the boundaries of the granite and continue into the surrounding country rocks. It must therefore be assumed that these schists were formed by the metamorphism of basic dike intrusions. As these metamorphosed dikes occur in entirely non-metamorphic intrusive rocks, the metamorphism of these basic rocks must have been brought about by relatively weak forces, too weak to affect the coarse grained acid granitic country rock.

The Volcano-Conglomeratic Complex

The Volcano-Conglomeratic Complex overlies the rocks of the two former complexes along a very pronounced unconformity. It comprises relatively small plutonic masses, partly of subvolcanic character, basic and acid extrusives, lavas as well as tephra, their dike equivalents — the Younger Dike Group — and finally the Eilat Conglomerate.

Rocks of the Volcano-Conglomeratic Complex constitute the whole of the Amram and Neshef massifs, occur in restricted areas in the Eilat and Timna massifs, but are absent from the Shahmon massif, with the exception of some dikes which should be attributed to this phase.

A. Plutonic masses

(a) *Timna Syenite*. The Timna Syenite forms a large part of the eastern block of the central Timna massif and also occurs as an isolated outcrop within the central block. The rock is coarse grained, pinkish red in colour, and very uniform in structure and composition. It shows a porphyritic texture, with phenocrysts of perthitic microcline forming more than half of the rock mass. Sometimes these crystals contain a core of oligoclase. The granular groundmass consists mainly of microcline and partly chloritized common hornblende; biotite is rare and oligoclase rare or absent; small amounts of quartz are usually present, and abundant accessory minerals

include sphene, zircon, apatite and magnetite. Accordingly, the rock should be classified as *biotite-hornblende-(quartz)-syenite*.

The chemical composition of this syenite is given in Table II, Nos. 55-57. The magma types are granosyenitic and K-nordmarkitic to K-gibelititic. The rock is slightly oversaturated, the quartz number varying from +15 to +26. k- and mg-values are very constant and similar to those of the Yehoshaphat Granite.

The Timna Syenite is attributed to the Volcano-Conglomeratic Complex, since field relationships show it to be the youngest rock of the Timna massif; since syenite dikes of similar composition cut the Eilat Granite; and — most important — because of its pronounced alkaline character.

(b) *Yehoshaphat Granite*. The Yehoshaphat Granite, which builds the northern half of Mount Yehoshaphat (Eilat massif), was not separated from the Eilat Granite by Bentor and Vroman (1955). However, as shown recently by S. Shiloni (1959), it represents a separate intrusion and differs petrographically from the Eilat Granite. The rock is gray-violet, almost devoid of mafic minerals, very dense and fine grained, with an average grain size of 0.5 to 1 mm. In contrast with the adjoining Eilat Granite which shows a typical arkosic weathering, that of the Yehoshaphat Granite is slabby. The average mineralogical composition of this rock is as follows:

quartz	25%
perthitic orthoclase	65%
albite	9%
biotite, very rare	
muscovite, and ore	1%

A typical feature of this granite is its constant cataclastic texture under the microscope.

The chemical composition is given in Table II, No. 49. The magma type is alkali-granitaplitic; the rock is typically alkaline with $T = 1.0$, and should be classified as *hololeucocratic biotite-alkali-granite*.

The Yehoshaphat Granite is attributed to the young Volcano-Conglomeratic Complex because of its alkaline character, and because it is intrusive not only into the Eilat Granite, but also cuts through dikes which are intrusive into the Eilat Granite and show close petrographic affinities with the Younger Dike Group. These contact relationships are exposed excellently on the lower north slope of Mount Yehoshaphat (N. Backler 1960).

(c) *Amram Granite-porphyry*. The Amram Granite-porphyry is well exposed in the northern part of the Amram massif. It occurs in the lower part of the section and is unconformably overlain by the lava flows of the Amram Quartz-porphyry. The rock is dark red, coarse grained and porphyritic, with phenocrysts up to 7 mm in size. The groundmass has a granular to hypidiomorphic texture. The rock is composed mainly of orthoclase and quartz, the latter in quantities rarely exceeding 10%. A small percentage of mafic minerals was originally present, but these have been

entirely transformed into chlorite or hematite. Hematite also stains heavily the orthoclase crystals and makes them almost opaque. This alteration is doubtlessly hydrothermal, a conclusion also borne out by the abundance of calcite in veinlets and nests.

Chemical analyses of the Amram Granite-porphyry are given in Table II, Nos. 50–51. The magma type varies from normalsyenitgranitic (?) to k-gibbelitic (?). Chemically, the rock is characterized by a relatively low si-parameter and high to very high fm and k-values, and clearly belongs to the alkaline suite.

In its present form, the rock is hydrothermally altered, mainly through the addition of iron-oxides. If the parameter fm is reduced to a value of 20, corresponding to that of the overlying quartz-porphyries, and the other parameters recalculated accordingly, Niggli values are obtained as shown in Table II, Nos. 50a–51a. They are practically identical with those of the Amram Quartz-porphyries, with the exception of the parameter si which is somewhat lower (compare Niggli values of No. 50a with No. 53 and No. 51a with No. 52). There can thus be no doubt that the Amram Granite-porphyry represents the subvolcanic facies of the Amram Quartz-porphyries slightly altered by subsequent volcanic activity. The position of this granite in the Volcano-Conglomeratic Complex is thus obvious.

B. Lavas, agglomerates and tuffs

(a) *Amram Quartz-porphyry and related tuffs and agglomerates.* The quartz-porphyry flows and related rocks are the most prominent member of the Volcano-Conglomeratic Complex. They build the whole of the Neshef massif extending for a long distance west across the border into Sinai; they are the most widespread rock in the Amram massif, where a thickness of more than 300 m can be observed; and they are known in smaller areas in the northern part of the Shahmon massif south of the Netafim Valley, and in the Eilat massif around the Yotam Plain.

The lava flows are superimposed upon each other and form a well layered sequence. Although the lava was very acid, the individual flows keep their thickness over long distances, the volcanism being of the plateau-lava type. The colour of the rock varies from bright green through red to violet and gray. The structure is mostly dense, but certain flows are amygdaloidal with amygdules filled mainly by chalcedony. A fluidal texture is generally well developed and certain flows are extremely rich in small xenoliths, mostly of granite. The rock is porphyritic, with sanidine and quartz as phenocrysts, usually 2 to 3 mm in size, set in a dense groundmass composed of alkali-feldspar, quartz and some ore minerals. Calcite, sericite and chlorite are secondary minerals. The texture of the groundmass is highly variable and changes from microgranular to granophyric, spherulitic, cryptocrystalline, hyalopilitic, vitreous or perlitic. The original glassy material has by now largely been devitrified.

Chemical analyses of the Amram Quartz-porphyries are given in Table II, Nos. 52–53. Although some variations can be observed in chemical composition, the magma type is always normal-alkaligranitic with high, and sometimes very high,

k-values. Except for its higher acidity the Amram Quartz-porphyry is chemically identical with the Amram Granite-porphyry.

In most of their occurrences the quartz-porphyry flows are accompanied by huge masses of *welded tuffs*. Usually these tuffs cannot be distinguished in the field from the lava flows; but under the microscope they show a well preserved pyroclastic texture. A solid unlayered mass more than 100 m in thickness in the central part of the Amram massif probably represents one continuous sequence of welded quartz-porphyry tuffs. Chemically the tuffs are very similar to the rocks of the flows, but sometimes they differ from them in the direction of still higher alkalinity, as shown by analysis 54, Table II. Leucoevitic, evisitic-pantelleritic, and evisitic-groruditic magma types are not uncommon, always distinguished by extremely high k-values of about 0.8.

Eruptive centres of this phase have been found at various places, generally surrounded by lava flows, non-welded tuffs and agglomerates. Usually they are accompanied by sedimentary conglomerates composed of fragments of various older igneous or metamorphic rocks cemented by tuffs.

(b) *Spilites, basalts and associated rocks.* Basic lava flows occur at several places, and particularly in the central Eilat massif, where they overlie the Eilat Granite and underlie the Eilat Conglomerate, and in the north-central part of the Shahmon massif overlying the Roded Quartz-diorite. At the latter location they reach a thickness of at least 30 m and are associated with lithic, vitric and crystal tuffs, as well as with conglomerates of fluvial origin. Feeder-dikes of these volcanics have been found west of the Yotam Plain, where they cut the Eilat Granite.

Most of these flows are spilitic in character. They are gray-green and weather into small cuboidal fragments. They are fine grained to aphanitic and sometimes contain xenoliths, mainly of granite. The rock carries rare phenocrysts of olivine and albite, the former largely transformed into chlorite and iddingsite. The ground-mass is ophitic and fluidal, and consists mainly of albite, intersertal chlorite and abundant ore. The chemical analysis of these spilites is given in Table II, No. 58.

Chemically these rocks are more akin to hornblende-trachy-basalts, such as those of the Dunedin district, New Zealand, or to the oligoclase-andesites of Hawaii than to true spilites, owing to their relatively high al- and k-values.

The rock is alkaline in character, the magma type being essexitakeritic.

These spilites are frequently associated with normal basalts and basalt tuffs mainly composed of pyroxene and labradorite. Some of the associated tuffs are intermediate in character and carry small amounts of quartz.

C. The Young Dike Group

A very large number of dikes of the Volcano-Conglomeratic Complex, the so-called "Young Dike Group", cut all other Precambrian rocks of the area. Normally, they are distinguished by their sharp contact with the country rocks and their straight and

continuous course, extending in some instances for more than 10 km. In general, the acid dikes have a strong positive morphological relief, while the basic ones form narrow depressional channels. The petrography of these dikes has been studied much less than that of the other rocks, and therefore, only a general outline can be given here. The major rock types present are: albite-diabase, trachyandesite, microdiorite, micromonzonite, quartz-porphyrity, microsyenite, microgranite and quartz-porphyrity. Of these, the first and last mentioned are by far the most widespread. Frequently two different rocks occur together in composite dikes. Chemically all these dike rocks — with the exception of the latest quartz-porphyrities — are markedly alkaline.

(a) *Albite-diabase*. Albite-diabases form the youngest Precambrian dikes. They are dark green to gray, dense, show very rare small phenocrysts, and are mostly weathered, with the exception of the chilled border zones which are dark gray and fresh. The rock is composed mainly of albite and pyroxene, the latter usually transformed into chlorite. Occasionally, some orthoclase is present, and apatite and ore minerals are abundant, as is secondary calcite. The chemical composition is given in Table II, No. 59. The magma type is lamprosommatitic to mugearitic. Although in general this composition is typical for albite-diabase, the parameter k is rather high, a fact which accounts for the occasional occurrence of some orthoclase in the rock.

Chemically, this albite-diabase is clearly different from the rock of the earlier spilite flows, the latter being clearly more acid, richer in alumina and alkalies, poorer in iron and magnesium, and definitely more sodic.

(b) *Intermediate rocks*. Intermediate rocks range from *trachy-andesites* to *microdiorites*, *quartz-porphyrities*, *porphyrites*, *micromonzonites* to *microsyenites* and *porphyrites*. These rocks are generally porphyritic; their feldspar is mainly andesine, occasionally oligoclase, and is accompanied in the more acid types by orthoclase. Among the mafic minerals augite and brown and green hornblende are prominent. In some of the acid types quartz is present in the groundmass. The texture is inequigranular, hypidiomorphic, and some rocks show a vesicular structure, the amygdulæ being filled by calcite, quartz, chalcedony or chlorite. The chemical composition of a *porphyrite* composed of acid andesine, augite, brown and green hornblende, much penninite and small amounts of quartz is given in Table II, No. 60. The magma type is monzonite-dioritic and clearly belongs to the potassic suite. A slightly more acid type is exemplified by the analysis given in Table II, No. 61. This rock is much less alkaline, the magma type being almost normal-quartzdioritic.

(c) *Quartz-porphyrities*. Quartz-porphyrity dikes are very abundant and constitute some of the most persistent dikes of the area. They may reach some tens of metres in width and several kilometres in length. The rock is a deep red, its texture is porphyritic with — sometimes very abundant — phenocrysts mainly of oligoclase and quartz in a groundmass, which was either originally vitreous or consists of an aggregate of quartz, oligoclase, orthoclase and sometimes biotite. A fluidal texture

is normally pronounced and some of the dikes show along their margin typical magmatic rolls (Tomkeieff 1946). Chemically two types can be distinguished: the composition of the first, and older group, is shown in Table II, No. 62; this type which can be correlated with the Amram Quartz-porphyry flows is alkaline with magma types ranging from K-gibellitic to si-syenitgranitic. The second, and younger type, (Table II, Nos. 63–64) is calc-alkaline with an engadinitgranitic magma type. The second group is higher in silica and alumina and characteristically lower in iron and alkalis.

These latter dikes do not fit into the differentiation diagram and have been omitted from figures 5 and 6.

D. Eilat Conglomerate

The Eilat Conglomerate, which corresponds to the Saramuj Series of L. Picard (1941), builds an area of about 4 km² in the north-central part of the Eilat massif, overlying either the Eilat Granite or spilite and quartz-porphyry flows. Its maximum preserved thickness exceeds 400 m. Among its rock fragments every Precambrian rock, metamorphic, plutonic and volcanic, including spilites and quartz-porphyrines, can be found. These rock fragments vary in size from less than 1 mm to blocks of several m³ without any sorting, with an average diameter estimated at about 7 cm. Some of the fragments are well rounded, but most are rather angular, and no trace of bedding can be observed.

An interesting feature of this conglomerate is the nature of its cementing material, which accounts for about 10% of the total rock mass and is locally individualised in irregular stringers and veinlets. This material is an originally glassy, volcanic rock which, according to chemical composition, should be designated as *lujavrite-obsidian*. Its colour varies in different shades of brown, and under the microscope it shows a well marked fluidal texture. The chemical analysis of this lava is given in Table II, No. 65. It is the most alkaline of all Precambrian rocks; its magma type is normalnatronsyenitic, with a strong tendency toward tavitic and normallujavritic magmas. In fact, the parameter alk exceeds al by 6.9 units. This magma seems to represent a differentiate of that which produced the slightly earlier spilite flows. Generally present only as cementing material, the obsidian becomes individualized locally in small and irregular veins and tongues within the conglomerate. The cementation of the conglomerate by this volcanic rock is so strong that its erosional relief is in no way different from the adjoining areas built of Eilat Granite. The conglomerate itself is cut by a large number of young Precambrian diabase and quartz-porphyry dikes.

E. Chronology of the Volcano-Conglomeratic Complex

The dissection of the Precambrian basement by contemporaneous and subsequent faulting, and the limited amount of work done up to the present time prevent the establishment of the exact order of events by which the Volcano-Conglomeratic Complex was built. The following chronological sequence, however, seems reason-

able: the oldest rocks of the complex are the spilite flows, which in any event underlie the Eilat Conglomerate. Their eruption was followed by the emplacement of microgranular intermediate dike rocks, as established by the fact that these have nowhere been found cutting the conglomerate. The next phase consisted of the eruption of the alkaline quartz-porphyry flows and the emplacement of the related subvolcanic Amram Granite-porphyry. The intrusion farther south of the alkaline Yehoshaphat Granite and its dike sequence of micro-granites probably occurred at about the same time. Thereafter, the Eilat Conglomerate accumulated and was percolated and cemented by the lujavritic lavas. This was followed by the intrusion of the non-alkaline quartz-porphyry dikes which cut the conglomerate in the south and the alkaline Amram Quartz-porphyry flows farther north. Shortly before the end of this phase and in connection with the large-scale tectonic break-up of the area, the emplacement of the albite-diabase dikes took place. This relationship is attested to by the fact that in most cases the young quartz-porphyry dikes are cut by those of albite-diabase, while in a few cases the reverse relationship has been found. Albite-diabase dikes, moreover, frequently follow Precambrian fault lines. Shortly afterwards, hydrothermal solutions ascended along these lines, bringing about their mineralization.

Although many overlaps and occasional recurrences can be observed, the general picture is that of one large volcanic cycle starting with the basic alkaline spilites and progressing with diminishing alkalinity through intermediate to acid volcanism with, at the end, a final reversal to the basic alkaline albite-diabase magma.

There is no evidence available to ascertain during what part of these events the emplacement of the Timna Syenite took place, but it happened probably early in this volcanic cycle.

APPENDIX

Dikes of doubtful (Precambrian) age

Many dikes, found in areas where only the Intrusive Complex is present, cannot be dated accurately. Those which show a close chemical and mineralogical relationship with dikes dated elsewhere do not present a problem. There are, however, some rocks, all of them basic, occurring only as dikes or small dike-like bodies within rocks of the Intrusive Complex, particularly in the Timna massif, which cannot be related to any of the dated rocks. These are briefly described in the following.

(a) *Olivine-dolerite*. Rocks of doleritic character occur in a dike-like (?) small intrusion in the Timna massif, cutting the Timna Granite. The rock is dark greenish and under the microscope has an ophitic texture. It is composed of labradorite with An_{50-66} , titaniferous augite frequently transformed into bastite, olivine generally altered to serpentine and magnetite, and rare chloritized biotite. Magnetite is an abundant, apatite a fairly frequent, accessory mineral.

Two chemical analyses of these rocks are given in Table II, Nos. 66-67. The magma types are normalgabbroidic to melagabbroidioritic, with slight essexit-

gabbroidic tendencies. These rocks could be related to the intrusion of the Timna Gabbro.

(b) *Trachy-andesite* (Andesites of Slatkine and Wurzbürger 1957). These rocks appear in a large number of thin dikes in all parts of the Timna massif. Their colour varies from brown to violet-brown and blackish gray. They are porphyritic, with phenocrysts of potassic-feldspar and plagioclase, the latter sometimes oligoclase and sometimes andesine. The groundmass is pilotaxitic and consists of feldspar cemented by intergranular chlorite. Accessory minerals are magnetite and ilmenite, secondary minerals epidote and calcite.

The chemical composition of these rocks is given in Table II, Nos. 68–69. The magma types are melaquartzdioritic to melanatronsyenitic. They combine high fm-values with extremely low ones of c. These rocks are younger than all the intrusive country rocks of Timna and even cut some of the quartz-porphyry dikes. They do not seem to be related to any of the better known Precambrian rocks.

Except for the exceptionally low c-values, these trachy-andesites can be fitted into the differentiation diagram of the Volcano-Conglomeratic Complex (Figure 5), and may therefore chronologically belong to it, and more particularly to the stage of the porphyrite dikes (cf. analysis 61).

(c) *Biotite-hornblende-meladiorite* ("Green-rock" of Slatkine and Wurzbürger 1957). In the central part of the Timna massif a small irregular intrusion is found, some 15 m in maximum width, composed of a green holocrystalline rock, containing idiomorphic andesine with An_{46} . The mafic minerals which form more than half of the total rock mass are mainly hornblende, generally with a core of biotite. Accessory minerals are abundant apatite, as well as magnetite and ilmenite. The chemical analysis is given in Table II, No. 70; its magma type is al-hornblenditic with a rather high si-value. This basic to ultrabasic rock, which should be termed *biotite-hornblende-meladiorite*, has no affinities, neither mineralogically nor chemically, with any other Precambrian rock. All that can be said about its age is that it is younger than the Timna Granite-porphyry into which it is intrusive.

(d) *Lamprophyre* (?) ("Aphanitic brown rock, andesite?" of Slatkine and Wurzbürger 1957). These rocks are dark brown, hard and compact, and have a porphyritic texture. Their mineralogical composition is difficult to determine because of a generally advanced stage of weathering. They carry phenocrysts of idiomorphic feldspar which is, at least partly, alkali-feldspar, and is considerably replaced by calcite. The groundmass is either hyalopilitic and made up of abundant feldspar microlites, in a glassy strongly calcitized matrix, or pilotaxitic and composed of feldspar and chlorite. Accessory minerals are abundant magnetite and ilmenite with some apatite. Secondary minerals are calcite, epidote and hematite. The chemical analyses are given in Table II, Nos. 71–72. The Niggli values, calculated after correction of CaO for calcite, give lamprosyenitic to lamprosommaitic magma types. This composition is similar to that of the latest albite-diorite dikes; a genetic link, however, is excluded by the very high-k value. Chemically, the rocks

resemble a lamprophyre, described by Michel-Lévy (Niggli 1923) from Charmes, Morvan. They are possibly *lamprophyric differentiates* of either the Timna Granite-porphry or the Timna Granite. They are younger than the meladiorite described above, which in turn is younger than the Timna Granite-porphry.

REMARKS ON THE FAULT HISTORY OF THE PRECAMBRIAN AREA IN THE SOUTHERN NEGEV

The Precambrian area in southern Israel has been strongly affected by the mid-Tertiary and younger phase of faulting which led, among others, to the formation of the Jordan-Arava Rift Valley system. In many places strata as young as Lower Eocene are faulted against Precambrian rocks, and even faults of Pleistocene age can be observed within the young Rift Valley fill.

On the other hand, the geological map of Eilat (Bentor and Vroman 1955) shows a number of faults of demonstrably Precambrian age. Detailed work carried out in the meantime by M. Ayal in the Eilat massif has shown this Precambrian faulting to be much more developed than had been supposed earlier. In fact, a very large number of Precambrian faults cut through all parts of the basement complex. They are characterized by intensive mylonitization extending frequently more than 20 m away from the actual fault zone. The age of some of the faults can be dated approximately. Two large faults in the central Timna massif are transgressed and obliterated by the Timna monzonite rock sequence. Their formation must, therefore, antedate the final stages of the emplacement of the Intrusive Complex. The same faults are also cut by some of the late Precambrian albite-diorite dikes (oral communication, U. Wurzbacher), although most of the dikes connected with the Intrusive Complex end abruptly against the fault planes.

The Precambrian age of many other faults is shown by the fact that the late Precambrian hydrothermal mineralizing solutions used them as channel ways. This mineralization is definitely of Precambrian age, as in no case does it cross the unconformity separating the Precambrian complex from the overlying "Nubian" sandstone sequence, the lower members of which are dated by fossil evidence as Lower Cambrian. It is, therefore, surprising that many of these old faults contain within the fault zone narrow, but long and continuous, remnants of squeezed-in Nubian sandstones of Paleozoic, and probably also Mesozoic age, and this even in areas from which the Nubian cover has long since been removed by erosion. The obvious conclusion is that these old faults were subsequently rejuvenated and were active again, in any case during the young Tertiary to Pleistocene faulting period, but probably also repeatedly between Cambrian and Tertiary time.

The faulting history of the Precambrian basement area can thus be summarized as follows: faulting started at the latest during the later part of the period in which the Intrusive Complex was emplaced. It increased in severity during the build-up of the Volcano-Conglomeratic Complex, and particularly in its final stages in which the albite-diorite dikes were emplaced. These faults were rejuvenated at the latest

in mid-Tertiary time, during the taphrogenetic phase of the Rift Valley. At this time, a large number of new faults, first of the tensional and later of the compressional type were formed (see also Bentor and Vioman 1960).

THE MAGMATIC HISTORY OF THE ISRAEL PRECAMBRIAN

The oldest Precambrian rocks are a thick geosynclinal sequence of mainly shaly, partly sandy and rarely calcareous sediments. Their deposition was accompanied by basic to ultrabasic geosynclinal magmatism (amphibolites). This rock sequence was folded and metamorphosed during the following orogenic cycle. Concentrically arranged metamorphic zones from the biotite-garnet to the sericite-chlorite stage can still be recognized. Late in this orogenic cycle large-scale intrusive activity of typically calc-alkaline character took place (Intrusive Complex), starting with basic rock types (Eilat Gabbro) and trending successively towards more acid types (Roded Granite). Some of these intrusions probably caused surface volcanism, as shown by the pyritic quartz-porphyry dikes of Timna, genetically related to the Timna Granite-porphyry, and by the schist-dikes of the Eilat massif, representing, now metamorphosed, basic subvolcanic intrusions. During the later part of this cycle, folding was accompanied by faulting. The final magmatic intrusions were again basic (Timna Gabbro), but chemically different from the initial basic magmatism. The monzonitic rock sequence of Timna may have resulted from the hybridizing influence of this late-orogenic gabbro on earlier granites. The superheat needed can be explained by the assumption that this recurrence to basic magmatism was already connected with late-orogenic deep-seated faulting.

Following the folding phase, the area was uplifted and dissected by tensional faults. These movements led to large-scale erosion which uncovered part of the central intrusive bodies. Thereafter, magmatic activity was renewed, but from now onward it is characterized by strongly alkaline affinities. The first eruptions were basic (spilite flows and associated basalts), but magmatic evolution again ran the whole course toward acid end-members (Amram Quartz-porphyry). Most of the intermediate types survive only in subvolcanic dikes, but acid lava flows are still preserved in considerable thickness. Post-kinematic plutonic intrusions of the same period are represented by the Timna Syenite, the Amram Granite-porphyry, and the Yehoshaphat Granite.

In the large basins huge thicknesses of mountain waste (molasse) accumulated, which were quickly transformed through impregnation with an extremely viscous, highly alkaline, lujavritic lava into the volcano-sedimentary Eilat Conglomerate.

Volcanism of the acid type continued, although with diminishing alkalinity (younger quartz-porphyries). A final phase of intense faulting led to the concluding phase of alkaline volcanism, which is again basic (albite-diabase dikes). The immediately following phase of hydrothermal mineralization constitutes the end of the magmatic history of this area which has never since been renewed, not even

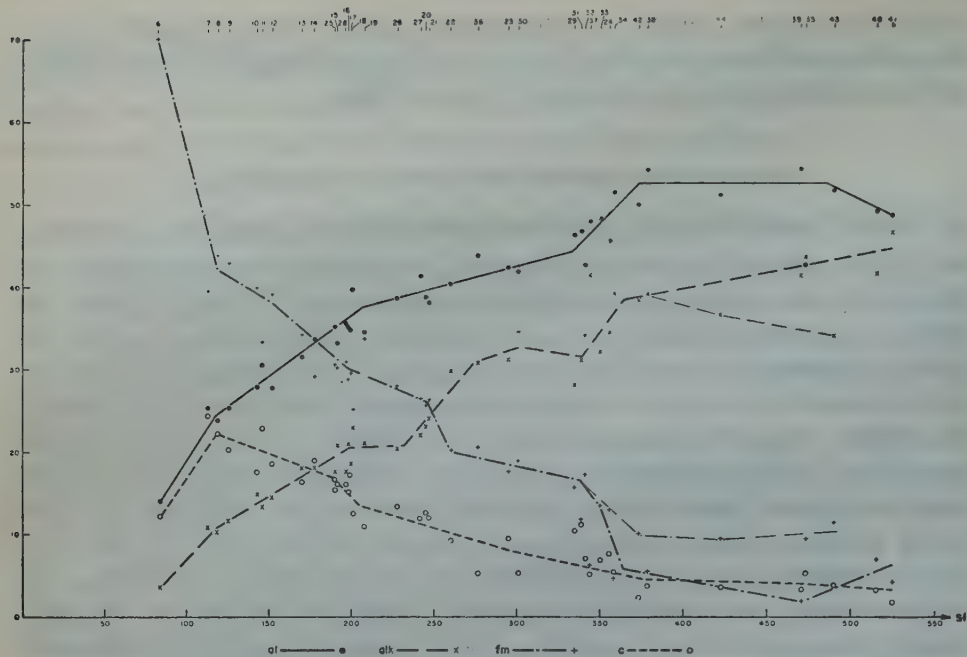


Figure 3
Differentiation diagram of rocks of the Intrusive Complex

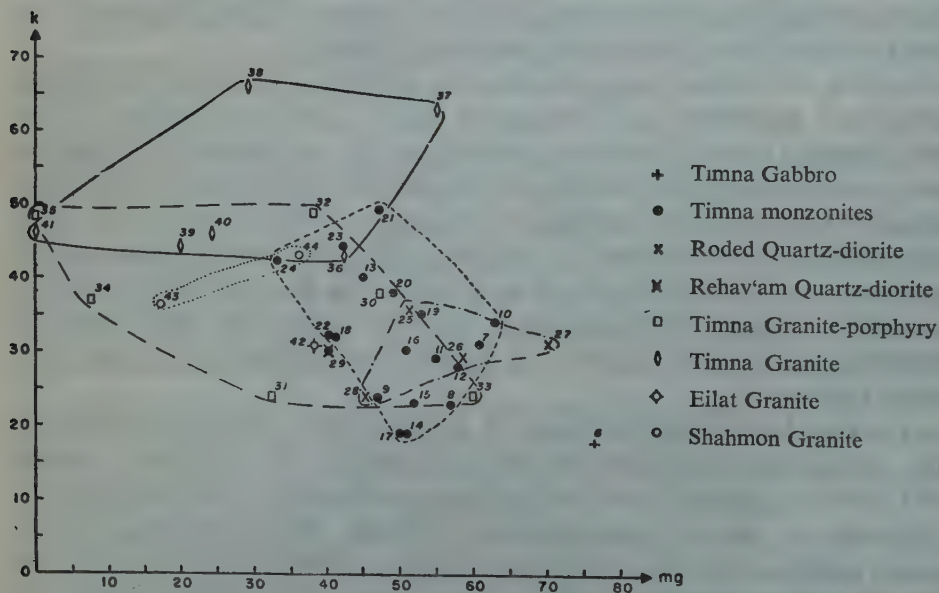
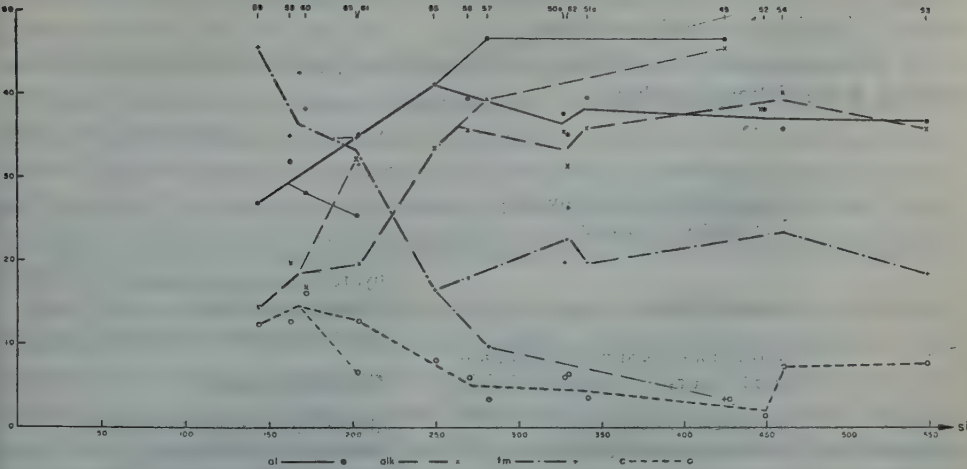


Figure 4
k-mg-diagram of rocks of the Intrusive Complex



Figures 5
Differentiation Diagram of the rocks of the Volcano-Conglomeratic Complex

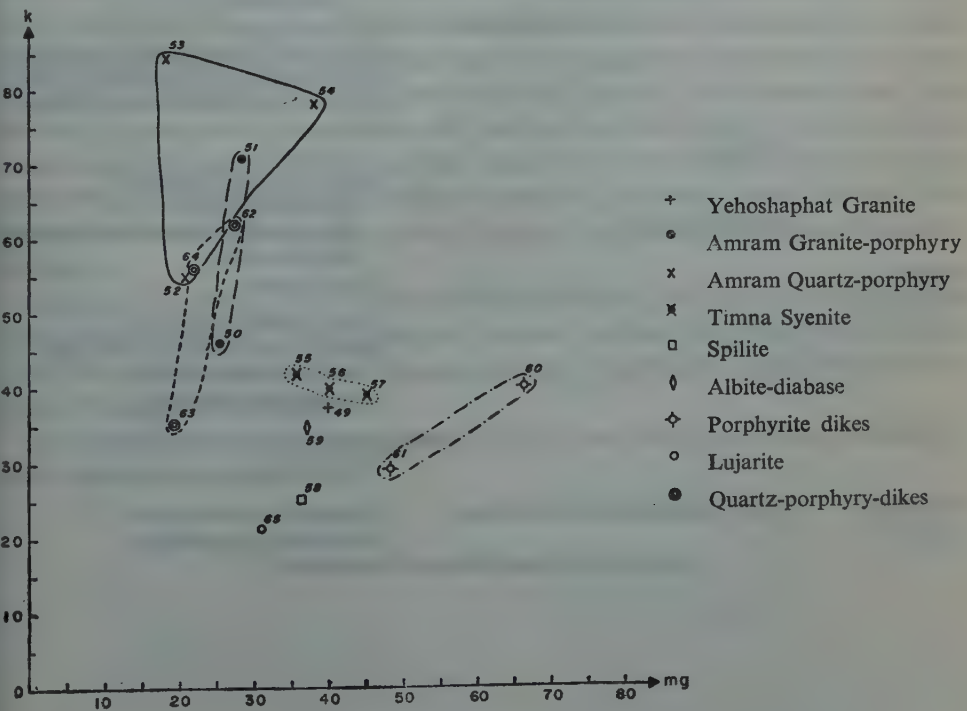


Figure 6
k-mg-Diagram of the rocks of the Volcano-Conglomeratic Complex

during the intensive faulting accompanying the break-down of the Rifi Valley system in Tertiary to Pleistocene time.

The tecto-magmatic development of the area during the Precambrian is summarized in the following table:

	Deposition of early Cambrian fluvatile sediments	
		erosion
	intense faulting	hydrothermal mineralization albite-diabase dikes calc-alkaline quartz-porphyry dikes
	erosion and clastic sedimentation; continuation of volcanic activity	Eilat Conglomerate
Volcano- Conglomeratic Complex	large-scale volcanism, some hypabyssal intrusions	alkaline quartz-porphyry dikes, Amram Quartz-porphyry intermediate dikes spilite flows, tuffs and agglomerates
		intrusions of Yehoshaphat Granite Amram Granite-porphyry Timna Syenite
		uplift, faulting and erosion
		Intrusion of Timna Gabbro and form- ation of monzonite sequence of Timna. Dike intrusions (pyritic quartz-porphy- ries)
	faulting	phase of granitic intrusions: Shahmon Granite Eilat Granite followed by pegmatite and aplite dikes
	end of folding	Timna Granite
Intrusive Complex		Timna Granite-porphyry phase of quartz-dioritic intrusions: Rehav'am Quartz-diorite Roded Quartz-diorite
		basic intrusions: Eilat Gabbro
Metamorphic Complex	Intense folding and metamorphism	Formation of mica-schists, Taba Gneiss, amphibolites
	geosynclinal sedimentation and magmatism	

The differentiation diagram of the rocks composing the Intrusive Complex is given in Figure 3, the corresponding mg-k-diagram in Figure 4. The diagrams, based on 39 analyses, represent a typical calc-alkaline province with iscfaly at 178. Even in the acid rocks the parameter al exceeds alk by about 10 units. At a si-value of about 360, differentiation splits into two trends. In the main trend, best represented by the Timna Granite, alk increases with increasing si, fm-values are similar to c and very low. The other trend, represented mainly by the Shahmon Granites, shows alk-values which decrease with increasing si, while the parameter fm is conspicuously higher than c.

The differentiation diagram of the igneous rocks of the Volcano-Conglomeratic Complex is given in Figure 5, the corresponding mg-k-diagram in Figure 6. These diagrams are much less clear, partly since they are based on 16 analyses only, but mainly because most of the analyses belong to dike rocks which show locally a much more pronounced chemical variability. Nevertheless, the differences from the diagrams of Figures 3 and 4 are obvious. This is a typically alkaline sequence with isofaly at 200; extreme values of the parameters are reached already at si-values of about 280, and from here toward the acid end the curves are almost horizontal. Again, the acid part of the diagram shows two differentiation trends which separate from each other at an si-value of about 250. The main trend starts with the average type of the Timna Syenite and leads to the Amram Granite-porphyry and the related Amram Quartz-porphyry. The al and alk curves practically coincide and in some instances T is negative; fm-values are around 20, i.e. very high for acid rocks, and at least 10 units higher than for equally acid rocks of the Intrusive Complex. The minor trend branches off with the acid members of the Timna Syenite and leads to the Yehoshaphat Granite and possibly onward to the latest quartz-porphyry dike rocks. Compared with the main trend the minor one is less alkaline and has low fm-values.

The lujavritic magma, at the basic end of the diagram, does not fit into the general differentiation scheme. It represents an extreme increase in alkalies with a sharp drop in the al- and c-values. This magma, therefore, represents a local differentiation trend of hyperalkaline character.

The detailed petrological consequences to be drawn from these data are reserved for a separate paper.

Niggli Values*

	1	2	3	4	5	6	7	8	9	10	11	12	13
si	231.5	318.4	337.9	477.4	85.0	83.6	114.3	118.4	125.4	142.6	145.5	151.7	170.0
al	41.0	48.4	41.6	47.1	13.7	14.1	25.4	23.8	25.3	27.8	30.5	27.7	31.5
fm	36.8	21.3	13.9	12.5	56.3	69.8	39.4	43.7	42.9	39.8	33.3	39.3	34.1
c	8.4	5.8	11.6	1.5	26.3	12.4	24.3	22.2	20.2	17.5	22.8	18.5	16.3
alk	13.8	24.5	32.9	38.9	3.7	3.7	10.9	10.3	11.6	14.9	13.4	14.5	18.1
k	0.34	0.21	0.54	0.45	0.35	0.18	0.31	0.23	0.24	0.34	0.29	0.28	0.40
mg	0.40	0.48	0.50	0.30	0.57	0.76	0.61	0.57	0.47	0.63	0.55	0.58	0.45
ti	4.9	0.3	0.9	1.9	6.5	2.4	2.1	3.4	5.6	1.8	2.4	3.0	3.7
p	0.2		0.3	0.0	0.2	0.2	0.0	0.7	0.3	0.2	1.0	0.3	0.7
qz	+76.3	+120.4	+106.3	+221.8	-29.8	-31.2	-29.3	-22.8	-21.0	-17.0	-8.1	-6.3	-2.4

* All values are calculated after correction of CaO for calcite.

1. Garnetiferous mica-schist 1424/8812, No. E.P. 763; analyst: Gaon.
2. Taba Gneiss, Shahmon massif 14160/88835, No. T.V. 53; analyst: Bodenheimer-Heizler.
3. Taba Gneiss, Southern Eilat massif, 1409/8822, No. B.T. 815-M 1; analyst: Bodenheimer-Gaon.
4. Taba Gneiss, Northern Eilat massif, 1427/8872, No. E.P. 744; analyst: Gaon.
5. Amphibolite, Southern Shahmon massif, 1421/8891, No. T.V.L. 9; analyst: Bodenheimer-Vogel.
6. Timna Gabbro, central block of

- Timna massif, 1476/9101, No. S.W. 196; analyst: Bodenheimer-Heizler. (Slatkine-Wurzbarger, 1957).
7. basic gabbro-diorite, Timna massif, 1478/9098, No. B.T. 3127, analyst: Bodenheimer-Gaon.
8. gabbro-diorite, Timna, 1486/9087, No. B.T. 3073, analyst: Gaon. (Slatkine-Wurzbarger, 1957).
9. gabbro-diorite, Timna, No. S.W. 600; analyst: Gaon. (Slatkine-Wurzbarger, 1957).
10. gabbro-diorite, Timna massif, 1494/9089, No. B.T. 3085; analyst: Gaon.
11. gabbro-diorite, Timna massif, 1477/

- 9097, No. S.W. 56; analyst: Gaon. (Slatkine-Wurzbarger, 1957).
12. diorite, Timna massif, 1495/9088, No. B.T. 3104; analyst: Gaon.

13. monzonite, Timna massif, 1489/9084, No. B.T. 3101; analyst: Gaon. (Slatkine-Wurzbarger, 1957).

Magma Type

1. —
2. natron-rapakivitic ? (T very high)
3. engadinitic to yosemitic
4. engadinitic
5. hornblende to isitic
6. hornblende to hornblende-peridotitic
7. orbic to leucompharitic
8. normalgabbrodioritic
9. normalgabbrodioritic
10. lamprophyritic (c low) to monzonitic (c low)
11. normaldioritic
12. lamprophyritic (c low)
13. si-monzonitic

TABLE II (continued)
Chemical Analyses

	14	15	16	17	18	19	20	21	22	23	24	25	26	27
SiO ₂	57.63	58.20	59.45	59.49	57.98	60.16	63.19	63.49	63.89	66.99	70.20	57.36	62.09	63.55
Al ₂ O ₃	18.58	17.74	17.82	17.72	19.50	16.86	16.91	16.52	16.89	16.20	15.23	17.83	17.73	18.27
Fe ₂ O ₃	2.89	3.15	2.88	2.70	3.01	3.55	2.20	2.45	2.54	1.83	1.37	2.50	1.80	—
FeO	3.01	2.55	2.45	2.80	2.34	2.20	1.94	2.06	0.86	1.16	0.72	3.09	2.15	2.54
MgO	3.16	3.16	2.91	2.96	1.97	3.48	2.18	2.12	1.38	1.14	0.58	3.13	3.00	3.20
CaO	5.73	4.54	4.26	4.79	3.63	2.88	3.03	2.83	2.15	2.00	1.41	4.34	3.36	3.64
Na ₂ O	4.90	5.04	4.54	4.72	4.70	4.12	3.86	3.32	5.16	4.05	4.01	3.83	4.00	4.13
K ₂ O	1.77	2.32	2.94	1.67	3.34	3.44	3.65	4.71	3.70	4.87	4.55	3.28	2.50	2.70
TiO ₂	1.26	1.14	0.98	1.30	1.33	1.74	0.92	1.02	0.67	0.63	0.50	1.20	0.92	1.33
P ₂ O ₅	—	0.45	0.40	0.37	0.39	0.36	0.22	0.27	0.41	—	—	—	—	—
MnO	0.12	0.09	0.10	0.07	0.10	0.10	0.08	0.10	0.39	0.04	0.05	—	—	—
CO ₂	—	—	—	—	0.23	—	—	—	—	—	—	—	0.08	0.18
Cl	0.23	—	—	—	—	—	—	—	0.07	—	0.20	—	—	—
SO ₃	0.10	—	—	—	—	—	—	—	—	—	—	—	—	—
H ₂ O—	0.03	0.15	0.31	0.41	0.17	0.19	0.24	0.20	0.40	0.21	0.16	tr.	0.25	—
H ₂ O+	1.28	1.29	0.99	0.90	0.90	1.19	1.40	1.14	1.59	0.96	0.05	0.26	0.36	0.13
Total	100.69	99.82	100.03	99.90	99.59	100.27	99.82	100.23	100.10	100.08	99.60	99.90	99.20	100.59
O corr. for Cl	—0.05	—	—	—	—	—	—	—	—	—	O corr. for Cl	—0.05	—	—
100.64	—	—	—	—	—	—	—	—	—	—	99.55	—	—	—

TABLE II(continued)
Chemical Analyses

	28	29	30	31	32	33	34	35	36	37	38	39	40	41
SiO ₂	58.55	69.79	67.31	70.63	69.62	71.10	69.48	75.78	64.32	68.41	70.05	75.98	77.29	77.19
Al ₂ O ₃	17.81	16.28	15.83	16.37	14.69	16.48	16.76	11.49	17.88	16.11	16.93	14.80	12.42	12.00
Fe ₂ O ₃	2.94	0.95	2.83	1.26	1.80	0.85	0.95	1.66	2.47	0.64	1.00	0.33	0.94	0.77
FeO	3.45	1.43	—	0.85	0.97	0.61	0.14	0.21	1.06	—	—	—	0.07	—
MgO	2.76	0.89	1.34	0.51	0.90	1.08	0.04	tr.	1.39	0.45	0.20	0.05	0.16	—
CaO	4.62	2.21	1.04	2.11	1.25	1.29	1.28	0.79	1.16	0.94	0.28	0.51	0.47	0.19
Na ₂ O	4.00	4.17	4.93	5.02	3.67	5.08	4.89	3.71	4.33	3.09	2.56	3.85	3.48	3.81
K ₂ O	2.00	2.76	4.60	2.39	5.33	2.42	4.40	5.18	5.00	8.07	7.38	4.47	4.38	4.93
TiO ₂	1.00	0.20	0.50	0.61	0.51	0.57	0.51	0.56	0.77	0.43	0.16	—	0.14	0.12
P ₂ O ₅	—	0.10	0.16	0.10	0.42	tr.	tr.	tr.	0.13	0.23	tr.	—	—	—
MnO	—	0.04	0.07	0.03	0.04	tr.	0.03	tr.	0.06	0.07	0.02	tr.	0.04	tr.
CO ₂	0.15	0.15	—	—	—	—	0.25	—	—	—	—	—	—	—
Cl	0.37	—	—	—	—	—	—	—	0.18	—	—	—	—	—
SO ₃	tr.	—	—	—	—	—	—	—	0.17	—	—	—	—	—
H ₂ O—	0.34	0.22	0.31	0.23	0.27	0.02	0.23	—	0.41	0.28	0.43	0.05	0.03	—
H ₂ O+	1.71	0.69	1.13	0.46	0.88	1.08	0.94	1.06	1.39	0.55	1.20	0.13	0.15	0.28
Total	99.70	99.88	100.05	100.57	100.35	100.58	99.90	100.44	100.72	99.27	100.21	100.60	100.01	100.01
								O corr.	O corr.			O corr.		
								for Cl	for Cl			for Cl		
								—0.04	—0.04			—0.01		
								100.68	100.68			100.59		

	28	29	30	31	32	33	34	35	36	37	38	39	40	41
si	198.0	335.2	300.8	339.2	342.2	350.6	358.5	473.0	266.7	344.4	378.9	470.6	515.2	524.9
al	35.5	46.1	41.5	46.4	42.5	47.9	51.1	42.3	43.5	47.7	53.9	53.9	48.8	48.2
fm	31.0	15.6	18.8	11.8	17.1	13.3	4.6	9.4	20.7	6.1	5.5	1.9	6.8	4.1
c	16.0	10.4	5.1	11.0	6.5	6.8	5.3	5.2	5.2	5.1	1.6	3.3	3.2	1.6
alk	17.5	27.9	34.6	30.8	33.9	32.0	39.0	43.1	30.6	41.1	39.0	40.9	41.2	46.1
k	0.24	0.31	0.38	0.24	0.49	0.24	0.37	0.48	0.43	0.63	0.66	0.44	0.46	0.46
mg	0.45	0.41	0.47	0.32	0.38	0.60	0.07	0.00	0.42	0.55	0.29	0.20	0.24	0.00
ti	2.6	0.9	1.6	2.3	1.8	2.1	1.9	2.6	2.5	1.5	0.7	0.0	0.8	0.4
p	0.3	0.3	0.3	0.9	0.9	0.0	0.0	0.0	0.2	0.3	0.0	0.0	0.0	0.0
qz	+28.0	+123.6	+62.4	+116.0	+106.6	+122.6	+102.5	+200.6	+44.3	+80.0	+122.9	+207.0	+250.4	+240.5
28.	Melanocratic granite, Shahmon massif, 1423/8903, No. T.V. 71; analyst: Bodenheimer-Heizler.			Tinna Granite-porphyr, Timna massif, 1486/9094, No. S.W. 55; analyst: Bodenheimer-Heizler (Slatkine-Wurzbürger, 1957).				burger, 1957).			Gaon.			
29.	Rehav'am Quartz-diorite, Ellat massif, 1409/8855, No. B.S. 258; analyst: Gaon.			Tinna Granite-porphyr, Timna massif, 1485/9093, No. S.W. 261; analyst: Gaon. (Slatkine-Wurzbürger, 1957).				38. Tinna Granite, Timna massif, 1476/9079, No. B.T. 3044; analyst: Bodenheimer-Gaon.(Slatkine-Wurzbürger, 1957).			40. Tinna Granite, Timna massif, 1477/9112, No. B.T. 3089; analyst: Gaon.			
30.	Tinna Granite-porphyr, Timna massif, 1485/9087, No. B.T. 3065; analyst: Gaon. (Slatkine-Wurzbürger, 1957).			Tinna Granite-porphyr, Timna massif, 1490/9095, No. S.W. 58; analyst: Bodenheimer-Heizler. (Zlatkine-Wurzbürger, 1957).				39. Tinna Granite, Timna massif, 1500/9100, No. B.T. 3087; analyst: Bodenheimer-Gaon.			41. Tinna Granite, Timna massif, 1455/9114, No. B.T. 2717; analyst: Bodenheimer-Gaon.			
31.	Tinna Granite-porphyr, Timna massif, 1476/9088, No. S.W. 85; analyst: Gaon. (Slatkine-Wurzbürger, 1957).			Tinna Granite, Timna massif, 1470/9085, No. E.P. 820; analyst: Bodenheimer-Heizler.				36. normalquartzdioritic			36. yosemiticgranitic (c low, fm high) to adamellite (c low)			
32.	Tinna Granite-porphyr, Timna massif, 1490/9085, No. B.T. 3102; analyst: Bodenheimer-Gaon. (Slatkine-Wurzbürger, 1957).			Tinna Granite, Timna massif, 1479/9078, No. B.T. 3048; analyst: Bodenheimer-Gaon.(Zlatkine-Wurzbürger, 1957).				28. leucoquartzdioritic			37. apligranitic			
								30. granosyenitic			38. apligranitic			
								31. leucoquartzdioritic			39. apligranitic			
								32. engadiniticgranitic			40. apligranitic			
								33. natronapaktivic			41. alkaligranitit			
								34. apligranitic						
								35. alkaligranitit						

TABLE II (continued)
Chemical Analyses

	42	43	44	45	46	47	48	49	50	51	52	53	54
SiO ₂	71.67	76.58	73.13	73.56	76.39	69.43	75.70	74.35	66.40	63.99	75.05	77.03	70.56
Al ₂ O ₃	16.11	13.60	14.90	15.90	14.38	14.63	13.52	13.99	13.12	12.70	11.10	8.94	6.84
Fe ₂ O ₃	1.27	1.60	0.84	0.98	1.67	2.75	1.58	0.47	5.09	7.80	3.57	2.86	3.16
FeO	0.28	0.29	0.50	0.34	0.51	0.94	tr.	—	0.55	0.13	—	—	—
MgO	0.50	0.20	0.40	1.07	—	1.70	—	0.18	0.96	1.59	0.49	0.34	1.00
Ca	0.65	0.56	0.56	—	—	0.81	0.42	0.58	1.22	0.61	0.24	1.00	5.13
Na ₂ O	5.20	3.50	3.69	3.19	3.29	4.87	4.46	5.30	4.02	1.96	3.04	0.80	1.42
K ₂ O	3.60	3.00	4.20	3.45	2.68	2.66	3.21	4.63	5.19	7.70	5.50	6.85	7.56
TiO ₂	0.31	tr.	0.70	—	—	0.47	0.14	tr.	0.72	1.43	0.51	0.37	0.74
P ₂ O ₅	tr.	—	—	—	—	—	—	—	1.12	0.26	tr.	—	—
MnO	0.03	—	—	0.05	0.06	—	—	—	0.11	0.10	0.04	—	—
CO ₂	0.20	—	—	—	—	0.37	—	—	—	—	—	—	3.22
Cl	—	—	0.06	—	—	0.10	—	—	—	—	—	—	—
SO ₃	—	0.08	—	—	—	0.29	—	—	—	—	—	—	—
H ₂ O-	0.16	—	0.19	0.24	0.18	0.11	0.11	0.05	0.35	0.50	0.62	—	0.12
H ₂ O+	0.47	0.80	0.39	0.82	0.95	0.93	0.64	0.32	1.25	1.56	0.44	—	0.71
Total	100.45	100.21	99.56	99.60	100.11	100.06	99.78	99.87	100.10	100.33	100.60	98.19	100.46

Ocorr.

for Cl

-0.01

99.55

Nigili Values

	42	43	44	45	46	47	48	49	50	50a	51	51a	52	53	54
si	374.5	490.4	422.6	424.2	505.2	335.4	476.2	425.8	303.3	328.3	272.7	341.9	450.0	548.7	461.2
al	49.6	51.2	50.7	53.9	56.0	41.5	49.8	47.1	35.1	38.0	31.9	40.0	38.8	37.2	26.3
fm	10.0	11.2	9.4	15.6	11.5	25.8	7.6	3.4	26.3	20.0	36.1	20.0	20.9	18.8	25.5
c	2.2	3.8	3.5	0.0	0.0	1.7	2.6	3.4	5.7	6.2	2.8	3.5	1.4	7.7	7.4
alk	38.2	33.8	36.4	30.5	32.5	31.0	40.0	46.1	32.9	35.8	29.2	36.5	38.8	36.3	40.8
k	0.31	0.36	0.43	0.41	0.35	0.27	0.32	0.37	0.46	0.46	0.72	0.72	0.55	0.85	0.78
mg	0.38	0.17	0.36	0.62	0.00	0.47	0.0	0.40	0.25	0.28	0.28	0.21	0.18	0.38	0.38
tl	1.3	0.0	3.1	0.0	0.0	1.7	0.4	0.0	2.5	2.7	4.6	5.7	2.2	2.1	3.5
p	0.0			0.0	0.0		0.0		2.2	2.4	0.5	0.6	0.0		
qz	+121.7	+255.2	+177.0	+202.2	+275.2	+111.4	+216.2	+141.4	+71.7	+85.1	+55.9	+95.9	+194.8	+303.5	+241.5
42.	Eilat Granite, Eilat massif, 1403/8850, No. B.S. 220; analyst: Bodenheimer-Heizler.														
43.	Shahmon Granite (microcline-albite-granite), Shahmon massif, 1413/8911, No. T.V. 42; analyst: Bodenheimer-Heizler.														
44.	Shahmon Granite (oligoclase-microcline-quartz-monzonite), Shahmon massif, 1412/8894, No. T.V.L. 7; analyst: Bodenheimer-Heizler.														
45.	Two-mica-garnet-granite, dike in old schists, Eilat massif, 1431/8829, No. B.T. 1037; analyst: Bodenheimer-Gaon.														
46.	Two-mica-garnet-granite, dike in old schists, Eilat massif, 1428/8831, No. B.T. 1039; analyst: Bodenheimer-Gaon.														
47.	Micro-granite, dike in Rehavam Granite, Eilat massif, 1397/8845, No. N.B. 128; analyst: Bodenheimer-Harpaz.														
48.	pyritic quartz-porphry, dike in Timna Granite-porphry, Timna massif, "diagonal wadi", No. S.W. 525; analyst: Bodenheimer. (Slatkine-Wurzbarger, 1957).														
49.	Yehoshaphat Granite, Eilat massif, 1402/8846, No. B.S. 264; analyst: Bodenheimer-Heizler.														
50.	Amram Granite-porphry, Amram massif, 1445/8973, No. B.T. 3174; analyst: Bodenheimer-Gaon.														
50a.	Analysis 50, recalculated for fm = 20.														
51.	Amram Granite-porphry, Amram massif, 1460/8976, No. S.W. 282; analyst: Gaon.														
51a.	Analysis 51 recalculated for fm = 20.														
52.	Amram Quartz-porphry welded tuff (?), Amram massif, 1441/8968, No. S.W. 468; analyst: Gaon.														
53.	Amram Quartz-porphry, lava flow, Amram massif, 1456/8964, No. S.W.														
54.	Amram Quartz-porphry, welded tuff, Amram massif, 1456/8963, No. S.W. 302; analyst: Bodenheimer-Heizler.														
50.	K-gibellitic(?)														
50a.	normalalkaligranitic														
51.	normalsyenitigranitic (? fm high, c low)														
51a.	normalalkaligranitic														
52.	normalalkaligranitic														
53.	normalalkaligranitic														
54.	leucoviscitic to eviscitic-pantelleritic to eviscitic-gronditic														

Magma Type

TABLE II (Continued)
Chemical Analyses

	55	56	57	58	59	60	61	62	63	64	65	66	67
SiO ₂	62.96	64.30	65.78	53.83	47.98	56.74	59.47	68.30	70.09	74.36	58.78	43.80	44.48
Al ₂ O ₃	17.73	16.11	18.67	18.15	15.44	15.79	17.47	12.44	15.94	12.30	12.59	15.79	13.58
F ₂ O ₃	2.05	2.20	1.05	6.43	12.22	2.63	0.35	4.97	3.40	3.10	7.62	11.70	12.39
FeO	1.35	0.99	0.46	3.20	0.65	2.80	5.53	0.43	—	tr.	1.51	3.79	3.20
MgO	1.01	1.18	0.67	2.80	3.76	5.60	3.01	1.04	0.42	0.45	2.13	4.40	6.04
CaO	1.89	1.36	0.70	4.03	3.86	5.46	3.64	1.28	0.81	0.38	1.78	7.48	7.04
Na ₂ O	5.10	5.35	5.87	5.18	3.32	3.50	4.25	2.55	4.50	2.65	7.66	1.34	2.76
K ₂ O	5.56	5.41	5.68	2.51	2.72	3.50	2.57	6.43	3.90	5.11	3.15	1.10	1.44
TiO ₂	0.72	1.64	0.60	2.15	3.20	0.82	1.66	0.80	0.30	tr.	2.05	5.53	4.67
P ₂ O ₅	0.20	0.15	—	—	—	—	—	—	—	—	—	0.41	0.65
MnO	0.08	0.09	0.13	—	—	0.39	0.11	—	0.43	—	—	0.47	0.22
CO ₂	—	—	—	—	—	0.21	—	0.07	0.08	—	—	—	—
Cl	—	—	—	—	—	tr.	0.45	0.25	0.31	—	—	—	—
SO ₃	—	—	—	—	—	—	—	—	—	—	—	—	—
H ₂ O—	0.37	0.21	0.27	0.12	3.16	0.18	0.64	0.21	—	0.24	0.55	0.87	0.20
H ₂ O+	0.50	0.52	0.34	1.85	4.50	2.38	1.11	1.14	0.54	1.02	2.41	3.43	3.93
Total	99.52	99.51	100.22	100.25	100.81	100.00	100.26	99.91	100.72	99.61	100.23	100.11	100.60
						O corr.			O corr.				
						for Cl			for Cl				
						—0.05			—0.02				
						99.95			100.70				

TABLE II (continued)
Chemical Analyses

	68	69	70	71	72		68	69	70	71	72
SiO ₂	50.78	52.27	53.29	49.10	50.76	si	157.8	163.7	137.7	139.8	149.4
Al ₂ O ₃	16.10	18.34	13.86	16.52	17.06						
Fe ₂ O ₃	7.82	6.16	5.21	5.45	4.34	al	29.5	33.6	21.1	27.7	29.6
FeO	1.77	2.98	3.98	3.91	3.48	fm	43.8	43.8	60.0	47.0	47.3
MgO	4.40	4.50	10.85	6.05	6.58	e	5.8	4.7	12.1	10.3	12.3
CaO	4.76	1.38	4.36	4.57	4.33	alk	20.9	17.9	6.8	15.0	10.8
Na ₂ O	5.06	4.03	1.61	2.13	1.41						
K ₂ O	2.82	2.76	1.73	5.12	3.59	k	0.27	0.32	0.41	0.61	0.62
TiO ₂	1.13	1.95	1.49	2.05	1.31	mg	0.47	0.48	0.68	0.55	0.61
P ₂ O ₅	0.52	0.36	0.35	0.53	0.35						
MnO	0.17	0.08	0.08	0.13	0.12	ti	2.6	4.5	2.9	4.3	2.8
CO ₂	2.36	—	tr.	0.94	0.35	p	0.7	0.6	0.3	0.7	0.4
Cl											
SO ₃											
H ₂ O—	0.12	1.53	—	—	0.12	qz	-25.8	-7.9	+10.5	-20.2	+6.2
H ₂ O+	2.72	4.11	3.81	4.05	5.95						
Total	100.53	100.45	100.62	100.55	99.75						
68. trachyandesite, dike in Timna Granite, Timna massif, 1455/9070, No. B.T. 2567; analyst: Bodenheimer-Heizler.						1466/9106, No. S.W. 25C; analyst: Gaon.					
						Magma Type					
						68. melagranitic (si low) to melagranitic					
						69. melagranitic (c very low)					
						70. al-hornblende (si high)					
						71. lamprophyritic to lamprogranitic					
						72. lamprogranitic					
69. trachyandesite, dike in Timna Granite, Timna massif, 1458/9069, No. B.T. 2560; analyst: Gaon.						72. lamprogranitic					

REFERENCES

1. AYAL, M., 1959, *The Geology and Petrography of the Eilat Massif, Southern Negev* (unpublished M. Sc. thesis, Hebrew University, Jerusalem).
2. BACKLER, N., 1960, *The Petrography of Mount Yehoshaphat and Mount Yehoyahin, Southern Negev, Israel* (unpublished report).
3. BENTOR, Y. K. AND VROMAN, A., 1955, *The Geological Map of Israel, Series A: The Negev, Sheet 24: Eilat* (Geological Survey of Israel, Jerusalem).
4. ——— AND ———, 1960, *The Geological Map of Israel 1:100,000, Sheet 16: Mount Sdom* (Geological Survey of Israel, Jerusalem).
5. BLAKE, G. S., 1935, *The Stratigraphy of Palestine and its Building Stones* (Govt. of Palestine, Printing and Stationary Office, Jerusalem).
6. BLANCKENHORN, M., 1914, Syrien, Arabien und Mesopotamien, *Handbuch der Regionalen Geologie*, 5, 4, fasc. 1, Heidelberg.
7. HULL, E., 1886-1889, Memoirs on the Geology and Geography of Arabia Petraea, Palestine and adjoining Districts etc. (*Palestine Exploration Fund, Survey of Western Palestine*, IX, London).
8. LARTET, L., 1869, Essai sur la Géologie de la Palestine et des Contrées avoisinantes, telles que l'Egypte et l'Arabie etc, II, *Ann. Soc. Geol.*, 1^{re} année, pp. 5-116.
9. MICHEL-LEVY, Quoted in: NIGGLI, P., 1923, *Gesteins- und Mineral-provinzen I*. Berlin, (p. 290 Nr 345).
10. PICARD, L., 1941, The Precambrian of the North Arabian-Nubian Massif, *Bull. Geol. Dept. Hebr. Univ.*, 3, 3-4, Jerusalem.
11. POSNER, E., 1954, *Report on the outcrops of eruptive rocks of the Timna region* (unpublished report, Geol. Surv. Israel).
12. SHILONI, S., 1959, *The Geology and Petrography of the Eilat Conglomerate, Southern Israel* (unpublished M. Sc. thesis, Hebrew University, Jerusalem).
13. SCHUERMANN, H. M. E., 1949, The basement rocks of the northern part of the eastern desert of Egypt, *Bull. Soc. Roy. Géogr. Egypte*, XXIII, 35-61.
14. — — — 1954, Remarks on stratigraphy, tectonics and metamorphoses with reference to the Pre-Cambrian in Egypt, *Geologie en Mijnbouw*, 8, 315-320.
15. — — — 1956, Das Praekambrium der arabischen Wueste Aegyptens, *Geol. Rundschau*, 45, 179-193.
16. — — — 1957, The Precambrian of Egypt, east of the River Nile, *Geologie en Mijnbouw*, 5, N. Series, 165-171.
17. TOMKEJEFF, S. I., 1946, Magmatic Rolls, *Nature*, 158, 420-423.
18. WEISSBROD, T., 1960, *The Petrography of the Shahmon Massif, Southern Negev, Israel* (unpublished M.Sc. thesis, Hebrew University, Jerusalem).
19. WURZBURGER, U., 1959, *The geology and petrography of the Amram Mountains, Southern Israel* (unpublished M.Sc. thesis, Hebrew University, Jerusalem).
20. SLATKINE, A. AND WURZBURGER, U., 1957, Eruptive rocks of Timna (Negev), *Geol. Survey of Israel*, 14, Jerusalem.

THE GEOLOGY OF MOUNT GILBOA

A. FLEXER

Department of Geology, The Hebrew University of Jerusalem

ABSTRACT

Mt. Gilboa located at the junction of the Jordan Valley and the Emek Jezreel (Esdraelon) depression, is built of sediments attaining a total thickness of 1200m, and ranging in age from Upper Cenomanian to Middle Eocene. The Middle Eocene strata are unusually thick. An erosion surface characterized by appreciable relief separates the Eocene beds from the underlying Senonian beds. The main structural pattern is that of faulted tilted blocks. Post-faulted volcanic rocks are encountered, among which a small doleritic intrusion with associated thermal metamorphism is of special interest.

INTRODUCTION

Mount Gilboa constitutes the north-eastern branch of the Ephraim Mountains. This mountain block has a rectangular form with a maximum height of 500m above sea level.

The comparatively steep NE escarpment of Mt. Gilboa faces the Emek Jezreel (Harod Valley) in the North; its eastern slopes face the Jordan Valley (Beit Shean). To the West it is bordered by the Taanach Valley, and in the South the international border with Jordan separates it from the Samarian Eocene Synclinorium. The geology of this region has been previously described by Picard (1928, 1929, 1955); Willis (1928) and Blake (1936, 1939). The present paper records new observations made by the author during 1958–1959. The surveyed area is about 80 square kilometers and has been mapped on the scale of 1:20,000.

LITHOLOGY AND STRATIGRAPHY

The area is built of sedimentary and volcanic rocks, with subsidiary intrusive phenomena.

1. Sedimentary rocks

The main rock types are dolomite, limestone, chalk and flint. The sequence of the lithologic units is given below, the description beginning with the older beds.

(1) *Deir Hanna formation (dhf)*

Dolomite—yellow, finely crystalline, soft, very thickly-bedded*, with abundant chert and quartzolite.

* The term thickness adopted in this work is in accordance with Ingram (1954). The terms Deir Hanna formation and Sakhnin Dolomite were introduced by Golani (1961) and Bi'na Limestone by Shadmon (1959).

Thickness: only 140m exposed.

Age: Upper Cenomanian.

(2) *Sakhnin dolomite (sd)*

Dolomite—grey, coarsely crystalline, hard and porous; massive and cliff forming at the base, but well-bedded at the top.

Thickness: 200m.

Age: Upper Cenomanian.

(3) *Bi'na limestone (bl)*

Limestone—yellowish-white, lithographic, stylolitic, thickly-bedded; alternating with coarsely crystalline, brown limestone. There are lateral transitions to coarsely-crystalline grey dolomite, and to a large quartzolite rudistid reef.

Thickness: 40m.

Age: Cenomanian-Turonian.

(4) *The "Chalk unit"* (s)*

Chalk, — white, massive and jointed, with a thick cover of nari; it is hard at the base. Massive, hard, brecciated flint is encountered in several places.

The unit varies in thickness from 100m in the center of the area to over 200m along its flanks.

Age: Senonian, Maestrichtian and Paleocene.

(5) *Meroz formation (mf)***

Limestone, yellowish-brown or grey, lithographic to sublithographic, hard with flint nodules.

The limestone is well bedded and there are intercalations of green clay.

Thickness: 200m.

Age: Lower to Middle Eocene.

(6) *Jzreel "marble" (im)*

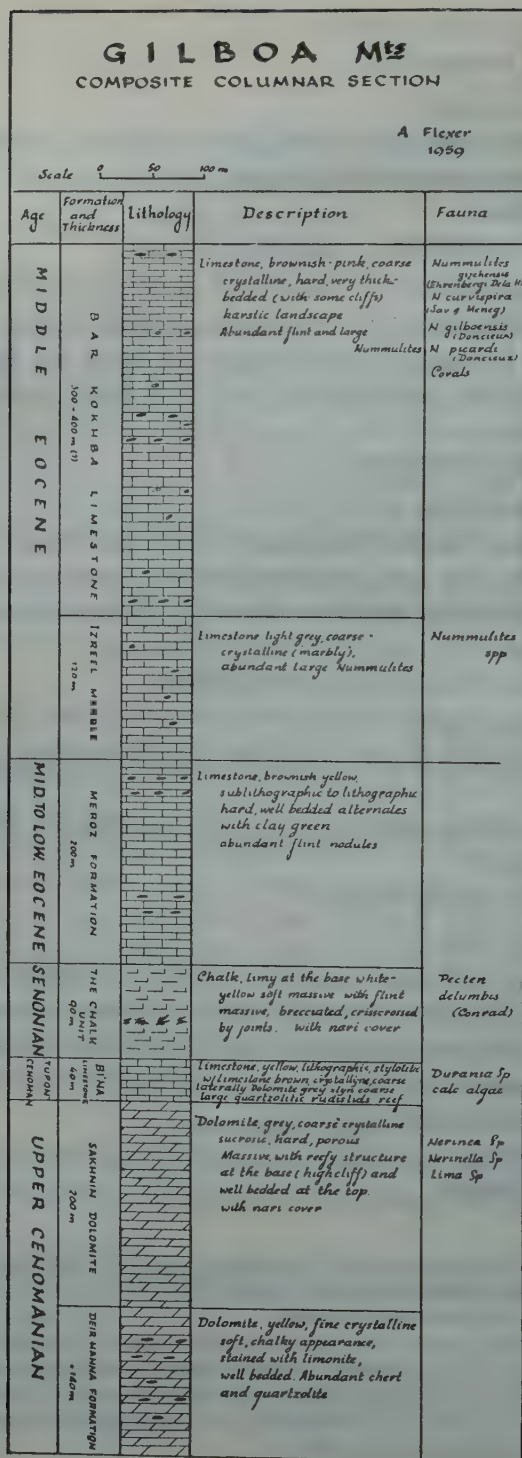
Limestone, greyish-brown, coarsely crystalline ("marbly"), with many large nummulites silicified on the outer surface. At a few localities the rocks have a pseudo-conglomeritic appearance though no fault is evident near by. The lateral continuity of this phenomenon is difficult to check in the field, and the degree of its persistence is unknown.

Thickness: 120m.

Age: Middle Eocene.

* As this unit, all over Northern Israel, is at present under investigation, it is hoped that type sections with formal names of formations will be published in the future. The term "Chalk unit" is therefore to be considered as provisional.

** Again only provisional names are given to the following three formations (5-7), of Eocene age. They are distinguished by a peculiar calcareous facies, and are well developed in the eastern part of Northern Israel (Gilboa, Givat Hamoreh, Nazareth Hills, Mount Arbel, Safad region and Nahal Dishon). A broad regional correlation has yet to be made. In its absence these provisional names are presented (Flexer 1959).



(7) *Bar Kokhba Limestone*¹ (*bkl*)

This formation is built of two alternating lithologic units;

(a) yellowish-brown, lithographic, hard and well-bedded limestone, with interbedded horizons of flint nodules;

(b) marbly, nummulitic limestone forming cliffs up to 20m each. The landscape formed by both these types is karstic, and characterized by numerous caves. The total thickness is as yet unknown for the top of this formation lies beyond the border with Jordan. However, it is estimated to be 300–400m.

Age: Middle Eocene.

(8) *Younger Sediments*

The younger sediments occur as terraces of conglomerates along the mountain borders (Picard 1934, Nir 1960). This conglomerate consists of rounded to subangular Eocene limestone pebbles with some basaltic components, embedded in a soft marly matrix.

Their age is Pleistocene.

A disconformity between Eocene and Senonian strata

In the eastern part of Mt. Gilboa, in the Nahal Avinadav exposuue (coordinates 216/206), Middle Eocene strata overlie disconformably² Senonian sediments. i.e. the Jzreel formation rests directly on the "Chalk unit", the intervening Meroz formation is missing (Figure 1, Plate 1). The contact between the Senonian Chalk and the Eocene limestone is very sharp.

The erosion surface was probably caused by submarine currents and not by the effects of subaerial exposure. In contrast to Mishor Hava (Bentor and Vroman 1956,

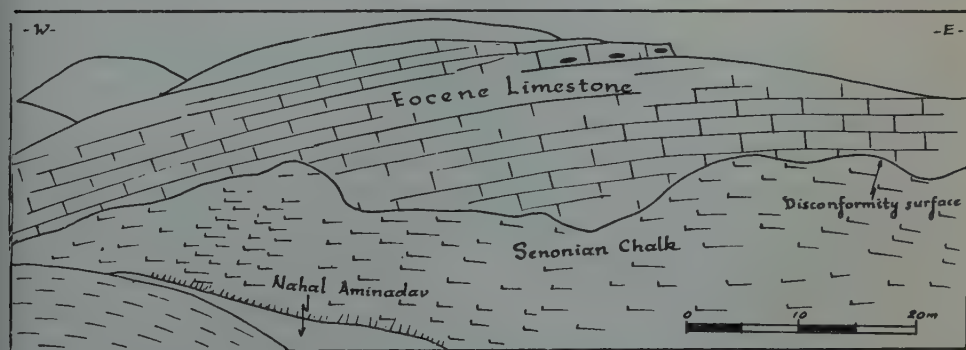


Figure 1
Erosion surface between Senonian and Eocene sediments
in Nahal Avinadav (216/206). After Plate 1

1. This formation has been previously studied by Picard (1928). The microfauna (examined by Duncieux) indicated an Upper Lutetian age or Lower Mokattan stage. The term Bar Kokhba has been in use for some time, but has not been published so far.
2. For the meaning of this term the reader is referred to Dunbar and Rodgers (1958, p. 119).



plate 1
The Nahal Avinadar exposure, see Figure 1

Starinsky 1961) no lateritic layers or limonitic crusts were found on the surface or just below the surface.

As it has proved impossible to measure the strike and dip of the Senonian beds directly beneath the Eocene strata the author's earlier suggestion (1959) of an angular unconformity remains unproved.

Discordances of various kinds between the Senonian and Eocene have been recorded in the Levantine countries and in Egypt by many authors.

Regional Correlation

The four formations of the Upper Cretaceous epoch (1-4), encountered in the Gilboa, resemble much their adjoining formations over all Galilee, especially those of the Nazareth Hills (Golani 1961, Weiler 1961).

The Eocene formations may be correlated only with those of Northeastern Israel (as mentioned above), while the Eocene formations of Northeastern Israel are distinguished by chalky facies, and indicate pelagic environments (Rabinovitch 1954, Arad 1955, Greenberg 1961).

II. Volcanic rocks

About ten exposures of basic volcanic rocks are encountered on Mt. Gilboa. These occur as small independent extrusive bodies and as an intrusive plug.

(1) The extrusive rocks

The lavas are all basalts of the alkali-olivine-basalt type. They can be divided into two types:

- a. Basalts with phenocrysts of olivine only: this group occurs in the northern part of the area (see map)

- b. Basalt with phenocrysts of olivine and plagioclase: this group occurs in the eastern part of Mt. Gilboa.

It is evident that a relationship exists between the location of the volcanic bodies and the presence of some of the major faults.

The lava-flows spread over a faulted relief, and accumulated over the down-thrown blocks. This phenomenon indicates that the basaltic bodies are younger than the main phase of faulting of Mt. Gilboa.

(2) *The intrusive rocks*

Near Kibutz Heftsibah (1894/2139), a small intrusion (of some $60 \times 40\text{m}$) cuts through the rocks of the Sakhnin dolomite. The intrusion is of an irregular shape (Figure 2), and composed of an alkaline dolerite.

The dolerite itself shows highly metamorphic changes due to the assimilation of calcareous sediments, and has itself been the cause of high-grade thermal metamorphism of the adjacent dolomites. (Oppenheim, internal report, Hebrew University, 1960).

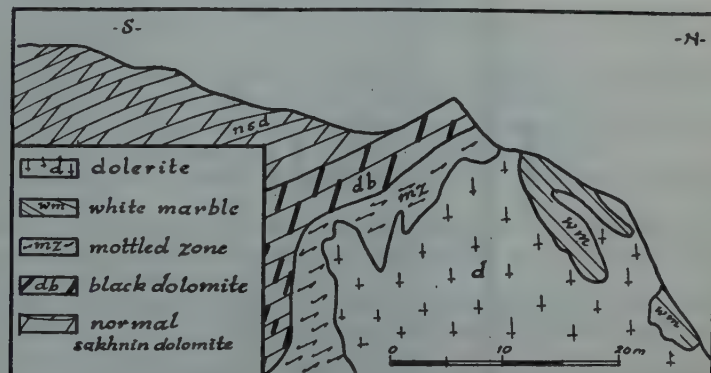


Figure 2

Simplified sketch of Dolerite intrusion near Heftsibah 1894/2139

STRUCTURE

Faulting is the dominant tectonic element of this region. Mt. Gilboa is bounded on the northern and eastern parts by three big border faults, having a maximum throw of not less than 500m.

As a result of these movements, two independent tilted blocks may be distinguished:

1. The Central Gilboan block.
2. The Jeszreel block.

It is these tectonic features which determine the present morphology of the mapped area.

The tilted block of central Mt. Gilboa has the structure of a half-dome, and bears

a certain interesting resemblance to the northern Carmel structure (Karcz 1959). However, it should be mentioned that Mt. Gilboa is but the northern exposed part of the large synclinorium of Samaria (Picard 1943).

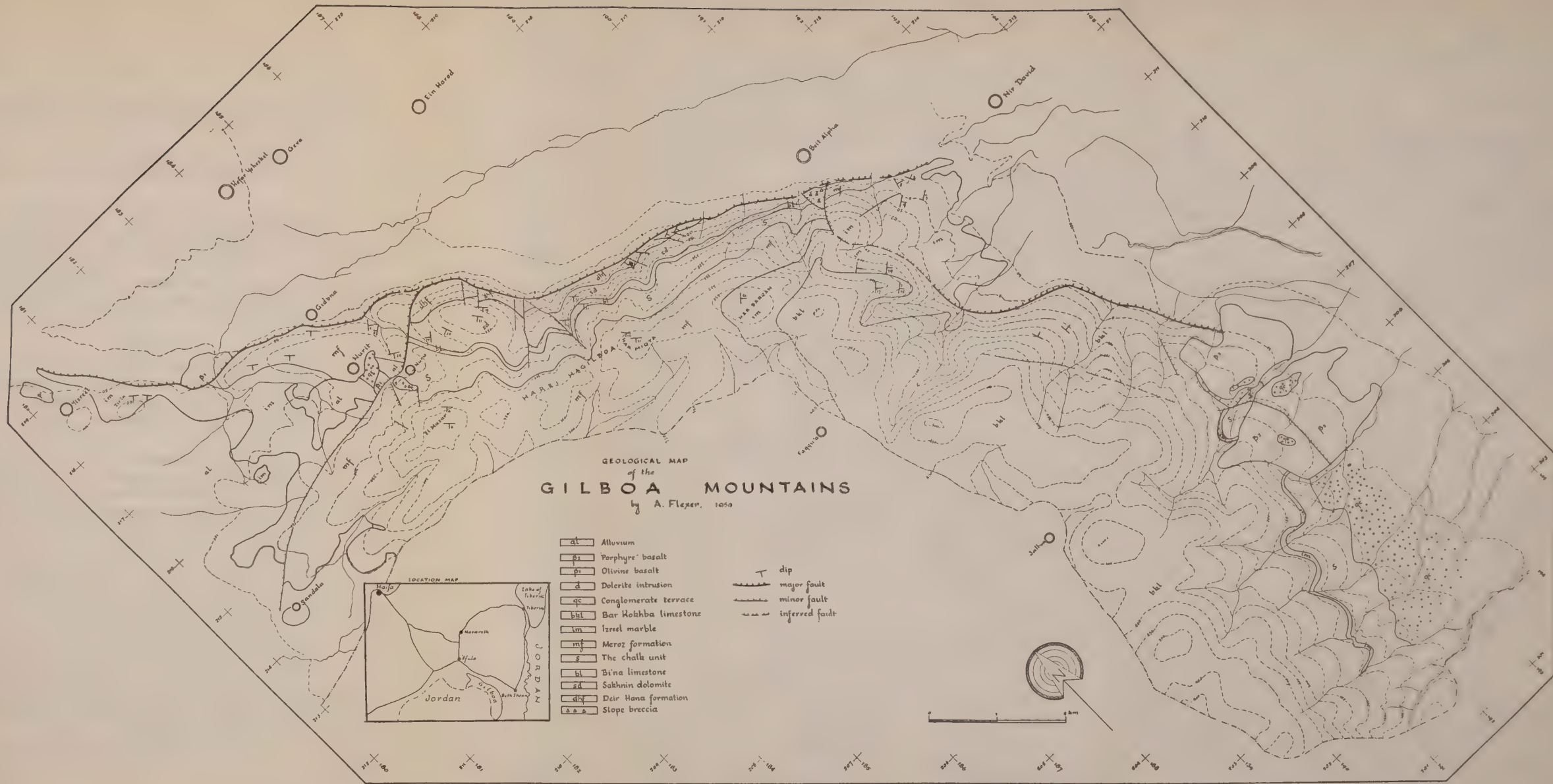
ACKNOWLEDGEMENT

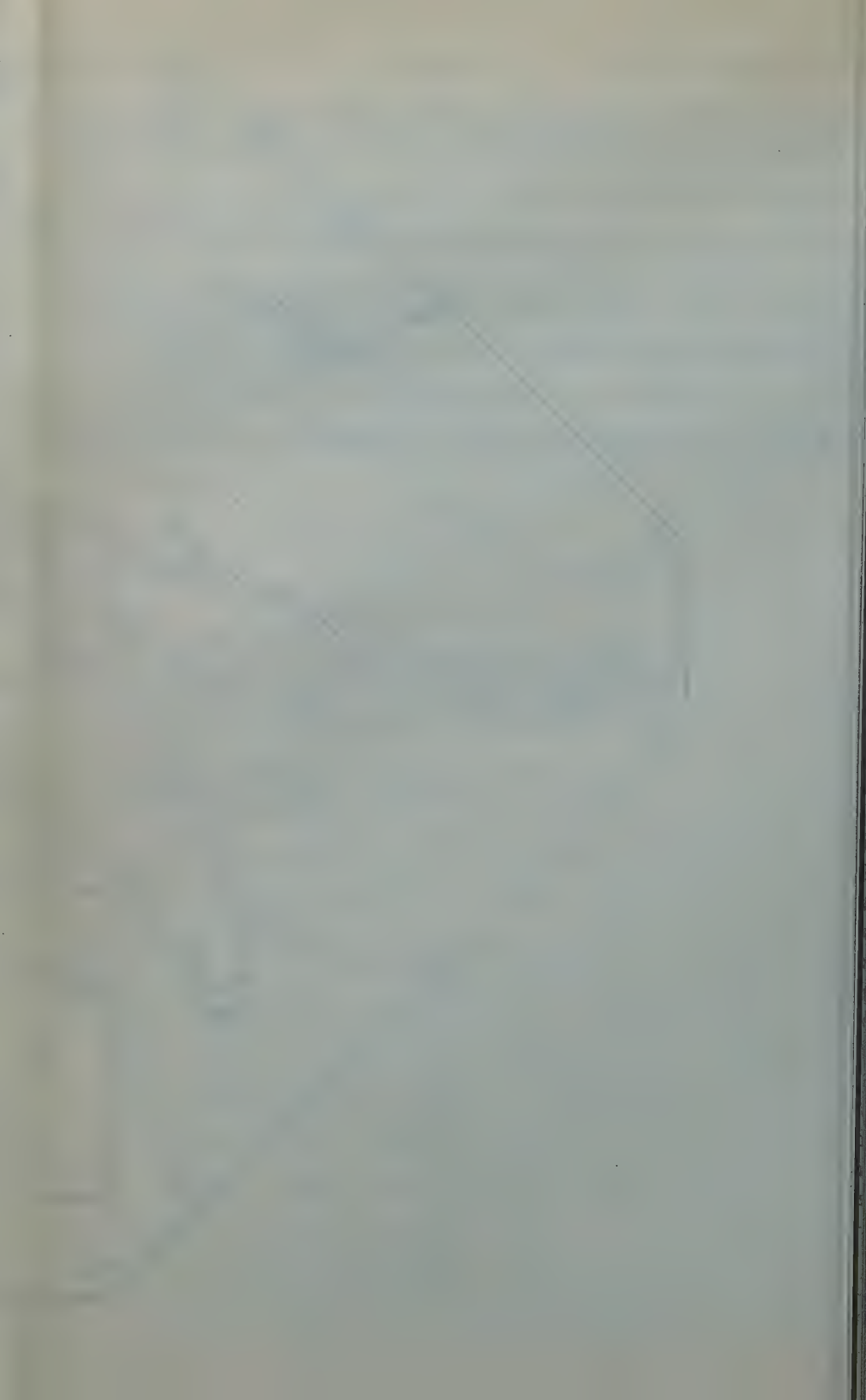
The author wishes to express his thanks to Prof. Picard for his guidance in the present study, to "agudat Ha'meim of Emek Harod" for its support of the work, and to his friends in the Geological Department of the Hebrew University and the Geological Survey of Israel for their criticism of the manuscript.

REFERENCES

1. ARAD, A., 1959, Geology of Ephraim Mts., *Geol. Dept. Hebr. Univ. Jerusalem*. (Unpublished M.Sc. thesis. In Hebrew).
2. AVNIMELECH, M., 1946, On Nautilus libnoticus Foord and Crick in the Senonian of Palestine, *Ann. and Mag. Nat. Hist. Ser.*, 10, Vol. 12, 523-528.
3. BALL, M. AND BALL, D., 1953, Oil prospects of Israel, *Bull. Am. Ass. Petr. Geol.*, 36, 10.
4. BENTOR, Y. AND VROMAN, A., 1951-1960, Geological map of Israel 1:100,000. Sheets: Abda, Nahal Arava, Sdom, *Geol. Survey of Israel, Jerusalem*.
5. BENTOR, Y. AND VROMAN, A., 1954, A structural contour map of Israel, *Bull. Res. Council of Israel*, 4, (2), 125-135.
6. BENTOR, Y. AND VROMAN, A., 1956, Unconformities between the Turonian and Eocene in the Ramon anticline, *Bull. Geol. Soc. of Israel*, 3, 57-64. (In Hebrew).
7. BLAKE, G. S., 1936, *The Stratigraphy of Palestine and its building stones*, Govt. Press. Jerusalem.
8. BLAKE, G. S., 1939, Geological map of Palestine 1:250,000, Jerusalem.
9. BLAKE, G. S. AND GOLDSCHMIDT, 1941, *Geology and Water Resources of Palestine*, Pal. Gov. Printer, Jerusalem.
10. CUVILLIER, J., 1930, *Révision du Nummulitique égyptien*, Thèse Sc. Paris, Mem. Inst. d'Égypt.
11. DAQUE, E., 1903, Mitteilungen ueber den Kreidecomplex von Abu Roash bei Kairo, *Sdr. Palaeontogr.*, 30, 337-392.
12. DUNBAR, O. AND RODGERS, J., 1958, *Principles of Stratigraphy*, John Wiley, New York.
13. FLEXER, A., 1959, Geology of the Gilboa Mts., *Geol. Dept. Heb. Univ. Jerusalem*. (Unpublished M.Sc. thesis. In Hebrew).
14. GOLANI, U., 1961, Cenomanian-Turonian lithostratigraphy of Central Galilee, *Bull. Res. Council of Israel* (In press).
15. GOLDBERG, A., 1959, Nari in Israel, *Geol. Dept. Heb. Univ. Jerusalem*. (Dissertation in Hebrew).
16. GREENBERG, J., 1961, Geology of Kefar Hachores region, *Geol. Dept. Heb. Univ. Jerusalem* (Unpublished M.Sc. thesis. In Hebrew).
17. HAUN, J. D. AND LE ROY, L. W., 1958, *Subsurface Geology in Petroleum Exploration*, First ed., Colorado School of Mines, Golden, Colorado.
18. INGRAM, J. R., 1954, Terminology for the thickness of stratification and parting units in sedimentary rocks, *Bull. Geol. Soc. America*, 65, 937-938.
19. KARCZ, Y., 1959, The Structure of the Northern Carmel, *Bull. Res. Council of Israel*, 8G, (2-3), 119-130.
20. NIR, D., 1960, Recherches granulométriques dans les oeds de la région de Beth-Chean, *Bull. Res. Council of Israel*, 9G, (4), 192-206.
21. PICARD, L., 1928, Ein Eocanprofil des Gilboas in Palastina, *Centralblatt f. Min. Abt. B.*, pp. 578-582.
22. PICARD, L., 1928, Zur Geologie der Kishonebene, *Zeitschr. Deutsch. Palast. Vereins*, 51, 5-72, Leipzig.
23. PICARD, L., 1929, Zur Geologie der Besanebene. Ibid. 52, 24-90.
24. PICARD, L., 1934, Zur Geologie der Gebietes zwischen Gilboa und Wadi Fara, *Centralblatt f. Min., Abt. B.*, pp. 27-32.

25. PICARD, L., 1943, Structure and Evolution of Palestine, *Bull. Geol. Dept., Heb. Univ.*
26. PICARD, L., 1955, Geological map of Israel 1:100,000, Sheet: Nazareth. *Geol. Survey of Israel.*
27. PICARD, L., 1959, Geology and oil exploration of Israel, *Bull. Res. Counc. of Israel*, **8G**, (1), 1-30.
28. RABINOVITCH, D., 1954, Geology of Shafar-Amer region, *Geol. Dept. Heb. Univ. Jerusalem*, (Unpublished M.Sc. thesis. In Hebrew).
29. SCHULMAN, N., 1959, The geology of Central Jordan Valley, *Bull. Res. Counc. of Israel*, **8G**, (2-3), 63-90.
30. SHADMON, A., 1959, The Bi'na Limestone, *Geol. Surv. Bull. No. 24.*
31. STARINSKY, A., 1961, Geochemical anomalies in Mishor-Hava, *Geol. Dept. Heb. Univ. Jerusalem*, (Unpublished M.Sc. thesis. In Hebrew).
32. WEILER, Y., 1961, Geology of the Nazareth Hills and Mt. Tabor, *Geol. Dept. Heb. Univ. Jerusalem*, (Unpublished M.Sc. thesis. In Hebrew).
33. WILLIS, B., 1928, Dead Sea problem: Rift valley or ramp Valley? *Bull. Geol. Soc. America*, **39**, 490-542.
34. WILLIS, B. AND PICARD, L., 1932, The Jordan Valley and Judean Highlands, *Geol. Magaz.* **69**, 97-107.





DISTRIBUTION OF LOWER TURONIAN AMMONITES IN ISRAEL AND THE NEIGHBOURING COUNTRIES*

RAPHAEL FREUND

Department of Geology, The Hebrew University of Jerusalem

ABSTRACT

Distribution maps of the Lower Turonian ammonites in Israel and the neighbouring countries show that the ammonites occur along several strips trending SW-NE. It is discussed whether this indicates a slight pre- and intra-Lower Turonian folding, or changes in marine environment. The Lower Turonian ammonite isofacies lines traverse the present fold and fault structure.

Senonian sediments directly overlying the ammonite bearing strata indicate a considerable pre-Senonian erosion. The distribution of the ammonites on both sides of the Dead-Sea graben may support the hypothesis of a sinistral strike-slip movement of 100km.

INTRODUCTION

A considerable number of Lower Turonian ammonites was collected since the end of the last century in Syria, Lebanon, Palestine and Egypt. The fauna was determined and described by Blanckenhorn (1890), Solger (1903), Fourtau (1904), Eck (1909, 1910, 1914), Douvillé (1912, 1928), Greco (1915), Taubenhaus (1920) and Jasse (1937, 1940, 1954).

Douvillé (1910, p. 60) noted that the hippurites and Lower Turonian ammonites found by Zumoffen near Beyrouth are replaced towards the north of these localities by radiolites of European types. He thought that this was due to a colder Turonian sea in the north. Dubertret (1937), finding the ammonites further in the north at Djebel Ansariyeh, did not accept Douvillé's climatic explanation, but suggested (1944, pp. 26-27) that the facies changes in the Turonian layers were due to pre-Turonian uplifting of Mt. Lebanon (and perhaps also Anti-Lebanon) above sea level. He further attributed the Lower Turonian ammonite occurrence on the eastern side of the Beqaa, recorded by Vautrin (Dubertret and Vautrin, 1937), to a Turonian sea reaching the Beqaa from the south.

Blanckenhorn (1912, 1931 p. 10) noted that Lower Turonian ammonites are abundant in Trans-Jordan while they are absent in Cis-Jordan. This is most likely due to the fact that he worked mainly in the northern Dead Sea area. Blake (1936, 1940) and Wetzel and Morton (1959) show in their columnar sections that the ammonites occur on the eastern side of the Dead Sea, disappearing to the south and to the

This article is based on a part of the author's Ph.D. thesis carried out at the Hebrew University, Jerusalem, under the guidance of Prof. L. Picard.

Received April 16, 1961

north. Avnimelech (1950) assumed a sedimentary gap between the Cenomanian and the Turonian in the Jerusalem area, indicated by the absence of Lower Turonian fauna and by the presence of conglomerates.

During the last decade several surveying geologists had found Lower Turonian ammonites in the Western Galilee; later Vroman (1958) and Freund (1959) noted that the ammonites occur along a narrow strip with a N30°E trend. The latter author suggested that this strip was deposited in a pre-Turonian syncline.

DISTRIBUTION MAPS

MAP No. 1 is an isopach-contour map of the Yirka formation in the Western Galilee and the Daliya marl (?= Ein Hod marl of Karcz 1959) on Mt. Carmel. Both formations consist of yellow limestones and marls carrying Lower Turonian ammonites, and attaining a maximum thickness of 80m. The thickness figures in the Galilee were obtained by plane-table, air-photos and columnar section measurements. The information on Mt. Carmel was obtained from the geological maps of Kashai (1958), Karcz (1959) and Vroman (1960). Several bore-holes penetrated the Turonian and Upper Cenomanian beds in Haifa-Bay. Only four of them encountered the yellow marls of the above mentioned formations (Mandel and Arad 1958; and information of the G.S.I.* Hydrogeology Division).

The characteristic fossils of the Yirka fm. are: (Table I) *Thomasites rollandi* (Thomas and Peron), *Choffaticeras luciae* Pervinquièrre, *Pseudaspidoceras salmuriensis* (Courtyiller) *Fagesia* spp., *Neoptychites cephalotus* (Court.) and *Romaniceras* sp. These ammonites are abundant in the Yirka fm., but only the last two species which characterize the upper part of the Yirka fm. are found in the Daliya marl. No other Lower Turonian ammonites were found elsewhere in Northern Israel*.

The NW boundary of the Yirka fm. is almost a straight line trending N30°E while the SE boundary is wavy; the broader parts of the strip coincide with the present horsts while the narrow ones with the grabens. Three of the bore holes seem to indicate a SW extension of the same band. The equidimensional area occupied by the Daliya marl on Mt. Carmel is somewhat shifted to the SE off this trend. The formations wedge out and do not interfinger laterally with other formations. The irregular thinning of the Yirka fm. in the middle of its area of occurrence is due to rudist-reefs which occur below and above this formation.

MAP No. 2 and the stratigraphic cross section (Figure 1) show the distribution and thickness of the Lower Turonian ammonite bearing formations in the Negev (Southern Israel). The information was obtained from numerous columnar section studies carried out by the author during 1960, from the geological maps

* G.S.I. — Geological Survey of Israel

** Kashai (1958) mentions *Pseudaspidoceras* cf. *armatum* Perv. from the base of Muhraqa limestone which underlies the Daliya marl, but this determination is doubtful.

Shaw (1947), Bentor and Vroman (1951 ff.), from unpublished works and from fauna collected by A. Aker, I. Ariyeh, A. Barzel, J. K. Bentor, M. Brown, A. Galai, P. Grader, J. Nir, A. Parnes, M. Raab, E. Rosental, A. Shilo, and Z. Shiftan, part of which the Geological Survey of Israel has so kindly put at my disposal.

The ammonites are easily grouped into three main successive zones, which usually correspond to three definite rock units.

The sequence of the *lower zone* begins with *Pseudaspidoceras* of the group of *P. footeanum* (Stoliczka), *Paravascoceras cauvini* (Chudeau), *P. crassum* Furon and "*Vascoceras*" *niloticum* (Douvill  ). The ammonites are embedded in soft marly limestone which interfingers laterally with hard concretionary limestone devoid of any ammonites. The ammonites of the lower zone are found in the northern part of the Negev in a ENE trending band which crosses the present fold structure (indicated by the Cenomanian-Turonian boundary of the new geological map 1:250,000 by Picard and Bentor, in press), and reaches the SW end of the Dead Sea. The above mentioned assemblage is best developed in the SW but degenerates towards the NE.

From the NW flank of the Hamakhtesh-Hagadol anticline and further to the NE these ammonites are followed in the sequence by *Thomasites rollandi* (Th. and Per.), *Vascoceras triangulare* Faraud and *Coilopoceras* sp. On the eastern side of the Hamakhtesh-Hakatan anticline the first assemblage of the lower zone is represented only by a thin layer with few ammonites, followed by beds containing the second assemblage and abundant *Paravascoceras* (?) *pioti* (Fourtau). A zone of large *Exogyra olisiponensis* Sharpe occurs below the lower zone in the central part of this band.

The characteristic fossils of the *middle zone* are: *T. rollandi* (Th. and Per.) *Choffaticeras segne* (Solger), and *Pachyvascoceras durandi* (Th. and Per.). These ammonites are crowded in a hard grey, detritic, coarse limestone up to 15m thick. This zone occurs in the northern part of this region in an elliptical area elongated to the NE. It extends from the vicinity of Mt. Arif in the SW, crosses diagonally the Ramon anticline and overlaps the lower zone near Ma'ale Ha'aqrabim. *C. segne* are rarely found further north. The ammonites of the middle zone disappear to the SE through the wedging out of their rock unit which indicates a shore environment. In the NW the upper zone overlaps the middle one; the boundary of the latter is not exposed.

The ammonite assemblage of the *upper zone* differs only to a small extent from that of the Yirka fm. in Western Galilee. The characteristic fossils are: *T. rollandi* (Th. and Per.), *Choffaticeras luciae* Perv., *Fagesia* spp., *P. salmuriensis zerhalmensis* Perv., *Neoptychites cephalotus* (Court.) and *Hoplitoides* sp. (the last one was found so far only in the Southern Negev). The rock unit in which these ammonites occur attains a maximum thickness of 15m and consists of soft, white-yellow marl, chalk and limestone. The geographic position of the upper zone is parallel to that of the middle zone, shifted 12km to the NW. The ammonites of this zone are usually rare and

STRATIGRAPHIC SECTION OF LT AMMONITES ROCK UNITS

Central and southern MEGEV

(Columnar sections projected on a $S 60^{\circ} E - N 60^{\circ} W$ line)

$S 60^{\circ} E$

$N 60^{\circ} W$

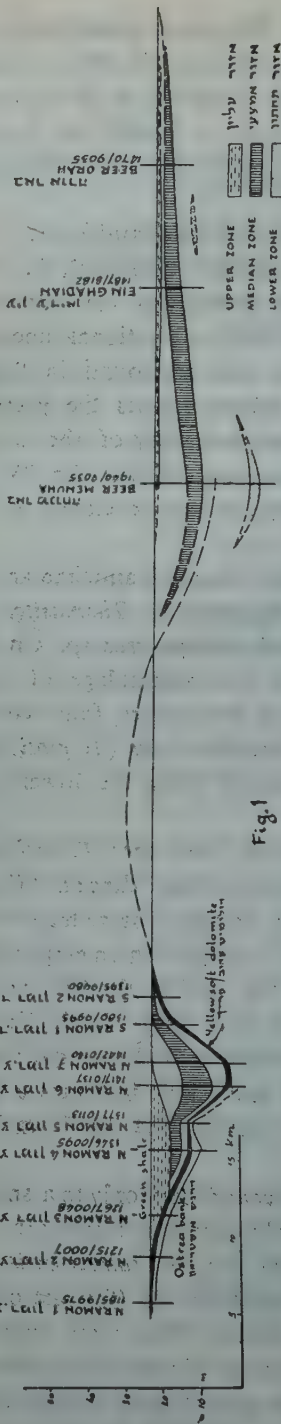


Fig.1

SCHEMATIC PROJECTED CROSS-SECTION OF THE LOWER TURONIAN AMMONITES DISTRIBUTION IN ISRAEL AND NEIGHBOURING COUNTRIES

התוך רוחב מושלך סכמטי
של תפוצת אמוניטים מגיל טורון התחתון
בישראל ובסביבותיה

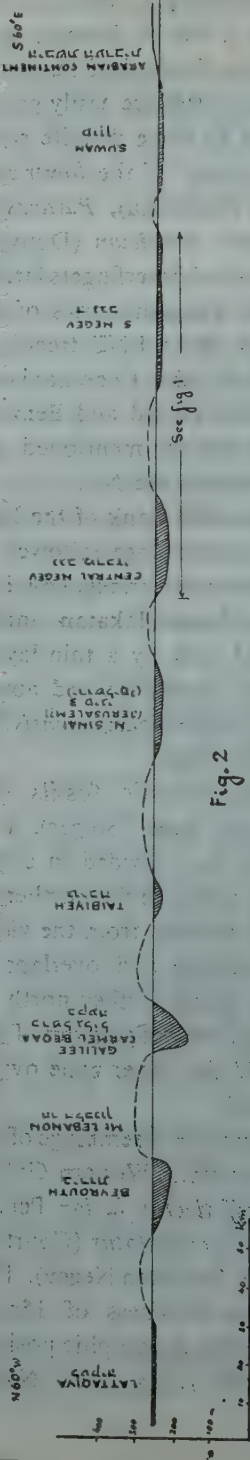


Fig.2

TABLE I
Zones of Lower Turonian ammonites in Israel*

	Mt. Carmel	Western Galilee	Northern Negev	Ramat Kvuda	Central Negev	Southern Negev
80m	<i>Romaniceras deverianum</i> <i>Neptychites cephalotus</i>	25m <i>Romaniceras deverianum</i> <i>Neptychites cephalotus</i> <i>Pseudaspidoceras</i> sp.				
Daliya marl	<i>Choffaticeras</i> sp.	40m <i>Choffaticeras luciae</i> <i>Choffaticeras segne</i> <i>Choffaticeras pavillieri</i> <i>Choffaticeras discoidale</i> <i>Thomasites rollandi</i> <i>Thomasites jordani</i> <i>Neptychites cephalotus</i> <i>Mammites nodosoides afer</i> <i>Pseudaspidoceras salmuriensis</i> <i>Fagesia thevestensis</i> <i>Fagesia</i> spp.		10m <i>Choffaticeras luciae</i> <i>Thomasites rollandi</i> <i>Hoplitoides</i> sp.	10m <i>Choffaticeras luciae</i> <i>Choffaticeras</i> (?) <i>stricta</i> <i>Choffaticeras pavillieri</i> <i>Thomasites rollandi</i> <i>Thomasites jordani</i> <i>Pseudaspidoceras salmuriensis</i> <i>Mammites</i> sp. <i>Neptychites cephalotus</i> <i>Fagesia</i> spp.	1m <i>Choffaticeras luciae</i> <i>Choffaticeras mokattanica</i> <i>Thomasites rollandi</i> <i>Pseudaspidoceras salmuriensis</i> <i>Hoplitoides</i> sp.
		15m Yirka formation <i>Choffaticeras segne</i> <i>Choffaticeras discoidale</i> <i>Choffaticeras pavillieri</i> <i>Thomasites rollandi</i>	<i>Choffaticeras segne</i> <i>Pachyvascoceras harttiiformis</i>		10m <i>Choffaticeras segne</i> <i>Choffaticeras discoidale</i> <i>Choffaticeras pavillieri</i> <i>Thomasites rollandi</i> <i>Pachyvascoceras durandi</i> <i>Pachyvascoceras harttiiformis</i>	5m <i>Choffaticeras segne</i> <i>Choffaticeras discoidale</i> <i>Choffaticeras pavillieri</i> <i>Thomasites rollandi</i> <i>Pachyvascoceras durandi</i> <i>Pachyvascoceras</i> spp.
Upper part		? <i>Choffaticeras</i> sp. (juvenile)	5m <i>Choffaticeras</i> sp. (juvenile) <i>Coilopoceras</i> sp. <i>Paravascoceras</i> (?) <i>pioti</i> <i>Thomasites rollandi</i> <i>Vascoceras triangulare</i> <i>Pseudaspidoceras</i> sp. <i>Paravascoceras cauvini</i> <i>Paravascoceras crassum</i> <i>Paravascoceras tavense</i> "Vascoceras" <i>niloticum</i> <i>Pseudaspidoceras footeanum</i> <i>Pseudaspidoceras</i> spp. "Acanthoceras" sp.			<i>Choffaticeras</i> sp. (juvenile) <i>Paravascoceras</i> sp. (juv.)
Lower part			15m			<i>Pseudaspidoceras</i> cf. <i>footeanum</i> <i>Paravascoceras cauvini</i> <i>Vascoceras</i> sp.

* Uncommon and new species not mentioned. Numbers indicate the maximum vertical distribution.

well preserved. Near the NW boundary the thickness of the rock unit diminishes to 0.6–0.3m., and poorly preserved crushed limonitized ammonites are very abundant. This most likely indicates a thanatocoenosis on a shore line.

A peculiar assemblage of Lower Turonian ammonites occurs in Ramat Kvuda, near the ruins of the ancient town Subeita (NW corner of the map). It comprises *T. rollandi* (Th. and Per.), *Choffaticeras luciae* Perv. and *Hoplitoides* sp. and differs somewhat from the upper zone assemblage. It probably extends into Sinai.

In the Southern Negev the ammonites of the middle zone occur in a four-meter thick layer. The ammonites of the upper zone follow in a very thin but persistent bank whereas the ammonites of the lower zone are found sporadically. The lower zone is underlain by a zone of *E. olisiponensis* Sharpe which in turn overlies a zone of *Neolobites* sp. and *E. flabellata* Goldf. (Cenomanian). The NW boundary of this distribution area is not exposed here and the SE boundary is probably near Eilat.

Map No. 2 shows that the two higher zones have the same trend as the Yirka-Daliya formations in Northern Israel. In Figure 1 (compare map No. 1) it is seen that the thinner the zones, the wider is their distribution area. A facies indicating shore environment is evident on every exposed boundary of the higher zones. The distribution trend of the lower zone diverges by about 30° from that of the upper zones.

MAP No. 3 shows the occurrence of Lower Turonian ammonites in Israel and the neighbouring countries. The information was obtained from literature, from unpublished reports and from Transjordanian and Egyptian fossils deposited in the H.U.J.* and the G.S.I. collections.

Since the ammonites are large and easily detectable in the field, they are considered as very rare or non-existent in areas from which they were not recorded by geologists who investigated the Cenomanian-Turonian stratigraphy. Nevertheless four cases are known where at localities from which no ammonites have been recorded by one investigator, others have discovered them.

The northernmost occurrence of Lower Turonian ammonites is described by Dubertret (1937, pp. 15–22) from three localities east of Lattaquia (SL 1, SL 2, SL 3)**. These ammonites are embedded in three meters of chalk covered by Senonian sediments. Further to the south (SL 4) the facies becomes dolomitic and no ammonites are mentioned.

Zumoffen (in Douvillé 1910, p. 59) describes the well known Turonian in the area NW of Beyrouth, which includes the "niveau calcaire à ammonites" — 20–30m of chalk and marl (SL 11). Dubertret (1937, 1944 p. 22, 1947 etc) noted that he himself did not find again these ammonites at the same locality, but that they are very abundant in a thin layer further north, near Maat (SL 9). The abundance of the ammonites in a thin layer (in comparison with their scarcity in a thick

* Hebrew University of Jerusalem.

** Locality numbers on map No. 3; see references in Table No. II.

and soft layer) may indicate here again a shore-line in the NW. Further North (SL 7) the ammonites are rare; on the northern side of Nahr el Djos (SL 6) they were not found. Near Beyrouth, at Nahr el Arech (SL 12) the ammonite bearing strata disappear: "sans doute est-il disparu par laminage" (Dubertret and Vautrin 1937 p. 66).

Ammonites were found on the eastern side of the Beqaa by Diener (1886) and again by Vautrin (op. cit. and later works). They are found in soft chalks from the neighbourhood of Baalbeck (SL 13) in the NE, through Nebi Chit (SL 14) and Majdal Anjar (SL 15) to Quaroun (SL 16) (Dubertret et al. 1949-1951). The Lower Turonian ammonites of the eastern side of the Beqaa seem to belong to the extension of the Carmel-Galilee band of distribution. The thickness of the chalks seems to be considerable, although no detailed measurements of the 200-300m thick Turonian are available. On the western side of the Beqaa the ammonites are absent (SL 18); this seems to be also true for the higher parts of Mt. Lebanon. (SL 19) (Dubertret 1944, p. 26; Heybroek 1942, p. 373). Jux and Omara (1960a, p. 64; 1960b, p. 474) and Dubertret (in Arambourg 1958, pp. 205-7) note the absence of these ammonites in the Palmyra range (SL 5, SL 17).

The ammonite assemblage found in Syria-Lebanon resembles that of the Galilee (Basse 1937, 1940, 1954).

Lower Turonian ammonites were not found so far in the northern part of Transjordan (Blake 1936, 1940, Wetzel and Morton 1959). Blackenhorn found at Es Salt (J 2) in 1894 several specimens which were determined erroneously by Taubenhau (1920, p. 44) as *T. rollandi* (Th. and Per.). These ammonites actually belong to the above mentioned *Paravascoceras(?) pioti* (Fourtau) which are found again on the SW side of the Dead Sea (see map No. 2). Ammonites seem to disappear again towards the South (J 15). Still further South ammonites of the middle and upper zones are very abundant. Wetzel and Morton (1959, p. 144) give the figure of five metres for the ammonites' vertical distribution in one place. This thickness as well as the lithology of the overlying and underlying rock units show a close resemblance to those of the Southern Negev. Further South (J 11 and on) the ammonites disappear again, whereas on the opposite Negev side of the Deae Sea graben they are present. At Suwan (J 13) and probably at Hasa (J 14) the ammonites re-occur (Wetzel and Morton 1959, p. 146).

No records of Lower Turonian ammonites are available from the Judean region which is situated mostly outside Israel. One *Choffaticeras* was found by A. Gluck in 1934 in a well near Taibiyeh (I 3). Berner (1960, p. 6) noted a more chalky and less dolomitic lithology — a facies characteristic of ammonite bearing areas (Freund 1959) — of the Upper Cenomanian in bore holes at this area. Blake (1936, p. 51) mentions fossiliferous chalk below the Upper Turonian limestones at Deir Divan (I 4), 15km NE of Jerusalem. Ammonites, however, were not yet found there. Other localities in Israel are shown in the accompanying maps.

Much of the information concerning the Sinai Peninsula (S) and the Eastern

TABLE II
List of Lower Turonian ammonites occurrences shown on map 3

No.	Locality	Reference	Description
<i>Syria and Lebanon (SL)</i>			
SL 1	Khan el Djioz	Dubertret, 1937, p. 21	2-3m platy chalk with L.T.a.* covered by Senonian chalk.
SL 2	Ein el Tiné	" p. 15	3m chalk with L.T.a., covered by glauconitic chalk and conglomerate.
SL 3	Qalaat-Mhelbe	" p. 22	3m platy chalk, rare L.T.a covered by phosphatic conglomerate.
SL 4	Mohamad Joufine, Jaoubet Borghal	" p. 33	Dolomitic section with few fossils.
SL 5	Palmyra	Jux and Omara, 1960b, p. 474	No L.T.a. found.
SL 6	Nahr el Jos	Dubertret, 1944, p. 24	"
SL 7	Zéne, Sourate, Boksmaya	"	Thin layer of marl with L.T.a., no hippurites.
SL 8	Rouna, Aabrine	"	Marl with abundant L.T.a.
SL 9	Maat	"	Alternation of marl and limestone, a thin layer rich in L.T.a. above hippurites.
SL 10	Eddé, Ghorfin	" pp. 22-24	L.T.a. in a considerable vertical distribution.
SL 11	Ghazir	" p. 22	30m of marl, L.T.a. rare, found by Zumoffen (Douvillé 1910).
SL 12	Nahr el Arech	" 1937, p. 66	The marls with L.T.a. disappear.
SL 13	Baalbeck-Rayak	" 1950a, p. 25	Marl with L.T.a.
SL 14	Nebi Chit	" 1937, p. 67	Chalk with L.T.a.
SL 15	Majdal Anjar (S. of)	" 1950b, p. 41	10m of marl with L.T.a. followed by rudist limestone (hippurites etc)
SL 16	Quaroun-Baaloul	Jux and Omara 1960a, p. 64	No L.T.a. mentioned
SL 17	Damascus	Dubertret, 1950a, p. 25	"
SL 18	Zahlé-Schmistar	" 1950b, p. 41	"
SL 19	Djezzine	"	"
<i>Israel (I)</i>			
I 1	Western Galilee	Map 1	Up to 90m of chalk and limestones with abundant L.T.a.
I 2	Mt. Carmel	"	L.T.a. rare.
I 3	Taibiyeh	G.S.I. collection	<i>Chiofaticeras</i> found by Gluck.
I 4	Deir Divan	Blake, 1936, p. 51	Chalky limestone with gastropods, no ammonites mentioned.
I 5	N. Negev	Map 2	"
I 6	S. Negev	"	"
<i>Transjordan (J)</i>			
J 1	El Zerka Suweilih road	Wetzel and Morton 1959, pp. 140-142	No ammonites found. <i>E. olisipensis</i> .
J 2	Es Salt	Blanchenhorn 1894, H.U.J. coll. Taubenhaus 1920, p. 44	<i>Paravascoceras</i> cf. <i>pioti</i> Fourtau similar to those found on the SW side of the Dead Sea
J 3	7km from Amman	Blake 1940, p. 87	Concretional limestone with abundant pelecypodes and small ammonites.
J 4	Ein Humra	Wetzel Morton 1959, pp. 141-2	A bed with <i>Thomasites</i> , <i>Pseudotisotia</i>
J 5	Wadi Mujib	Blake, 1936, p. 52	L.T.a.
J 6	Ed Dirra (near Kerak)	Wetzel Morton 1959, p. 144	5m limestone with L.T.a.
J 7	Wadi Hesa	H.U.J. coll.	Several <i>Chiofaticeras</i> found by L. Picard.
J 8	La'aban, Police station	Blake 1940, p. 86	21m of shales with L.T.a.
J 9	Tafleh	Blake 1936, p. 51	Marls with L.T.a.
J 10	Wadi Musa, near Petra	Wetzel Morton 1959, p. 147	No L.T.a.
J 11	Naqb Ishtar	" p. 146	No L.T.a.
J 12	Suwan	" "	<i>Neophychites</i> and <i>Thomasites</i> less than 50m above Nubian sandstone.
J 13	Hasa	" "	<i>A. deverianum</i> .
J 14	S. of Naur	" "	No ammonites mentioned.
J 15	"	Blake 1936, p. 51	"
<i>Sinai (S)</i>			
S 1	Gebel el Moghara	S.O.C.E. 158	No L.T.a. found.
S 2	Gebel Helal	S.O.C.E. 157	<i>Thomasites jordani</i> and other L.T.a.
S 3	Gebel Helal	Blake 1940, p. 82	Limestone with flint and large ammonites.
S 4	Gebel Minshera	Moon and Sadek 1921, p. 110	Did not find ammonites.
S 5	Gebel Minshera	S.O.C.E. 153	36m of light 1mst. and fossiliferous marly limestone with <i>Neophychites</i> , <i>Leonicer</i>
S 6	Gebel Kherim	S.O.C.E. 152	12m of chalky limestone, varying soft and hard, large ammonites.
S 7	Gebel Yeleg	Moon and Sadek 1921, pp. 101-2	In the NE <i>Duranita</i> marks the Turonian base. L.T.a. are not mentioned
S 8	Gebel Fallig	Moon and Sadek 1921, p. 96	L.T.a. are not mentioned.
S 9	Gebel Fallig	S.O.C.E. 155	L.T.a. are not mentioned.
S 10, 11, 12, 13	SW of Gebel Yeleg	Moon and Sadek 1921, pp. 101-2	Limestone with flint and large ammonites.
S 14	Gebel Giddi	Moon and Sadek 1921, pp. 85-86	Large ammonites, <i>Leonicer</i>
S 15, 16, 17	Gebel Umm Khushelb	Moon and Sadek 1929, p. 93	No ammonites were found in the NW and SW domes.
S 18	Gebel Hamra	S.O.C.E. 136	48m of fossiliferous chalky 1mst. Lower part softer, contains abundant ammonites, <i>Leonicer</i> .
S 19	Gebel Raha	Barthoux 1922, p. 70	No ammonites recorded
S 20	Ein Sudr	Moon and Sadek 1921, pp. 77-8	"
S 21	W. Gharandel, W. Akhal	Moon and Sadek 1921, p. 82	No ammonites recorded.
S 22	W. Gharandel	?Barthoux 1922, pp. 71-2	Many <i>Vascoceras</i> , <i>Thomasites</i> , <i>Pseudotisotia</i> .
S 23	G. Edemat	S.O.E.C. 110	26m of light grey sandy and chalky fossiliferous 1mst. Many L.T.a., <i>Thomasites</i> , <i>Leonicer luciae</i>
S 24	G. Tih	Greco, 1915	L.T.a.
S 25	G. Tih	Bail 1916, pp. 136-9	Abundant L.T.a., <i>L. segne</i> , <i>T. rolland</i>
S 26	4 km NW off Bir Nasb	Bail 1916, p. 136-9	Abundant L.T.a., <i>L. segne</i> , <i>T. rolland</i>
S 27	G. Farsh el Ghazlan	Barron, 1907, p. 149	30m of 1mst. and shales, large L.T.a.
S 28	Sheikh Atiya	Douvillé 1928	Numerous L.T.a.
S 29	G. Rigm	S.O.E.C. 105	19m of marls and sandy shales with <i>Thomasites</i> and <i>Leonicer</i> .
S 30	W. Fairan, G. Nazazzat	S.O.E.C. 108	31m of shales. <i>Exogyra</i> , ammonites?
S 31	G. Araba	S.O.E.C. 104	16m of limestone with <i>Vascoceras</i> below <i>Leonicer</i>
S 32	G. Naqus	S.O.E.C. 103	10m of marly and chalky 1st., rare <i>Thomasites</i> .
S 33	G. Husva	Barthoux 1922, p. 70	Abundant L.T.a.
		Barron 1907, p. 149	No ammonites recorded
		S.O.E.C. 101	No ammonites recorded.
		S.O.E.C. 102	3m of gypsiferous fossiliferous 1mst., <i>Leonicer quasi</i> .
<i>Eastern Desert (Egypt) (E)</i>			
E 1	Rod el Hamal (Wadi Araba)	S.O.E.C.	No L.T.a. mentioned.
E 2	W. Askar el Bahari	S.O.E.C. 27	9m of shaly limestone; <i>Leonicer</i> spp.
E 3	G. Thelemet (Wadi Araba)	S.O.E.C. 26	18m of slightly sandy, marly 1mst. <i>Leonicer</i> spp. <i>Thomasites</i> spp.
E 4	G. Shaira (Wadi Araba)	S.O.E.C. 22	16m limestone with <i>Leonicer</i> , <i>Pseudaploceras</i> cf. <i>footeanum</i> .
E 5	St. Paulus convent	Greco 1915	Numerous L.T.a. collected by Figari Bey.
E 6	S. Gallala plateau	Fourtau 1904	<i>C. quasi</i> and <i>A. pioti</i> .
E 7	W. um Tarfa	Douvillé 1928	Numerous L.T.a.
E 8	W. um Tarfa	Greco 1915	Numerous L.T.a.
E 9	Head of Wadi Um Arta	S.O.E.C. 18	28m of alternating 1mst. and shale, <i>L. segne</i> below <i>L. luciae</i>
E 10	Wadi Mor	S.O.E.C. 19	15m of shaly and sandy 1mst. <i>Paravascoceras</i> below <i>Leonicer</i> .
E 11	W. Hawashieh	Douvillé 1928	L.T.a.
E 12	Hea of Wadi Abu Had	Eck 1914	L.T.a., Schweinfurth's collection.
E 13	G. Gharamul	Solger 1904	<i>Chiofaticeras segne</i>
E 14	G. Zeit	Douvillé 1928	L.T.a.
E 15	Sufr el Dib	S.O.E.C. 16	27m of shales and 1mst., <i>Paravascoceras</i> below <i>Leonicer</i> .
E 16	W. Qena, W. Seil	S.O.E.C. 15	25m of nodular marl, <i>Vascoceras</i> sp.
E 17	Abu Roush (Cairo)	S.O.E.C. 14	No L.T.a. recorded
E 18	S. of Wadi Mellaha	S.O.E.C. 11	No L.T.a. recorded.
E 19	S. part of Wadi Qena	S.O.E.C. 10	18m 1mst. <i>L. luciae</i> .
E 20	G. Abu Sharel Bahari	S.O.E.C. 8	No L.T.a. recorded.
		S.O.E.C. 5	No L.T.a. recorded.
		S.O.E.C. 13	No L.T.a. recorded.

Desert (E) was taken out of unpublished columnar sections made by E. J. Foley, H. W. Haight, K. D. White, F. Iskander, S. Soliman and A. Bandali for the Standard Oil Company of Egypt during 1940–1942, and were handed over to the Hebrew University of Jerusalem for fauna determination; L. Picard had determined at that time their ammonite fauna. Further information was found in the numerous paleontological works mentioned above and in the geological works of Beadnell (1902), Barron (1907), Ball (1916), Moon and Sadek (1921) and Barthoux (1922).

The northern boundary of the ammonite occurrence in Sinai is distinct. Its trend is similar to that of the lower zone in the Central Negev. The position of the southern boundary is less clear, mainly in the eastern part of Sinai. In the area between G. Raha (S 19) and Rod el Hamal (E 1) ammonites seem to be absent. Unfortunately, no special attention was paid to the exact vertical distribution of the Lower Turonian ammonites in Egypt, yet it does not exceed 30m.

The faunal assemblage resembles that of Southern Israel; even the same sequence of ammonite zones could be detected in some detailed sections (E 8, E 9, E 12).

The main results derived from the maps are:

1. All the distinct and well defined boundaries and isofacies lines (solid line on maps) trend NE. They diverge somewhat to the north in the northern parts and to the east in the southern parts. Besides, there is a difference in the trend between the lower and upper zones which was detected only in the Northern Negev. The inferred boundary lines may be wrong in position and direction.
2. The ammonites of the middle and upper zones disappear laterally through the wedging out of their rock units, sometimes showing indications of a shore environment in the NW and SE. The ammonites of the lower zone disappear through the facies change in their rock unit. The whole Upper Cenomanian–Turonian section seems to be less dolomitic and more chalky in the ammonite distribution areas.
3. The thickness of the ammonite bearing strata is: 3m in Lattaquia, 20–30m in Beyrouth, 80–90 m in Carmel–Galilee–Beqaa, up to 30m in Northern Negev, and not exceeding 10m in the Southern Negev. Curiously enough, the width of the ammonite distribution areas seems to be in inverse proportion to their thicknesses (see cross sections, Figures 1 and 2).

As shown in Figure 2 the distances between the centers of the ammonite distribution areas, when projected on a NE–SW section, are roughly 40–50km. The situation in central Israel and in Sinai is not clear.

4. The Lower Turonian ammonites are always embedded in detritic limestones, chalks and marls, regardless of the underlying and overlying rocks, which may be rudist reef limestones in the north, limestones and shales in the Negev

or shales and sandstones in east Transjordan, south Sinai and the Eastern Desert.

PALEOGEOGRAPHIC INTERPRETATION

As pointed out above (p. 1) Dubertret showed that the paleogeography of the Lower Turonian is not consistent with the simple ecological explanation proposed by Douvillé. However, before accepting his tectonic explanation, we should reconsider other causes which could have influenced the distribution of the ammonites. Thus, a current may cause local differences in marine environment along narrow belts. A current may be favourable to a certain group of organisms, may prevent the deposition of soft mud and may also supply the Mg solution for the dolomitisation of the limestones. On the other hand, areas outside this current may be favourable to another group of organisms, and soft sediments may be deposited. We could explain in this way the facies changes in the Cenomanian-Turonian rocks, but it is highly doubtful that several (about eight) such currents could have existed contemporaneously in a parallel and well spaced order. Furthermore, currents could not have formed the shore features on the boundaries of the ammonite distribution areas.

One is inclined, therefore to follow Dubertret's hypothesis, attributing a tectonic cause to the Lower Turonian facies changes. Tectonic movement formed long ridges, some of which even emerged and formed shallow islands (bordered by shore lines); but also the submerged parts of the ridges were unfavourable to ammonites and marly sedimentation. As the channels in which the ammonites lived were apparently filled up by Lower Turonian sediments and the overlying strata were deposited on a flat surface, the land-sea relief could not be much higher than the thickness of the thickest sediments (90m in the Galilee)*. The special conditions prevailing in such long shallow bodies of water, so far away from the deep sea may be the cause for the flourishing of the big (up to 60 cm) ammonites which outnumber any other Cretaceous assemblage in Israel.

As the distribution areas of the Lower Turonian ammonites are parallel and well spaced, and no fault could be detected along them, it seems sound to assume that the relief was formed by a slight folding which formed long shallow synclines and anticlines. The synclines become shallower and wider towards the Arabian shield (SE). The same phenomenon towards the NW (in Beyrouth and Lattaquia) may indicate another shield in this direction.

The isofacies lines are usually transverse to the present fold and fault structure. It thus seems that the parallelism between the ammonite occurrences and the present structure in Lebanon, as noted by Dubertret (1944), is accidental, and the later structures should not be regarded as the continuation of pre-Turonian tectonic movements.

* Gignoux (1955, p. 455) estimates a depth of 50-100m for the wide Cretaceous transgressions.

The tectonic movements apparently began already in the Upper Cenomanian, as indicated by the dolomite-chalk facies changes which have a similar geographic position in the rocks of this age, as those occurring in Turonian strata.

POST TURONIAN TECTONIC MOVEMENTS

The Lower Turonian ammonites, being a good marker, both vertically (stratigraphic) and horizontally (geographic), may elucidate some later tectonic movements.

1. Sediments of Senonian age directly overlie the Lower Turonian rocks in Gebel Ansariyeh (Syria), Elkosh (Western Galilee) and the NW flank of Hamakhtesh-Hakatan anticline. The 80m or more of Upper Turonian limestones are missing. This gap is due to erosion, being in close relationship with the present anticlines in the Negev; but in the Galilee no such regular pattern was observed, except some relationship to fault lines.

2. Strike slip movement is assumed for some faults in Israel. Lower Turonian ammonites occurring on both sides of these faults may throw some light on this problem.

In map No. 1 the Daliya marl is shifted 8-10km to the SE off the Yirka fm. band. This might be explained by strike slip movement along the large NE border fault of Mt. Carmel. However, the apparent shift may be due to the en échelon position of the Lower Turonian synclines.

Bentor and Vroman (1954, p. 126) consider the transverse faults of the Central Negev (Zin, Ramon, Badad, Faran) to be strike slip faults. As far as the continuation of the Lower Turonian isofacies lines on both sides of the Ramon fault could show, no considerable strike slip movement occurred here since the Lower Turonian. The same applies to the Zin fault, as the Kvuda assemblage has not yet been found further East in the Northern Negev anticlines.

Far more convincing in this respect is the theory, developed lately by Quennell (1956, 1958) on a strike slip movement of 100km to the north of Transjordan along the Dead Sea Rift. The present-day position of two separate Lower Turonian ammonite assemblages on both sides of the rift valley (S Negev - E Dead Sea; SW Dead Sea - Amman, see map No. 3), confirms this theory. It is interesting to note that no such movement is indicated by the same criteria along the Gulf of Suez, and that the Beqaa ammonite occurrence is not considerably shifted off the Carmel-Galilee band.

ACKNOWLEDGEMENTS

The author is greatly indebted to Prof. L. Picard for his encouragement and guidance in the present investigation and to the Hebrew University authorities for the permission to publish this paper. Thanks are due to N. Shulman, M. Raab and Z. Reiss for the constructive criticism of the manuscript, and to A. Yakin for drafting the maps and sections.

REFERENCES

- ARAMBOURG, C., DUBERTRET, L., SIGNEUX, J. AND SORNAY, J., 1958, Contribution à la Stratigraphie et à la Paleontologie du Crétacé et du Nummulitique de la marge NW de la Péninsule Arabique, I. Stratigraphie par L. Dubertret, *Notes et Mémoires sur le Moyen Orient*, T.7, pp. 193-251.
- ARIYE, I., 1959, Stratigraphy and Paleontology of the Eastern Jeroham range. M.Sc. thesis for the Hebrew University, Jerusalem, (in Hebrew).
- AVNIMELECH, M., 1950, Sur les lacunes de la sédimentation crétacée dans les environs de Jérusalem, *C.R.Ac.Sci.*, T.230, 1088-1090.
- BALL, J., 1916, The Geography and Geology of West Central Sinai, *Minist. Finance, Egypt*, 219 pp.
- BARRON, 1907, Topography and Geology of Peninsula of Sinai (Western part). *Surv. Dept. Cairo*.
- BARTHOUX, J., 1922, Chronologie et description des Roches Ignées du Désert Arabique, *Mém. Inst. Egypte*, T.V, 260 pp.
- BASSE, E., 1937, Les céphalopodes crétacés des massifs côtiers Syriens, *Haut Commiss. Republ. Franc. Syrie-Liban.*, Vol. 2, pt. 2, Etudes Pal., pp. 165-230, pls. 8-11.
- BASSE, E., 1940, Les céphalopodes crétacés des massifs côtiers Syriens, *Haut Commiss. Republ. Franc. Syrie-Liban.*, Vol. 3, pt. 2, pp. 412-490.
- BASSE, E., 1954, Sur une ammonite nouvelle du Turonien du Liban, *Haut Commiss. Republ. Franc. Syrie-Liban.*, Vol. 5, p. 199-204, pl. IV.
- BEADNELL, H. J. L., 1902, The Cretaceous region of Abu-Roash, *Geol. Surv. Egypt, Report*, 1900, pt. II, 46 pp.
- BENTOR, Y. K. AND VROMAN, A., 1951-1957, The Geological map of Israel on a scale of 1:100,000 ser. 1, Southern Israel. Sheet 18: Ovdar; Sheet 16: Har Sdom; Sheet 19: Nahal Arava.
- BENTOR, Y. K. AND VROMAN, A., 1954, A structural contour map of Israel (1:250,000) with remarks on its dynamical interpretation, *Bull. Res. Counc. of Israel*, 4, 125-135, 4 figs., map.
- BERNER, U., 1960, Subsurface geology of the eastern coastal plain, M.Sc. thesis for the Hebrew Univ. Jerusalem, (in Hebrew).
- BLAKE, G. S., 1935-1936, *The Stratigraphy of Palestine and Its Buildings Stones*, Jerusalem, Printing and Stationary Office, 133 pp.
- BLAKE, G. S., (in IONIDES) 1940, *A report on Geology, Soils and Minerals and Hydrogeological correlations of Transjordan*, London, 372 pp.
- BLANCKENHORN, M., 1890, *Beitraege zur Geologie Syriens: Die Entwicklung des Kreidesystems in Mittel und Nord Syrien*. 135 pp. Cassel.
- BLANCKENHORN, M., 1931, Geologie Palästinas nach heutiger Auffassung, *Zeitschr. deutsch. Paläst. Ver.*, Vol. 54, 50 pp., 1 pl.
- BROWN, M., 1961, The Geology of the Imara and Sherif anticlines, N. Negev, M.Sc. thesis for The Hebrew University, Jerusalem, (in Hebrew).
- DIENER, C., 1886, *Libanon*, Wien, 412 pp.
- DOUVILLE, H., 1910, Etudes sur les Rudistes, *Mém. Soc. Géol. Fr.*, No. 41, Rudistes du Liban pp. 52-75.
- DOUVILLE, H., 1912, Evolution et classification des Pulchelliidés, *Bull. Soc. Géol. Fr.*, Sér. 4 Vol. 11, pp. 285-320.
- DOUVILLE, H., 1928, Les Ammonites de la craie supérieure en Egypte et au Sinai, *Mém. Acad. Sci. Inst. Fr.*, Vol. 60, 41 pp., 7 pl.
- DUBERTRET, L., 1937, Le Massif Alaouite ou Djebel Ansariyeh, *Haut Commiss. Répub. Franc. Syrie-Liban.*, Vol. 3, pp. 9-42.

- DUBERTRET, L. AND VAUTRIN, H., 1937, Révision de la stratigraphie du Crétacé du Liban, *Haut Commiss. Répub. Franc. Syrie-Liban*, Vol. 3, pp. 43-74.
- DUBERTRET, L., 1944, Sur le Turonien (Crétacé Moyen) du Liban, *Publ. techn. et scient. de l'étude fr. d'Ingénieurs de Beyrouth*, (Liban), No. 6, 7 pp.
- DUBERTRET, L., 1947, Problèmes de la géologie du Levant, *Bull. Soc. Geol. Fr.*, 5e Sér., t. 17, pp. 23-27. fig. 8-10.
- DUBERTRET, L. ET AL., 1949-1951, Carte géologique du Liban au 50,000. a) Feuille de Rayak; b) Feuille de Djezzine.
- ECK, O., 1909, Neue Ammoniten aus der oberen Aegyptischen Kreide, *S. B. Naturf. Fr. Berl.* No. 3, p. 179.
- ECK, O., 1910, Vorläufige Mitteilung über Cephalopoden der Schweinfurthschen Sammlung, *Monatsber. d. deutsch. geol. Gesel.*, Vol. LXII, pp. 379-386.
- ECK, O., 1914, Die Cephalopoden der Schweinfurthschen Sammlung, *Zeitsch. d. deutsch. geol. Gesel.*, Vol. LXVI, pp. 179-216.
- FOURTAU, R., 1904, Etude de la faune crétacique d'Egypte, *Bull. Inst. Egyptien*, Sér. 4, Vol. IV, pp. 231-349.
- FREUND, R., 1959, On the stratigraphy and tectonics of the Upper Cretaceous in Western Galilee, *Bull. Res. Counc. of Israel*, 8G, (1), 43-50.
- FREUND, R., 1960, Type sections of three formations in Western Galilee, *Bull. Res. Counc. of Israel*, 9G, (2-3), 159-160.
- GIGNOUX, M., 1955, *Stratigraphic geology*, 682 pp., 4th edition, in English, San Francisco.
- GRECO, B., 1915, Fauna cretacea dell'Egitto, *Pal. Ital.*, Vol. XXI 1915, pp. 189-231, pls. 17-22.
- HEYBROEK, F., 1942, La géologie d'une partie du Liban Sud, *Leidsche Geologische Mededeelingen*, Vol. 12, Liefer. 2, p. 251-470.
- JUX, U. AND OMARA, S. M., 1960, Die Qasyoun — Antiklinale bei Damascus (Syrien), *Zeit. d. deutsch. geol. Gesel.*, B.112, T.1, pp. 62-74, text figs.
- JUX, U. AND OMARA, S. M., 1960, Der geologische Aufbau der Umgebung von Palmyra in Syrien, *Geol. Rundschau*, Vol. 49, T.2, pp. 467-486, pl. 14.
- KARCZ, J., 1958, The structure of the Northern Carmel, *Bull. Res. Counc. of Israel*, 8G, (2-3), 119-130.
- KASHAI, E., 1958, The Geology of Eastern and Southwestern Carmel, Ph.D. thesis, Hebrew Univ. Jer., (in Hebrew).
- KASHAI, E., 1958, A note on the revision of the stratigraphy of the Southern Carmel, *Bull. Res. Counc. of Israel*, 7G, (2-3), 164-165.
- MANDEL, S. AND ARAD, A., 1958, First report on the geo-hydrology of the Western Galilee. Tel-Aviv (in Hebrew).
- MOON, E. W. AND SADEK, H., 1921, Topography and Geology of Northern Sinai; Survey of Egypt, *Petrol. Research Bull.*, No. 10, Cairo.
- NIR, J., 1959, The Geology of the Fault-Scarps, SW Dead Sea, M.Sc. Thesis, The Hebrew University, Jerusalem, (in Hebrew).
- PICARD, L. AND BENTOR, Y. K., Geological map of Israel on 1:250,000 (in publication).
- PICARD, L. AND KASHAI, E., 1958, On the lithostratigraphy and tectonics of the Carmel, *Bull. Res. Counc. of Israel*, 7G, (1), 1-26.
- QUENNEL, A. M., 1956, Tectonics of the Dead Sea rift, *Geol. Surv. of Tanganyika*, (Unpublished).
- SHAW, S. H., 1947, *Southern Palestine. Geological Map on a Scale of 1:250,000 with Explanatory Notes*. Jerusalem, Palest. Govt. Print.
- SOLGER, F., 1903, Ueber die Jugendentwicklung von *Sphenodiscus lenticularis* etc., *Zeitsch. d. deut. geol. Gesel.*, Vol. 55, pp. 69.-84

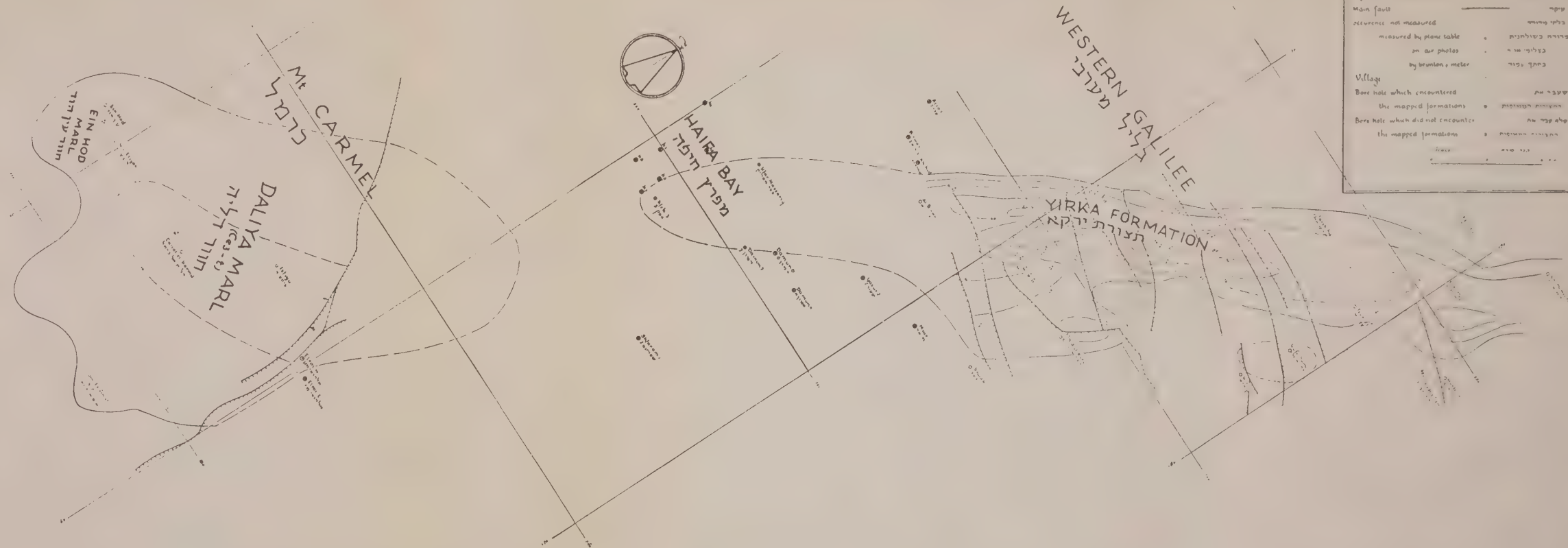
- Standard Oil Company of Egypt, 1940-1941, Columnar sections by E. J. Foley, H. W. Haight, K. D. White, F. Iskander, S. Soliman, A. Bandali. (unpublished reports).
- TAUBENHAUS, H., 1920, Die Ammoneen der Kreideformation Palästinas und Syriens, *Zeitsch. d. deutsch. Palästina-Vereins.*, Bd. XLIII, Heft 1-2.
- VROMAN, A. J., 1957, The Cenomanian-Turonian boundary in Northern Israel, (Preliminary note). *Bull. Geol. Surv. Israel*, No. 17, pp. 1-2.
- VROMAN, A., 1960, Note on Rock Units of Mt. Carmel, Israel, *Bull. Geol. Surv. Israel*, No. 27.
- WETZEL, R. AND MORTON, D. M., 1957, Contribution à la géologie de la Transjordanie, *Notes et Mém. sur le Moyen Orient*, T.7 (1959), pp. 95-191.
- ZUMOFFEN, G., 1926, *Géologie du Liban*, Paris, 166 pp.

תל אביב
1952

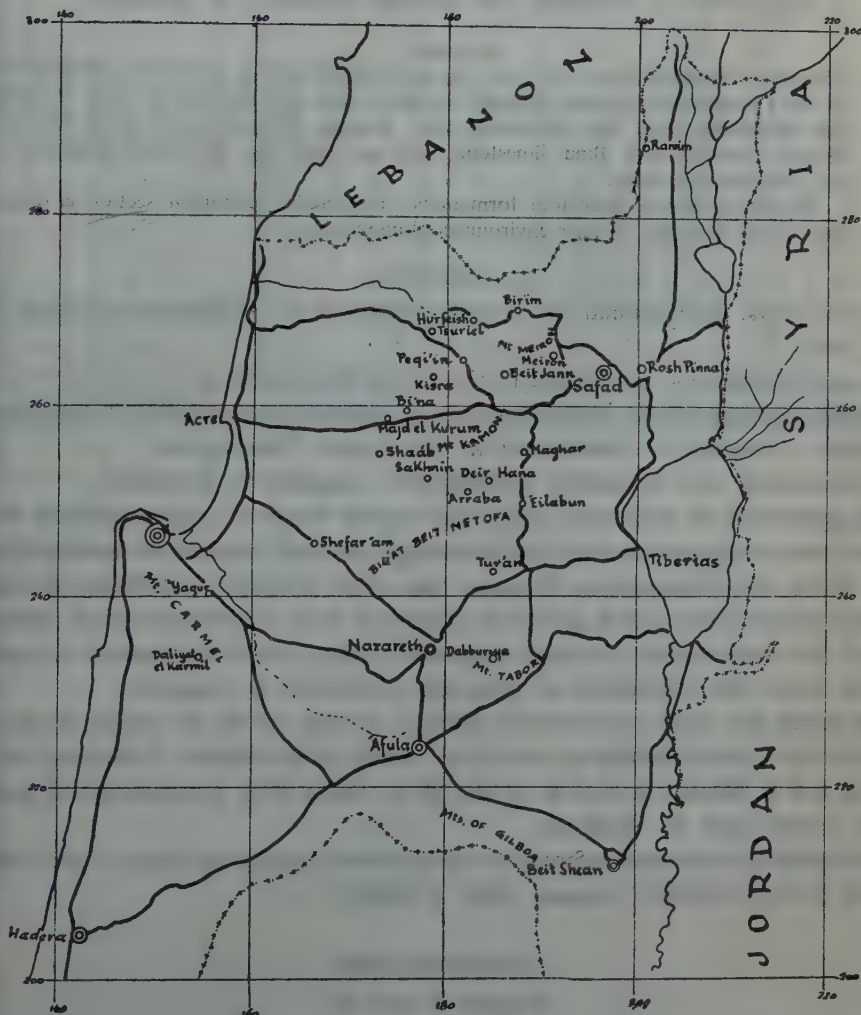
Map No. 1
ISOPACH MAP OF YIRKA FORMATION AND DALIYA MARL - Northern ISRAEL
מפת שוה-עובי של תצורת ירקא וחורר דליה בצפון ישראל

מקרא LEGEND

Isopach contour line	קו שווה עובי
Inferred isopach contour line	קו שווה עובי מניח
Main fault	הפסק עיקרי
recurrence not measured	נקודה בליק מניח
measured by plane table	פרומה בשולחנות
on air photos	בצלילי אוויר
by Brunton, meter	במחש, מטר
Village	ישוב
Bore hole which encountered the mapped formations	קרוח שפגש את התצורות המפותחות
Bore hole which did not encounter the mapped formations	קרוח שלא פגש את התצורות המפותחות
Scale	מסל



Scale = 1:500,000



ON THE CENOMANIAN-TURONIAN LITHOSTRATIGRAPHY OF CENTRAL GALILEE

U. GOLANI

Department of Geology, The Hebrew University of Jerusalem

ABSTRACT

Instead of the vague terms Ce_1 , Ce_1 , Ce_3 etc., usually used to denote the different parts of the Cenomanian-Turonian sequence in the Galilee and the Carmel, four formations are introduced here. The formations are: Kamon Dolomite, Deir Hana formation, Saknin Dolomite and Bina limestone. They are valid for the Central Galilee and the neighbouring areas.

The description of these four formations with detailed columnar section is followed by a short summary of their environmental condition.

INTRODUCTION

For many years, the Cenomanian-Turonian stages of the Galilee were divided into four parts:

1. Lower Dolomite — attributed to the Lower Cenomanian.
2. Dolomites and Chalks containing chert — referred to the Middle Cenomanian.
3. Upper Dolomite — determined as the Upper Cenomanian.
4. Lithographic and Crystalline Limestone — regarded as Turonian.

The separation of these four parts was mainly based on reconnaissance work without measuring sections and/or determining the exact boundaries between them. As a result, the Cenomanian-Turonian was often divided by different markers.

In the present paper, which gives in a condensed form, the stratigraphical information on the Cenomanian-Turonian sequence of the Central Galilee and the neighbouring areas, the introduction of three new formations is suggested.

The results are based on measured sections, carried out by the author in several places of the Central Galilee and on M.Sc. theses (of the Hebrew University) of R. Freund and E. Eliezri, as well as on the Ph.D. thesis of E. Rosenberg and papers by P. Grader and A. Shadmon.

The reader is, moreover, referred to the published geological maps of the Galilee (Picard 1956, 1:100,000, Vroman 1958, 1:50,000).

A. KAMON DOLOMITE

(Figures 1 and 2)

Lower Cenomanian (Ce_1) Picard, 1:100,000 maps, 1956.

Lower Cenomanian (L.C.) Grader, 1958.

Received February 3, 1961.

SECTION No 4

KAMON DOLOMITE
M^{ts} KAMON
Eastern slope of Mt Kamon above the mills
Coordinates: 180025716 to 1636925726
Attributed to snow. Thickness measured by tape and Brunton
14th January 1991
By Uri Golani

KAMON DOLOMITE
M^{ts} KAMON
Eastern slope of Mt Kamon above the mills
Coordinates: 180025716 to 1636925726
Attributed to snow. Thickness measured by tape and Brunton
14th January 1991
By Uri Golani

KAMON DOLOMITE
M^{ts} KAMON
Eastern slope of Mt Kamon above the mills
Coordinates: 180025716 to 1636925726
Attributed to snow. Thickness measured by tape and Brunton
14th January 1991
By Uri Golani

[illegible]

2	3	4	5	6	7	8	9	10	11	12	13	14	15	16	17	18	19	20	21	22	23	24	25	26	27	28	29	30	31	32	33	34	35	36	37	38	39	40	41	42	43	44	45	46	47	48	49	50	51	52	53	54	55	56	57	58	59	60	61	62	63	64	65	66	67	68	69	70	71	72	73	74	75	76	77	78	79	80	81	82	83	84	85	86	87	88	89	90	91	92	93	94	95	96	97	98	99	100
---	---	---	---	---	---	---	---	----	----	----	----	----	----	----	----	----	----	----	----	----	----	----	----	----	----	----	----	----	----	----	----	----	----	----	----	----	----	----	----	----	----	----	----	----	----	----	----	----	----	----	----	----	----	----	----	----	----	----	----	----	----	----	----	----	----	----	----	----	----	----	----	----	----	----	----	----	----	----	----	----	----	----	----	----	----	----	----	----	----	----	----	----	----	----	----	----	----	-----

2	3	4	5	6	7	8	9	10	11	12	13	14	15	16	17	18	19	20	21	22	23	24	25	26	27	28	29	30	31	32	33	34	35	36	37	38	39	40	41	42	43	44	45	46	47	48	49	50	51	52	53	54	55	56	57	58	59	60	61	62	63	64	65	66	67	68	69	70	71	72	73	74	75	76	77	78	79	80	81	82	83	84	85	86	87	88	89	90	91	92	93	94	95	96	97	98	99	100
---	---	---	---	---	---	---	---	----	----	----	----	----	----	----	----	----	----	----	----	----	----	----	----	----	----	----	----	----	----	----	----	----	----	----	----	----	----	----	----	----	----	----	----	----	----	----	----	----	----	----	----	----	----	----	----	----	----	----	----	----	----	----	----	----	----	----	----	----	----	----	----	----	----	----	----	----	----	----	----	----	----	----	----	----	----	----	----	----	----	----	----	----	----	----	----	----	----	-----



Figure 1

Kamon Dolomite and Deir Hana formation on the southern slope of Mt. Kamon



Figure 2

Typical appearance of the Kamon Dolomite. West of Acre-Safad road near Farod Spring

Cenomanian, Lower part (Ce₁) Vroman, 1:50,000 maps, 1958.

Sajur Dolomite; R. Freund (unpublished report), 1958.

Name adapted from Mt. Kamon (Jebel Kamana) in the Central Galilee, on the southern side of Acre-Safad road, near the village of Rama.

The type section was taken on the eastern slope of Mt. Kamon (coord. 18500/25716 to 18439/25726). Section No. 1.

Boundaries

Top and base boundaries are very distinct both in field and on air photographs. The lower boundary of the Kamon Dolomite is very sharp; dolomite layers are found without any transitional zone above the limestones and marls of the Tsalmon formation*.

Upon the hard banks which distinguish the top Kamon Dolomite there follow soft yellow dolomites with chert, referred in the following chapter to the Deir Hana formation.

Description

The thickness of the Kamon Dolomite is 197 m. It is comprised of four main types of dolomites with many transitional varieties.

1. Dolomite, white crystalline, very fine grained, dense and of chalky appearance;
2. Dolomite, light gray to gray, crystalline, medium to coarse grained, hard, compact. Resembles closely the Mizzi Yahudi dolomite of Jerusalem.
3. Dolomite, white to light gray, crystalline, medium grained, very porous, soft to friable, with sugary appearance. Resembling the Kiryat Anavim Dolomite near Jerusalem.
4. Dolomite, somewhat clayey, yellow, fine to medium grained, medium hardness. Found mostly in the lower part of the formation.

The colour of the Kamon formation is white, gray light-yellow and-brown with all transitional shades.

All the dolomites are crystalline, ranging from very fine to coarse, but mostly they are fine to medium grained. The hardness of the rocks varies between soft and very hard. Most of the dolomites of this formation are porous. The porosity, however, varies considerably from one rock-type to another.

The different dolomite types are randomly distributed through the whole section; therefore, the formation cannot be subdivided into members.

Thin marl laminae (mostly few mm, but sometimes up to 10cm thick) appear between the dolomite beds, especially in the lower part of the formation. The marl is mostly undetectable in the field, but may be seen in new road cuts or in other artificial exposures.

* The Tsalmon formation consists of about 45m, of limestone and yellow marls, rich in macrofossils and belongs to the Upper Albian stage. This term has not yet been introduced into the literature.

The thin mail beds are often covered by a nari (caliche) crust. But in contrast to the normal nari found on chalks, this nari has a travertine and tuffa texture and a "flow" structure on the surface. Rain and ground water—which percolates vertically through the dolomite layers—stop on top of the thin marl laminae and flows out laterally to the surface. There, after the water evaporates, the carbonates are precipitated. That is the most likely hypothesis for the appearance of "nari" on purely dolomitic rocks.

A few thin layers of quartzolite (silicified dolomite) and several horizons of idiomorphic quartz crystals (up to 2 cm) are found in the upper half of the formation. Very scattered brown chert nodules are present near the top of the formation.

The bedding is good to very good. Beds are between 0.5 to 4.0 m thick, usually 1–1.5m.

Small cliffs 2–3m high and terraces 1–2m wide, caused by the various dolomite types (Figure 2), interrupt the otherwise uniform slope profiles of the Kamon Dolomite. The vegetation is poor in comparison with that of the overlying Deir Hana formation.

The Kamon Dolomite is practically devoid of fossils; except for some very badly preserved impressions and cavities.

Distribution

The Kamon Dolomite can be traced without any considerable change, at least from the Valley of Yezreel (*Esdraelon*) to the northernmost Galilee. It outcrops along a N–S line along the structural backbone of Galilee. There are four other localities where a full section of the formation is exposed.

(1) *Mt. Netofa* (Jebel Hazwa)

The thickness of the Kamon Dolomite in Mt. Netofa cannot be determined accurately because of the many faults. According to some measurements (made by the author), the thickness of the formation is about 170–190m, which is almost the same as in the type locality. The dolomite types, the bedding, the morphology and the overall appearance are the same as on Mt. Kamon.

A layer of 2–4m, of dark, yellow dolomite separates here the Tsalmon formation from the Kamon Dolomite. This yellow dolomite is the northern tongue of the Kesullot Dolomite* of the Nazareth hills.

(2) *Mt. Kesullot* (Nazareth Hills) and *Mt. Tabor*

In this southernmost exposure, the Kamon Dolomite lies above the Kesullot Dolomite.

The thickness of the Kamon formation here is about 160–170m. The general rock character is the same as in the type locality, but there are possibly, less dolomite varieties. No fossils have been found.

* Kesullot Dolomite is a formation of about 70 m, composed of alternating thick yellow dolomites and thinner yellow marls. This term has not yet been introduced into the literature.

(3) *Mt. Ha'ari (above Rami region)*

The stratigraphy of Mt. Ha'ari has been worked out by I. Eliezri (1959). He found that the Kamon Dolomite (called by him "Lower Cenomanian" or Haari Dolomite) attains a thickness of about 150m. Comparing his columnar section with other detailed sections, it is obvious that his upper boundary compared with the Kamon Dolomite as defined here is about 30m too low.

The many dolomite varieties, the good bedding and the horizons of milky quartz crystals are the same as in the type locality of Kamon. The more cliffy morphology and V shapes of the young wadis is due to the fact that the formation outcrops on very steep slopes caused by the big Majd el Kurum fault scarp and to higher topographic position (800 m against 300 m at Kamon) and consequently higher rainfall.

Eliezri mentions *Cerithium elias* Boehm and *Nerinea cochleae formis* Conr. in the Kamon Dolomite of Mt. Ha'ari, yet the exact locality is not given.

(4) *Ramim (Manara) and Naftali Mountains*

The stratigraphy of this region has been worked out by E. Rosenberg (1960).

The thickness of the Kamon Dolomite here is 280 m. According to the description given by E. Rosenberg, there is no doubt that this is, in fact the Kamon Dolomite. The present author believes, however, that the upper part of the section belongs to the overlying Deir Hana formation, which would reduce considerably its thickness and bring it nearer to that of the type section.

The age of Kamon Dolomite

The Lower Cenomanian age of the Kamon Dolomite is inferred from the position of the formation between Albian limestones and marls containing *Knemiceras* and *Acanthoceras* bearing chalks of the Deir Hana formation to which an Upper Cenomanian age is attributed.

It is not yet known, however, whether the lithological boundaries of the formation coincide with the time lines. It is not unlikely that the lower part of the Kamon Dolomite belongs to the Upper Albian (Vraconkian stage).

Correlation

The stratigraphical relations of the Kamon Dolomite to the Yagur Dolomite in the Carmel (350 m) and the so-called Lower Cenomanian of the Judean Mountains (over 200 m) has not yet been clarified. It is believed that these formations are identical. More work has to be done to verify this assumption.

B. DEIR HANA FORMATION

(Figures 3,4,5,6,7)

Middle Cenomanian (Blake 1936, 1:250,000).

Middle Cenomanian Ce₂ (Picard 1956, 1:100,000; Vroman, 1958 1:50,000)



Figure 3

Deir Hana formation with its three members on the southern slope of Jebel Abarya



Figure 4

Deir Hana formation, Nahal Kercn, 2 km south of Sasa. Hard banks of dolomite alternating with soft chalky beds



Figure 5
Chert lens in hard dolomite, Deir Hana formation, Mt. Tabor



Figure 6
Chert laminae in soft "chalky" dolomite, Deir Hana formation, Sasa-Hurfeish road



Figure 7

Chert nodules and lenses, Deir Hana formation near Sasa

Upper Cenomanian, lower part U.C.1 (Grader 1958).

Peqi'in formation (Freund 1959)*.

The formation is named after the village of Deir-Hana in Central Galilee (coord. 1845/2507). The type section was taken on the southern slope of Mt. Kamon (coord. 18252/25656 to 18240/25654. Section No. 2.

Boundaries

Lower boundary: The well-bedded gray and white dolomites of the Kamon Dolomite are overlain by yellow dolomites with thin layers of chert and many chert nodules of the Deir Hana formation. The lower part of these yellow dolomites is quite soft and frequently covered with soil, nari and dense vegetation.

Upper boundary: The beginning of very hard gray dolomites — (Mizzi Yahudi type) of the Sakhnin formation and the abrupt disappearance of the flints marks the upper boundary of the Deir Hana formation.

Description

In the type section, the Deir Hana formation attains a thickness of about 200m. Although the Deir Hana formation consists mainly of dolomite, it differs from the underlying Kamon Dolomite and the overlying Sakhnin Dolomite by the abundance

* This name was invalidated by Freund. (refer to Bull. Res. Council. Israel Vol. 9G, 2-3, 159, 1960).

of chert beds and nodules, the dominance of a light yellow colour and a far softer morphology.

The Deir Hana formation can be sub-divided into three members:

1. *The lower dolomite member: well-bedded, yellow dolomite with chert, 52.0m.*

The main rock type of this lower member is a light yellow, crystalline, very fine to medium grained dolomite. Some beds of very fine grained white dolomite are also present in the section. Here and there, calcareous dolomite is encountered. The rocks are very compact, but not very hard.

It has been observed in thin sections that most of the rocks of this unit are built of very small xenomorphic dolomite crystals, in a very closely packed texture.

The permeability of the rocks is very low. Only a small part of the dolomites is porous and the pores are small and not very abundant.

Rocks of this unit are well bedded. Beds are approximately 1m thick and some of them have a very fine lamination.

Chert is very abundant in this member. The colour of the chert is brown to gray brown. It appears in horizons of small lenses or nodules and in irregular thin layers. Quartz concretions are irregularly scattered within the dolomite beds.

The slopes, formed by the well bedded yellow dolomite with chert, have the form of stairs, the edges of which are rounded. This morphology is very typical of this unit.

There is very little nari, on the exposures of this lower member and only on a few calcareous beds.

No fossils have been found in the lower member of the Deir Hana formation.

2. *The median chalk member: chalk, dolomite, limestone with chert, 105m.*

The member consists of many rock types which are described below in the order of decreasing abundance:

- (1) Chalk, yellow to white, soft, with chert nodules; the chalk is mostly covered by nari and soil.
- (2) Dolomite partly calcareous, yellow to white, soft, crystalline, very fine to medium grained; with thin chert beds and chert nodules.
- (3) Dolomite partly calcareous, gray, fine to medium grained, hard, massive.
- (4) Limestone, sometimes slightly dolomitic, yellow, crystalline, fine grained, hard, with chert nodules.

As most of the rocks are chalk and soft dolomite, the bedding is not very well expressed. Hard gray dolomite and limestone in banks 1–2m thick, occasionally stands out of the nari-and soil covered soft chalky rocks.

Soil and nari development and a very gradual slope profile distinguish this prevalent chalky member of the Deir Hana formation; on it, one finds cultivated fields and olives.

3. *The upper dolomite member: prevalent dolomite, some chalk, 40m.*

The uppermost 40m of the Deir Hana formation consist mainly of light-gray to

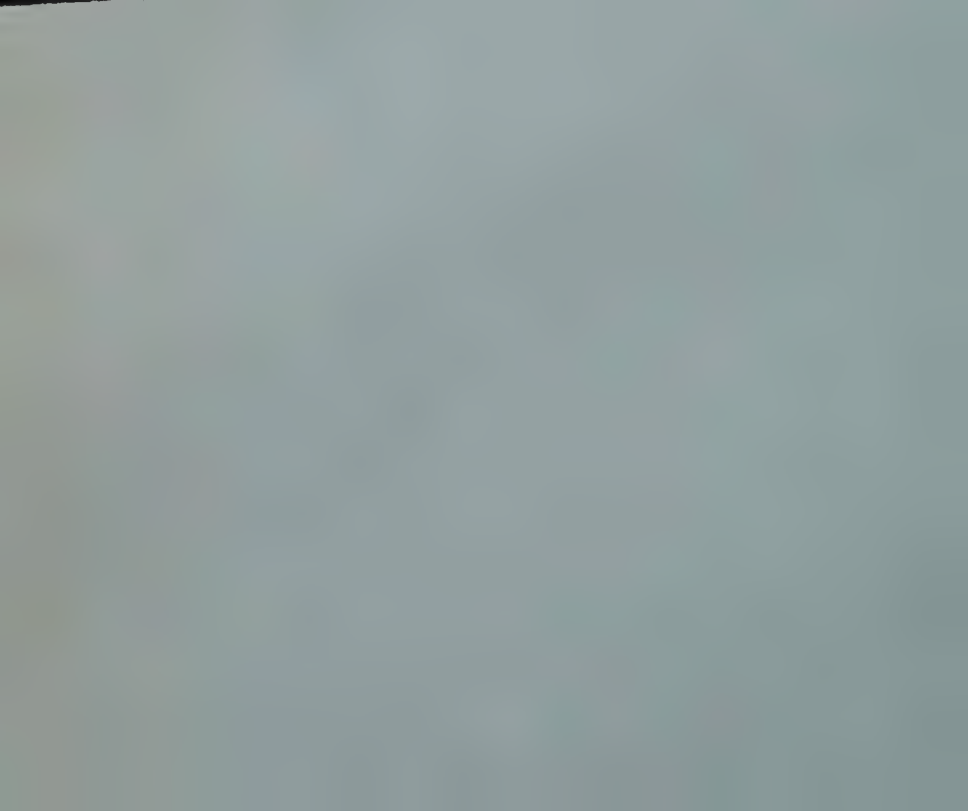
SECTION N. 2
SAMPLES
W 30 to W 73

DEIR HANA FORMATION

SOUTHERN SLOPE OF MT. KAMON WEST OF WADI KAMANA
Coordinates: 10252125050 to 10240126654
Dip: 10° N 40 W. Thickest measured by tops and Brunton 20 Jan. 1955
By Uvi Golani

SERIES	STAGE	FORMATION	MEMBER	LITHOLOGY	THICKNESS IN METERS	DESCRIPTION
S	N	U	P	D	E	Dolomite, light grey, medium grained
U	A	D	E	I	F	Dolomite light grey fine grained w/ flint layers 1-10 cm thick
C	T	M	O	A	R	Dolomite light grey fine grained w/ flint layers 1-10 cm thick
A	M	I	N	O	N	Dolomite light grey fine grained w/ flint layers 1-10 cm thick
C	F	R	E	O	D	Dolomite light grey fine grained w/ flint layers 1-10 cm thick
R	E	H	A	N	Z	Dolomite light grey fine grained w/ flint layers 1-10 cm thick
P	P	I	R	E	D	Dolomite light grey fine grained w/ flint layers 1-10 cm thick
U	U	D	E	F	I	Dolomite light grey fine grained w/ flint layers 1-10 cm thick

KAMON DOLOMITE



white crystalline fine grained dolomites. Some dolomitic limestone, some soft fine grained yellow dolomites and some bright yellow chalk are also present.

Irregular chert layers, 2–10cm thick, are found within medium to thick dolomite beds.

This member could be united with the overlying Sakhnin Dolomite; however, the presence of chert, chalk beds and soft dolomite, definitely missing in the Sakhnin Dolomite, ties this member to the Deir Hana formation.

In the type-section of Mt. Kamon, fossil remains were not found, but some bioscromes of Rudists occur in the upper member approximately 2–3km west of Mt. Kamon.

Facies changes within the Deir Hana formation

The Deir Hana formation appears in two different facies. The first one is the dolomitic facies typically represented at Mt. Kamon (as described above) and distributed primarily in Central Galilee (from Mt. Gilboa through the Nazareth hills, Mt. Tir'an, Mt. Netofa to Mt. Kamon and their vicinities).

The second facies consists of cherty-chalk and limestone, almost devoid of dolomites, and is described briefly in the chapter "The distribution of the Deir Hana Formation". The most typical distribution of this facies is found in the area of Ramim (Manara). A transitional mixed facies is noted at Mt. Meron, Beith Jann (Eliezeri) and Sasa (Grader).

The distribution of the Deir Hana formation

1. Dolomitic facies

The most typical development of the dolomitic facies is discussed in the previous chapter on Mt. Kamon. At Mt. Netofa and Mt. Tir'an, the Deir Hana formation, about 180 m thick consists mainly of yellow dolomites with nodules and thin layers of chert. The middle part of the formation is somewhat softer and includes yellow chalk with chert nodules. As the soft middle part, however, is not well developed, the formation can hardly be divided here into three members.

In the Nazareth hills, the thickness of the Deir Hana formation is about 160–180 m. It is difficult to fix here its lower boundary because of the gradual merging of the gray Kamon Dolomite into the yellow dolomites, with chert nodules of the Deir Hana formation.

The upper boundary, however, is very sharp. A cliff of some 30–40m and more of hard gray dolomite overlies the yellow and light gray dolomites with chert nodules. The triple division is well developed and resembles that of Mt. Kamon.

On Mt. Gilboa (A. Flexer 1959), only the upper 142 m are exposed, closely resembling in rock-character the upper two members of the Deir Hana formation at Mt. Kamon.

Chalky facies

In the region of Ramim (Manara) and Misgav Am, according to E. Rosenberg

(1960), the Deir Hana formation attains a thickness of 110m. The formation shows 15m of silicified limestone, followed by a unit 95m thick of chalk and shaly chalk. The chalk contains many brown chert nodules and layers, and quartz concretions. Crystalline limestone, built of Rudists debris, with reef structure, is found in this thick chalky unit. The chalk is overlain by beds of pink limestones which become harder towards the top of the formation.

"In the region of Rosh Hanikra, or the Mediterranean coast, the formation is composed of soft white chalk containing small black nodular chert. The lower part contains *Acanthoceratids*. More than 300 m are exposed on the Israel side." (Grader 1958).

According to Freund (1958), only the upper 40m of the chalky facies of the Deir Hana formation outcrop near Majd-el-Kurum and Yanuch in the Yirka-Pequim region of W. Galilee. The section shows white chalk with some limestone beds containing chert nodules and lenses.

Finally there is much similarity between the chalky Deir Hana facies of the Northern Galilee and that of the Carmel (Kashai 1958).

The age of the Deir Hana formation

The fauna found in the chalky facies of the Deir Hana formation indicates an upper Cenomanian age. The chalky formation of the Carmel has the same stratigraphical position. No fossils have been found in the dolomitic facies.

C. SAKHNIN DOLOMITE (Figure 8)

Upper Cenomanian-Turonian C_3 -t (Picard 1956).

Cenomanian, Upper part Ce_3 (Vroman 1958).

Unit U.C.2 (Grader 1958).

Rosh Tsurim Dolomite (c-ta) (Freund 1959).*

The formation is named after the village of Sakhnin in Central Galilee (coord. 178/252). The type section was measured on the northern slope of Mt. Kamor (coord. 18200/25695 to 18090/25671). See section No. 3

Boundaries

At the lower contact, the hard gray dolomites of the Sakhnin Dolomite overlie sharply the soft yellow dolomites and chalks with chert of the Deir Hana formation.

The upper boundary is also easily detected. Normally, the hard gray dolomite of the Sakhnin Dolomite is covered by well bedded lithographic limestone belonging to the Bi'na Limestone (e.g. Sh'ab region). Where the Bi'na Limestone is absent the Sakhnin Dolomite is overlain by chalk of Senonian age (e.g. S-W section at Beit Netofa).

* See note on page 9.



Figure 8
Shakhnin Dolomite, north-western slope of Mt. Kamon

Description

The Sakhnin formation at Mt. Kamon (205.5 m thick) consists of hard, medium to coarse crystalline dolomites. At the base of the formation, the colours of the rocks are mostly white to light gray; upward, the colours turn dark gray to brown gray. The bedding is fair to good. The beds are mostly thick to very thick, but in some parts of the section the beds are only 30–50 cm thick. In many places, the dolomitic beds show a pseudobreccious structure, very clearly recognized on weathered surfaces, but on freshly exposed rocks, such as in road cuts or quarries, it is hardly detectable.

The Sakhnin Dolomite forms a dark gray, rough, rocky landscape distinct from any other Galilean formation (Figure 8). No macro- or micro-fossils have been found in this formation.

Distribution

The Sakhnin Dolomite extends over large areas of the Galilee without considerable changes in facies or thickness. Some limestone beds may occur here and there, and reefs are occasionally encountered.

The Sakhnin Dolomite of Mt. Tir'an consists over its entire thickness of 170 m. of gray to white dolomite beds with some quartzolite layers.

East of Khirbet Mazlakhit, in the NE part of the Beit Netofa valley (coord. 825/247a), some calcareous beds made up of Rudists are found in the lower part of the formation.

In the Nazareth hills, the 200 m thick formation starts with a reef dolomite, the

thickness of which varies from 40m in the west to 30m in the east. Towards the top some of the beds are calcareous.

On Mt. Gilboa, the Sakhnin Dolomite differs somewhat from the type section of Mt. Kamon. The formation can, according to Flexer (1959), be divided into three parts:

- a) The lower cliff-forming part attaining a thickness of 63m, is built of gray, hard dolomite and corresponds to the cliffs of the Nazareth hills.
- b) The well bedded part attains a thickness of 121m. The lower section of this part consists of light coloured dolomites with very little chert; the upper section consists of white calcareous dolomites.

The well bedded unit forms a lapiés landscape, similar to that formed by the Sakhnin Dolomite in other places of the Galilee.

- c) The well bedded part, is overlain by 14m of gray to light red dolomites with a brecciated structure mostly covered by nari.

In the Peqi'in and Sasa regions (Grader 1958, Eliezri 1959), the Sakhnin Dolomite is similar to the type section in Mt. Kamon. The thickness is about 200m.

To the West, along a N-S line, the Sakhnine Dolomite passes abruptly into a group of calcareous formations (Freund 1959). This very sharp facies-change is limited however to a strip (3-4 km wide) in the Yirka-Yanuch region. West of this strip, the Sakhnin Dolomite reappears again.

The Sakhnin Dolomite is found in normal development east of the valley of Beit Netofa and from there northwards through the Safad region up to Misgav-Am in the northern part of the upper Galilee. Since the Sakhnin Dolomite is situated between the Upper Cenomanian Deir Hana formation and the Bi'na Limestone, the age of this formation is best attributed to the uppermost Cenomanian and/or Lower Turonian.

It is possible, however, that in some places the Sakhnin Dolomite represents only the upper part of the Upper Cenomanian. This is the case, for instance in the region of Majd-el-Kurum, where the Bi'na Limestone represents late Cenomanian and Turonian stages (Shadmon 1959).

D. BI'NA LIMESTONE

Turonian (t) (Picard 1955, Vroman 1958).

Kisra Limestone (Freund 1959),

Bi'na Limestone (Shadmon 1959).

Description and type section of the formation in the Bi'na and Majd-el-Kurum regions are given in Shadmon's publication (1959).

Although the Bi'na Limestone is not very thick, it is found with only minor lithological variations in many parts of the Galilee.

The bedding of the Bi'na Limestone is very good, beds are mostly 1-3 m thick. On the surface rocks are light gray and attain a very typical karstic landscape, with many small solution cavities (Figure 9).

SECTION N-5
SAKHIN DOLOMITE
NORTHERN SLOPE OF M. KAMON

SAMPLES:
1. 7. 10. 13.

Coordinates 10°50'50" N. 100°00'10" W.
Dip 10° N 40° W. Thickness measured by tape and Brunton

Date 27-1-1958
By T. H. Gahm

CH. 5	STAGE	CRUST	DIAG. LITHO.	SAMPLE NO.	THICKNESS	DESCRIPTION
				1	100.11	Unconformity, reddish white, crystalline
				2	100.12	Dolomite, grey, coarse grained, crystalline
				3	100.13	Dolomite, light grey, coarse grained
				4	100.14	Dolomite, light grey, medium grained
				5	100.15	Dolomite, light grey, coarse grained
				6	100.16	Dolomite, light grey, medium grained
				7	100.17	Dolomite, light grey, coarse grained
				8	100.18	Dolomite, light grey, medium grained
				9	100.19	Dolomite, light grey, coarse grained
				10	100.20	Dolomite, light grey, medium grained
				11	100.21	Dolomite, light grey, coarse grained
				12	100.22	Dolomite, light grey, medium grained
				13	100.23	Dolomite, light grey, coarse grained
				14	100.24	Dolomite, light grey, medium grained
				15	100.25	Dolomite, light grey, coarse grained
				16	100.26	Dolomite, light grey, medium grained
				17	100.27	Dolomite, light grey, coarse grained
				18	100.28	Dolomite, light grey, medium grained
				19	100.29	Dolomite, light grey, coarse grained
				20	100.30	Dolomite, light grey, medium grained
				21	100.31	Dolomite, light grey, coarse grained
				22	100.32	Dolomite, light grey, medium grained
				23	100.33	Dolomite, light grey, coarse grained
				24	100.34	Dolomite, light grey, medium grained
				25	100.35	Dolomite, light grey, coarse grained
				26	100.36	Dolomite, light grey, medium grained
				27	100.37	Dolomite, light grey, coarse grained
				28	100.38	Dolomite, light grey, medium grained
				29	100.39	Dolomite, light grey, coarse grained
				30	100.40	Dolomite, light grey, medium grained
				31	100.41	Dolomite, light grey, coarse grained
				32	100.42	Dolomite, light grey, medium grained
				33	100.43	Dolomite, light grey, coarse grained
				34	100.44	Dolomite, light grey, medium grained
				35	100.45	Dolomite, light grey, coarse grained
				36	100.46	Dolomite, light grey, medium grained
				37	100.47	Dolomite, light grey, coarse grained
				38	100.48	Dolomite, light grey, medium grained
				39	100.49	Dolomite, light grey, coarse grained
				40	100.50	Dolomite, light grey, medium grained
				41	100.51	Dolomite, light grey, coarse grained
				42	100.52	Dolomite, light grey, medium grained
				43	100.53	Dolomite, light grey, coarse grained
				44	100.54	Dolomite, light grey, medium grained
				45	100.55	Dolomite, light grey, coarse grained
				46	100.56	Dolomite, light grey, medium grained
				47	100.57	Dolomite, light grey, coarse grained
				48	100.58	Dolomite, light grey, medium grained
				49	100.59	Dolomite, light grey, coarse grained
				50	100.60	Dolomite, light grey, medium grained
				51	100.61	Dolomite, light grey, coarse grained
				52	100.62	Dolomite, light grey, medium grained
				53	100.63	Dolomite, light grey, coarse grained
				54	100.64	Dolomite, light grey, medium grained
				55	100.65	Dolomite, light grey, coarse grained
				56	100.66	Dolomite, light grey, medium grained
				57	100.67	Dolomite, light grey, coarse grained
				58	100.68	Dolomite, light grey, medium grained
				59	100.69	Dolomite, light grey, coarse grained
				60	100.70	Dolomite, light grey, medium grained
				61	100.71	Dolomite, light grey, coarse grained
				62	100.72	Dolomite, light grey, medium grained
				63	100.73	Dolomite, light grey, coarse grained
				64	100.74	Dolomite, light grey, medium grained
				65	100.75	Dolomite, light grey, coarse grained
				66	100.76	Dolomite, light grey, medium grained
				67	100.77	Dolomite, light grey, coarse grained
				68	100.78	Dolomite, light grey, medium grained
				69	100.79	Dolomite, light grey, coarse grained
				70	100.80	Dolomite, light grey, medium grained
				71	100.81	Dolomite, light grey, coarse grained
				72	100.82	Dolomite, light grey, medium grained
				73	100.83	Dolomite, light grey, coarse grained
				74	100.84	Dolomite, light grey, medium grained
				75	100.85	Dolomite, light grey, coarse grained
				76	100.86	Dolomite, light grey, medium grained
				77	100.87	Dolomite, light grey, coarse grained
				78	100.88	Dolomite, light grey, medium grained
				79	100.89	Dolomite, light grey, coarse grained
				80	100.90	Dolomite, light grey, medium grained
				81	100.91	Dolomite, light grey, coarse grained
				82	100.92	Dolomite, light grey, medium grained
				83	100.93	Dolomite, light grey, coarse grained
				84	100.94	Dolomite, light grey, medium grained
				85	100.95	Dolomite, light grey, coarse grained
				86	100.96	Dolomite, light grey, medium grained
				87	100.97	Dolomite, light grey, coarse grained
				88	100.98	Dolomite, light grey, medium grained
				89	100.99	Dolomite, light grey, coarse grained
				90	100.100	Dolomite, light grey, medium grained

SECTION No. 4

BI'NA LIMESTONE

24th Jan. 1955

SAMPLES:

NORTH OF Mt. KAMON

By Uri Golani

K-104 to K-115

Coord: 18093/25868 to 18070/25906

Dip: 15° N 23° W

Thickness measured with Brunton

SERIES	STAGE	FORMATION	SAMPLE NO.	LITHOLOGY	TOTAL THICKNESS	THICKNESS	LITHOLOGICAL DESCRIPTION
UPPER CRETACEOUS	SENONIAN (SANTONIAN)						Chalk, light brown-white, hard, compact, with fauna
	Turonian	BI'NA LIMESTONE			80.0	15.0	Limestone, lithographic, white, w/ Stylolites, interbedded w/ Limestone brown to the top layers of limestone, light yellowish brown, 2-20m thick
			115				
			114		65.0	25.0	Limestone lithographic, white with Stylolites layers 1-4m. thick
			113				
			112				
			111		40.0	16.0	Limestone, crystalline, white, to the top more compact layers 1-2m thick
			110		24.0	3.5	Limestone reddish white, coarse, to the top whiter & more compact
					20.5	1.5	Limestone lithographic karstic
			109		19.0	3.5	Limestone lithographic, white with stylolites
			108		15.5	4.25	Limestone yellowish white crystalline, fine grained.
			107		11.25	1.75	Limestone crystalline, reddish white.
			106		9.5	1.5	Limestone lithographic, light brown-white
			105		8.0	3.5	Limestone lithographic white
			104		7.5	3.0	Limestone reddish-white crystalline
	UPPER CRETACEOUS	BI'NA LIMESTONE			4.5	1.5	Dolomite, light grey, coarse grained.

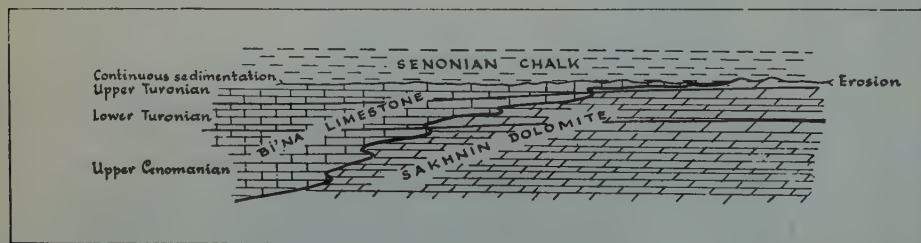


Figure 9
Bi'na Limestone near Majd-el-Kurum

Many microfossils and debris of large fauna are found in this formation. A full list of microfossils, from the Bi'na Limestone by Z. Reiss, is given in Shadmon's paper and determined as Cenomanian-Turonian, without a clear boundary between the two stages. Freund (1959) has shown that in some areas in the western Galilee, the Bi'na Limestone begins later in the Turonian (possibly Upper Turonian) whereas in other places, this formation still belongs to the Upper Cenomanian.

In some places, as for example in the area SW of the Beit Netofa valley, the dolomitic rocks of the Sakhnin Dolomite were deposited, while in other places, the calcareous sediments of the Bi'na Limestone were formed contemporaneously.

This relationship is schematically shown in the following sketch:



In some places, (Nazareth hills) the Bi'na Limestone (usually 20-40m thick) is absent due to pre-Senonian erosion.

North of Mt. Kamon, 1km south of the village of Nahf, the Bi'na Limestone attains a thickness of 78.5m and is composed of lithographic limestone with some beds of crystalline limestone.

On Mt. Gilboa (Flexer 1959), the Bi'na Limestone attains a thickness of 40m. In some places dolomite beds and Rudists reefs appear within the lithographic limestone complex.

In the Wadi Ein Mimla, east of the village of Eylabun (coord. 19284/25157), the Bi'na Limestone attains a thickness of 41.5m and is built of lithographic limestone interbedded with gray crystalline dolomite.

A narrow strip of Bi'na Limestone is exposed along the eastern side of the Galilee, but nowhere is the formation so well developed as in the Majd-el-Kurum region in Western Galilee.

Other thickness-figures of the Bi'na Limestone:

Near the village of Sha'ab	over 100m
Around Kisra	over 5.5m
Tzuriel	over 25m
Ramin region	over 100m

E. HISTORY OF SEDIMENTATION

The Aptian transgression which covered the Galilee continued throughout the Albian and the Cenomanian-Turonian.

The supply of fine clastics (clays) diminished gradually towards the end of the Albian; the section shows limestone beds with thin marl layers between them.

In late Albian or early Cenomanian, a new sedimentary factor was introduced: dolomitization.

It is believed today by most authors, that dolomitization is a process between the newly deposited calcitic or aragonitic material and the sea water, in a broad shallow sea (the penecontemporaneous theory).

This depositional environment dominated in the Galilee (and perhaps in the Judean and Ephraim Mountains). The very thin marl laminae found in the lower part of the Kamon Dolomite, indicate that the supply of clastic material almost came to an end.

Tectonic movements starting in early Upper Cenomanian time brought to an end the uniform depositional conditions. Differential subsidence (or perhaps slight folding) caused the formation of different depositional environments. This subsidence is best manifest in southern Israel where the Upper Cenomanian transgression advanced over the Negev as far as Eilat and Sinai.

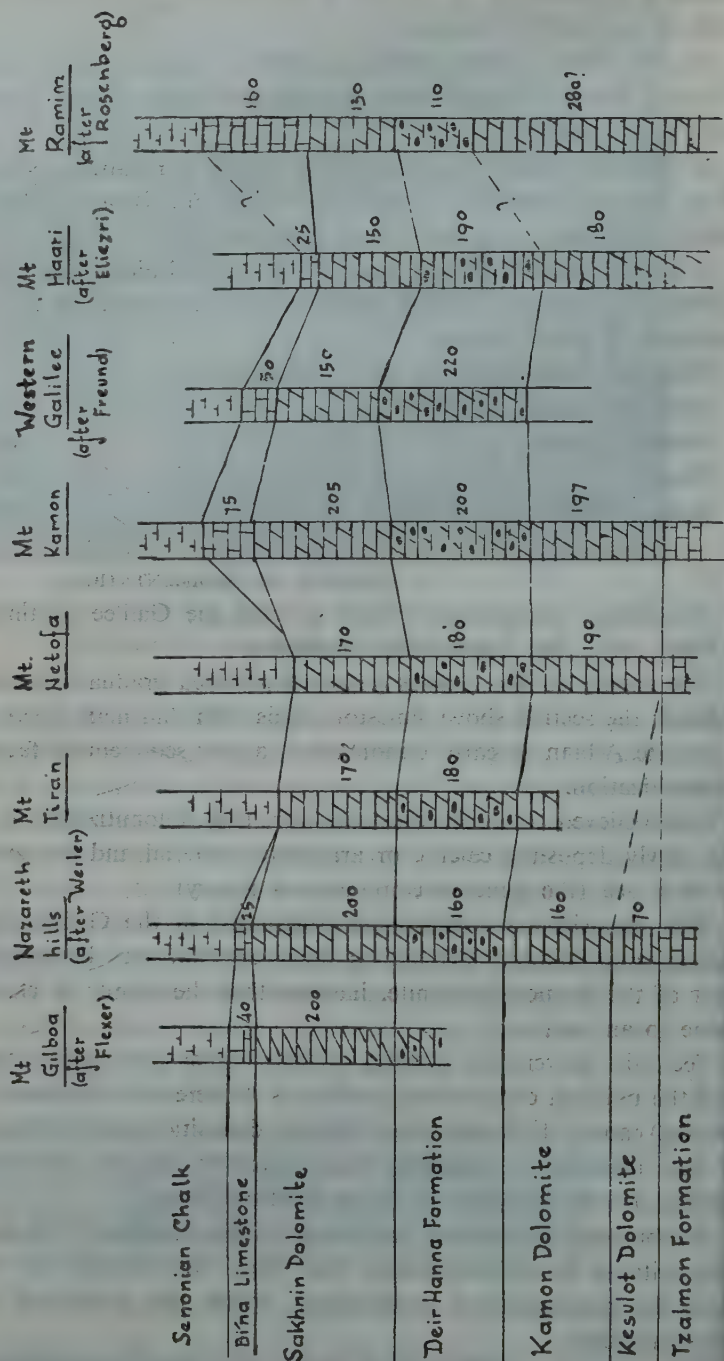
A submarine ridge existed in Central Galilee which under the prevailing conditions was suitable for dolomitization. The ridge was encircled by deep basins (deeper than the dolomitization depth-limit), where the calcareous sediments escaped dolomitization.

The extensive supply of silica to the early Upper Cenomanian sea is reflected

Correlation Chart

of the Cenomanian-Turonian Formations
of the Galilee

Vertical Scale 1:1000



by the richness of chert nodules and layers in the Deir Hana formation. The deposition of silica was not affected by the different environments; in consequence, chert is equally present in both the dolomitic and the chalky facies of this formation.

The rise of the sea floor in the later Upper Cenomanian caused the return of conditions favourable for dolomitization. In the Western Galilee, however, limestones and chalks were deposited in a narrow synclinal basin (2–5 km wide) (Freund 1959). The rising sea floor enabled the development of the many reefs found in the Sakhnin Dolomite.

In the late Upper Cenomanian, apart from the Western Galilee syncline, there existed some places where the carbonate sediments were not affected by dolomitization (Majd-el-Kurum region for example). In these places, the Bi'na Limestone is found.

In most places no marked change in depositional conditions occurred during the early Turonian. In the Western Galilean syncline, chalks and limestones were deposited (Freund 1959). In the Eastern and Central Galilee and at Mt. Gilboa, Sakhnin Dolomite depositional conditions continued.

Towards the end of the Turonian, the deposition environment of the Bi'na Limestone spread almost all over the Galilee. This environment was of shallow water as indicated by its rich microfauna (Shadmon 1959).

At the end of the Turonian or at the beginning of the Senonian, some areas emerged above sea level and were subjected to erosion. In a few localities in the Nazareth hills, an erosional unconformity is apparent between the Sakhnin Dolomite and the overlying Senonian chalk. In one or two cases, conglomerates are found.

From the Senonian age onward, conditions of sedimentation changed radically. The sea deepened considerably and chalks were uniformly deposited.

REFERENCES

- BALL, M.E. AND BALL, D., 1953, Oil Prospects of Israel, *Bull. Amer. Ass. Petr. Geol.*, 36:10.
- BLAKE, G.S., 1936, *The stratigraphy of Palestine and its building stones*, Jerusalem.
- ELIEZRI, I., 1959, *The Geology of Beit Jann region*, Unpublished M.Sc. thesis of the Hebrew University, Jerusalem.
- FLEXER, A., 1959, *The Geology of Mt. Gilboa*, Unpublished M.Sc. thesis of the Hebrew University, Jerusalem.
- FREUND, R., 1959, On the stratigraphy and tectonics of the upper Cretaceous in Western Galilee, *Bull. Res. Council of Israel*, 8G.
- 1958, *The Geology of Yirka-Peqi'in region (Hebrew)*, Unpublished M.Sc. thesis of the Hebrew University, Jerusalem.
- GOLANI, U., 1957, *The Geology of Mughar region*, Unpublished M.Sc. thesis of the Hebrew University, Jerusalem.
- 1957, *The Geology of Beit Netofa valley*, Unpublished report for TAHAL (Water planning of Israel).
- 1956, *The Tunnel of Eylabun*, Final geological report for TAHAL, unpublished.
- GRADER, P., 1958, Geological outlines of the Sasa region, Galilee, *Bull. of the Geol. Survey of Israel*.
- KARCZ, Y., 1959, The structure of the Northern Carmel, *Bull. Res. Council of Israel*, 8G.
- KASHAI, E., 1958, A note on the revision of the stratigraphy of the Southern Carmel, *Bull. Res. Council of Israel*, 8G (2–3).

- PICARD, L., 1938, The Geology of new Jerusalem, *Bull. Geol. Dept. Hebrew University*, II, No. 1.
- PICARD, L., Structure and Evolution of Palestine, *Bull. Geol. Dept. Hebr. Univ.*, IV, No. 2-4.
- PICARD, L., 1950, The structural pattern of Palestine, *Bull. Res. Council. of Israel*, IV, (1).
- PICARD, L., 1958, Geological background on petroleum, drilling in Zichron Yaakov, *Bull. Res. Council. of Israel*, 7G (1).
- PICARD, L., Geology and oil exploration of Israel, *Bull. Res. Council. of Israel*, 8G (1).
- PICARD, L., 1956, The geological map of Israel, 1:100,000, Serie A, Northern part, *Geol. Survey of Israel*, Jerusalem.
- PICARD, L., 1959, *Geology and oil exploration of Israel*, Fifth World Petroleum Congr., New York, Sect. I., Pap. 16:1-22, Ill. (also in *Bull. Res. Council. of Israel*, 8G, (1) 1-30, Ill., map, May 1959).
- PICARD, L. AND KASHAI, E.: Lithostratigraphy and Tectonics of the Carmel.
- ROSENBERG, E., 1960, Geologische Untersuchungen in den Naftalibergen, Mitteilungen aus dem Geologischen Institut der Eidg. Techn. Hochschule und der Universität Zurich.
- SHADMON, A., 1959, The Bi'na Limestone, *Bull. Geol. S. Isr.* No. 24.
- VROMAN, A., 1958, Geological Map of Israel, 1:50,000. Series I, Galilee, *Geol. Survey of Israel*, Jerusalem.
- VROMAN, A., 1960, Note on the Rock Units of Mount Carmel, Israel, *Bull. Geol. Survey of Israel*, 27.

NEOGENE GAS PROSPECTS IN THE CENTRAL COASTAL PLAIN, ISRAEL

P. GRADER AND G. GVIRTZMAN
Geological Survey of Israel

ABSTRACT

Though numerous showings of gas have been found in sediments of Neogene age in drillings in the Coastal Plain of Israel, no commercial production of gas has yet resulted. This failure has generally been attributed to the lack of suitable reservoir conditions within the Neogene sequence. The formations encountered, however, in the recently completed National Park No. 1 well provide potential reservoir targets, hitherto unknown. In this drilling, 20 m of conglomerates and tuffs and 187 m of vesicular basalts were found. The conglomerates are rather tight, but the basalts are highly porous and permeable in parts; a test over the upper part of this volcanic complex flowed salt water to the surface. Petrographic studies have shown the possibility of dividing the upper, mainly parts of the Neogene section into grain-size units. Correlation of these units over the Coastal Plain may indicate trends of increasing porosity and permeability within the Neogene sequence and thus outline areas of prospective gas accumulation. A new formation name is proposed for the marls, conglomerates and volcanics of Neogene age — Ramat Gan Formation.

INTRODUCTION

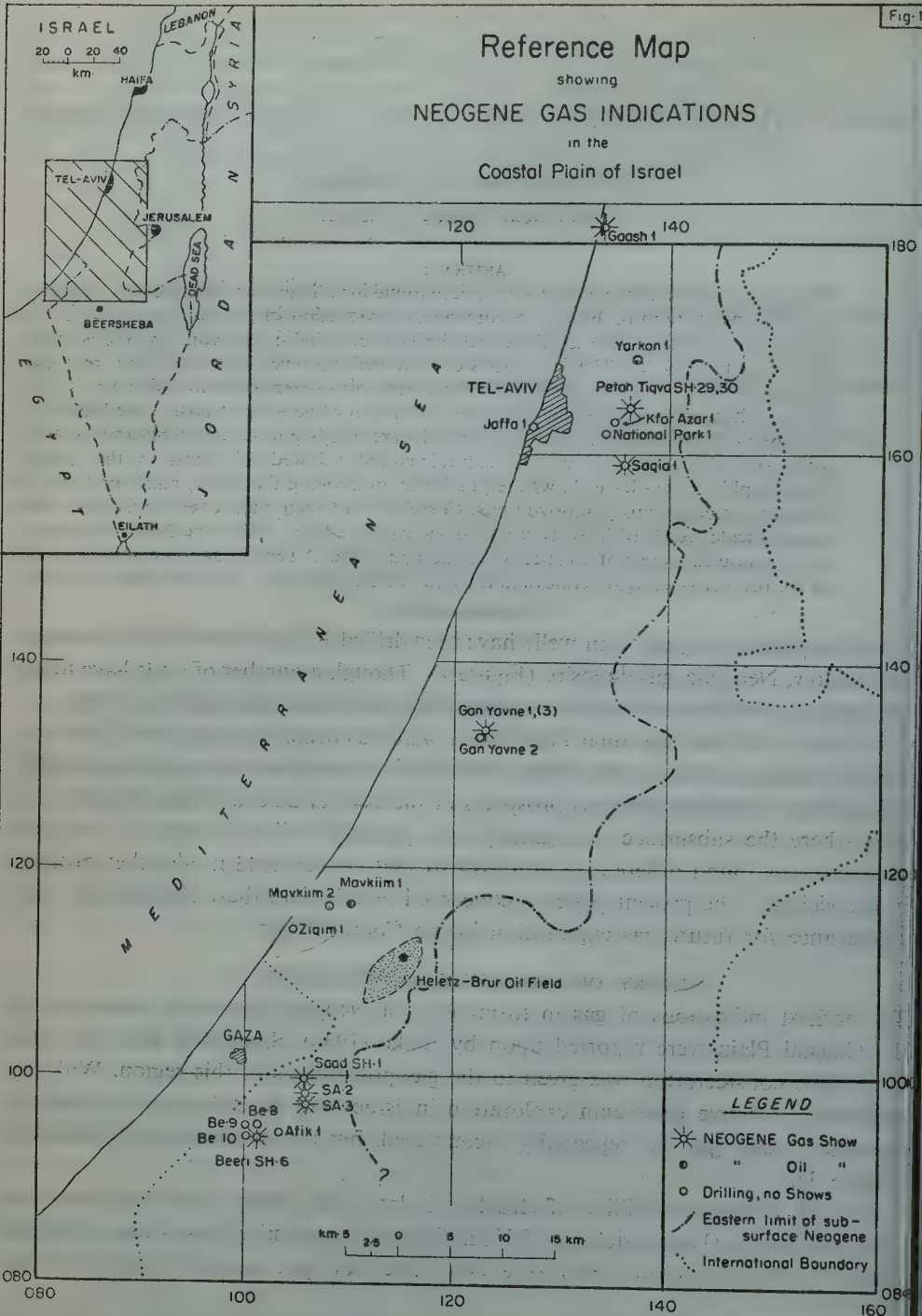
Over the past seven years, ten wells have been drilled in the Coastal Plain in search for shallow, Neogene gas deposits (Figure 1). Though a number of wells have found encouraging indications of gas, no commercial production has resulted to date.

In April 1960, the National Park No. 1 well was drilled 8 kms east of Tel Aviv. Though no gas was found, the results of this drilling have provided valuable geological information enhancing the gas prospects of the Central Coastal Plain. Drilled in an area where the subsurface stratigraphy was generally believed known, a Neogene sequence was found different in lithology to that encountered in all other drillings in the vicinity. The present paper is concerned mainly with these changes and their significance for future gas exploration in the Coastal Plain.

HISTORY OF SHALLOW GAS EXPLORATION

The earliest indications of gas in formations of Neogene age in the subsurface of the Coastal Plain were reported upon by Blake (1936). Since that time and until 1953, little consideration was given to the gas possibilities of this region. With the beginning of active petroleum exploration in Israel and the subsequent drilling of numerous wells, gas was repeatedly encountered, but not in commercial quantities (Figure 1).

In 1954, during the drilling of structure holes in the Petah Tiqva area, gas was discovered at the shallow depth of 256 m. The most interesting shows were found in wells P.T. 29 and P.T. 30, which for a short time blew gas, sand and water from the



upper part of the Sakie beds (Israel American Oil Co. Progress Reports No.'s 3 and 5, 1954). Sternberg (1956), who studied these gas occurrences, concluded that the gas emanated from three zones, and designated them as the "Lower", "Middle" and "Upper" gas sands. Owing to the limited lateral extent of these sands, he did not believe that sufficient reserves would be found.

In 1955, during the drilling of the Gan Yavne Well No. 1, a blow-out of gas occurred in the Neogene section at a depth of 922 m. The gas caught fire and "burned about 30 m high and for about 30 minutes before it went out of its own accord" (Israel American Oil Co. Progress Report No. 7, 1955). Franklin concluded that, as no reservoir rocks could be detected on the electric logs, "the gas came from small tight fissures in very thin seams of silty shale". Following this blow-out, interest in the oil and gas prospects of the Neogene formations was revived (Behr 1956). However, after two additional wells drilled on the Gan Yavne structure failed to find any indications of gas, this interest diminished. With the discovery of oil in Heletz in the latter part of 1955, the centre of interest shifted entirely to the oil prospects of the Lower Cretaceous sands.

It was not until 1957, when gas was found during drilling in the Neogene section in three of the Saad structure holes, that the shallow gas possibilities came again into prominence. Interest was further strengthened when the Beeri structure hole No. 6 blew out, and continued to blow uninterruptedly for 12 days. Tschopp and Wiener (1958) concluded that the gas and water were issuing from a Cenomanian reservoir truncated by the Neogene marls, and that the gas entered the reservoir "by lateral migration from the onlapping Sakie and/or Paleocene — Danian — Senonian wedge further down flank".

It was generally believed however, that the main source of the gas found in the numerous wells drilled in the Coastal Plain could be attributed to the shales and marls of the Neogene; that, if suitable reservoir rocks could be found within this sequence under favourable structural or stratigraphic conditions, a commercial accumulation of gas might be located. After the Beeri discovery, the prospection for shallow gas was directed to a search for porosity within or at the base of the Neogene and followed three main trends:

1) *The search for old eroded Cenomanian highs truncated by Neogene formations*

In 1959, three additional wells were drilled on the flanks of the eroded Beeri structure within a radius of 1 km of Beeri Sh. 6 (Figure 1) (Lapidoth, Israel Oil Prospectors Corp.). No gas was found in these wells, and Cohen (1960) concluded that the Beeri field, being less than 1 sq. km, was of no commercial value.

2) *The search for reefs or sand bars within or at the base of the Neogene section*

In a number of wells drilled, beds of massive anhydrite were encountered, e.g. Gan Yavne, Mavkiim. Barriers were postulated as being located somewhere to the west of the wells in which anhydrite was found. These barriers were thought to be responsible for a temporary closing of the basins from the open seas, resulting in

the deposition of anhydrite. In June 1960, a second well, Mavkiim No. 2, was drilled 2 km to the west of Mavkiim No. 1 (Lapidoth, Israel Oil Prospectors Corp.). At a depth of 1036 m, anhydrite was penetrated. The well was continued down to 1045 m, when a high pressure flow of salt water from above the anhydrite zone made it necessary to abandon the well.

3) *The search for coarser clastics (sands, gravels, conglomerates) within the Neogene section*

Grader (1958) showed that low gravity anomalies provided an effective means for the delineation of erosion channels over the main structural trend of Heletz-Brur and that this association might extend to other parts of the Coastal Plain; that one might "find significant changes in the lithology of the formations within these channels" where "suitable reservoir conditions for gas and oil may exist". Neev (1960) described in detail the existence of one such major pre-Neogene erosion channel breaching the Beeri-Saad structure, and predicted the presence of coarser clastics within the channel. These predictions were borne out with the drilling of Afik No. 1 in 1959 (Lapidoth, Israel Oil Prospectors Co.), which encountered more than 100 m of channel fill at the base of the Neogene, composed of silts and sands.

The search for porosity in the Neogene formations was extended to the Tel Aviv area with the drilling of Gaash No. 1 (Nov. 1959), and Jaffa No. 1 (Feb. 1960) (Israel National Oil Co.). Gaash No. 1 was located on an E-W trending structural nose as outlined by a seismic reflection survey. Though minor shows of gas were reported during the drilling, no porous beds could be detected on the electric logs. In the Jaffa No. 1 well, over 2000 m of Neogene formations were drilled. No indications of gas were noted, and no porous beds were encountered.

NATIONAL PARK NO. 1

The National Park No. 1 well was spudded in April 1960 by the Israel American Oil Co. on their Ramle licence. A gravity survey carried out in 1954 over the entire Coastal Plain resulted in the discovery of a major gravity "high" over the Petah Tiqva structure. Most of the earlier geological and geophysical investigations in this area were therefore concentrated on this "high". In order to delineate the subsurface structure, thirty-three shallow wells were drilled and a detailed seismic survey was carried out. E-W seismic lines across the southern plunge of the structure indicated a N-S trending fault on the west flank of the structure (Behr 1958). The presence of such a fault or flexure was also inferred from the total gravity maps where a well pronounced change in gradient occurs. To the west of this fault a number of marked gravity "lows" are found. The National Park No. 1 well was located at the southern end of one of these major low gravity anomalies (Figure 2). As indicated already, it was believed that such gravity lows reflected, in part, old erosion channels; that within these channels coarser clastics might be found providing suitable reservoir conditions for the entrapment of gas.

The main lithologic units encountered during the drilling of the National Park No. 1 well can be summarized as follows (Figure 3):

Quaternary	0 - 186 m	predominantly sand and sandstones
	186 - 240 m	marls
	240 - 243 m	a bed of friable macro-fossils
	243 - 860 m	marls
Neogene	860 - 880 m	alternations of coarse conglomerate and tuffs
	880 - 1067 m	vesicular basalt
	1067 - 1154 m	marls
	1154 - 1174 m	chalk and flint
Turonian- Cenomanian	1174 - 1188 m	algal limestone

The well was abandoned at 1188 m depth, in formations of Turonian-Cenomanian age.

The marly portions of this sequence have all the characteristics of the "Sakie marls" and contain a fauna of Neogene age. These marls are composed of approximately 2/3 calcareous matter (including organogenic debris) and 1/3 clastics and clay minerals. However, as considerable ambiguity has arisen in the past regarding the usage of "Sakie" for describing all the post-Turonian (mainly Neogene) marl occurrences in the Coastal Plain of Israel, this Neogene sequence of marls as found in the National Park No. 1 well is herein designated the *Ramat Gan Formation*. This formation can be divided into a lower and upper member (as yet unnamed) and a middle volcanic complex termed the *National Park Volcanics* (Figure 3). Though these marls are very uniform in lithology, detailed petrographic studies have shown the possibility of dividing the upper member of the Ramat Gan Formation into sub-units. The lack of such subdivisions in the Neogene has hitherto been a major obstacle in studying the nature and distribution of these sediments in the Coastal Plain.

Though the presence of almost 200 m of basalt in the National Park No. 1 well is a surprising feature, it is by no means anomalous to the region. Drake (1872) noted "an outbreak of basalt, very friable from exposure" between the villages of Abu Shushe and Sydun. Blake and Goldschmidt (1947) record that from 29-125 m depth in the Wilhelma drilling (Figure 2), "decomposed basaltic material, hard at base, was encountered but not penetrated", and that in the Al Yahudiya well "the yellow olive clays encountered from 16-39 m depth might also be a volcanic ash bed". Avnimelech (1936) records three exposures of basalt in the area: near Abu Shushe (142/140); near Mansura (138/139); near Umm Kalkha (138/136) (also Picard and Avnimelech 1937). Vesicular basaltic pebbles were also found in a base conglomerate of a Pliocene exposure (138/138) by Avnimelech (1953). He deduces from this outcrop that "the volcanism must be younger than Helvetian but older than Lower Pliocene".

Picard (1943) noted that the basaltic complex of Burdigalian age in the Suez Gulf area, which is overlain by conglomerates and lagoonal deposits of Vindobonian

age, is similar to the volcanics found in the northern coastal plain of Syria, where they are also overlain by conglomerates and evaporites. Picard concluded that "Miocene eruptiva are not definitely established in the Coastal Plain region of Palestine (basalt and palagonite tuffs of the Ramleh region), though they are widely distributed in the Miocene continental deposits of Palestine and the neighbouring countries".

The thick basalt complex found in the National Park drilling bears affinities to the basalts occurring in the Suez Gulf area and Syria as described by Picard. Interestingly enough, the National Park volcanics are overlain by conglomerates and tuffs, and less than 8 km to the west, in the Jaffa No. 1 boring, though no volcanics were found, an evaporite section was encountered (Figure 4). It should also be noted that lagoonal deposits within the Neogene section are widespread and have been found in many drillings in the Coastal Plain of Israel.

Some interesting features have been noted in the basalts of the National Park No. 1 drilling. The National Park Volcanics can be divided into a "Lower" and "Upper" part by a thin 5 m horizon containing basaltic fragments covered by limonite and clay material. This layer is clearly reflected on the electric logs where the resistivity curves become featureless and "flat". The oxidized iron cover and the clay material seem to have resulted from sub-aerial erosion and resemble a fossil soil similar to the recent residual reddish soils of the Lower Galilean plateau basalts. Some thin horizons of red clayey material which are intercalated between basalt sheets in the continental Neogene plateau basalts of Galilee have been considered by Bentor (1957) as evidence of sub-aerial weathering. Bentor and Vroman (1951) also pointed out that the "Main Basalt Flow" at the base of the Lower Cretaceous in Machtesh Ramon is a sub-aerial flow rather than a sill, because of the presence of red clayey material at the top of the basalt.

The lower 35 m of the "Lower Basalt" are very vesicular and a core from this part shows flow structures (Plate IB). The upper 79 m of the "Lower Basalt", though more massive and granular with some phenocrysts, contain larger vesicles which are filled with calcite and zeolites. The "Upper Basalt" above the fossil-soil horizon is again extremely vesicular and displays a scoria structure. Weathering effects and chloritization are found to be very intense over the entire basalt complex, especially in the higher parts of the "Upper Basalt" and in the lower portions of the "Lower Basalt".

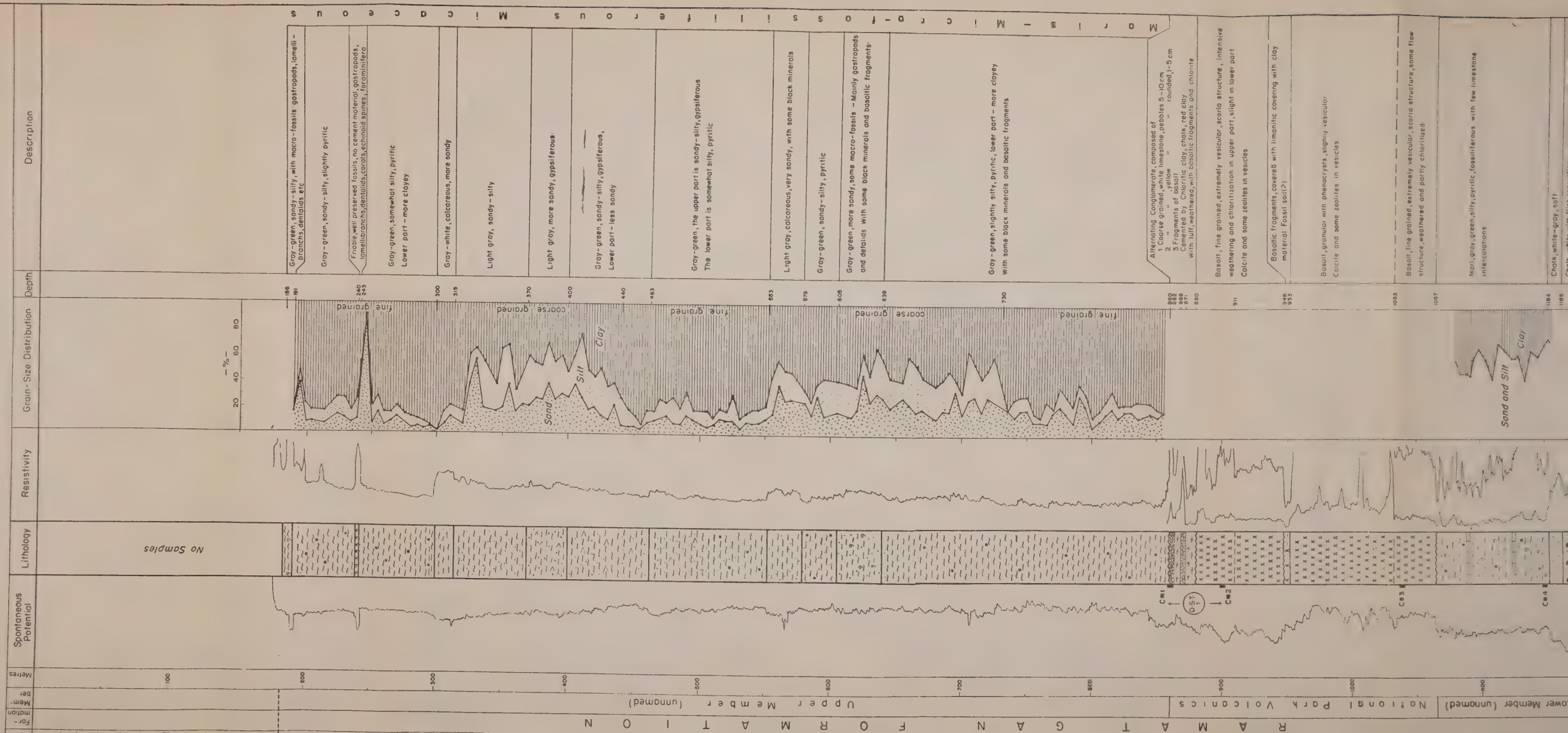
The presence of a gravity low over the basalt would at first appear to be contradictory. However, a number of density measurements made on the basalt cores show that these basalts have densities similar to the Neogene marls. For the more vesicular basalt type, an average density of 2.04 was determined. The more massive, slightly vesicular and weathered basalts showed an average density of 2.23. These densities are comparable with the Neogene marl densities of 2.27 for the more chalky portions and 1.98 for the more shaly parts. Thus there is little density contrast between the marls and the basalts. The main density contrast occurs between the Neogene section (marls and basalts) and the Turonian-Cenomanian limestones

COMPOSITE LOG
NATIONAL PARK

Coords: E 133994 / N 162002

by
G GVIRTZMAN
Oil Division
Geological Survey of Israel

Fig 3

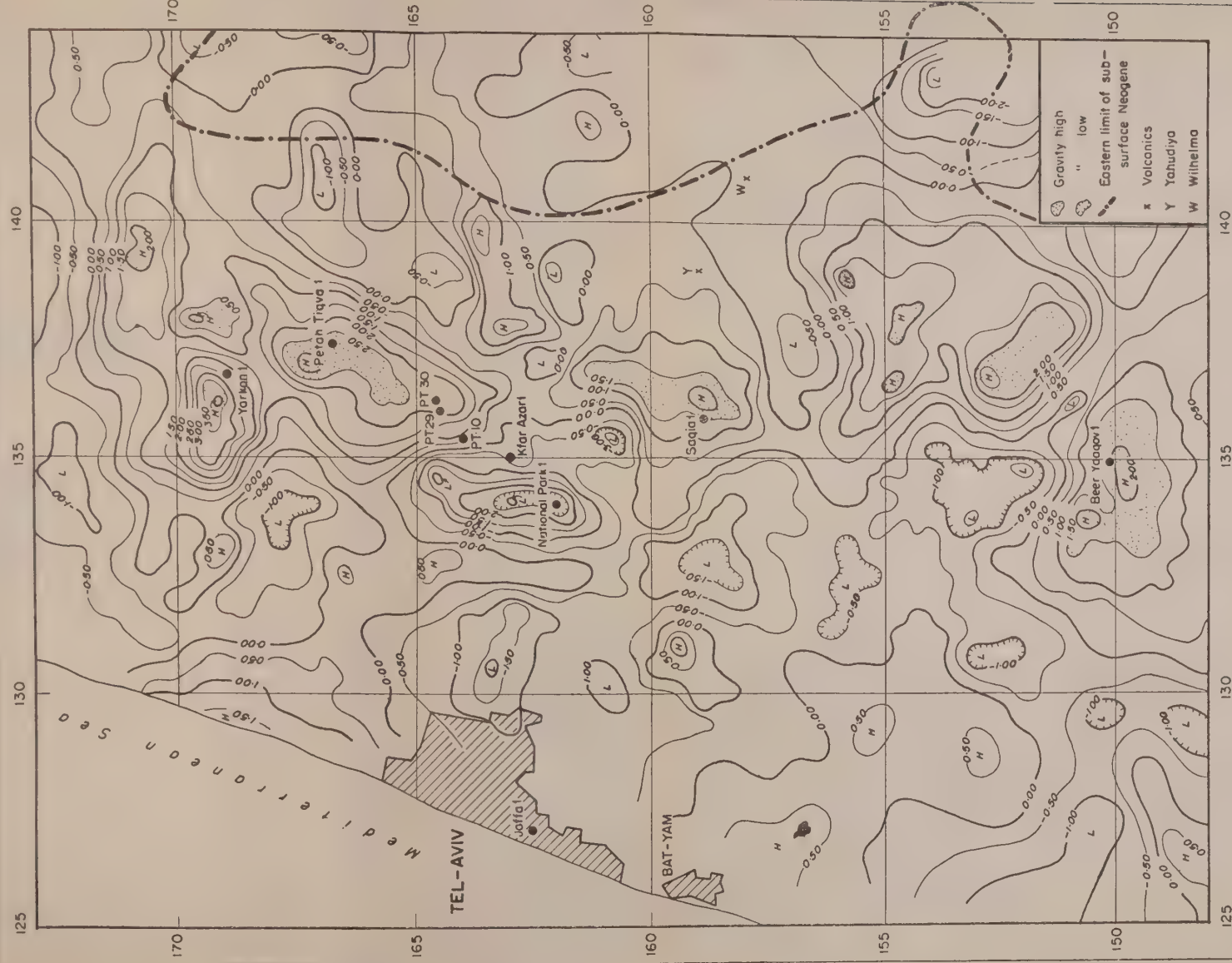




RESIDUAL GRAVITY MAP CENTRAL COASTAL PLAIN of ISRAEL



Contour Interval: 0.5 milligal

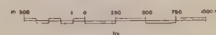




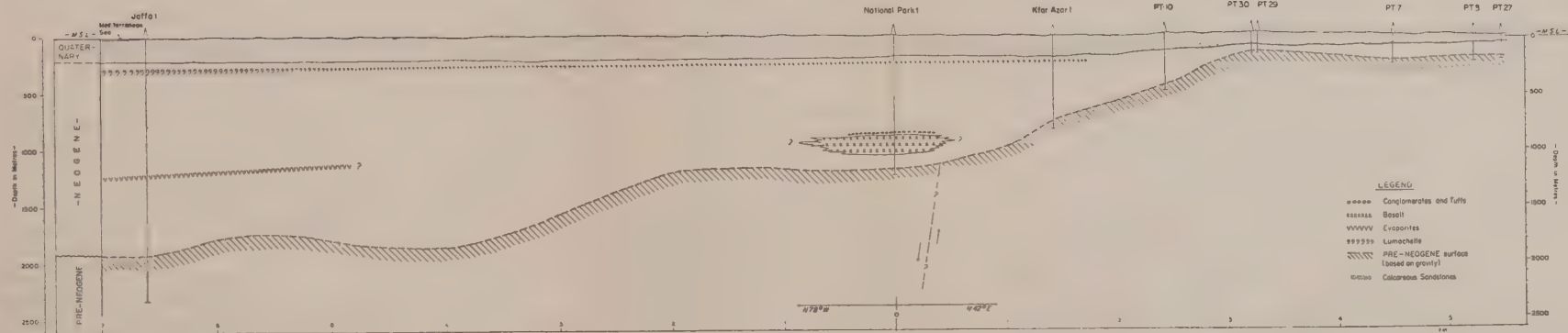
GEOLOGICAL CROSS SECTION through CENTRAL COASTAL PLAIN

Jaffa 1 - National Park 1 - Kfar Azar 1 - PT.29

Horizontal & Vertical Scale



P. GRADER and G. GIVERTZMAN





(density of 2.46) and dolomites (density of 2.86). Thus, as has been found in other parts of the Coastal Plain (Grader 1958), gravity measurements in the Ramle area reflect mainly the pre-Neogene erosion surface.

The place of eruption of the basalt is still unknown. It may be associated with the fault, which as first indicated by seismics, passes between the National Park No. 1 location and the Kfar Azar No. 1 well (Figure 4). It does appear though, that there were two phases of volcanism. In the first phase the basaltic flow emerged from the sea and erosion took place. Subsequently, a second basalt flow covered the eroded surface of the "Lower Basalt". The top of the "Upper Basalt" was in turn covered by fluviatile deposits (conglomerates) interbedded with tuffs.

PETROGRAPHIC ANALYSES

Over 150 samples (at intervals of 5 m) from the National Park No. 1 drilling were examined for grain size (excluding the basalt and non-marly portions of the rock sequence). Previous observations on the "Sakie marls" have shown that they are composed of sand, silt and clay in varying amounts. In order to arrive at a quantitative evaluation of these variations, a rapid analytical technique was used.

Because of errors resulting from contaminated sample cuttings, the determination of grain size by the classical pipette analysis method was not believed to be necessary. The clay fraction (and possibly some fine silt) was separated from the sample by dispersion in water and decantation. The remaining material (silt and sand) was analysed by the Emery settling tube method (Emery 1938). A measured volume was introduced into the tube, and the volume of material that settled within the time limit of sand-settling (coarser than 0.062 mm.) was determined. The material which was finer than 0.062 mm and which did not settle within this time is the remaining volume.

The composite results as shown in Figure 3, represent the percentage of the three fractions of the whole sample. Though absolute results of each sample are only approximated ($\pm 5\%$), the percentage variations along the rock sequence gives a reliable picture of the sedimentational characteristics of this sequence.

It is emphasized that the main divisions of the upper member of the Ramat Gan Formation, are based on grain size measurements, and not on mineral composition. The sand fraction is composed mainly of quartz grains and foraminifera. The silt fraction contains mainly fine calcite particles, foraminifera, quartz grains and pyrite. The clay fraction is composed of calcite and clay material in approximately equal proportions.

Based on these studies it was found possible to subdivide the marl sequence above the basalt into five parts (Figure 3):

- 1) 186-300 m gray-green sandy, silty, pyritic marls, predominantly *fine grained* (excluding friable macro-fossiliferous bed 240-243 m)
- 2) 300-440 m gray-green sandy, silty marls, gypsiferous in the upper part and mainly *coarse grained* (higher percentage of sand and silt)

- 3) 440-553 m similar to sub-unit (1) and characterized by its *fine grained* texture
- 4) 553-730 m gray-green sandy, silty marls, gypsiferous, *coarse grained*, containing basaltic fragments in the lower part
- 5) 730-860 m again similar to sub-unit (1), mainly *fine grained* and containing basalt fragments.

The change from fine grained to coarse grained sediments is generally a gradual one, as can be observed by the results of the granular study shown in Figure 3.

Interestingly enough, these major changes in sediment grain size (from fine grained to coarse grained sediments) are clearly reflected on the resistivity curves of the electric logs. Previous analyses of the electric logs over the Neogene interval have failed to yield correlative markers. A generally flat resistivity curve characteristic of shales, has precluded its use over this section for correlation purposes. It should be noted that some of the smaller electric "kicks" on the logs of the National Park No. 1 well, over the predominantly marly section of the Neogene, may be of significance for qualitative analysis and correlation.

The petrographic study has also shown that abundant particles of pyrite, a lower carbonate content and absence of gypsum are associated with the finer grained sediments; higher carbonate content, gypsum particles and almost no pyrite characterize the coarser grained sediments. These granular changes accompanied by a differing mineral composition, reflect changes in the environment of deposition. The coarse grained detritus with higher carbonate and sulfate content may indicate a lower rate of reduction of the bottom sediments, either at shorter distances from the continent or in a shallow basin; the fine grained detritus with its lower content of carbonate and sulfidic elements may indicate a higher rate of reduction, either in a deep basin or at a greater distance from the continent. It is believed that these changes are of a regional nature, and may reappear in nearby wells the samples of which have not yet been examined in detail.

CONCLUSIONS

Though no gas was found in the National Park No. 1 drilling, hitherto unknown potential gas-bearing reservoirs were discovered. In addition to the porous and permeable rudist limestones of the Turonian-Cenomanian, the conglomerates and vesicular basalts of Neogene age provide new targets in the search for shallow gas. Little is known today of their subsurface lateral extent in the Central Coastal Plain.

The conglomerates penetrated in the National Park No. 1 drilling were loosely cemented by clay and tuffaceous material and were thus of low porosity and permeability. Their reservoir properties, however, may improve towards the channel source. The basalts on the other hand, were highly porous and even permeable in parts. Core analysis has shown porosities ranging from 15-34% and a number of samples indicated permeabilities as high as 357 millidarcies. The fact that this section is

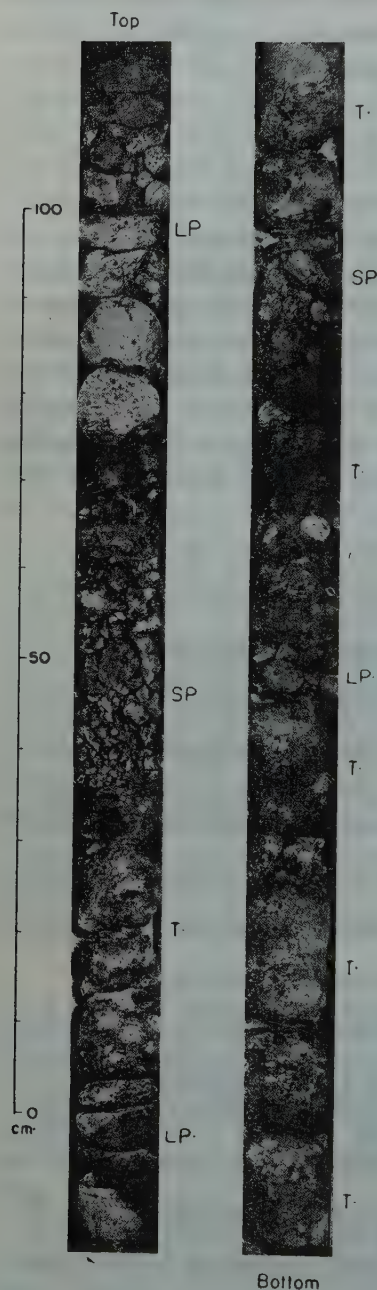
permeable is attested to by the results of a drill stem test made over the interval from 857-906 m, where 20 m of the coarse conglomerates and interbedded tuffs and 29 m of the "Upper Basalt" were open. These formations were permeable enough to flow salt water to the surface in 45 minutes. Of significance is the fact that these waters contain almost 60,000 p.p.m. chlorides. This indicates that these waters are confined within a closed trough and are in no way connected with the fresh water-bearing sands of the Quaternary or with the fresh water limestones of the Turonian-Cenomanian. It is quite possible therefore, that these formations may carry gas if they are structurally elevated at the rims of the trough.

From the detailed study of the National Park No. 1 samples, it has been found possible to subdivide the upper part of the Neogene section in this area into petrographic units based on grain-size. Further investigations may show that these grain-size units can be recognized in other wells of the Coastal Plain. If such correlation can be established, the stratigraphic study of the Neogene sediments will be greatly facilitated. It may also provide the necessary clues for outlining area of increasing porosity and permeability within the Neogene sequence and point the way to potential reservoirs of gas.

REFERENCES

1. AVNIMELECH, M., 1936, *Études Géologiques dans la Région de la Shéphélah en Palestine*, Grenoble.
2. AVNIMELECH, M., 1953, A New Pliocene outcrop in the Central Coastal Plain of Israel, *Bull. Res. Council of Israel*, **2**, 4.
3. BEHR, M.I., 1956, *Report on Oil and Gas Prospects of Neogene Formations in the Yavne Licence II/13*, Sharon Oil Corp., Tel Aviv (unpublished).
4. BEHR M.I., 1958, *A Geophysical Study of the Central and Southern Coastal Plain of Israel*, Unpublished Ph. D. thesis, Hebrew University.
5. BENTOR, Y.K., 1957, Cenozoic Volcanism of Israel, *XX Cong. Geol., Int. Sect. I*, Mexico.
6. BENTOR, Y.K. AND VROMAN, A., 1951, *The Geological Map of the Negev*, 1:100,000, Sheet 18: *Abde (Ovdat)*, Tel-Aviv.
7. BLAKE, G.S. AND GOLDSCHMIDT, M.J., 1947, *Geology and Water Resources of Palestine*, Jerusalem.
8. COHEN, Z., 1960, *The Beeri Gas Prospect*, Lapidoth, Israel Oil Prospectors Corp., Tel-Aviv (unpublished).
9. DRAKE, T., 1872, Report, *Palestine Exploration Fund-Quarterly Statement for 1872*.
10. EMERY, K.O., 1938, Rapid Method of Mechanical Analysis of Sands, *Jour. Sed. Petr.* **8**, 3.
11. GRADER, P., 1958, Geological History of the Heletz-Erur Area, Israel, I, *Geol. Survey of Israel, Bull.*, **22**.
12. ISRAEL AMERICAN Oil Co., 1954, Progress Reports No.'s 3, 5, 7 (unpublished).
13. NEEV, D., 1960, A Pre-Neogene Erosion Channel in the Southern Coastal Plain of Israel, *Geol. Survey of Israel, Bull.*, **25**.
14. PICARD, L., 1943, Structure and Evolution of Palestine, *Bull. Geol. Dept. Hebr. Univ.*, Jerusalem, **4**, 2-4.
15. PICARD L., AND AVNIMELECH, M., 1937, On the Geology of the Central Coastal Plain, *Bull. Geol. Dept. Hebr. Univ.*, Jerusalem, **1**, 4.
16. STERNBERG, C.W., 1956, *Petah Tiqva Shallow Gas Prospects*, Geological Survey of Israel, Jerusalem (unpublished).
17. TSCHOPP, H.J. AND WIENER, G., 1958, The Occurrence of Gas in the Beeri-Saad Area, *Bull. Ver. Schweizer. Pet.-ol-Geol. & Eng.*, **24**, 67.

PLATE I



A



B

A Core No. 1, 861 — 867 m.
Conglomerates and tuffs from top of National Park Volcanics.

L.P. — Large pebbles

S.P. — Small pebbles

T. — Tuffs

B. Core No. 3, 1040—1045 m
Vesicular Basalt. Note flow structure and alternations of vesicular and non-vesicular flows. The upper vesicles are filled with Calcite.

THE PLIO-PLEISTOCENE GEOLOGY OF THE ASHDOD AREA

A. ISSAR

Hydrogeology Division, Geological Survey of Israel, Jerusalem

ABSTRACT

Investigations carried out in the Ashdod area, which is part of the Southern Coastal Plain of Israel, have proved the occurrence of four major ingressions cycles also recognized in other parts of Israel, and assumed to be of Sicilian, Tyrrhenian I-II, and post-Tyrrhenian ages. The geographical extension of the ingressions and the distribution of the various lithological facies in the area are discussed.

The study is based mainly on sub-surface data.

INTRODUCTION

The present investigation was carried out by the author within the framework of geohydrological research of the Coastal Plain of Israel. This research is undertaken by the Hydrogeology Division of the Geological Survey of Israel in collaboration with the Hydrological Division of TAHAL (Water Planning for Israel). It also forms part of the author's Ph. D. thesis at the Hebrew University, Jerusalem, and is being carried out under the supervision of Prof. L. Picard.

The author wishes here to express his thanks to the latter as well as to Prof. Y. Bendor, Director, G.S.I. for permission to publish this paper.

AREA OF INVESTIGATION

The Ashdod area is part of the Southern Coastal Plain of Israel. It lies about 30km south of Tel Aviv and about 10km north of Ashqelon (see Reference Map, Figure 1). It is bounded in the West by the Mediterranean Sea, in the East by the Foothills region and in the South and North by the 125 and 140 E-W Israel (Palestine) grid system lines.

METHODS OF INVESTIGATION

Special problems of Pleistocene geology (lack of indicative fauna, alternation of facies, scarcity of outcrops in the area, etc.) make correlation between the numerous wells in this area difficult.

In order to solve the problems involved, the following methods have been applied:

- A. Macro- and microscopic analysis of all borehole samples for determination of:
1. their lithological composition (clay, silt, sand or gravel) and the mode of cementation (calcitic, limy, silty or limonitic);

On the basis of this analysis the various environments of deposition were determined and ingression—and regression—cycles recognized.

B. The latter cycles were followed in N-E to S-W geological cross-sections running along lines nearly parallel to the present day shoreline. Changes of facies, distribution of guide fossils and relative altitudes of typical stratigraphical complexes were used as criteria for correlation.

C. On the basis of the N-E to S-W geological cross-sections, E-W cross-sections were prepared showing the correlation of the various cycles of sedimentation.

D. Outcrops along the cross-section lines were examined and the data obtained were incorporated in the subsurface data.

ROCK TYPES AND FACIES

A. Sharon Formation (Issar 1960)

This term designates the marine to lagoonal clays, shales, silts and marls forming the base of the section studied.

The Sharon Formation includes the "Sakiebeds" of Loewengart (1928). Its age ranges from Neogene to Recent. The type-section of the Sharon Formation was established in a borehole at Kefar Shalem, and will be described (like those of the following formations) elsewhere.

The Sharon Formation is developed in four facies:

1. Deep marine
2. Shallow open sea
3. Shallow marine basins
4. Lagoonal and brackish.

B. *Pleshet Formation* (Issar 1960; *synon. with Calcareous Sandstone of Philistaea, Hull, 1885*).

This formation comprises the calcareous sandstone overlying the Sharon Formation. It is of Upper Pliocene to Recent age.

The type-section was studied in the Migdal (Ashqelon) well No. 5a. This formation is developed in three different facies:

1. Marine
2. Shore environment
3. Continental s. str.

C. Rehovoth Formation (Issar 1960)

This formation includes the continental loams (Hamra) and clays of red, brown and blackish colours. Its age is Pleistocene to Recent.

The type section was established in a well at Rehovot.

This formation occurs in two facies:

1. Soils
2. Swamp deposits

based on five observation wells which have been drilled at a small distance from the shore.

In Figure 2a, the lithologic sequence of the various boreholes is given, while in Figure 2b, the interpretation of the environment of deposition according to this section is shown.

The six rock complexes which are observed in this section show four cycles of

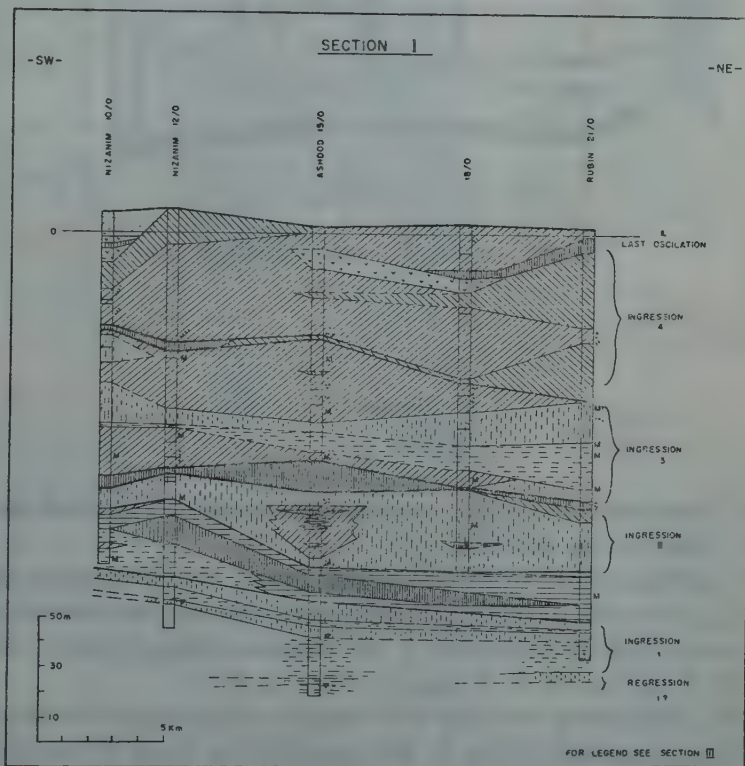


Fig 2b

1650

Figure 2b

marine deposition or ingression; each cycle begins and ends in a regressional phase.

The lowermost regression (regression No. 1 — M_1 Reiss — Issar 1960) is represented in this section by a change from marine clays to coralline and silty sandstone.

The four ingressions, Nos. 1-4 (M_{1a} - L_4 Reiss-Issar 1960) show a marked tendency to shallower conditions, from the bottom of the section to its top. This may point to the fact that the rate of sea penetration decreased from one ingression to the next.

Ingressions 2 and 3 (M_2 - M_{2a} Reiss-Issar 1960) are characterized by the occurrence of *Marginopora*.

Cross-section II (Figure 3) runs parallel to section I, at a distance of 4km from the

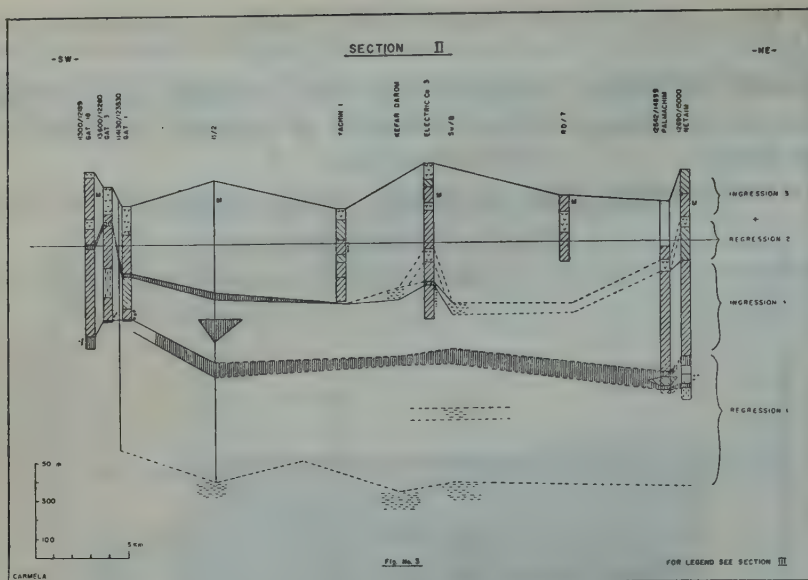


Figure 3

shore. Data from wells located at a small distance north and south of the Ashdod region were added to the section.

Only two ingressions may be observed in this section. The second one, containing *Marginopora*, shows a stronger continental influence than may be observed in section No. I. Moreover, while in section No. I, this ingression occurs between -50 to -150 metres m.s.l., in section No. II, it appears above sea level.

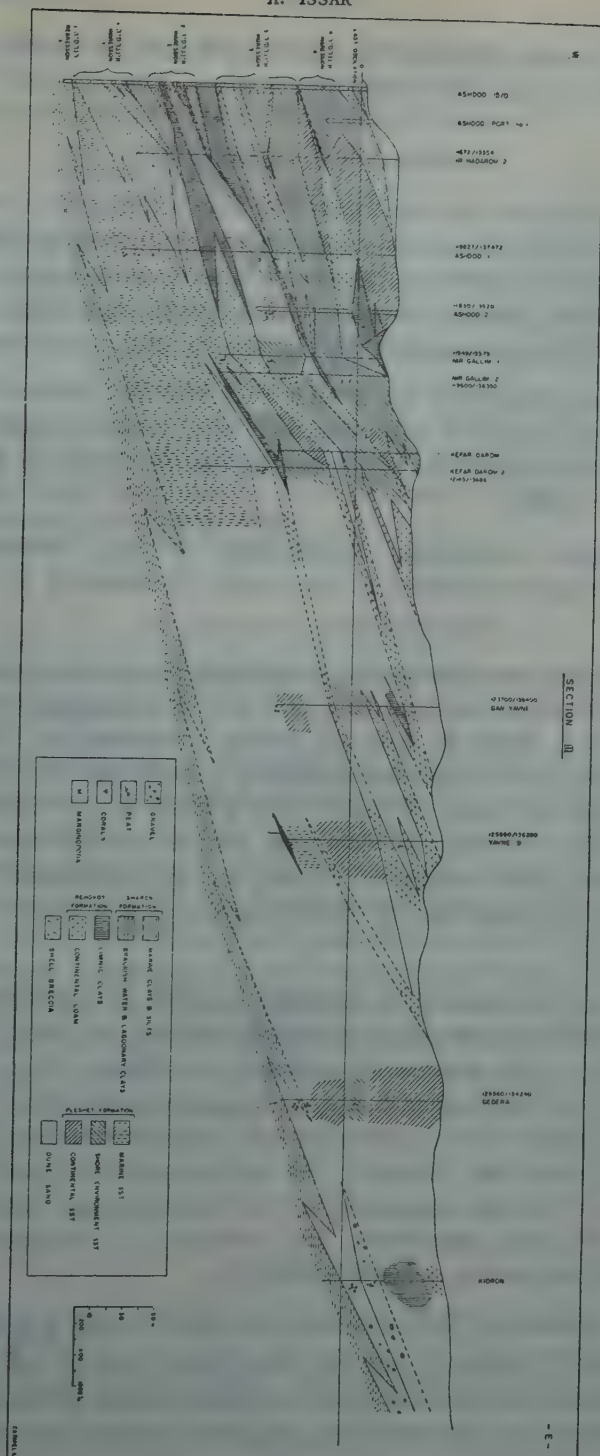
Section No. III (Figure 4) runs in an E-W direction 17km inland from the shoreline.

The sediments deposited during the first ingression are found in the western part of the section. These are Sharon clays, of a shallow open sea facies, alternating with algal limestone and calcareous sandstone containing corals. At a distance of approximately 5km from the coast, these layers pass into Pleshet sandstone of marine facies, and, some 10km from the coast, the sediments of the first ingression are found only as Pleshet sandstone of shore environment to continental facies.

Ahuzam gravel is found in the eastern part of the Coastal Plain alternating with, and overlying, sediments of the first regression and ingression.

The sediments of the second and third ingressions, which contain the *Marginopora* assemblage, become conglomeratic and detritic at a distance of about 3km from the coast. Approximately 4km from the coast, these layers appear in littoral to continental facies.

Marine sediments containing *Marginopora* cannot be found at a distance of more than 4km from the coast.



Sediments equivalent to those of the fourth ingression are found at a distance of about 1km from the coast in a continental facies.

CHRONOLOGICAL CORRELATION

It may be concluded from the above data that after a long period of marine transgression (Mio-Pliocene) one major regression and four main ingressions occurred in this region. The two middle ingressions are characterized by an assemblage containing *Marginopora*. Toward the end of the fourth ingression, an oscillation may be observed, but influenced in distribution by local conditions.

Correlating these events with the division suggested by Gignoux (1952), the first regression may be assumed to be of Calabrian age, the first ingression of Sicilian, the second and third ingressions of Tyrrhenian, and the fourth of post-Tyrrhenian age (Reiss-Issar 1960).

The *Marginopora* assemblage, characteristic of the Tyrrhenian, indicates that a warmer climate prevailed at that time (Avnimelech 1951, Reiss-Issar 1960).

In the Ashdod area, two occurrences of vertebrate remains were reported. The first one by Pilgrim (1941) who determined a skull of *Hemibos palestinus* from a well-sample near Gedera, at a depth of some 25 metres. According to Pilgrim, *Hemibos palestinus* may be of Villafranchian or slightly younger age. The site of this well is located between the wells of Gedera and Kidron shown in the eastern part of section No. III. It is obvious from this section that the layers found at a depth of 25 metres in the vicinity of Gedera are the continental facies (or the Villafranchian) of the upper part of the first regression assumed to be of Calabrian age.

The second find was reported by Avnimelech (1950). In a borehole near Yavneh (1248/1402 Israel grid system), *Elephas* bones were found at a depth of 74.6–75.2m (–35.6 to –36.2m m.s.l.). Avnimelech supposed the *Elephas* to be of the antiquess group and attributed a Tyrrhenian age to the marine sandstone found about 6m below the *Elephas* bones. The Yavneh well may be projected on section No. III between the wells Gan Yavneh and Yavneh 9. The marine sandstone found at the absolute depth of –35m in this area, is assumed to be of Calabrian age. As the species of the *Elephas* has not been determined, the divergence in interpretation between Avnimelech and the author remains unsettled.

Picard and Avnimelech (1937) described the log of a well drilled at Al-Kheimat east of Masmiye-El-Kabira. In this well, they found layers of soil and sand to a depth of 20m, sand and chert pebbles to a depth of 21m, sandstone and conglomeratic sandstone to 31.15m, and from this depth down to 86m, marls containing *Globigerina* in the lowermost part. They assumed a Quaternary age for the sand

pebbles and sandstone, and a Pliocene age for the marls. The Al-Kheima well may be projected approximately on the eastern end of section No. III. The conclusions drawn here correspond to those of Picard and Avnimelech.

TECTONICS

The dip of the layers of the first regression and ingression is $1/2^\circ$ to 1° ; it may be caused by tectonic movements or by sedimentary factors. The dip of the layers deposited by the second and third ingressions (Tyrrhenian) seems, however, more likely to be of a depositional nature. This assumption is based on the abrupt change of facies, from shallow-marine to continental sediments over a distance of about 4km. Moreover, as can be seen in section No. III, small changes of facies take place at a distance of about one kilometre from the shoreline, while the dip remains negligible. The same phenomenon has been observed in many other E-W cross-sections elsewhere in the Coastal Plain.

SUMMARY AND CONCLUSIONS

The events which occurred during the Pleistocene period in the Ashdod area may be summed up as follows:

At the end of the Pliocene or at the beginning of the Pleistocene, a regression occurred as a result of which the shoreline receded about 4km east of the present shoreline. During this regression, gravel layers accumulated at the eastern margins of the Coastal Plain (lower and upper gravel horizons, Picard and Avnimelech 1937). Following this regression, to which a Villafranchian age is attributed, a new ingression occurred which placed the shoreline about 5–6km east of the present shoreline. A Sicilian age is attributed to this ingression. The sea then retreated to the vicinity of the present shoreline and, during the Lower Tyrrhenian, advanced to about 3–4km of the present shoreline, later again retreating to the west. During the upper Tyrrhenian, it again advanced 2–3km east of the present shoreline. The post-Tyrrhenian shoreline was, in some places, in the vicinity of the present one, and in some places, a little more to the west.

REFERENCES

1. AVNIMELECH, M., 1950, On the finding of Elephas bones in a boring near Yavneh, Israel, *Ecl. geol. Helv.*, 43, No. 2.
2. AVNIMELECH, M., 1951, Contribution to the knowledge of the Quaternary oscillations of the shoreline in Palestine, *Proc. 1, Congr. Internaz. di Pleist. e Protoist. Mediter.*, Firenze, 1950.
3. GIGNOUX, M., 1952, Pliocène et Quaternaire marins de la Méditerranée occidentale, *Congr. Géol. Int. Alger*, T. 15.

4. HULL, E., 1885-1899, Memoirs on the Geology and Geography of Palestine, etc., *Palestine Exploration Fund*.
5. LOEWENGART, S., 1928, Zur Geologie der Küstenebene Palästinas, *Centralbl. F. Min. etc., Abt. B*, No. 9.
6. PICARD, L., 1943, Structure and Evolution of Palestine, *Bull. Geol. Dept., Hebrew University*, 4, Nos. 2-4.
7. PICARD, L. AND AVNIMELECH, M., 1937, On the Geology of the Central Coastal Plain, *Bull. Geol. Dept. Hebrew University*, 1, No. 4.
8. PILGRIM, G.G., 1941, A fossil skull of Hemibos from Palestine, *Annals and Magazine of Nat. History, London*, 2, No. 7.
9. REISS, Z. AND ISSAR, A., 1960, Subsurface Quaternary Correlations in the Tel Aviv Region, *Geol. Survey of Israel, Bull. No. 29*.

AIRBORNE SALTS — THE MAJOR SOURCE OF THE SALINITY OF OF WATERS IN ISRAEL

S. LOEWENGART

Department of Mining Engineering Israel Institute of Technology, Haifa

ABSTRACT

The majority of the salts in all waters of Israel and Jordan is traced back to air borne salts carried by seasonal rains into the country. The yearly salt precipitation at the coast amounts to 100–150 kg Cl⁻/ha and decreases geometrically towards the interior, at the fringe of the desert to about 10 kg. The precipitation is calculated indirectly in three different ways, all figures obtained being in good agreement with each other and with direct measurements previously made.

The yearly intake of air borne salts by the whole Rift Valley is calculated in the same way. The author arrived at a quantity of about 80×10^6 kg Cl⁻ per year, which — under present conditions — could have achieved the accumulation of all the salts supposed to be in the area, in 1.5–2 million years.

The size of the catchment area of the Yarkon (Rosh Ha-Ain) Springs is calculated on the basis of the quantity and the chemical composition of its salts.

The mechanism of continuous or interrupted influx of sea water into the karstic aquifer at the coast is explained.

The steady increase of salinity in the Pleistocene aquifer of the coastal plain is explained by the yearly precipitation of air borne salt on one side and the decrease of the quantities of water draining into the sea on the other. By the normal exploitation of the aquifer salts are recycled and accumulated. A formula is given for this process, the rate of which is inversely correspondent to the thickness of the aquifer.

In a previous paper (Loewengart 1958) the author tried to explain the quantitative and qualitative composition of the salt-content of Israel waters. He tried to follow the process of differentiation of sea salts when they meet with the carbonates of the mainland and when they undergo ion exchange. Many indications pointed to the aerial origin of the salts in the Pleistocene and limestone groundwaters of the Coastal Plain, especially the Cl⁻/Br⁻ ratio and the "Alkali Number".* It was impossible, however, to prove this conclusively and to make numerical estimates as regards the quantities of salt precipitation from the air.

One of the first studies dealing with the significance of airborne salts was probably Holland and Christie's (1909) now almost classical research in this field, concerning the Indian inland lakes of Rajputana. F.W. Clarke (1924), and later V.M. Goldschmidt (1958), attributed due importance to the airborne transport of salts, but they did not have sufficient material for numerical conclusions.

Conway (1942) in a very elaborate paper proved conclusively that the greatest part of the chlorides in inland waters originates from airborne salts. He suggested a mathematical formula which expresses the amount of precipitated chlorides as an

* (eq. $\frac{Na + K}{Cl} \cdot 100$)

exponential function of the distance from the coast-line. This calculation is based on a chlorinity map of the surface waters of the New England states. Here, the chlorinity amounts to about 6 ppm at a distance of 3km from the sea, but decreases to about 3ppm at a distance of 25km and to 1.5ppm at 50km, while there remains always a hard core of salinity of about 0.2 ppm over the whole interior of the United States. A comprehensive survey of the question is given by G.E. Hutchinson (1957) in his "Limnology". Great advances were made in the field of airborne salt research during the last five years, when meteorologists developed a new field of research — "Chemical Meteorology".

In 1959 Eriksson, the most prominent author in this field, published a comprehensive paper which presents all the data collected by him and other workers during the last few years. A short summary of the present state of knowledge, pertaining to the subject of this paper, follows:

1. During the year 1958, the amount of chlorides precipitated from the air was measured over the United States, Western Europe and Australia. The maximum precipitation over the Gulf Coast was about $20\text{kg Cl}^-/\text{ha}$. The minimum on the coast of Maine was about $7\text{kg Cl}^-/\text{ha}$. On the West Coast the maximum was about $36\text{kg Cl}^-/\text{ha}$ in the State of Washington, the minimum — about $4\text{kg Cl}^-/\text{ha}$ — was in Southern California. The methods of measurement were probably not uniform all over the world, as on the Atlantic coast of Europe much higher figures were obtained: $200\text{kg Cl}^-/\text{ha}$ on the Irish West coast, $148\text{kg Cl}^-/\text{ha}$ in Cornwall, from $40\text{--}130\text{kg Cl}^-/\text{ha}$ along the Atlantic coast of Scandinavia. In Australia, the whole West coast from West Australia through South Australia and Victoria lies between the 100 and $150\text{kg Cl}^-/\text{ha}$ isohyete.

2. Eriksson (1955) compared the measured rates of precipitation with those calculated from the run-off of some of the main rivers in Sweden, and showed that in some countries rain carries only about $1/3$ of the total airborne salts. In his opinion, the remainder precipitates as dry fallout. Similar conclusions are also drawn from the figures for the Mississippi Valley catchment area. In Australia, however, the quantity of Cl^- precipitations calculated from rainfall and from the river run-off is almost identical (Anderson 1945). The same is also true in Israel, as will be shown later.

3. The airborne salts created by wind and tides originate on the interface between the ocean-water and the air. They are lifted by turbulent currents into the air and reach their maximum concentration at a level of about 800m.

4. The chemical composition of the salts in sea- and in rainwater is very similar. This is true at least for those areas in which the average rainfall contains not less than about 2 ppm Cl^- as in Israel and Jordan. The differences in composition discussed by Eriksson (1959) show no uniform pattern. Eriksson rules out the possibility of fractional crystallisation of sea-salt in the air proper. Hutton (1958), Hutton and Leslie (1959) and Hingston (1958) bring comprehensive data on the chemical composition of rain waters in Southeastern and Western Australia, from which one arri-

ves at the conclusion that the original composition of the sea salts is largely preserved until their precipitation from the air. (See also Loewengart 1958). The reaction of small quantities of H_2SO_4 derived from the release of SO_2 from the biosphere (Eriksson 1958) and of HNO_3 with mineral dust floating in the air is probably responsible for small the excess of Ca and Na. Larger excess quantities of Ca and Mg are always connected with equivalent quantities of HCO_3^- originating in terrestrial dusts.

5. Man-made pollution, mainly through combustion, is partly responsible for the excess sulphates.

6. Partly relying on Anderson (1945), the following formula is given: if N (mm) is the yearly precipitation, E (mm) the yearly evaporation, C_n (ppm) the concentration of chlorides in the rain water, C_g (mm) the Cl^- concentration in the groundwater in a stationary state, then: $C_g = C_n \frac{N}{N-E}$.

SALT PRECIPITATION OVER ISRAEL AND JORDAN

On the basis of the above new data, tentative calculations of the amount of salt precipitated over Israel and Jordan can now be made. The quantity of airborne salt precipitation will be calculated in four different ways.

1. *Groundwater-spring method*

The chemical composition of waters of low chloride concentration seems to confirm the fact that the salts at least in these waters, are airborne (Loewengart 1958). For the whole area, without taking into account more or less theoretical evaporation rates, empirical infiltration rates are well known and we may rely within certain limitations on the data given by M. Goldschmidt (1958, 1959) and Santing (1958). In order to calculate the total quantity of Cl^- deposited on a unit of area (1 ha) we multiply the quantity of infiltration (mm) by 10^4 , and by the observed concentration in this specific area. As previously, we choose only representative minima of concentration for this purpose. If, for instance, the theoretical infiltration rate in a certain area is 360mm, and the concentration of a spring draining this area 20 ppm Cl^- , then the total Cl^- precipitation (kg Cl^- /ha) is therefore $0.360 \times 10^4 \times 0.02 = 72$.

Total infiltration in $\text{m}^3/\text{ha} \times \text{kg } \text{Cl}^-/\text{m}^3 = \text{precipitation kg } \text{Cl}^-/\text{ha}$. Only in the most favourable cases when a maximum infiltration rate is reached, does the possibility exist to base the calculation on M. Goldschmidt's (1958) empirical formula which reads simplified as follows: Total runoff = 0.9 (total precipitation in mm - 360) (M. Goldschmidt 1958). The quantities of storm water runoff in vadis, which are always less than 10%, are neglected in this calculation. They are mostly turned into infiltration in the same, or in another area, and their salts are, therefore, finally fed into the ground water. As in the above formula all areas with a precipitation less than 360mm are excluded; its value increases with higher precipitation figures and decreases with lower ones. By applying the system of represen-

Locality	District	Nature of the water	Cl- ppm () author	Precipitation (mm)	Actual runoff (author)	Calculated chlorine precipitation kg/ha
Ein Mushreifa	Near Rosh Hanikra	Karst spring	30-40 (Ch)	about 700	300 G.	108-120
Ein Malcha	Hule area	"	18-20 (Ch)	about 800	400 G.	72-80
Ein Faradia	Galilee	"	18-20 (Y)	790	390 G.	71-78
Ein Tsin	Safed	"	18-20 (Y)	about 740	350 G.	61-70
Nachal Amud	Safed area eastern drainage	"	20-22 (Y)	710	310 G.	62-68
Kabri springs	Acre plain	"	23 (average from 30 samples) (Y)	" 740	330 G.	
Nahal Betset (Karkara)	Western Galilee	"	23 (average from 4 samples) (Y)	" 923	475 G.	76 126
Nahal Wadi Keren	" "	"	28 (average from 8 samples) (Y)	" 680	520 G.	140
Haifa Bay Dunes	Coastal Plain	Pleistocene dune water	30 (minimum) (Y)	" 600	340 S.	102
Hadera Paper Fact	Central Coastal Plain	Pleistocene ground water	47 (Y)	" 600	225 S.	106
Ramat Gan	" "	" "	45 (Y)	" 532	175 S.	79
Bat Yam	" "	dune water	30 (Y)	518	325 S.	95
Rishon le Zion	" "	partly dune water	45 (Y)	" 518	145-325 S.	abt. 100
Migdal Ashkelon	Southern Coastal Plain	Pleistocene dune water	63 (Y)	" 450	275 S.	185 ?
Yad Mordekhai	" "	" "	75 (Y)	" 415	250 ? S.	187.5
Nir Am	" "	Pleistocene water	117 (Y)	" 450	100 S.	117
Hadassim	Central Coastal Plain	Pleistocene ground water	50 (Y)	" 550	225 S.	120
Yavne area	Southern Coastal Plain	Pleistocene water	80(T)	" 450	125 S.	100
Ashdod-Gat area	" "	" "	105 (T)	400	100 S.	105
Nahal Sorek	Central foothill area	Surface flow	16-26 (Y)	688	275 G.	58
Bittir (Betar)	Judean Mountains	Perched spring in cenomanian	24 (average from 20 analyses) (CH)	660	260 G.	62.5
Deir es Sheikh	" "	Perched spring	24 (CH)	640	235 G.	56
Ein Karem	" "	" "	30 (CH)	620	220 G.	66
Ras el Ain springs	Samaritan Hills	" "	20 (CH)	730	330 G.	66
Ein el Askar	Nablus Area Jordan	Eocene Limestone	18 (CH)	730	330 G.	60
Tafle Bosera springs	on the Moab	"			Probably less than 40	
Shobrek Ein Musa spring	Highlands Jordan	"	25-45 (T)	200-280 (T)		10 estimate

TABLE II
Chlorine precipitations from catchment areas

River	Chlorinity (ppm)	Average precipitation (not for calculation) (mm)	Yearly runoff $\text{m}^3 \times 10^6$	Catchment area (km ²)	Calculated Cl- precipitation kg/ha (kg)
Jordan up to Bridge of Jacob's Daughters	15	(average) (Y) 1946/47	480	1500	50-60
Its tributaries:					
Nahal Hermon (Banias)	14	1053 mm (1901-1930)	62.4	175	84
Hasbani	16	1147	70	152	112
Yarmuk	55	364 (B)		7250	34
	90	regular flow 248 (I)			
	15	storm water flow 223 (I)			
Rivers of Northern Gilead (Kufrinjah Rajib)	25	525	100-150	1250 (I)	25-35
Zerka (Jabok)	98	291			
Auja (Nahal Kelt)	30	525	60	2960 (I)	appr. 20
Ain Gedi	64	(BG)	22		33
Sered (Wadi el Hesa)	90	162	22	480 (BG)	about 29
Jordan Allenby Bridge (total catchment area)			23	1750 (I)	12
				16700	about 32

To Tables I. and II. Analytical and hydrological data taken from:

Y. Hydrological Yearbook of Israel (a-c)° B.G. Blake-Goldschmidt

Ch. Chemical analysis Palestine etc. I. Ionides

G. Calculated on Goldschmidt's formula B. Bardon.

S. Santing

tative minima of Cl^- concentration for a given sector we shall arrive according to the above formula at tentative values for airborne salt precipitation. (Table I). This procedure presupposes of course the uniformity of the area in question. Only in areas in which no impervious surface exists are the ideal figures of infiltration attained, otherwise infiltration may be restricted to about a quarter or even less. Rates of infiltration for the coastal plain of Israel which take account of the surface properties of the ground are given in the hydrological paper by Santing (1958) and are also used for this calculation.

2. Catchment area method

Following Anderson (1945) and Eriksson (1955, 1959) the total amount of Cl^- contained in the run-off of an area drained by a single river has been calculated. By dividing this quantity by the size of the catchment area, figures for airborne salt precipitation are obtained (Table II) which, although subject to many possible errors, have at least a tentative value.

3. Direct measurements

The most satisfactory way to obtain figures on precipitation of airborne salts is the actual measurement of the salt content of rain water. Measurements of this kind were carried out by Menchikovsky (1925). The Cl^- content of the rainwaters mentioned in these early papers (Table III) is in good agreement with the figures obtained by the independent procedures outlined in this paper. As in Australia, there seems to be no necessity to assume any dry fallout of airborne salts, as the quantities contained in the rain are entirely adequate.

Menchikovsky (1925) made during two seasons measurements in Tel-Aviv at a distance of about one km from the sea and the samples collected by him comprise about half of the total quantity of rainfall over the whole rainy season. For the figures obtained further inland however, no details of the collecting procedure are given. As already pointed out by Eriksson (1952) and others, the Cl^- concentration of each rainfall is to a first approximation an inverse function of the size of each rainfall. The present author has analysed the Cl^- concentration of rains in the Haifa Bay area at a distance of 3 km from the sea and found figures very similar to those of Menchikovsky. The bulk of the winter rains contained about 15 ppm Cl^- , but figures as low as 5 ppm and as high as 60 ppm were occasionally observed.

TABLE III.
Salinity Data from Menchikovsky (1925).

Locality	Average Cl^- in rain in ppm	Cl^- precipitation kg/ha/year
Tel Aviv (1km from sea)	25.3	140
Petah Tikvah	10.6	59
Ben Shemen	12.5	64
Ein Harod	10.6	42
Ayelet Hashahar	9.7	46

Remark: It is not known on how many measurements the figures, besides those of Tel Aviv are based.

4. Flood water method

An additional way to calculate precipitation is based on the salinities of storm water flows.

Table IV A-B gives figures of Cl^- concentrations for a number of storm water flows (taken from the Hydrological Yearbooks of Israel) which all belong to normally dry river beds which lead to the Mediterranean; an exception is Nahal Alexander which has a small perennial flow. All the samples were taken from gauging stations during storm flows which occur only a few times during winter. In respect to Cl^- , therefore, all these waters can be classified as pure rainwater in which no evaporation has occurred. The quantity of Cl^- picked up on the way is probably almost negligible, at least where storm flows had occurred previously. If small quantities of Cl^- are collected in this way they are probably compensated for by the intensity of the flood-producing rains which have a lower than average Cl^- content. By calculating salt precipitation from average salinities of these storm flow waters (regarded here as unchanged rainwaters) results are obtained which are — except in two cases — in good agreement with the results based on methods 1–3. The results for Nahal Alexander for the year 1949/50 seem too high and are more than twice the figure obtained by other calculations. This disagreement is probably due to the small perennial flow of this river which has a higher salinity than rainwater. The figure for Nahal Beersheba is about half of that obtained by other calculations. Ionides (1939) measured the Cl^- content in a flood in Aman and obtained 18ppm. This single figure obtained from Transjordan is not taken into account.

The calculated quantities of salt precipitation in Tables I–IV are plotted in Figure 1 against the respective distances from the sea in km. As precipitation decreases ex-

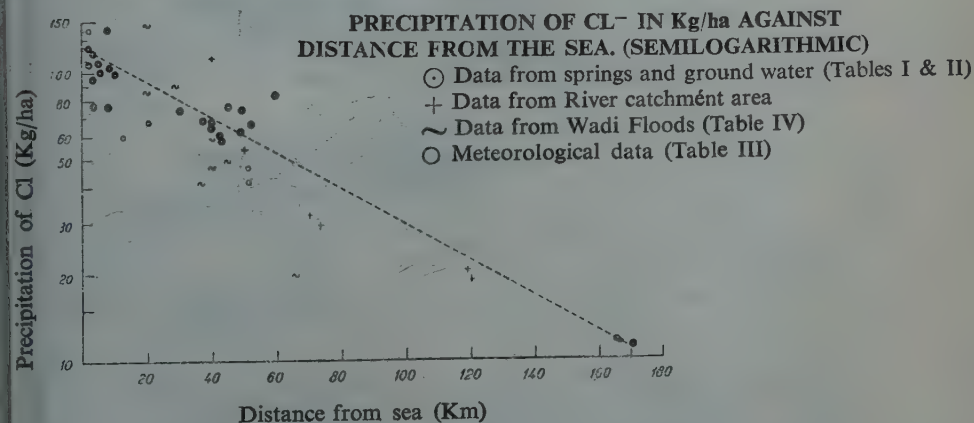


Figure 1

ponentially with increasing distance from the sea, the data is therefore plotted logarithmically. Thus a straight line is obtained on the basis of which a tentative map for salt precipitation has been drawn (Figure 2). The Isolines probably show too high

TENTATIVE SALT PRECIPITATION OVER ISRAEL AND JORDAN IN Kg/ha Cl^-

1:2 000 000

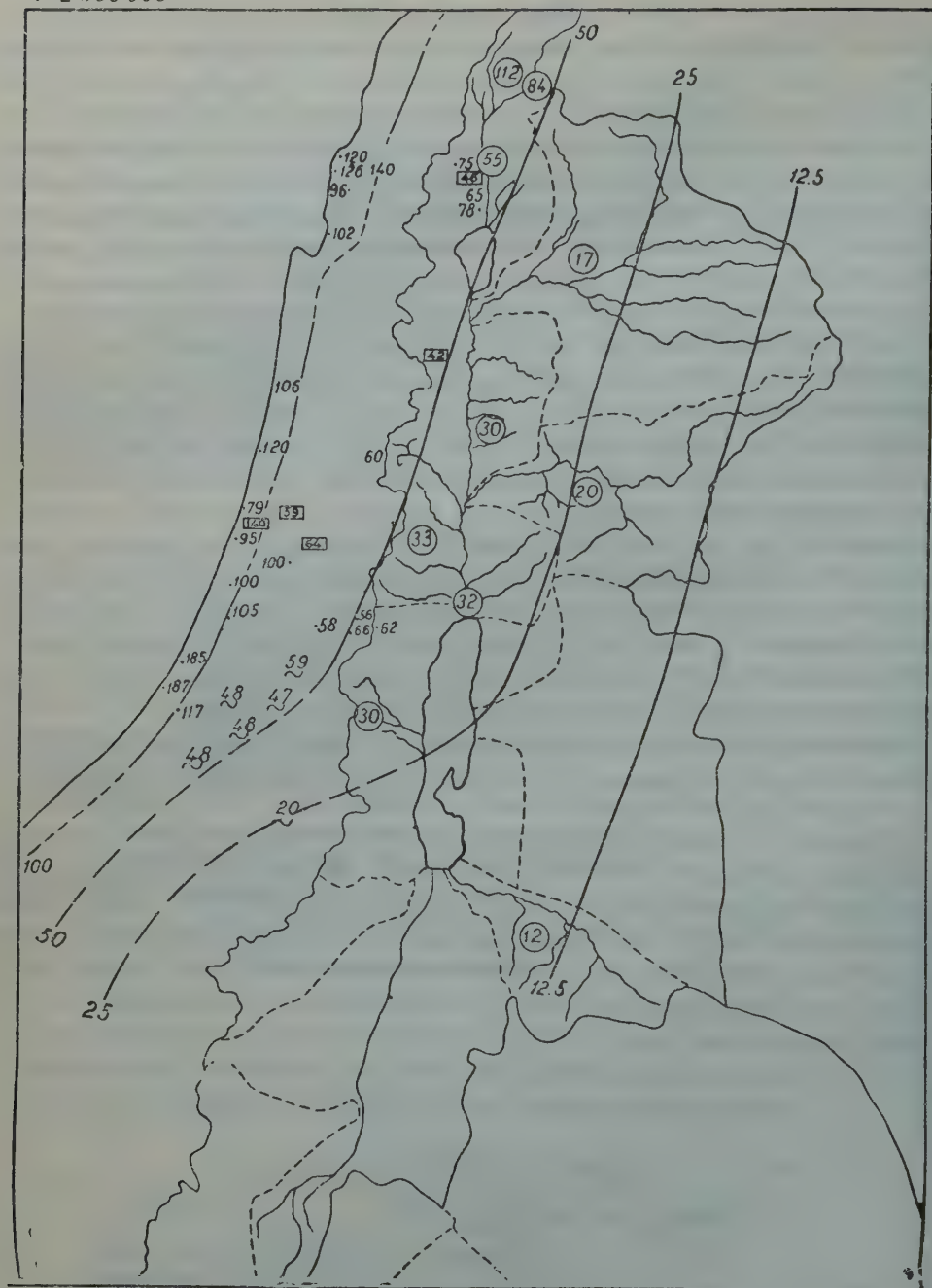


Figure 2

- calculated Cl^- precipitation from ground water and springs.
- calculated Cl^- precipitation from river catchment areas.
- Cl^- precipitation from rain observation (Menchikovsky).
- ~ calculated Cl^- from wadi floodwaters.

TABLE IVA

Cl⁻ concentrations of flood waters at specific dates (Hydrological Yearbooks of Israel)

ppm		ppm	
Nahal Hillazon at Yas'ur (Wadi Halazon near Birwa)			
14. 1.47	12	25. 1.47	16
21. 1.47	8	2. 2.47	24
21. 1.47	8	4. 2.47	24
22. 1.47	8	23.11.50	12
22. 1.47	12		
22. 1.47	10		
Nahal Alexander near Hadera, at Maabarot (Nahr Iskandaruna)			
24.12.48	36	20. 1.47	20
31. 1.49	27	2. 2.47	14.8
8. 2.49	32	25. 3.47	24.5
6.11.46	18		
14. 1.47	19.6		
Nahal Ayalon (Wadi Salame) at Nahalat Yitzhak near Tel Aviv			
1. 2.49	17	25.12.49	12
8. 2.49	24	27.12.49	8
		29.12.49	16
Nahal Govrim (Wadi Jaladiah) near Shafir (123E 123N)			
29.12.49	12		
17. 1.50	16		
23. 1.50	12		
Nahal Lakhish near Ein Tsurim (Wadi Qureiqui) (122.5E, 123.3N)			
29.12.49	8		
17. 1.50	16		
23. 1.50	10		
Nahal Shikmah at Yad Mordekhai (Wadi Hesi at Deir Suneid) (107E, 108N)			
18. 3.47	12		
19. 3.47	12		
Nahal Garar (Wadi Sharia) (113E, 087N)			
23.12.49	12		
29.12.49	20		
Nahal Beersheva Wadi Shaab at Beersheva (131E, 071N)			
23.12.49	4		
29.12.49	4		
17. 1.50	12		

Drainage area gauging points from Map No. 1, attached to Hydrological Yearbook, Jerusalem 1952).

TABLE IVB

Cl⁻ content of precipitations calculated from average compositions of flood waters (Table IVA) and average yearly rainfall. (Distances refer to median distance of catchment area in km from the sea)

Catchment Area	Average Cl ⁻ precipitation (ppm) (number of samples)	Average Rain precipitation (mm)	Calcul. Cl ⁻ kg/ha	Median Distance from sea (km)
Nahal Hillazon (Wadi Halazon at Birwa) Yas'ur	13 (10)	650	85	20
Nahal Alexander at Maavaroth	16.9 (5) in 46/47 29	629	126 178 ?	20
Nahal Ayalon (Wadi Salame at Nahalat Yitzhak	15.8 (5)	580	90	28
Wadi Jaladiah near Shafir	12.7 (3)	460	59	40
Nahal Lakhish (Wadi Qureiqui)	11.3 (3)	412	47	40
Nahal Shikmah (Wadi Hesi)	12 (2)	350	42	35
Nahal Garar (Wadi Sharia)	16 (2)	303	48	45
Nahal Beersheba (Wadi Saab at Beersheba)	6.7 (3)	280	19	65

values of salt precipitations for areas with low rainfall, in so far as they are not derived from river salinity data and too low values for areas of very high rainfall. From the above graph (Figure 1) a formula similar to that of Conway (1942a) and Seeflang quoted by Eriksson (1952) can be empirically derived:

$$N = 110 \times \frac{-c}{75} e$$

where N is the amount of salt precipitation in kg/ha and c the distance from the sea in km.

In the following chapters different aspects of the airborne salt approach are discussed.

THE DRAINAGE AREA OF THE RIFT VALLEY AND THE GEOCHEMICAL HISTORY OF THE DEAD SEA

The three main headwaters of the Jordan drain a mountainous and humid area where rainfall varies from 700 to 1200 mm/a. The average Cl⁻ concentration of the Jordan river, on leaving the Hula area, is only about 15 ppm. The salt precipitation value is therefore, between 50–60 kg Cl⁻/ha (See Table II). Still higher figures prevail for parts of this area, as for the Banias (84 kg Cl⁻/ha) and for the Hasbani river area (112 kg

Cl⁻/ha). The lowest Cl⁻ concentration observed in the area, was from the Dan (Tel el Kadi) waters—4ppm—(Hydrological Yearbook 1946/47) which arise in the same drainage area as the Hasbani (8 ppm Cl⁻). As usual the lowest figures refer to the rainy season in which rainfall sometimes turns entirely into runoff.

Important springs on the western side of the Rift Valley north of Lake Tiberias, like Ein Malcha, Ein Parod, Ein Tsin, (see Table I), show values corresponding to a precipitation of 60–80 kg Cl⁻/ha. However, only part of the salt carried by many springs of the Lake Tiberias area and farther south is derived from the current precipitation of airborne salt. As pointed out earlier (Loewengart 1958), another important source of salts in this area is residual evaporation brines. A criterion for distinguishing these two types of salts is the Cl⁻/Br⁻ ratio, which is about 300 in the ocean and in air borne salts, but considerably lower in the residual brines. A considerable proportion of the salts in the more saline springs discharging into Lake Tiberias and at least in part in springs of the Beisan (Beth Shean) district must be derived from residual brines.

A calculation of the overall salt precipitation of the catchment area of the Jordan (about 16700km² against about 40000km² for the whole Rift Valley) can be carried out by combining the Cl⁻ rates given by Ionides (1939) with the run-off given by Neumann (1958). The total amount of Cl⁻ carried annually by the Jordan River is, based on these figures, 320 × 10⁶ kg Cl⁻, but only 51.5–79.5 × 10⁶ kg Cl⁻ are to be regarded as supplied from the current precipitation of air borne salts as explained in the following Table and additional text.

TABLE V
Yearly Cl⁻ content in Jordan at Allenby Bridge (Jericho) in 10⁶ kg.

Total (Ionides and Neumann)	320	thereof yearly precipitation 51.5–79.5	
Specification:			
Jordan at outflow from Lake Tiberias	145	15–33	(Loewengart 1958)
Yarmuk	25	12.5	(Table II and text below)
Beisan Springs	56	12	(Loewengart 1958 and text below)
Inflow from western side, south of Beisan	4	4	(Table II and text below)
Inflow from eastern side, south of Yarmuk	8	8	(Table II and text below)
Not accounted for	82	0–10	(see below)

The total inflow of Cl⁻ into the Dead Sea, regarded as not derived from the recent cycle of air borne precipitation, is the result of the evaporation of an inland lake of the Late Tertiary and Pleistocene times, which received its oceanic salt components through the geological past from the continuous inflow of inland waters containing slight quantities of air borne salts. Most of the sodium chloride was deposited in the Dead Sea area while the residual brine spread out over all the parts of the Rift Valley in so far as it existed then. The deepening of the erosion basin in the Later

Pleistocene exposed these trapped solutions which are now drained by meteoric waters into Lake Tiberias and further south into the Jordan Valley.

From the 145×10^6 kg Cl^- leaving annually Lake Tiberias only 12×10^6 are provided by the inflowing Jordan, being no doubt of cyclic origin, plus perhaps another 3×10^6 from air borne salts over the area which is drained immediately into the Lake, all the rest would come from residual brines. It can be assumed that the springs draining into the Lake are mixtures of a residual brine, like the Tiberias Hot Springs (Cl^-/Br^- 75), — and such a brine was lately detected in many borings beneath the Lake (written reports from Israel Water Planning Ltd.) — with meteoric waters (Cl^-/Br^- 290). To obtain a 120 Cl/Br ratio for the outflow from the Lake (Loewengart 1958) an admixture of about 30×10^6 kg Cl^- out of air borne salt would be required, or correspondingly less for a Cl/Br ratio higher than 75. The author is here in full agreement with Dr. Taussig from Israel Water Planning Ltd., who proves such a mixing process by a number of calculations (unpublished report, 1960).

The most important tributary of the Jordan which carries even more water than the Jordan itself is the Yarmuk river. Burdon (1954) gives a total run-off figure of 580×10^6 m³/year and one Cl^- value of 55 ppm. Ionides gives 248×10^6 m³ run-off from regular flow, with an average Cl^- concentration of 90 ppm, and 223×10^6 m³ of storm water flow with an average Cl^- concentration of 15 ppm. These figures enable us to calculate the Cl^- precipitation for the unit of area. (See Table II). The Cl/Br ratio of the Yarmuk River water according to information received from Dr. Taussig is 187. It follows, therefore, that the Yarmuk receives half of its salts from brines and only half of the chlorides is derived from cyclic salts. This would reduce the precipitation figure for the Yarmuk area to 17 kg Cl^- /ha.

We are on more secure ground as regards the *Beisan Springs* and other waters flowing from the western side to the Jordan. From a number of springs in the Judean and Samarian hill region (Table I) the Cl^- precipitation can be easily calculated as between 50–70 kg/ha. Besides those springs with minimum salinities, generally about 20 ppm, on which the calculation was based (as for springs in the vicinity of Jerusalem and Nablus), there exist springs with higher salinities, such as from Anebt in the Nablus area with 60 ppm whose catchment areas do not comprise pure limestone areas like the former, but are partly covered by more impervious Senonian–Eocene marls, so that the cyclic salts in the water become more concentrated because of a lower rate of infiltration. (See chapter dealing with the Yarkon Springs, page 197). The springs of the Beisan district can be divided into two different groups (Loewengart 1958, p. 202). The group of less saline waters with an average 176 ppm Cl^- and a Cl/Br ratio of 257 can be regarded as a mixture of cyclic salts (Cl/Br 290) with the salts of the waters of the more concentrated group of springs (Cl/Br 166, Cl^- 770 ppm) in a relation of about 3:1. It can be safely assumed that the flow of groundwater for this area, before any residual brine is taken up, has already a basic salinity of about 120 ppm Cl^- of cyclic origin. Based on the figures of the total yield

of all the springs (about $35 \times 10^6 \text{ m}^3$ for the less — and 65 for the more concentrated), it may be a fair estimate to take about $12 \times 10^6 \text{ kg Cl}^-$ from the total supply of 56×10^6 as derived from current precipitation. Taking the precipitation figures from the map (Figure 1) as a basis, this would require an effective catchment area of about 2400km², in which are included very inefficient groundwater-collecting areas like Emek Jesreel and the Jenin Plain. This is a situation very similar to that in the catchment area of the Yarkon (Ras el Ein) Springs, to be described later.

The “Inflow from the western side” consists of an estimate of the whole inflow into the Jordan south of the Beisan Springs with $80 \times 10^6 \text{ m}^3$ (M. Goldschmidt 1959) and our estimate of a salinity of not more than 60 ppm Cl^- , which may be regarded as of entirely cyclic origin.

Similar calculations (see Table II) have been carried out on the basis of figures published by Ionides (1938), Wilson and Wozab (1954) for the catchment area of a number of small rivers draining the northern Gilead (Golan) area and for the Yabbok (Zerka) area, which together make up the “Inflow from the eastern side”.

It appears from Table V that the important quantity of $82 \times 10^6 \text{ kg Cl/year}$ is taken by the Jordan on its way from Lake Tiberias to the Dead Sea. The sources of this additional salinity are stated as “not accounted for”, but it can be assumed that the bulk of this quantity consists of residual brine. The Cl/Br ratio at Jericho is about 130 as against 120 in the outflow from Lake Tiberias and remains so, almost unchanged. It is known that all water borings in the Jordan valley (Jericho, Shuni, Jiftlik etc.), (Ionides 1938, Blake and M. Goldschmidt 1947) have met waters of very high salinity which probably are taken up by the Jordan in many small seepages.

The catchment area of the Dead Sea, excluding that of the Jordan Valley, comprises about 23, 300 km², for which the following estimate of air borne salt precipitation can be made:

	Size of Area	Kg Cl/ha	Total inflow in 10^6 kg Cl^-
Eastern slope of Judean Mountains	2500 km ²	30	~ 7
Trans-Jordan Highlands (Moab)			
drained into Dead Sea	9500 km ²	15	~14
Araba Valley	11300 km ²	5	~ 5

The estimate for the inflow of air borne salt into the Dead Sea from the Judean Mountains is taken from the data of the Ein Gedi Springs in Table II. The very important and strong Feshkha Springs, originating in this area, with a salinity of 1500–4000 ppm Cl^- , may have their salts from previous inundations of the Dead Sea into the Karst water, as according to Wilson and Wozab (1954) the chemical composition is very close to that of the Dead Sea water.

For the southern part of Transjordan (Moab) which drains into the Dead Sea an estimate of salt precipitation is made for the area of Nahal Sered (Wadi el Hesa) in Table II. In Table I Cl^- concentrations of a number of springs from the Highlands of Moab are given, which also point to precipitation figures of about 10 kg/ha. The reversal of salinity figures quoted in Table I from Ionides (1938) for the southern

and southeastern parts of the territory of Jordan together with the rainfall rates of nearby localities is very instructive. In particular the relatively low salinities of springs in the very arid parts of Transjordan should be compared with the high salinities of groundwaters and springs in the Southern Negev where rainfall conditions are similar. In order to recognize the tremendous influence played by the distance from the sea.

The most arid part of the Dead Sea drainage area is the *Nahal Zin and Arava Valley* South of the Dead Sea with about 11,300 km² and a yearly rainfall of 50–100 mm. Shiftan (1958) described the not unimportant underground flow, which has a Cl⁻ content of around 1000 ppm. This groundwater collects probably most of the precipitated air borne salts of the area in addition to those which may flow into this deep depression from west and east. The yield of this groundwater flow is estimated by Shiftan (verbal information) to be about 24×10^6 m³/year, which corresponds to an equal amount in kg Cl⁻. The chemical composition of this water shows no resemblance to the Dead Sea brine, however, the Cl/Br ratio of the water in Nahal Zin is 177 (Dr. Taussig, unpublished report 1960), and this fact proves that a large part (at least half) of these salts is cyclic salts emanating from the Dead Sea area, a possibility already foreseen by Shiftan (1958). By assuming that half of the remaining salts come from the adjoining areas, the total yearly precipitation over the Arava would come to 5 kg/ha per year.

THE ORIGIN OF THE DEAD SEA SALTS

It appears from the above calculations and estimates that under present conditions at least about 75×10^9 kg Cl⁻ are brought every year from the outside by rains from the Mediterranean with groundwaters and floods into the closed basin of the Rift Valley.

While for geological reasons a contact between the Rift Valley and the Mediterranean cannot be excluded, it is most probable that the salts of this basin represent the accumulation of air borne salts. As in both cases the salt-water is ultimately derived from the sea, the question cannot be easily decided by chemical reasoning. The almost entire absence of iodine in the Dead Sea (verbal information by Y. Bentor according to Eriksson (1952) is a characteristic feature of air borne salts. The accumulation of air borne salts must take place in a basin under all circumstances so long as it is closed, while the intrusion of the sea and all subsequent processes are always dependent on chance.

It has been calculated (Loewengart 1958) that in order to balance the quantities of Br⁻ in the Dead Sea at least 200×10^9 tons NaCl must be buried in the Rift Valley. This corresponds to 121×10^9 tons Cl⁻ in addition to 26×10^9 tons Cl⁻ which are present in the water of the Dead Sea. The recent oil-borings at Sdom and the test borings in the area of the Potash Works make this estimate probable. Only 1.5–2 million years would be necessary, under today's conditions, for the accumulation of this quantity of Cl⁻ and the corresponding quantity of other sea salts. The existence of the Rift Valley, however, goes back at least to the Miocene. It is true that the catchment area of the basin was originally much smaller and has grown steadily through lateral erosion. On the other hand during Pliocene and early Pleistocene

cene time the Mediterranean coast was much nearer to the Rift Valley than it is at present, and air borne precipitation of salt may have been higher than today. Under these conditions even a higher quantity of salt deposition through accumulation of air borne salts than the above figure could appear reasonable within the context of all other geological knowledge about the area.

In order to understand properly the development in the Rift Valley, one has to distinguish between the ocean-derived influx of air borne sea salt accumulating without interruption in such a landlocked basin, and the internal shiftings inside this basin, through evaporation of lakes and precipitation of salts, the distribution and redistribution of the residual brine (by the Jordan of today) caused by tectonic movements. The internal circulation does not, however, alter the overall salt-balance in the Rift Valley. The Dead Sea proper may also act as a source for the internal circulation of air borne salts.

EVALUATION OF A CATCHMENT AREA BY COMPARING THE INPUT OF PRECIPITATION

SALTS WITH THE OUTPUT OF SALT FLOW — THE ROSH HA-AIN (YARKON) SPRINGS

This group of springs, the largest in Israel, has a yearly flow of about $220 \times 10^6 \text{ m}^3$ and a peculiar composition. This water contains 170 ppm Cl^- , 126 ppm Na, 45 ppm SO_4 and has an "Alkali Number" of 112 (Loewengart 1958). M. Goldschmidt (1959) has calculated the probable catchment area of these springs and his calculation explains quite well the yield of these springs. This procedure is adequate to explain the quantities of water, but cannot be used in a study of the chemical composition of, and the quantity of salt in, the water. There is, in fact, a large difference between the salt content of the Rosh Ha-Ain springs and the Cenomanian-Turonian waters which, according to M. Goldschmidt, make up their main supply.

The opposite procedure, i.e. the definition of a catchment area by comparing the calculated quantity of precipitated salt with that contained in surface and underground flows was tried successfully in Victoria, New South Wales, and West Australia (Anderson 1945). The total quantity of air borne salt in the infiltration area makes it possible to define also those parts of it which contribute very small quantities of water, but relatively large quantities of salt.

The waters collecting in the Cenomanian-Turonian limestone area of the Judean Arch have a very low salinity of about 30 ppm Cl^- (Faria and Bittir Springs, Motsa boring). Waters in the same formation north of the Yarkon Springs, from Neve Janin in the vicinity of the Rosh Ha-Ain Spring to Qaqun about 50km farther north, carry salinities from 40 to 70 ppm Cl^- (see Issar's contour map 1959). Farther south, in the Lod region, the Cl^- content is nowhere below 150 ppm. Wells about 10km south of the Rosh Ha-Ain Springs in the Lod region carry 200 ppm Cl^- and another 10km farther south even 270 ppm Cl^- at an average. A characteristic feature of the Yarkon Springs is the high surplus SO_4^{--} and the high "Alkali Number" of the springs, which they share only with the groundwaters farther south in the foothill area. Surplus amounts of sulphate (above 1:10 in equivalents, which is the normal SO_4/Cl^- ratio in sea water) occur frequently.

In most unpolluted coastal areas the fall-out contains an excess of SO_4^{--} , corresponding to about 5–20 kg/ha. In the more humid parts of Israel, at rainfalls of about 500mm, the average excess sulphate in spring- and groundwater is about 4 ppm (Loewengart 1958) (see also Figure 3), corresponding to a fall-out of about 5kg SO_4^{--} /ha or somewhat less*. In the opinion of most authors (Eriksson 1959) this excess is derived from the release of sulphur compounds from the biosphere, especially over the coastal and shelf areas, and their subsequent oxidation.

In the case of the Yarkon Springs, however, the excess of sulphate is of a much higher order of magnitude, i.e., about 20 ppm. Excess sulphate rises with the increasing aridity in the groundwaters. In the southern Arava, with less than 50mm rainfall, it reaches up to 1000 ppm and exceeds sometimes even the quantities of Cl^- (Figure 3)**. This excess sulphate is connected with the retention of calcium sulphate in the ground, parallel with the decrease of precipitation and the decrease of permeability of the surface. The map of Figure 3 shows the distribution of excess sulphate in the area under discussion. South of the Rosh Ha-Ain-Yarkon Springs, in an area with 500mm rainfall, a sulphate excess of 20 ppm is found; this area has a surface of very limited permeability. Farther south west in the Coastal Plain, over a more or less pervious surface, the same value is reached already at about 400mm rainfall. The increase in sulphate is probably a world-wide phenomenon, although occasionally, as in the southern part of the United States, it is masked by the abundance of SO_4 from man-made sources, it can, however, be observed in the more saline (say above 400 ppm Cl^-) groundwaters of Australia, Tunis and South Africa, as is evident from the data given by Anderson (1945), Dickinson (1942), Schoeller (1948 A–B) and Bond (1946).

M. Goldschmidt (1958) considered as the catchment area of the Springs only the 850km² of the Judean Mountains, which indeed supply the bulk of the water. If however, the foothill zone will be regarded as part of the catchment area (Figure 4), a point which, as the author admits, is still disputed by Hydrologists, a more reasonable explanation for the salinity of the Yarkon springs become apparent. This zone has been defined by Stern, Jacobs and Schmorak (1956). It comprises about 1850km² and stretches to the south to the Beersheba gap, only one third of it has over 400mm of rainfall and it mostly consists of impervious marls of the Senonian and Eocene. The contribution of this zone in run-off to springs is probably very small, but as its air borne salts are drained into the groundwater, it must contribute considerably to the salinity of the spring as a whole.

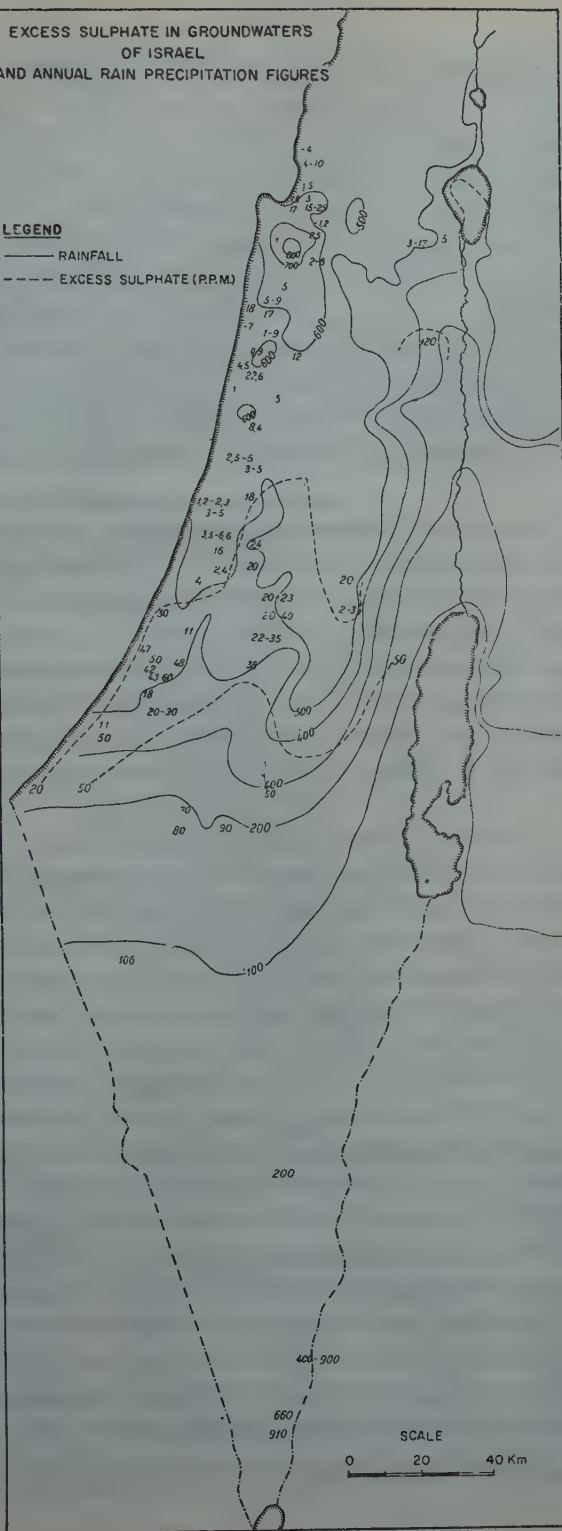
* In Western Australia under very similar conditions of climate and Cl^- concentration in rainwater, the excess sulphate in rainwater at the coast (Perth) has a mean value of 2 ppm and decreases more inland to about 1 ppm. (Computed from Hingston 1958). Taking into account the subsequent evaporation this figure is indeed very similar to that observed in Israel.

** (The data in Figure 3 are taken from Loewengart's paper 1958 for the north of the country. For the central and southern parts they are based on analytical data obtained from Israel Water Planning Ltd).

EXCESS SULPHATE IN GROUNDWATERS
OF ISRAEL
AND ANNUAL RAIN PRECIPITATION FIGURES

LEGEND

- RAINFALL
- - - - EXCESS SULPHATE (P.P.M.)



SCALE
0 20 40 Km

Figure 3

If infiltration rates, according to Goldschmidt's formula, would prevail, and given a Cl^- precipitation of 70 kg/ha (Figure 2), the salinity of the waters would correspond to figures under column A in Table VI. These figures which are taken at random from many available analyses (received from Israel Water Planning Ltd.) may be read in comparison to the actual Cl^- concentrations and so show the approximate rate of the increase of salinity through the imperviousness of the surface. For a precipitation of, say, 500mm the theoretical infiltration, according to Goldschmidt, is: $(500-360) \times 0.9 = 126$. Thus 70kg Cl^- in 1260m^3 would result in a salinity of 55 ppm Cl^- . The ratio of the actual infiltration (seen as a reciprocal value of salinity) to the theoretically expected is given in %. It is shown in Table VI that the contribution to the groundwater in this area is indeed very small, but still greatest on the border to the Cenomanian-Turonian hill region (Har Tuv and Gal On).

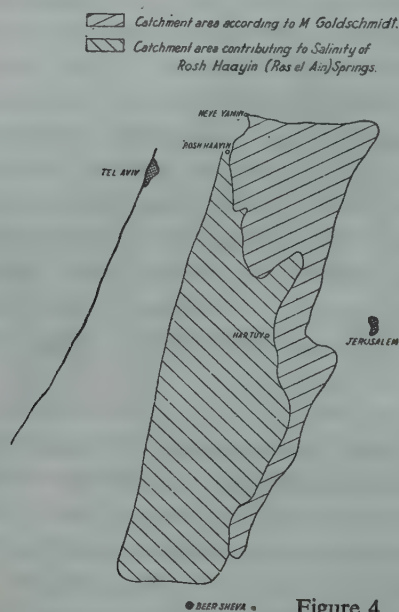


Figure 4

TABLE VI

Place	Average precipit. 1921-1950 (mm)	Cl^- (ppm)	Concentration Cl^- to be expected	% of infiltration to be expected	Actual infiltration in % from M. Goldschmidt's formula	Actual infiltration in % of total precipitation
on M. Goldschmidt's formula.						
Lod	500	260 (max)	55	25.2	21.2	4.6
Kfar Menahem	500	421	90	18.5	21.3	3.3
Gal On	400	300	200	11	66.6	5
Har Tuv	461	117	80	19.7	63	10.9
Ben Shemen	513	404	50	28	12.4	2.4

Analytical Data from Tahal (Israel Water Planning Ltd.)

The total quantity of Cl^- carried annually by the Rosh Ha-Ain Springs is 220×10^6

$\times 0.17 \text{ kg Cl}^-$ or $37.4 \times 10^6 \text{ kg Cl}^-$. Taking $70 \text{ kg Cl}^-/\text{ha}$ as a tentative Cl^- precipitation figure for the whole assumed catchment area of 2650 km^2 , the springs should contain about $18 \times 10^6 \text{ kg Cl}^-$. This is about half of the quantity observed, but it is much nearer to reality than if only the Cenomanian-Turonian catchment area is taken into account, since the latter would account for only 1/10 of the quantity of Cl^- . Only the foothill zone is able to supply the majority of the salts, the excess sulphate and causes the high Alkali Number. The Cl^-/Br^- ratio of the Yarkon Springs, according to Bloch et al. (1959): "Yarkon-Negev-line 172 ppm Cl^- , Cl/Br ratio 308", also points to the air borne origin of the salts of the Yarkon Springs.

A similar calculation could probably be made for the catchment area of the Tanninim (Crocodile or Zerka) river, a large part of the catchment area of which is also covered by impervious Senonian and Eocene. Mandel (1957) estimated infiltration rates in these later formations to be only 10% against 35% for the areas built of Cenomanian-Turonian strata.

THE CHEMISTRY OF GROUNDWATERS IN OTHER LIMESTONE FORMATIONS

The chemistry of groundwaters in the limestone formations of the country was described earlier (Loewengart 1958). It is now apparent that despite all differences in salinity these waters all fall into a single genetic category. Their composition is determined by the quantities of air borne salt precipitation, the amount of rain and the physical properties of the surface layers. A rather uniform rate of bicarbonates (5-6 meq.) is caused by relatively high CO_2 pressure, independent of the salinity. There is probably not much original (connate) salinity in the Senonian - Lower Eocene complex.

SALINITY DUE TO SEAWATER INTRUSION

In most of the limestone aquifers in the northern part of the country a more saline bottomwater, with 500-1000 ppm Cl^- is observed. This water is most evident at the mouth of the Tanninim River (Zerka Springs) at the southern end of the Carmel and in the Kurdani Springs in the Haifa Bay. It was shown earlier that the composition of these waters is very similar to that of seawater. No signs, however, have been observed here of the existence of an interface of seawater which undercuts the fresh water (Ghiben-Herzberg phenomenon). Besides the possibility of subrecent intrusions of seawater into the karstic aquifer (Loewengart 1958), there is probably also a perennial intrusion of seawater, at least along Mount Carmel. This process may operate as follows: the karstic groundwater drains through open channels into the sea, its slope being about 1m-2 per km. The amplitude of the tide is about 40cm. The elasticity of the groundwater body towards the tides is certainly not sufficient to follow its movements (Stern et al. 1956). At each tide heavier sea water is superimposed on the groundwater in the open channels and mixing takes place. As water intrudes from the sea on one side, and groundwater moves against it from the land, equilibrium results in a wedge of brackish water which sweetens and thins out towards the land. This wedge of brackish water forms the very strong springs at the mouth of the Tanninim River which contain about 1800 ppm Cl^- , while at the Rom-

an Bridge the water contains only 700 ppm and at the Shunie Spring (Benyamina) only 200 ppm. A brackish salt water body of the same origin probably undercuts the sweet water along the northern fringes of Mount Carmel and in the Haifa Bay. A similar case was observed at Miami in Florida by Brown and Parker (1945). There also a karstic aquifer drains into the sea. In contrast to the Israel coast line, the interface was drawn into the mainland by drainage channels, but similar to our zone, a wedge of brackish water stretches several kilometres into the mainland. whose thickness is about 6m, and Cl^- content reaches from 200 to 6000 ppm. The fluctuation of the tides (30-60cm) is also comparable to the conditions at our coast.

Such transition zones do not occur in clastic aquifers with slow groundwater movement. Here the interface is always sharply defined, as in the Pleistocene groundwater of the Coastal Plain. (Stern et al. 1956).

TABLE VII

Area	Infiltr. rate 1921-1950 (mm)	Representa- tive minimum of salinity (ppm)	Preci- pitations of Cl^- kg/ha	Average median Cl^- (ppm)	No. of samples	Thickness of aquifers (m)
Haifa Bay dune area	360	30	108	42	44	15-20
(Kiriath Haim)	Santing a. Golschmidt modified			(1933-38) 86 (1952-53)	28	
Tel Mond- Hezlia area	225	42.5	100	60	22	70-80
grid 190-170	Santing			(1933-38) 81 (1952-53)	13	
Yavne area grid 140-130	125 Santing	80	100	120 median 160 average (1952-53)*	25	50 ?
Ashdod-Gad area	100	105	105	175*	28*	50 ?
grid 130-120	(Lauting) excl. dune area					

* Calculated from analysis made by TAHAL (Water Planning for Israel), others from Hydrological Yearbooks of Israel.

THE SALINITY OF THE COASTAL PLAIN GROUNDWATER (PLEISTOCENE GROUNDWATER)

The economically most important groundwater in Israel is contained in the Pleistocene clastic formation of the Coastal Plain. Thanks to the numerous geological and hydrological investigations of this aquifer much data have been collected. Recently intrusions of seawater, mainly in Tel-Aviv and vicinity, have been reported. The causes have been found in overpumping, leading to the intrusion of seawater beyond a clearcut interface. Independently a slight but steady increase in salinity has been observed at many places the causes of which have not yet been studied. This phenomenon can be explained much more easily by the observation of air borne salt precipitation. In Table VII figures of average and median Cl^- contents are given for various

parts of the Coastal Plain aquifer. The Haifa dune area is a separate geographical unit, the other three areas have been chosen for convenience, according to Santing (1958).

As a representative area the *Herzliya-Tel Mond* sector is here discussed, a segment 20km from north to south, and about 14.5km from west to east. The average infiltration rate according to Santing (1958) is 225mm, i.e., 2250m³/ha Cl⁻ precipitation estimated with 100 kg/ha, therefore in the whole precipitation 44.4 ppm Cl⁻ to be expected. The thickness of the aquifer is estimated to be 75m and its porosity 25% (Santing 1958). The yearly intake of the aquifer in terms of thickness can be estimated, as was done by Blake and Goldschmidt (1947) in terms of seasonal movements of the water level. This procedure contains, of course, a simplification, as many changes occur inside the aquifer and permeabilities are very fluctuating. In the year 1952/53 the seasonal fluctuations according to the Hydrological Yearbook were between 30 and 250 cm in 26 wells of the area under discussion. The median value was 100cm. The storage capacity — defined as the time necessary to replenish the whole aquifer if theoretically emptied and with no outflow existing (Schoeller 1958) — can therefore be estimated as 75 years. In areas like these the pumped-out water is spent back over the same area. This is true, of course, for all areas where the water is used for irrigation and also for such populated zones which have no central sewage system. Under these conditions a formula may be developed for the increase in salinity in which appear the following expressions:

R = Average yearly replacement of the aquifer in m³

W = Average yearly net withdrawal (total pumping minus return flow) in m³ in so far as the water is spent over the area

A = The storage capacity of the aquifer in years (see above)

c_a = The original concentration of the water (Cl⁻ ppm) at the beginning of a period of p years

c_n = The final concentration after p years (ppm Cl⁻)

p = any number of years

Then the final concentration c_n is given by the following formula:

$$c_n = c_a \left[1 + \left(\frac{1}{A} \times \frac{W}{R} \times p \right) \right]$$

By using this formula for the aquifer described, and assuming that withdrawal and replacement were in equilibrium, the salinity in 20 years (from 1933–1953) should have increased as follows: (see Table VII)

$$c_n = 60 \times [1 + (1/75 \times 1 \times 20)] = \sim 76$$

As the observed figure in Table VII is slightly higher (81) than the figure obtained in the calculation it can be assumed that the withdrawal was slightly higher than the replacement.

When, in the above formula, p is taken as identical with A , salinity doubles under the provision that net withdrawal and recharge will balance each other ($\frac{W}{R} = 1$).

This formula seems to correspond with the observed facts in different regions, as will be shown below:

In the *Haifa Bay dune area* (Table VI) the approximate thickness of the aquifer is 15–20m, and the yearly fluctuation about 1m. In this area average salinity has doubled in the last 20 years. Most of the wells do not show any conspicuous draw-down. Most of the water is spent for irrigation of smallholdings and for domestic use, and no central sewage system exists, so that all the salts are infiltrated back into the groundwater.

A very thin aquifer, about 6m thick or less, exists in the *Acre–Naharia plain* (Blake and Goldschmidt M. 1947). Salinity in wells in Naharia, Shave-Zion, Bustan Hagalil and in the Acre Agricultural Station has sharply increased during the last 20 years, without any conspicuous draw-down of the water level. As a paradigm; Well No. 5A at the Acre Government stock farm increased its Cl^- content from 1932 to 1940 from 80 to 914 ppm. During the same time the water level remained constant apart from seasonal changes. Well number 5 in the immediate vicinity of the above well carried 140 ppm, in 1940, but 680 ppm in 1953. (Hydrological Yearbook). The water is entirely used for irrigation over the area, and the increase of salinity fits in with the above formula.

Even in areas in which the groundwater is not fully exploited an increase of salinity must occur, although at a lower rate — according to the above formula. According to Santing (1958) the aquifer in the *Hadera area* has a thickness of about 25–30m, but is not entirely exploited. In this area Well WR 267B (N 204.92 E 141.390) had in 1934 80 ppm and in 1953 112 ppm Cl^- . Well WR 275B (N 202.12 E 141.865) had in 1934 70 ppm and in 1953 90 ppm. (Hydrological Yearbook).

In the *Rehovot–Rishon area* the aquifer has probably a thickness of 30–60m and a number of wells here show almost no change in salinity. However, Well WR 1178 (N 145.73 E 33.48) in Rehovot had in 1934 a Cl^- content of 40 ppm and in 1953 of 95 ppm. The groundwater map in the Israel Atlas (Stern 1959) shows a considerable draw-down cone in this zone. In a part of this area the increase is due to over-pumping, but this is partly compensated through the reversed W–E inflow from the entirely untapped dune area. A number of wells in this area which show low and stable salinity almost over two decades probably exploit a water horizon whose intake is over this untapped dune area, into which no additional salts are redrained by irrigation.

As a *negative proof* for the *accumulation of salts* may be taken the case of the Kurdani Textile factory in the Haifa Bay, which pumps its water from a very narrow aquifer in the dune sands between Haifa and Acre. In spite of exploiting this aquifer considerably, Cl^- concentration has remained stable over the years, because the water used is drained off into an open channel outside the original catchment area.

Conclusions: In many cases the salt-balance of groundwaters can be used for hydrological calculations, especially for a determination of the infiltration rate. When more data are available on the salinity of the rain precipitation, calculations

of infiltration rates, as made by Y. Cahane and E. Behr (1957) for Emek Hefer, will be considerably facilitated.

The practical importance for further research is stressed by Eriksson (1958) who wrote: "A systematic well planned investigation of the sea salt content of ground-water, riverwater and precipitation would be most useful in assessing the water economy, not only of arid regions, but of most areas of the world."

ACKNOWLEDGEMENTS

The author is indebted to Prof. Y. Ben-Tor for his painstaking proof-reading of the manuscript and for various remarks which led to improvements of the text. The author also wants to thank Dr. D.H. Yaalon for his valuable assistance in reading and suggesting changes in the manuscript. The author further wants to thank Dr. K. Taussig for supplying him with a host of analytical data together with valuable critical remarks on his former paper, as well as Messrs. Cahane and Aisenstein — also from Israel Water Planning Ltd. — for the analytical data of water analyses.

Thanks are due to many others who helped the author with various problems connected with this paper.

REFERENCES

1. ANDERSON, V.G., 1945, Some affects of atmospheric evaporation and transpiration on the composition of natural waters in Australia, *Journ. Proc. Austral. Chem. Inst.*, **12**, 41–68, 83–98.
2. BLAKE, G. AND GOLDSCHMIDT, M., 1947, *Geology and Water Resources of Palestine*, Jerusalem.
3. BLOCH, M.R., KAPLAN, D., SCHNERB, J., 1959, The Bromide Content in the Halogenides of food and body fluids, *Bull. Res. Counc. of Israel*, **8A**, 156–165.
4. BOND, G.W., 1946, A Geochemical Survey of the Underground Water Supply of the Union of South Africa, *S.A. Geological Survey Memoir* No. 41.
5. BROWN, R.H. AND PARKER, G.G., 1945, Salt Water Encroachment in Lime-Stone at Silver Bluff Miami, Flo., *Econ. Geology*, **XL**, 235–262.
6. BURDON, D., MAZLOUM, S. AND SAFADI, C., *Groundwater in Syria*, Assoc. Internationale de Hydrologie Scientifique, Rome 1954, Tome II, pages 376–387.
7. BURDON, D., Infiltration rates in the Jarmuk basin of Syria-Jordan. Ibidem, pages 348–355.
8. CAHANE, I. AND BER I., 1957, The Hydrological Situation in Emek Hefer, Tahal (Water Planning for Israel, Tel Aviv, Hebrew).
9. Chemical analyses of Waters, etc. *Irrigation Services Governm. of Palestine*, Jerusalem 1948.
10. CLARKE, F.W., 1924, The Data of Geochemistry, *U. S. Geological Survey, Bull.* 770. 5th edition, Washington.
11. CONWAY, E.J., 1942, Mean Geochemical Data in Relation to Oceanic Evolution, *Proc. Royal Irish Acad.*, **48 B**, 159.
12. CONWAY, E.J., 1942, The Chemical Evolution of the Ocean, *Proceed. Royal Irish Acad.*, **48**, 161.
13. DICKINSON, S.B., 1942, The Monaree Station Saline Groundwaters and the Origin of their Saline Material, *Transact. of the R. Soc. of South Australia*, **66** (1).
14. ERIKSSON, E., 1952, Composition of Atmospheric Precipitation, *Tellus* **4**, 215–231, 280–303.
15. ERIKSSON, E., 1955, Airborne Salts and the Chemical Composition of River Waters, *Tellus* **7**, 243–250.
16. ERIKSSON E., 1958, The chemical climate and saline soils in the arid zones, *Arid Zones Research XI, Climatology*, Unesco 1958, pp. 147–181.
17. ERIKSSON, E., 1959, Atmospheric Transport of Oceanic Constituents in their Circulation in Nature, *Tellus* **11**, 1–72.
18. GOLDSCHMIDT, M. AND JACOBS, M., 1958, Precipitation over and Replenishment of the Yarkon and Nahal Hatteninim Underground Catchments, *Hydrological Paper N. 4, Hydrological Service*, State of Israel.

19. GOLDSCHMIDT, M., 1959, On The Water Balances of Several Mountains Underground Water Catchments in Israel and their Flow Patterns, *Hydr. Paper N.3*, Ibidem.
20. GOLDSCHMIDT, V.M. 1958, *Geochemistry*, Oxford.
21. HINGSTON, F.J., 1958, The Major Ions in Western Australian Rainwaters, *Comm. Scient. and Ind. Res. Org., Div. of Soils, Adelaide*.
22. HOLLAND, T.H. AND CHRISTIE, W.A.K., 1909, The Origin of the Salt Deposits of Rajputana *Bull. Geological Survey, India*, **38**, 154-186.
23. HUTCHINSON, G.E., 1957, *A Treatise of Limnology*, Vol. I.
24. HUTTON, J.T., 1958, The Chemistry of Rainwater with particular reference to conditions in South Eastern Australia, *Arid Zone Research X, Climatology*, Unesco 285-290.
25. HUTTON, J.T. AND LESLIE T.I., 1958, Accession of Non-Nitrogenous Ions dissolved in Rainwater to soils in Victoria, *Aust. Journ. of Agricultural Res.* **9**, No. 4, 492-507.
26. HUTTON, J.T., 1958, Rainwater Analysis, *Commonwealth Scient. and Ind. Res. Org., Division of Soils, Adelaide*.
27. Hydrological Yearbook of Israel 1946/47, Jerusalem 1950
 B " " " 1948/50 " 1952
 C " " " 1952/53 " 1955
28. ISSAR, A., 1959, Remarks on the Subsurface Geology of the Coastal Foothill Regions of Israel, *Geological Survey of Israel Bull.* **23**.
29. IONIDES, M.G., 1939, *The Water Resources of Transjordan and their Development*, Crown Agents for the Colonies, London, 1939.
30. LOEWENGART, S., 1958, Geochemistry of the Waters in Northern and Central Israel and the Origin of Their Salts, *Bull. Res. Council of Israel*, **7G**, 176-205.
31. MANDEL, S., 1957, Geohydrology of the Tanninim River Catchment Area, *Water Planning for Israel*, Tel Aviv.
32. MENCHIKOVSKY, F., 1929, Composition of Palestine Waters Accord. to the Natural Conditions of the Land, *Agric. Experiment, Station*, Tel Aviv (Hebrew).
33. MENCHIKOVSKY, F., 1925, (Hebrew), The Chemical Composition of Rain River in Tel Aviv, *Bull. of Agric. Res. Station, paper B, Tel Aviv*.
34. MENCHIKOVSKY, F., 1925, The chemical composition of Rain Water in Tel Aviv, *Bull. of Agric. Res. Station, paper B, Tel Aviv*.
35. Meteorological Yearbook of Israel (Hebrew), Tel Aviv, 1958.
36. NEUMANN, J., 1958, Tentative Energy and Water Balances for the Dead Sea, *Bull. Res. Council of Israel*, **7G**, 137-162.
37. PIPER, H.M., GARRETT, H.A., 1953, Native and Contaminated Groundwaters in the Long Beach Santa Ana Area, California, *U.S. Water Supply Paper*, 1136.
38. SANTING, G.E., 1958, Groundwater in the Coastal Plain, *Suppl. Report Water Planning for Israel*, Tel Aviv.
39. SCHOELLER, H., 1948, A. Les Modifications de la Composition Chimique de l'Eau dans une Meme Nappe, *Union Geodesique et Geophysique International Assoc. International Hydraul. Scient.*, Oslo, pp. 124-189.
40. SCHOELLER, H., 1948 B, Les Variations de la Composition Chimique de l'Eau dans les Nappes Souterraines, Ibidem, pp. 130-144.
41. SCHOELLER, H., 1956, *Geochimie des Eaux souterraines Appl. aux Eaux du Gisement de Petro* Paris.
42. SCHOELLER, H., 1958, *Arid Zones Hydrology, Recent Developments*, Unesco, Paris.
43. SHIFTAN, 1958, An Artesian Aquifer of the Southern Dead Sea Basin, *Bull. Res. Council of Israel*, **7G**.
44. STERN, W., JACOBS, M. AND SCHMORAK, S., 1956, Hydrogeological Research Coastal Plain Underground Water South of Nahr Rubin, Report to Ford Foundation, Jerusalem.
45. STERN, W., 1959, Groundwater Map with Text in Atlas, Israel, Jerusalem, (Hebrew).
46. TODD, DAVID, K., 1959, *Groundwater Hydrology*, New York.
47. WILSON AND WOZAB, 1954, Chemical Composition of Waters in Jordan, *Assoc. Internationale Hydrologie*, Rome. 170-178.

A LOWER CRETACEOUS VOLCANO IN MAKHTESH RAMON (SOUTHERN ISRAEL)

EMANUEL MAZOR

Israel Atomic Energy Commission

ABSTRACT

In the north-eastern area of Makhtesh Ramon, which lies in the southern part of Israel, a basalt hill is exposed with a summit 70m above its surroundings and an area of 1 sq. km. This hill is composed of mainly olivine basalt and partly of tuff. It is approximately hoof-shaped, with a low centre and a drainage outlet towards the south. It is postulated that this structure is the result of a volcanic eruption which started with an explosion of tuff, followed by the eruption of basaltic lava streams. During the last stage of this eruption the interior pressure was released and the part above the feeding neck sank. The volcano erupted in Early Cretaceous and was covered by sandstones of the Lower Cretaceous Kurnub formation, which preserved it until it was uncovered by recent erosion.

INTRODUCTION

In the north-eastern part of Makhtesh Ramon (Ramon erosion cirque, Central Negev) a black hill commanding the area is located, at coordinates 138/007 (Figure 1). The hill has a relative height of 70m and covers an area of about 1 sq. km. It is part of

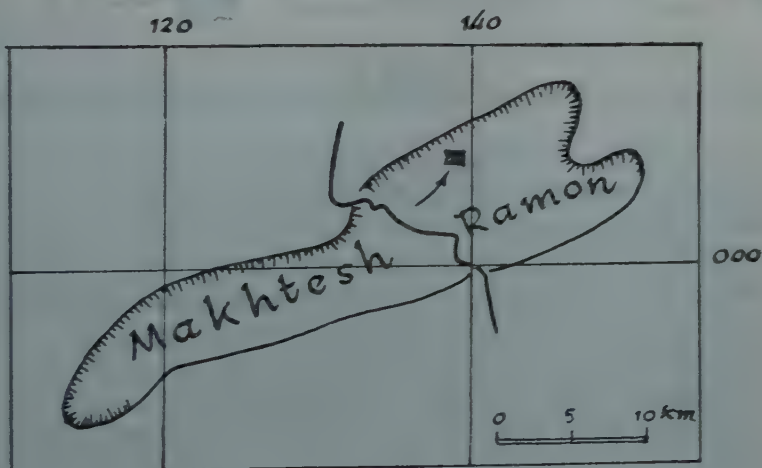


Figure 1.
Location map.

large olivine-basalt complex, exposed along the rims of the erosion cirque in small patches in the north-eastern part and in large outcrops to the south-west. In the latter area, this basalt constitutes a number of high black hills, called Karnei Ramon (Horns of Ramon). Previous investigations (Bentor and Vroman 1951, Posner 1955)

have shown that this basalt was extruded at the beginning of the Lower Cretaceous in two main flows. It is exposed also at Mount Arif, 15km south, and at Jebel-Arif-En-Naga in Sinai, about 30km west of Ramon. Generally, in the north-eastern part of Makhtesh Ramon the basalt outcrops are limited in area and have a thickness of only a few metres. Thus the hill under discussion is exceptional as regards its height, its extensive area and also, as shown below, in the complexity of its composition (Figure 2).

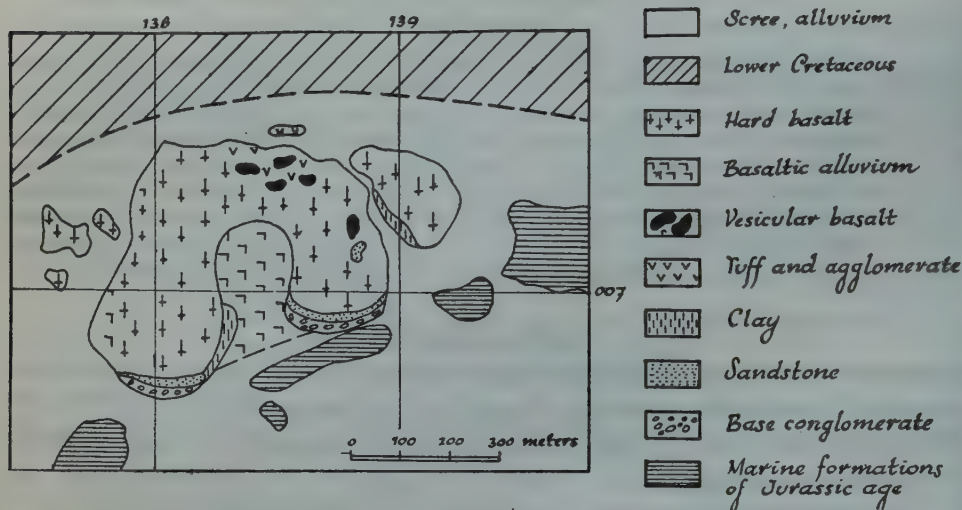


Figure 2.

Geological map of the basalt body. The legend also serves for the subsequent figures.

DETAILED DESCRIPTION

The general form of the basaltic body is that of a hoof. At the eastern, northern and western sides the structure consists of a hilly half cirque, some tens of metres higher than the surrounding area (Photo 1), while the centre and the southern side are relatively low (Figures 3, 4 and Photo 2). In the central depression are a few small basalt hills which protrude from the basaltic talus. The rock for the most part is hard olivine basalt which cleaves in prismatic columns, mostly hexagonal (Photo 3), or weathers in a concentric manner (Photo 4). Detailed petrographic study of the rock has not been included in the present work. On the northern slopes highly vesicular basalt and even scoria are found; the vesicles being partly filled with calcite. At the base of the northern slope occurs a fine grained tuff of basaltic composition. About 30 metres north of the northern margin of the hill, a clearly bedded heterogeneous rock is present, composed of quartz grains and rounded pieces of basalt of various sizes (Photo 5). Apparently, this rock represents an agglomerate that includes quartz grains of the Jurassic or Lower Cretaceous sandy country rock. On the eastern slope a large block of hard sandstone (Photo 6) is exposed, isolated from any other outcrops of sandstone. In its composition and texture this rock resembles

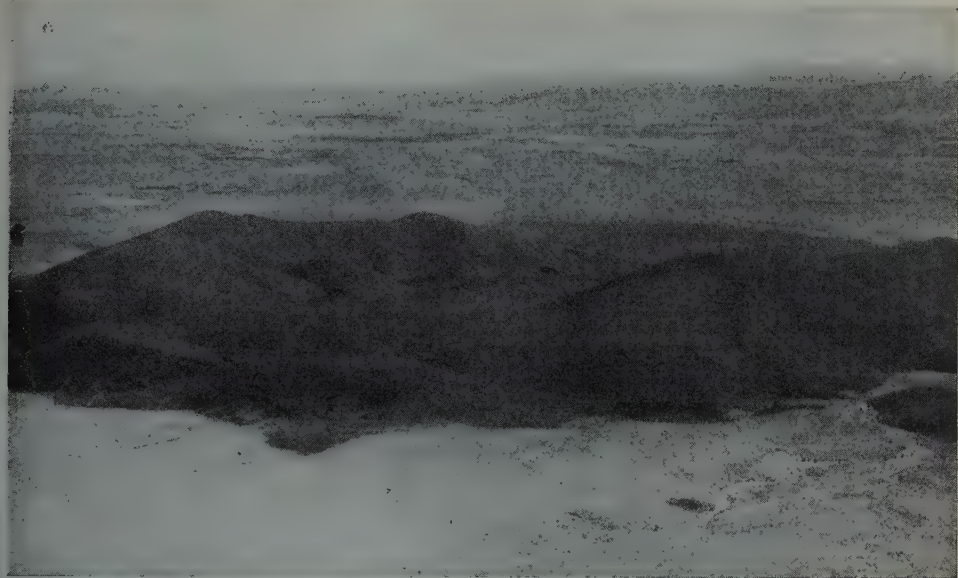


Photo 1.

The volcano, viewed from the northern cliff of Makhtesh Ramon. Note the raised rims and the southern outlet.



Photo 2.

he outlet through which the lava flowed at the final stage of the eruption. Viewed from the centre of the volcano southwards.

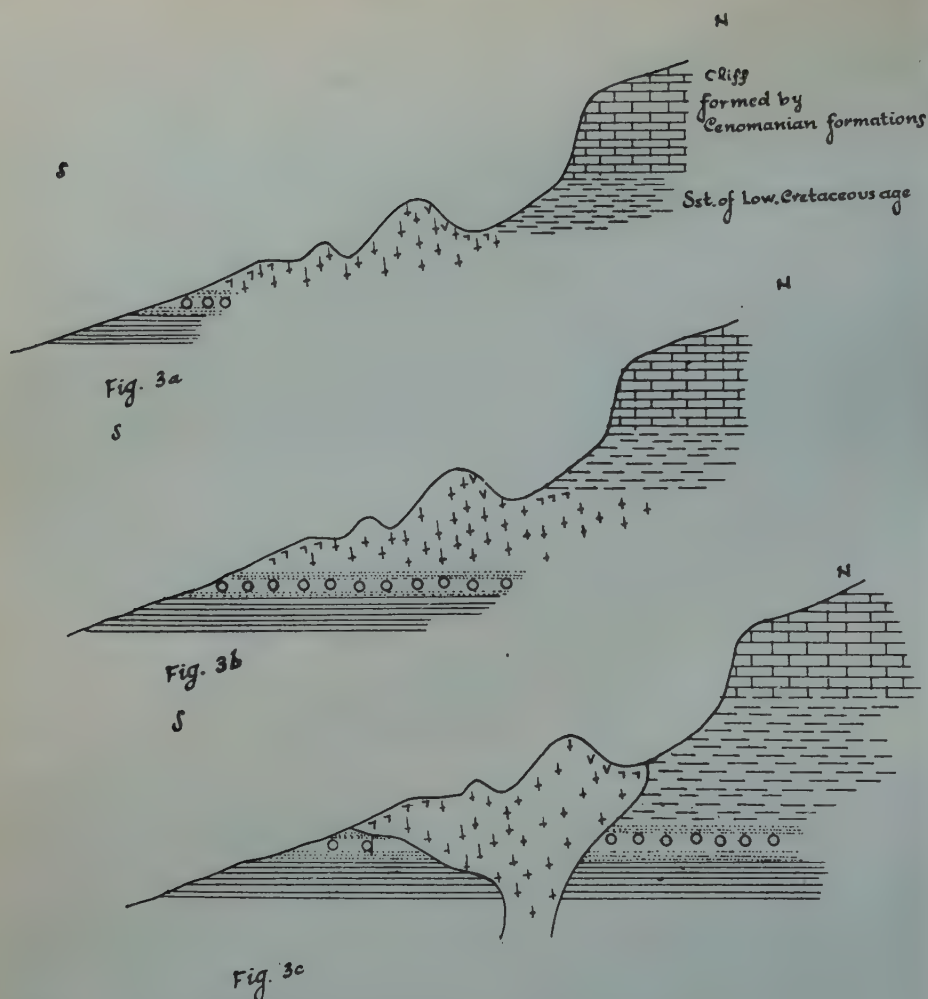


Figure 3A Cross section north-south through the volcanic structure.
 3B Explanation of the above section as part of a large flow sheet..
 3C Explanation of the above section as a volcano.

the Jurassic and Lower Cretaceous sandstones and can only be a relic of the country rock which was forced upwards by the rising lava. Nearby a vein of leuco-dacite* about 20cm thick, cuts the basalt (Photo 7).

GENESIS OF THE STRUCTURE

It is hard to determine the relationship between the basalt and the sedimentary rocks in the field because contacts are covered by thick talus accumulations. Shaw (1947), considers the basalt to be a sill. However, Bendor and Vroman (1951), and Bendor (1952) in a more detailed account describe the basalt as surface flows.

* Determined by Eitan Sas, Hebrew University.



Photo 3

Basalt prisms, mostly hexagonal, distorted by further pressure of the lava during process of cooling and jointing.



Photo 4.
Concentric weathering
of basalt.



Photo 5.
Well bedded agglomerate, about 30m north of the main body.



Photo 6.
A sandstone block lifted by the lava.

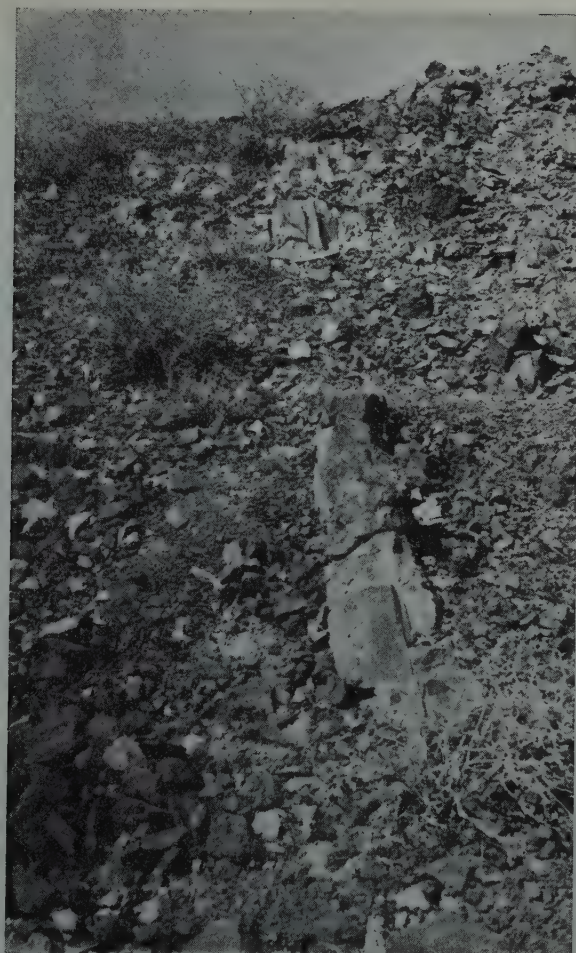


Photo 7

A leucodacite (?) vein, cutting through the basalt.

The present author in a previous report (1955), considered also the basalt hills in the Ramon to be flows as shown in figures 3B and 4B. According to the new data above, it seems (Figures 3 C and 4C) that the hill considered here represents a volcano in which the lava collected around the feeding neck and then flowed away (Figure 5A). When the pressure was released the fluids in the feeding neck subsided, resulting in the formation of a central depression (Figure 5B). The characteristic morphology of a circle with high margins and a low centre was maintained in spite of subsequent erosion (Figure 5C). In the final stage of activity the lava breached the core and flowed out through the southern exit (Photo 2). At the present time the northern margins are a little lower than the eastern and western ones, as is understandable, taking into

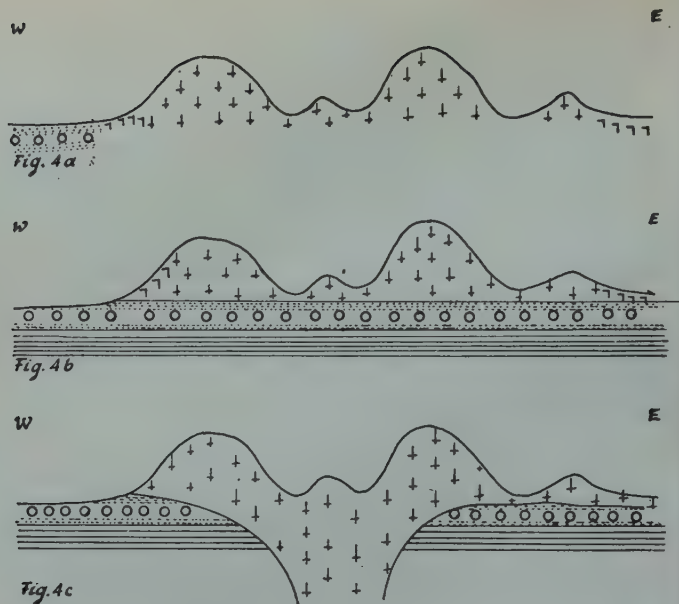


Figure 4A The east-west section as seen in the field.
 4B Explanation of the above section as part of a large flow sheet.
 4C Explanation of the above section as a volcano.

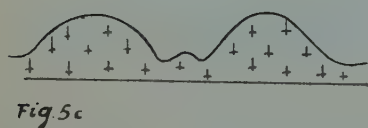
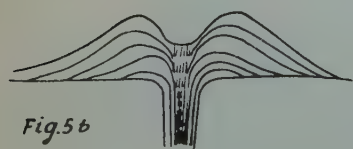


Figure 5A The main eruption stage.
 5B Subsidence of the centre as a result of a fall in pressure at the final stage of eruption.
 5C The present form of the hill as shaped by erosion.

consideration the tilting that the body received during the warping of the Ramon anticline. Reconstructing the situation as it was before the tilting, it may be seen that the northern part was higher while the southern outlet was even lower than it is today.

As the northern base of the hill is built of tuff and nearby are found outcrops of agglomerate, it appears that the volcanic eruption started with an initial explosion followed by main effusion of lava.

CONCLUSIONS

The hill under discussion seems to be a volcano of a well known type (as found, for example, in central and eastern Africa). The volcanic activity consisted of two phases, the first of which was explosive and resulted in the formation of tuff and agglomerate, while in the second and main phase lava was erupted accompanied by uplifting of fragments of the sandy country rock. At the end of this latter stage the pressure was released and the centre of the volcano subsided. The whole complex was tilted northwards by the warping that formed the present Ramon anticline.

If the explanation of a volcano is accepted the question of the origin of the basalt flow in the north-eastern part of the Ramon is partly answered. It will be necessary to survey again the large basalt hills at the south-western part of Makhtesh Ramon in order to verify whether volcanoes also existed in this area.

REFERENCES

- SHAW, S.H., 1947, *Southern Palestine, Geological map*, 1:250.000, with explanatory notes, Jerusalem.
- BENTOR AND VROMAN, 1951, *Geological map of the Negev*, 1:100.000, with explanatory notes. Tel-Aviv, (in Hebrew).
- BENTOR, Y., 1952, Magmatic intrusions and lava sheets in the Ramon area of the Negev (Southern Israel), *The Geological Magazine*, Vol. LXXXIX, 129-140.
- POSNER, E., (Mazor), 1955, The Magmatic Phenomena in Makhtesh Ramon, *M. Sc. Thesis*, (unpublished, Hebrew) presented to the Hebrew University.

ON THE OCCURRENCE OF *PSEUDOPYGURUS* LAMBERT IN SOUTHERN ISRAEL

A. PARNES

Department of Geology, The Hebrew University of Jerusalem, the Geological Survey
of Israel

ABSTRACT

Pseudopygurus hathirae sp. nov. from the Callovian of Makhtesh Hathira in the Negev is described. The phylogenetic relations of the genus are discussed and a diverging evolution of *Pygurus* and *Pseudopygurus* from a common root is suggested.

INTRODUCTION

Lambert (1911 p. 24) has introduced the generic name *Pseudopygurus*, Genotype: *Ps. letteroni* Lamb., based on a specimen found in the Sequanian beds of Tonnerre, Yonne (France), similar to *Pygurus blumenbachi* Koch and and Dunker, but differing from it by the heterogenous frontal ambulacrum. A short diagnosis of the unique type, is given without figure in Lambert and Thiery (1921, p. 358).

Two specimens belonging to *Pseudopygurus* found in North-Eastern Somaliland are described and figured by G. Checchia-Rispoli (1941) as *Pseudopygurus letteroni* Lambert. To the three hitherto known specimens of *Pseudopygurus* are now added two specimens found in Makhtesh Hathira, Negev (Southern Israel). The occurrence of this genus in Israel, thus forms a link between the two far distant regions, Since the form is so rare and the specimens found in Israel show some differences, their description, may contribute to the discussion of the phylogenetic relationships of the genus.

OCCURRENCE

The specimens of *Pseudopygurus* have been found in the crestal area of the Hathira anticline, near the site of drill D7 (coordinates 1492/0385), south of where Nahal Matmor enters Nahal Hathira (Wiener 1955, p. 43, figure 3). The Jurassic strata dip away from both sides of N. Matmor and are slightly displaced by SW-NE trending faults of small throw (several metres). The strata, highly fossiliferous, consist mainly of coralligenous marls, and limestones. In the part of the section between N. Matmor and N. Hathira eight horizons, well characterized by lithology and fauna, can be distinguished. Their thicknesses vary, sometimes at short distances, the true thicknesses being often obscured by slides. The geologists of P.D.P. (Petroleum Development (Palestine) Ltd.) have measured in the corresponding part of the section a thickness of 30 m (Shaw 1947, p. 20). A generalized section shows (thickness estimated, based on comparison of different outcrops in the area):

8. Top: hard limestone with rarely and badly preserved mollusca; about 1 m.
7. Marls with interbeds of coral limestone (predominantly *Calamophyllia*)

Received August 14, 1960

with: *Nautilus*, *Erymnoceras*, large *Pholadomya*, *Homomya*, *Mytilus*; about 7 m.

6. Soft marl with abundant Calcispongiae, Crinoid stems and ossicles (*Millecrinus*), radiols of Echinids (mostly *Cidarids*), *Eligmus*, rare: *Erymnoceras*, *Pseudopygurus hathirae* sp. nov.; about 3 m.
5. Marls containing a rich fauna of diverse corals (*Astrocaenidae*, *Thamnasteriidae*, *Calamophyllidae*, *Microsolenidae*, *Montlivaltiidae* etc.) accompanied by *Stromatoporidae*, *Calcispongiae*, *Brachiopoda* (*Somalirhyrchia*, *Terebratulids*) and various *Mollusca*; about 5 m.
4. Coral limestone (*Calamophyllia*, *Actinastraea*), hard, mostly crystalline, with *Stromatoporidae*, large pelecypods (*Pholadomya*, *Homomya*, *Mytilus*); about 2m.
3. Ferruginous brown to violet sandstone, fossiliferous, with "*Trocharea*", *Calamophyllia*, *Actinastraea*, *Bothriopneustes* sp. of *somaliensis* (Currie), various *Gastropoda*, common *Exogyra nana*, rare: *Nautilus*, *Erymnoceras*; average 3 m.
2. Clay shales with streaks and bands of gypsum; about 7 m.
1. Base: Hard white to greyish crystalline limestone with *Calamophyllia* and *stromatoporids*. about 2 m exposed.

A detailed list of the fauna is given by Hudson (1958, p. 418).

Only two specimens of *Pseudopygurus hathirae* sp. nov. have been found, one by G. Wiener on the "NW side of drill D 7, near the base of the exposed Jurassic"; the other by G. Gill together with *Erymnoceras* in the soft marls rich in remains of *Echinidae*, some 20 m above the base of the exposed Jurassic (horizon 6, coordinates: 1488/0386).

PALEONTOLOGICAL DESCRIPTION

Family Archiaciidae Cotteau 1869

Genus *Pseudopygurus* Lambert 1911

Genotype: *Pseudopygurus letteroni*; Lambert 1911; Checchia-Rispoli 1941.

Lambert, J.M., 1911, p. 24; Lambert J.M. et Thiery, P., 1921, p. 358; Checchia-Rispoli, G., 1941, pp. 870-874, text figs. 1-3; Mortensen, Th., 1948, p. 323, text fig. 297.

Original diagnosis (Lambert et Thiery, loc. cit.): "Lampadiforme, déprimé, sinueux en avant, rostré en arrière, rappelant la forme des *Echinopygus* et notamment celle du *E. Blumenbachi*, dont il se distingue seulement par son pétale impair différent des autres, simple, composé de pores arrondis, séparés par un granule.

Type unique: *P. letteroni* Lambert op. cit. (1911) du Séquanien de Tonnerre".

Pseudopygurus hathirae sp. nov.

(pl. I fig. 1-6 and text fig. 1.)

Derivation of name from the type locality Makhtesh Hathira, Negev, Southern Israel.

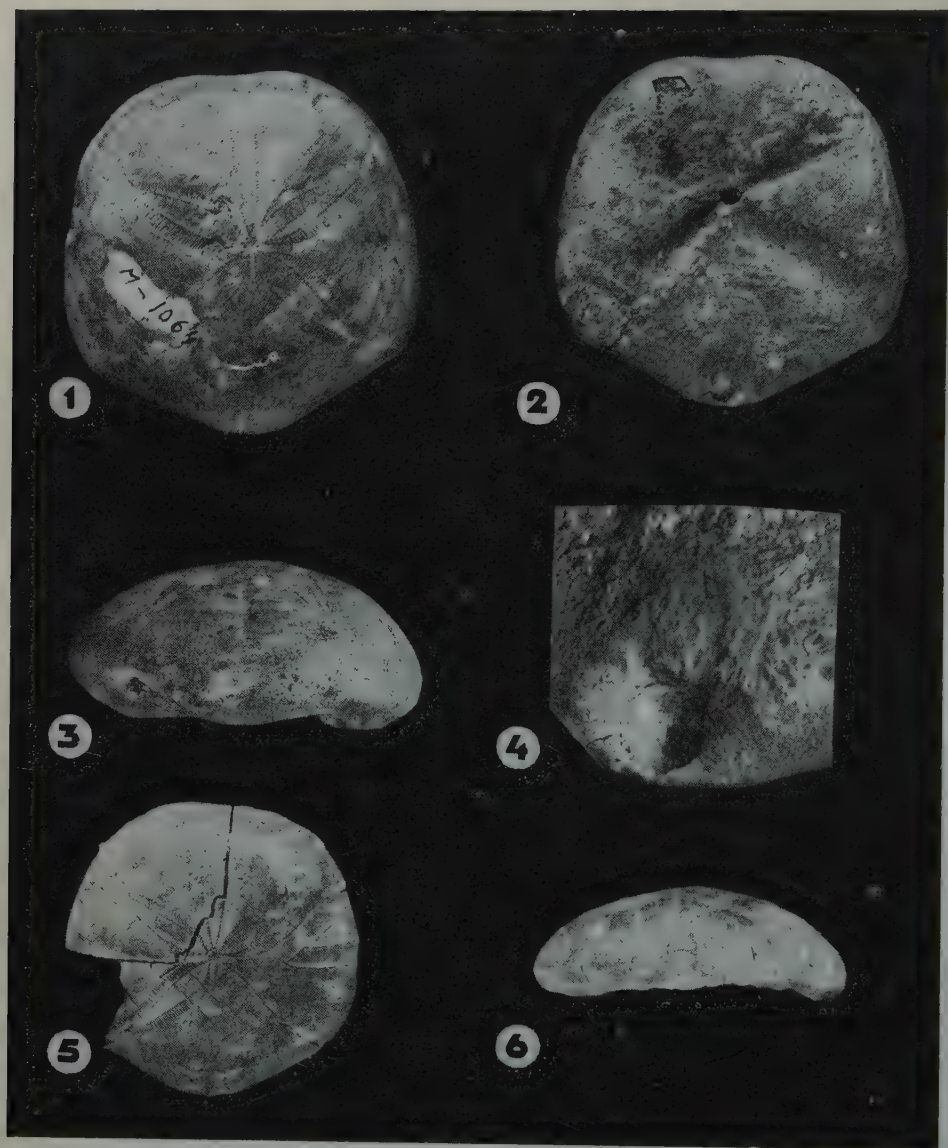


Plate I

Pseudopygurus hathirae sp. n.

Figures 1-4: M 1064, Holotype; 1. adapical face 2. adoral face, 3. lateral view, 4. anus, enlarged.
 Figures 5-6: HU 20855, paratype; 5. adoral face, 6. lateral view.
 All figures natural size except as indicated.

Level: Middle Callovian.

Material examined: two specimens, Holotype, deposited in the Collection of the Geological Survey of Israel, No. M 1064; paratype in the Department of Geology, Hebrew University, Collection No. 20855

Diagnosis: *Pseudopygurus* of subpentagonal outline, adapical face arched asymmetrically, apex central, frontal ambulacrum with pore zones parallel, paired petals lanceolate, anus acuminate posteriorly (aborally).

Dimensions:

	Length	Width	Height
Holotype	44 mm	44 mm	20 mm
Paratype	39 mm	39 mm	13 mm

Description: Outline pentagonal-rounded; posterior margin obtusely trigonal, subrostrate; periphery sharply rounded. Adapical face low arched, forming in profile a slightly asymmetric curve; apex and summit central, anterior part of shell slightly higher and sloping more abruptly than the posterior part. Adoral face concave, tumid; peristome pentagonal, in a deep depression, excentric anteriorly; adoral ambulacral areas shallow near the periphery, deepen and widen towards the peristome; floscelle formed by well developed bourrelets and leaf shaped phyllodes. Periproct inframarginal, placed at the extremity of the rostrum, on a raised subtriangular, obliquely truncated area; anus longitudinally oval, narrow, round anteriorly (adorally), the posteriorly acuminate end encroaching the point of the rostrum. Tubercles small, scrobiculate, perforate (crenulation not observed).

Apical disc monocyclic, tetrabasal, plates distinct; madreporite plate central, the net of pores encroaching inner margin of genital 2; four genital plates, genital pores large, genital 5 absent; five ocular plates, contiguous with the madreporite, separating the genital plates; the two posterior oculars enlarged, contiguous. Plates of apical disc bordered with granules.

Ambulacral system heterogenous. Frontal ambulacrum subpetaloid, open, length of petal nearly $2/3$ of the distance from apex to ambitus; pore zones, subparallel, very slightly diverging near anterior margin; pores quite small, round; pore pairs oblique, with a granule in each pair, close (40 pore pairs in each zone of the petal); extrapetal plates become larger, pore pairs distant and minute.

Paired ambulacral petals unequal, anterior pair somewhat shorter; petals lanceolate acuminate at the apex, widen rapidly, then converge toward the ambitus; pores in thin slits, external slit more elongated; pore pairs conjugate, separated by flat ridges ornamented by a row of moniliform granules; petal ends narrowly open; extrapetaloid pore pairs distant, marginal, not conjugate; pores minute, scarcely visible, with a granule in each pair.

Adoral ambulacral areas with large simple plates near the circumference, pore pairs distant, oblique; near peristome phyllodes deeply sunken, leaf shaped with compound plates; pore pairs first in triplets, then crowded, multiserial, arranged fanlike in oblique rows.

Interambulacral plates near ambitus increase in height, especially on the adoral circumference, bear three to five rows of tubercles, their sunken scrobicules surrounded by larger granules, some mammillate.

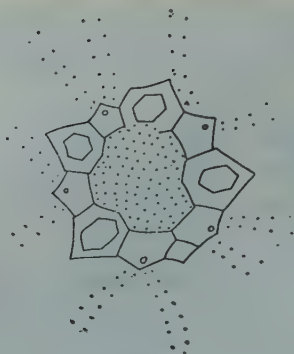


Figure 1

Pseudopygurus hathirae sp. n. Diagram of apical disc of holotype — enlarged.

Relationships: *Pseudopygurus hathirae* sp. nov. is in most details similar to *Pseudopygurus letteroni* Lambert from Somaliland (Migiurtina) described by Checchia-Rispoli. There are however some pronounced differences.

1) The specimens from Israel are as long as wide, well pentagonal, the angle of the posterior margin formed by straight lines, whereas the Somaliland species is wider than it is long, the posterior margin fortly sinuous, the circumference transversely trapezoidal.

2) The Israel specimens are aborally almost regularly rounded with apex central not corresponding with the excentric peristome; the asymmetry, although remarkable, is slight, against the gibbous, strong asymmetrical, conical shape of the Somali specimen with its summit strongly excentric and apex, corresponding with the peristome.

3) The paired ambulacral petals of the Hathira specimens are of lanceolate shape widest near the apex; the Somaliland species have the greatest width in the middle of the petals.

4) The anus of *Pseudopygurus letteroni* from Somaliland is acuminate anteriorly, that of the specimens from Hathira posteriorly.

5) The leaf-shaped phyllodes of the Israel specimens are more deeply depressed than the shallower little widened phyllodes of the Somaliland species.

6) The pore zones of the frontal ambulacrum are divergent in the Somaliland species, parallell in the Hathira specimens.

It seems that these differences justify the separation of the specimens from Hathira as a distinct species.

A g e : *Pygurus blumenbachi* is a Rauracian species and earlier than *Pseudopygurus letteroni* from the Sequanian of Tonnerre. The species of Somaliland have been found in a "thick banked, coarse sandy limestone, bearing a rich fauna of Brachiopods and Ostreids, directly above the sandstone with which the local sedimentary series

begins" (Checchia-Rispoli 1941, p. 873). From a similar horizon in a nearby locality Stefanini (1932, p. 48) has identified: *Somalirhynchia africana* Weir and *Terebratula pelagica* Roll.

The level of *Ps. hathirae* sp. nov. corresponds with the lower part of the section termed by Hudson (1958, p. 418) *Eligmus-Erymnoceras* Limestones and Marls. From the upper beds of this section Hudson has listed: *Erymnoceras* aff. *dorothea* Spath, *Thysanolytoceras* cf. *adeloides* (Kudernatsch), *Pachyceras* sp. sp.; he mentions also that echinoid debris are common. The age of these beds is according to Hudson—Lower-Middle Callovian.

Diagnosis of the genus: Considering the characters of *Pseudopygurus hathirae*, the diagnosis of the genus proposed by Checchia-Rispoli (1941, p. 874) may be emended as follows: Lampadiform echinid, sinucus anteriorly, subrostrate posteriorly. Apex monocyclic tetrabasal, central or excentral anteriorly. Ambulacral system heterogenous; frontal sulcus shallow; unpaired ambulacrum composed of two rectilinear zones of small, round, equal pores. Paired ambulacra petaloid with unequal conjugate pores. Phyllodes with multiserial pore pairs. Peristome in deep depression, pentagonal, surrounded by a well developed floscelle. Periproct infra-marginal, longitudinally oval; tubercles small, scrobiculate, perforate, (crenulate).

Phylogenetic considerations: The conclusions of the authors concerning the origin of the genus *Pseudopygurus* have been based on the surprising similarity of *Ps. letteroni* Lamb. to *Pygurus blumenbachi* Koch and Dunker and on the age priority of this latter species. It seemed obvious that there is a case of direct descent, that gave rise to a new lineage as suggested by Lambert (1911, p. 34): "il semble réellement que l'on assiste ici à la genèse d'une forme nouvelle dont les différences, encore indécises, en s'accroissant au cours des âges, conduiraient aux *Archiacia* du Crétacé". This view was joined by Mortensen (1948, p. 319), who considers it "evident that *Pseudopygurus* must be closely related to *Pygurus*, differing from this latter only by reduction of the pores in the frontal ambulacrum and it is very likely that we have here a direct line of descent". He also concluded that "It is in good accordance herewith that *Pygurus blumenbachi* is the older of the two, from the Rauracian" (ibid, p. 324).

The specimens from Hathira, although almost regularly rounded on adapical face, exhibit well the Archiaciid tendencies "to having the anterior part with the apical system raised" (ibid, p. 318). However, in view of the importance of the ambulacral structure, the opinions of the authors are undecided, even contradictory. If the direct lineage *Pygurus*—*Pseudopygurus* were true, the changes of the ambulacral characters could not be of far-going importance. Mortensen (ibid, p. 96) regards that "the primary importance ascribed to the ambulacral structure affords only generic, not family characters, the phyllod structure of the Cassiduloids showing all degrees of development of the phyllodes and bourrelets". Lambert even seems to doubt if the difference of the ambulacral structure is of generic significance (1924, p. 358): "Nous mentionnons ici ce genre, peut être théorique, en raison de l'import-

tance sans doute exagérée, attribuée par tous les auteurs au caractère de l'hétérogénéité des pétales". The absence of a link between the Jurassic *Pseudopygurus* and the Cretaceous *Archiacia* aroused therefore the doubts of Mortensen (ibid, p. 320): "I do not think the family of the Archiaciids as here limited, in conformity with Lambert and Thiery, a natural family. It is by no means improbable, that the reduction of the pores of the frontal ambulacrum, the essential character of the family, may have developed along different lines".

Now, the opinion that *Pseudopygurus* arose directly from *Pygurus blumenbachii* by the reduction of the frontal ambulacrum cannot be maintained, since the *Pseudopygurus* from Hathira is much older. But the supposition in itself does not seem conclusive. The significance of the phyllode structure is indeed not clear. It may be assumed that the arrangement of the pores, crowded in the peristomal region is liable to change. This is certainly not the case of the frontal ambulacrum, which by its position in a region of regular growth exhibits no tendency to undergo rapid structural changes. It seems, therefore, to be a constant character of great importance for family distinction. The frontal ambulacrum of *Pseudopygurus* is a well specialized linear ambulacrum with pore-pairs not conjugate, like the subpetaloid ambulacrum of the Spatangidae, and seems by no means to be a reduced petal of *Pygurus*. It is difficult to conceive the way by which it could be transformed suddenly from the frontal petal of *Pygurus* specialized in another direction. It may therefore be that both genera represent rather a parallel evolution diverging in Middle Jurassic times from a common root, that lead not only to generic but also to family distinction of the two lines.

REFERENCES

- CHECCHIA-RISPOLI, G., 1941, Sul genere "Pseudopygurus" Lambert, Atti di Reale Acc. d'Italia Rend. Class Sc. Fis. Mat. et Nat., Roma, ser. 7, 2, fasc. 10, pp. 870-874.
- CURRIE, E. D., 1925, Jurassic and Eocene Echinoidea, Monogr. Geol. Dept. Hunterian Mus. Glasgow Univ., 1, pp. 46-78, pls. VIII-X.
- HUDSON, R. G. S., 1958, The Upper Jurassic Faunas of Southern Israel, Geol. Mag., 95, 5, pp. 415-425.
- LAMBERT, J. M., 1911, Notes sur quelques Echinides Eocéniques des Corbières septentrionales. Ann. Univ. Lyon, N.S. 1, fasc. 30, p. 24.
- LAMBERT, J. M. ET THIERY, P., 1921, Essai de nomenclature raisonné des Echinides, Chaumont: Librairie Ferrière, 1909-1925.
- MORTENSEN, TH., 1948, A Monograph of the Echinoidea, 4, pl. 1, Holecypoids, Cassiduloidae, Copenhagen.
- SHAW, S. H., 1947, Southern Palestine, Geological Map with Explanatory Notes, Govt. of Palestine, Jerusalem.
- STEFANINI, G., 1932, Cenni sulle località fossilifere Giurassiche della Somalia, Paleontogr. Italica, 32, pp. 35-48.
- WIENER, G., 1955, Geology and Mineral Deposits of Makhtesh Hathira (Southern Israel), Bull. Swiss Ass. Pet.-Geol. and Eng., 21, 61, pp. 41-56.

LOWER CRETACEOUS MICROFACIES AND MICROFOSSILS FROM GALILEE

Z. REISS

Geological Survey of Israel, Paleontology Division, Jerusalem

ABSTRACT

A generalized composite columnar section and 92 photomicrographs of selected typical microfacies illustrating the surface Lower Cretaceous sequence of Northern Galilee are briefly discussed. A comparison between these strata and the subsurface early Cretaceous sequence of the Southern Coastal Plain is shown on a diagram, indicating diachronous facies distribution; this is held to be the cause for the restricted occurrence of *Hensonella* and of *Iraqia* in Galilee and their absence in the Southern Coastal Plain.

INTRODUCTION

A considerable amount of research on early Cretaceous strata of Israel has been carried out during the last years by the Geological Survey of Israel, by the Hebrew University Department of Geology, by Israel Mining Industries, Ltd., as well as by various oil companies in connection with geological mapping and economic minerals and oil exploration programs.

Published results deal mainly with subsurface early Cretaceous formations of the Southern Coastal Plain (Grader and Reiss 1958; Grader, Reiss and Klug 1960; Grader 1960; Picard 1958, 1959; Tschopp 1956, etc.). Information on the surface formations of early Cretaceous age in Galilee and in the Negev is contained mostly in unpublished reports and theses (Golani 1956; Nevo 1956; Rosenberg 1955, 1957, *et al.*), as well as in publications by Avnimelech, Parnes and Reiss (1954), Bentor and Vroman (1951), Blake (1935), Picard (1943, 1951, 1959), Shaw (1947), etc.

Serious difficulties have been encountered by all investigators of the Lower Cretaceous of Galilee with regard to sampling, measuring and establishing exact sequences of the exposed strata; these difficulties are due to the complicated fault-pattern of this region, as well as to land-slide topography and talus masses covering extensive areas. Magafossils are relatively rare and often badly preserved.

Therefore correlation by microfossils and microfacies is of considerable importance in stratigraphic work in this region. During 1956-1958 the author has examined large numbers of samples from outcropping early Cretaceous strata of Galilee, partly collected by himself but mainly submitted by various investigators. Of these samples only about 900 were found to be reliable and they form the basis of the present paper.

THE LOWER CRETACEOUS SEQUENCE OF NORTHERN GALILEE

The accompanying photomicrographs illustrate the marine surface early Cretaceous sequence of Northern Galilee. As detailed investigations of these strata by V. Boskovitz and U. Golani are now in progress at the Hebrew University, only a very brief summary of the sequence is given here. The accompanying composite section is intended to convey a highly generalized picture of the sequence and to show the position of the reliable samples from which the photomicrographs of some typical microfacies have been taken. Thicknesses indicated are maximum ones ascertained so far. They are often highly variable within the area under consideration and decrease generally from west to east. Certain doubts still exist with regard to the true thicknesses of some units; for this reason the lithological column on the accompanying diagrams appears broken in the case of the so-called "Orbitolina-series".

For the sake of convenience an open nomenclature is used here for the various lithostratigraphic units, but the names in use up to the present for the early Cretaceous units of Galilee (mostly invalid and inadequate) are indicated on the accompanying columnar section and mentioned in the text.

The Lower Cretaceous sequence of Northern Galilee is composed of four main complexes (from bottom to top): a sand complex with subordinate clays and marls, generally regarded as of pre-Aptian ("Neocomian") age; a sandy, oolitic, shaly and marly complex with clastic limestones, regarded to be of early Aptian age; a shaly limy, partly detritic and oolitic complex with intercalations of variegated clays, sands and iron-oolites, to which a late Aptian to earliest Albian age has been attributed; and a limy-dolomitic complex with shale intercalations, considered generally to be of Albian-Vraconian age.

The *lowermost complex* represents Wealdian deposits (Grader and Reiss 1958, Picard 1959) and contains some land-plants and — toward the top — lignite. Its base is not exposed and its maximum thickness not yet ascertained.

The overlying complex, *Unit LCrSIIIa*, is characterized by an alternation of oolitic and detritic sandy limestones, shales and marls, as well as by marine sandstones. Iron-oolites and lignite occur in places. Lateral variation over short distances is considerable. The fossil assemblage is characterized mainly by various Textulariidae, Verneulinidae, Valvulinidae, Miliolidae, Ophthalmidiidae, Lenticulininae, as well as by *Choffatella decipiens* Schlumb., *Pseudocyclammmina hedbergi* Maync and spp., *Orbitolina* spp., *Nautiloculina* nov. sp., rare *Trocholina* and *Neotrocholina* (ex gr. *infragranulata* (Noth)), *Cuneolina* and "*Praecuneolina*" spp., *Nezzazata* spp., *Valvulammina* (?) sp., and by fragments of molluscs, echinoids, ophiurans, bryozoans, rare corals and some Dasycladaceae. The assemblage indicates a possibly very late Barremian to early Aptian age, the latter appearing more probable (cf. Grader and Reiss 1958, Picard 1959).

The next higher complex consists of two units. *Unit LCrSIIIb* is composed of — usually cliff-forming — compact, generally fine grained, partly shaly limestones,

often sublithographic and containing intercalations of oolitic and detritic limestones and rarely of shales. The foraminiferal fauna is essentially the same as that of the underlying Unit LCrSIIIa and comprises occasionally *Barkerina* sp. The limestones contain *Nerinea pre-fleuriaui* Delp. (known from the Aptian of the Lebanon) and an abundance of fragmental Dasycladaceae and Codiaceae. Many of the occurring genera and species (*Cylindroporella*, *Arabicodium*, *Salpingoporella mühlbergi* Lor., *Acicularia*, *Munieria*, *Permocalculus*, etc.) have been recorded from the Barremian-Aptian of the Middle East by Elliott (1959). Particularly conspicuous in the microfossil assemblage is *Hensonella cylindrica* Elliott; it is restricted in Galilee to Unit LCrSIIIb. The fossil assemblage makes an early-middle Aptian age for this unit probable. The overlying Unit LCrSIIIc is composed of an alternating sequence of oolitic, detritic limestones, variegated shales and clays, compact limestones, sometimes sublithographic, rare sand-intercalations and strata containing iron-oolites and -concretions. Chamosite occurs occasionally. The so-called "Zumoffen"-cliff (a name used by comparison with the "Banc de Zumoffen" in the Lebanon), usually regarded as of early Albian age, is included here together with the so-called "Orbitolina-series" in a single unit, because both belong to the same lithofacies type and sedimentary cycle, as well as because of their essentially identical fossil assemblages. Incidentally, too much reliance has been placed by various authors on the assumed persistence of morphological prominence of the "Zumoffen"-cliff in Galilee: as shown by the writer's microscopic analysis the prominent cliff at Menara (Ramim) regarded as "Zumoffen" is formed by rocks belonging to the "Orbitolina-series", while the characteristic oolitic, detritic strata comparable with the Zumoffen cliff of the Lebanon occur at Menara higher in the section, but are not cliff-forming.

Unit LCrSIIIc carries abundant specimens of *Orbitolina* and comprises two fossil assemblages: a lower one, occurring in the lower part of the "Orbitolina-series" and essentially identical with that of the underlying unit LCrSIIIb, with the exception of *Hensonella* and containing considerably less algal remains (*Permocalculus*, *Acicularia*); and an upper one, occurring in the upper part of the "Orbitolina-series" and in the "Zumoffen" (s.str.), characterized by the absence of *Trocholina*, *Neotrocholina*, *Nautiloculina* and by the appearance of various Cretaceous pelagic foraminifera (*Hedbergella*) and of some Anellida. Echinodermata debris occurs often abundantly. The megafauna of this unit is composed mainly of species of *Cardium* and *Holcypus*. A (middle-late) Aptian age is probable for this unit.

The uppermost early Cretaceous complex of Northern Galilee is composed of Unit LCrSIV which comprises the so-called "Knemiceras layers" and unnamed strata referred to as "Vraconian".

The unit is composed of shaly limestones, sublithographic limestones, some skeletal and fragmental limestones, calcareous shales, as well as of dolomitic limestones and apparently secondary dolomites, which occur particularly in the upper part of the unit. The fossil assemblage of the lower part of this unit is characterized by Textulariidae, Miliolidae, *Cuneolina* and "*Praecuneolina*" spp., *Nezzazata* sp.,

Valvulammina (?) sp., *Orbitolina*, *Simplorbitolina* sp., *Dietyoconus* (?) sp., *Praeglobotruncana* sp., by frequent Cretaceous "globigerinids" and globotruncanids ("Globigerina" *washitensis* Carsey, *Hedbergella* spp.), various *Pseudocyclammina*, as well as by the absence of *Choffatella* (two fragments found are considered reworked) and extreme scarcity of Lagenidae. The megafauna comprises *Knemiceras*, *Heteraster delgadoi* Lor., *Exogyra* ex gr. *weatherfordensis* Cragin (det. A. Parnes). This assemblage points to an Albian age for this part of the unit (compare also Avnimelech, Parnes and Reiss, 1954).

The upper part of Unit LCrSIV is characterized by the gradual disappearance of the fauna mentioned above, of which mainly Miliolidae, *Nezzaza'a*, *Valvulammina* (?), *Cuneolina* and "*Praecuneolina*" and rare Textulariidae persist, by more frequent molluscan (including rudist) debris and by the occurrence of *Iraqia simplex* Henson. The highest part of the unit was generally considered to be of Vraconian age, although it is at least in part correlative with strata of the Lebanon considered by Heybroeck (1942) to be of Cenomanian age. In Galilee, the Vraconian-Cenomanian boundary is usually placed on a lithological basis only at the beginning of the massive dolomites regarded as of early Cenomanian age and containing occasionally *Strombus* sp. and *Nerinea* ex gr. *cochlaeformis* Conr. This usage is followed here, the status of the Vraconian stage being uncertain and the fossil evidence being insufficient (see also below).

DEPOSITIONAL ENVIRONMENTS

As already pointed out by Picard (1959), the stratigraphic sequence of the Lower Cretaceous of Galilee reflects "progressive sedimentary evolution... from the early or continental stage to the epicontinental and finally to quasi-pelagic conditions". Analysis of microfacies and faunas largely supports his interpretation of depositional environments of the various units.

The Wealdian deposits accumulated in Northern Galilee since the regression of the Jurassic Sea and until the beginning of Aptian times. Some of these deposits might be estuarine (Heybroeck 1942). The regression started at the close of the Jurassic, reached its peak in the Southern Coastal Plain in late Hauterivian times (Grader and Reiss 1958, Grader 1960) and the latter area remained in the littoral zone during the Barremian. Renewed transgression of the sea from the northwest started at the close of the Barremian and the sea reached Northern Galilee in early Aptian times. Clastic, oolitic, occasionally lignitiferous marine sediments containing warm — and shallow — water fauna and flora (Unit LCrSIIIa) were laid down in a turbulent, littoral, warm water environment. During middle Aptian times Northern Galilee remained within the limits of the epinerithic-littoral zone of a slowly transgressing sea. The fine-grained limestones containing abundant debris of calcareous algae belonging to groups whose living representatives thrive in tropical and sub-tropical waters at a depth of less than 50 meters (mainly Dasycladaceae, some Codiaceae and no Corallinaceae occur in Unit LCrSIIIb) have been probably deposited

ed in quiet, shallow and warm waters and are comparable to the "algal debris facies" rocks of Elliott (1958) characteristic of the later Lower Cretaceous in the Middle East. These deposits of Unit LCrSIIb contain intercalations of oolitic, pseudoolitic, detritic, *Trocholina*-bearing limestones providing evidence of a turbulent, current-swept littoral environment. Intercalations of the same type occur in the middle Aptian shales in the Southern Coastal Plain (Unit LCrIIb, Grader and Reiss 1958). General and gradual deepening of the sea over large areas during these times is, therefore, indicated, although the contemporaneous recurrence, both in Northern Galilee and in the Southern Coastal Plain, of littoral, turbulent conditions during an essentially undisturbed shelf sedimentation might point to minor tectonic movements. Such movements might also account for the recurrence of littoral sands in the early Aptian Unit LCrSIIa of Galilee. These *widespread* oscillations would have to be attributed to tectonic activity, assumed by Grader (1960) to have affected the Southern Coastal Plain in early Aptian times. Some of the *local* alternations of fine- and coarse-grained sediments, i.e. of undisturbed and turbulent conditions might, however, be genetically interrelated and of purely sedimentary origin. Thus, accumulation of oolitic, fragmental sediments carried by currents in a littoral environment might have produced (oceanographic) sills behind which fine mud particles and larger algal fragments of low specific gravity accumulated in "troughs" protected from the influence of currents (also Elliott 1958). Filling up of these troughs might have led again to agitated bottom conditions and to renewed influence of currents on the type of sedimentation.

The sediments of Unit LCrSIIc show that essentially shallow and warm water conditions reigned in Northern Galilee throughout later Aptian times, although a general tendency to deeper water conditions is progressively evident. Increase of distance from the shore accounted probably for higher salinity and for the appearance of pelagic foraminifera. Oscillations of depth caused again recurrence of oolitic strata (including the "Zumoffen") as well as iron-oolites and even sands in Unit LCrSIIc. Again part of these oscillations might be due to sedimentary factors, although contemporaneous erratic thicknesses changes in the Southern Coastal Plain and even thinning of strata towards the west in that area may point to continued tectonic activity, as assumed by Grader (1960).

Both lithology and fauna of the Albian sediments point to their deposition in an environment relatively far from the shore (frequency of pelagic foraminifera and scarcity of "larger" ones). The Albian sea encroaches upon vaster areas and in the Negev marine, *Knemiceras*-bearing sandy, shaly and oolitic limestones occur as intercalations in continental sandstones of "Nubian" type. Some areas like Northern Galilee remained nevertheless within the limits of rudist reef-talus formation, as well as of the Orbitolinidae and Miliolidae. Coarse molluscan debris occurs in late Albian-Vraconian strata. Conditions of this warm sea favoured the subsequent formation of dolomites which characterize late Albian and especially early Cenomanian deposits over considerable areas.

The distribution of early Cretaceous facies types in Northern Galilee reflects three main factors: transgression and continued subsidence of the area during Aptian-Albian times (Picard 1959), minor tectonic movements affecting larger areas (Grade 1960) and local rapid changes due to sedimentary causes. These factors determine diachronous facies distribution and lateral facies shifts summarized schematically on the accompanying diagram. The latter is intended to compare the distribution of facies types in the Southern Coastal Plain with that in Northern Galilee.

As can be seen from the diagram, the same sequence of facies types can be recognized in both areas; they are, however, diachronic until Albian times. Diachronism is more pronounced in the lower part of the column and less so in its higher part, or — in other words — more prominent in the group of shallower water facies. Thus, a facies type characterizing Hauterivian-early Barremian deposits in the Coastal Plain occurs in early Aptian times in Northern Galilee; the algal debris facies characteristic of late Barremian deposits in the Coastal Plain is widespread in middle Aptian times in Galilee. Sediments of Albian age on the other hand, are very similar in both regions, although they are thicker and apparently more dolomitized in the Coastal Plain (dolomitisation starting possibly also earlier) than in Northern Galilee.

The distinction between planes of isofacies and synchronous surfaces is, therefore, of particular importance in stratigraphic work on early Cretaceous formations of Israel. It presents a considerable problem, whose partial solution seems to lie in a future more detailed study of microfossils and microfacies from large amounts of material and from various areas.

Two characteristic microfossils, *Iraqia* and *Hensonella*, are recorded here for the first time from Israel. Their occurrence in the Lower Cretaceous of Galilee and apparent absence in the Southern Coastal Plain seem to be due to the facies-shifts mentioned above.

OCURRENCE OF *IRAQIA SIMPLEX* HENSON

Specimens of this foraminifer have been found in various samples of Unit LCrSIV of Northern Galilee. They have apparently been mistaken by various investigators for *Orbitolina*.

Iraqia has been described by Henson (1948) from Iraq and recorded by him also from Iran. The systematic position of *Iraqia* has been discussed by Henson (op. cit.), by Ciry and Rat (1953) and by Douglass (1960).

The stratigraphic range of *Iraqia* is given by Henson (op. cit.) as Lower to Middle Cretaceous. The type-locality of *Iraqia* was considered to be probably of Aptian age (P. Vienne in Henson, op. cit.), as Albian by Ciry and Rat (op. cit.) and by Smout (1956) as "either Cenomanian or so high in the Lower Cretaceous that a Cenomanian occurrence would not be surprising". Dunnington, Wetzel and Morton (1959) state, however, that the type locality of the species "lies some 700 feet below

the top of the Qamchuqa limestone" of Iraq, which is now considered to be of Albian age and that *Iraqia* ranges "through the lower part of the Albian and upper part of the Aptian". Douglass (1960) assigns now to *Iraqia* also the species *Dictyoconus valentinus* Almela occurring in Spain in strata regarded as of Cenomanian age.

Available records seem to indicate that *Iraqia* occurs in the Middle East mainly in early Cretaceous strata, although a very early Cenomanian age is not excluded for some of its occurrences.

Hitherto, *Iraqia* has not been found in samples from wells drilled in the Southern Coastal Plain. This might possibly be due to insufficient sample recovery (zone of "blind drilling", see Grader and Reiss 1958). On the other hand, it seems probable that its absence in the samples examined from the Coastal Plain is due to the fact that there water depth was too great at that time to allow the existence of "simple" Orbitolids, like *Iraqia*; this group seemed to favour moderately shallow and warm waters with fine grained, calcareous sediments and little clastic material. These conditions reigned in Northern Galilee in late Albian times.

OCCURRENCE OF *HENSONELLA CYLINDRICA* ELLIOTT

Abundant fragmental specimens of this species of unknown affinities occur in Unit LCrSIIIb throughout Galilee and are confined to it. Their occurrence has been to be an important and reliable means of correlation in this area.

Hensonella has been described by Elliott (1959) who has discussed its systematic position. Elliott was reluctant to assign *Hensonella* to the calcareous algae (although it resembles strongly a dasycladacean) particularly on account of the *irregular* "cracks and fissures", which are not regarded by Elliott as verticils of side branches, and because of the peculiar inner lining, coating the aragonitic cylinder. Elliott suggested the possibility of *Hensonella* being a scaphopod.

The rich material from Northern Galilee examined by the present writer belongs definitely to *Hensonella cylindrica* and all specimens examined show clearly the characters of this species as described by Elliott (op. cit.). However, Elliott's figured specimens do not show the distinct pores in the aragonitic wall of the specimens of Galilee (see figs. 93-107), nor does he describe this feature. Indeed, the pores are not easily seen in random sections, although they occur in all suitably sectioned specimens, as shown on the accompanying photos.

The structure shown by the specimens from Galilee seems to speak against scaphopod affinities and strongly suggests that *Hensonella* is in fact a dasycladacean alga. It might also be significant that it occurs in algal facies only (also Elliott 1959).

Hensonella is known from the Iraqi Kurdistan, from Kirkuk and from Persia (Elliott, op. cit.). As far as its stratigraphic range is concerned, Elliott records *Hensonella* as occurring "throughout the Lower Cretaceous but especially abundant at the Upper Barremian-Aptian levels". Its type level is given as "Lower Cretaceous, about Barremian level".

In Galilee, *Hensonella* occurs in undoubtedly Aptian (about Middle Aptian)

strata, but is absent at other levels. This is probably due to the fact that the only suitable (algal) facies for the occurrence of *Hensonella* in Galilee is that of the middle Aptian Unit LCrSIIB. In the Southern Coastal Plain this facies occurs in the late Barremian Unit LCrIId, but *Hensonella* is absent from it (Grader and Reiss 1958 and see Elliott's (1950, p. 230) remark). Possibly *Hensonella* did not occur at all in the region of Israel before the Aptian. Conditions suitable for its occurrence in Aptian times in this region, as known up to the present, have existed in Northern Galilee only.

REFERENCES

1. AVNIMELECH, M., PARNES, A. AND REISS, Z., 1954, Mollusca and Foraminifera from the Lower Albian of the Negev (Southern Israel), *Journ. Paleontology*, **28**, 6.
2. BENTOR, Y. AND VROMAN, A., 1951, *The Geological Map of the Negev*, 1:100,000, Sheet 18: Ovdat, Tel-Aviv (Hebrew).
3. BLAKE, G.S., 1935, *The Stratigraphy of Palestine and Its Building Stones*, Govt. Printing and Stationery Office, Jerusalem.
4. CIRY, R. AND RAT, P., 1953, Description d'un nouveau genre de foraminifère *Simplorbitolina manasi*, nov. gen., nov. sp., *Trav. Lab. Géol. Fac. Sci. Dijon, Bull. Sci. Bourgogne*, **14** (1952-1953).
5. DOUGLASS, R.C., 1960, Revision of the family Orbitolinidae, *Micropaleontology*, **6**, 3, New York.
6. DUNNINGTON, H.V., WETZEL, R. AND MORTON, D.M., 1959, *Léxique Stratigraphique Internationale*, **3**, *Asie, fasc. 10a, Iraq. Mesozoic and Paleozoic*, CNRS, Paris.
7. ELLIOTT, G.F., 1958, Algal Debris-facies in the Cretaceous of the Middle East, *Paleontology*, **1**, 3, London.
8. ELLIOTT, G.F., 1959, Fossil calcareous algal floras of the Middle East with a note on a Cretaceous problematicum, *Hensonella cylindrica* gen. et sp. nov., *Quart. Journ. Geol. Soc. London*, **115** (1959), 3.
9. GOLANI, U., 1956, *The Geology of the Hazwa-region*, M. Sc.-thesis, The Hebrew University, Jerusalem (unpublished).
10. GRADER, P. AND REISS, Z., 1958, On the Lower Cretaceous of the Heletz area, *Bull. Geol. Survey of Israel*, **16**, Jerusalem.
11. GRADER, P., REISS, Z. AND KLUG, K., 1960, Correlation of sub-surface Lower Cretaceous units in the Southern Coastal Plain of Israel, *ibidem*, **28**.
12. GRADER, P., 1960, Geological history of the Heletz-Brur area, Israel. Part II. Lower Cretaceous, *ibidem*, **31**.
13. HENSON, F.R.S., 1948, Larger imperforate Foraminifera of South-western Asia, *Mem. Brit. Mus. Nat. Hist.*, London.
14. HEYBROECK, F., 1942, La géologie d'une partie du Liban sud, *Leidsche Geol. Med.*, **12**.
15. NEVO, A., 1956, *Report on the Lower Cretaceous of the Rami region*, Geol. Survey of Israel (unpublished).
16. PICARD, L., 1943, Structure and Evolution of Palestine, *Bull. Geol. Dept., Hebr. Univ., Jerusalem*, **4**, 2-4.
17. PICARD, L., 1951, Geomorphogeny of Israel, Part 1: Negev, *Bull. Res. Council. of Israel*, **1**, 1-2.
18. PICARD, L., 1958, Geological background on petroleum drilling in Zikhron Yaaqov (S. Carmel) *Ibidem*, **7G**, 1.
19. ROSENBERG, E., 1955, *Report on the iron-ore of Menara*, Geol. Survey of Israel (unpublished).
20. ROSENBERG, E., 1957, *Geologische Untersuchungen in the Naphthali Bergen*, Ph.D.-thesis, Univ. of Zurich (unpublished).
21. SHAW, S.H., 1947, *Southern Palestine, Geological Map on a scale of 1:250,000 with Explanatory Notes*, Palest. Govt. Printer, Jerusalem.
22. SMOUT, A.H., 1956, Three new Cretaceous genera of foraminifera related to the Ceratobuliminidae, *Micropaleontology*, **2**, 4, New York.
23. TSCHOPP, H.J., 1956, The Oilfind of Heletz, *Bull. Swiss. Ass. Pet.-Geol. & Eng.*, **22**, 63.

EXPLANATIONS OF PHOTOMICROGRAPHS

Note: Numbers refer to samples deposited in the collections of the Paleontology Division, Geological Survey of Israel. Letters following descriptions indicate locations (see reference map): R — Rami (Har Haari, Har Hazon), H — Hazwa, M — Menara (Ramim). The order of the photomicrographs follows the stratigraphic sequence from bottom to top (see composite section).

Photos 1 — 14. Unit LCrSIIa — Lower Aptian.

- 1-2. Detritic, oolitic, pseudoolitic, sandy limestone with "*Praecuneolina*" (P), *Choffatella* (C), debris of molluscs, echinoderms and bryozoans. 1671-H.17.5x.
- 3-4. As above with *Orbitolina*. 1673-H.17.5x.
5. Oolitic, detritic, sandy limestone with calcite-filled fissures. 1674-H.17.5x.
6. Sandstone with rare organic debris. 1514-H.17.5x.
7. Detritic sandstone with corals (septa seen light-gray on left side of photo). 1509-H.17.5x.
8. Oolitic, pseudoolitic, detritic, strongly sandy limestone with *Orbitolina*. 1676-H.17.5x.
9. Oolitic, pseudoolitic, detritic, sandy limestone with debris of molluscs, echinoderms and bryozoans. 1561-H.17.5x.
10. Oolitic, pseudoolitic, detritic, strongly sandy limestone with miliolids and bryozoans (B). 584-M.21x.
11. As above with debris of molluscs and echinoderms. 1563-H.17.5x.
12. Sandstone with rare molluscan debris. 1713-H.17.5x.
13. Detritic, pseudoolitic, sandy limestone with *Orbitolina*, verneuiliids and molluscan debris. 593-M.21x.
14. Detritic, partly shaly limestone with *Choffatella* (C) and debris of molluscs, echinoids and calcareous algae. 1715-H.21x.

Photos 15—32. Unit LCrSIIb — (Middle) Aptian.

15. Detritic, shaly limestone with miliolids and abundant debris of dasycladaceans. 596-M.21x.
16. Detritic limestone with debris of Dasycladaceae, Codiaceae and *Hensonella* (H). 597-M.21x.
17. Detritic, partly oolitic limestone with *Nezzazata* (N) and various organic debris. 598-M.21x.
- 18-19. Shaly limestone with abundant Dasycladaceae (*Cylindroporella*). 599-M.21x.
20. As above with *Pseudocyclammina* (Ps.), *Nezzazata* (N), miliolids and *Hensonella* (H). 788-R.17.5x.
21. Shaly limestone with "*Praecuneolina*" (P), *Salpingoporella* (Sa) and var. algal debris. 789-R.17.5x.
22. Detritic, "granular" and pseudoolitic limestone with valvulinids, textulariids, miliolids, *Nezzazata* and some algal debris. 1725-H.21x.
23. Detritic, shaly limestone with *Orbitolina* and debris of molluscs and algae. 602-M.21x.
24. Shaly limestone with textulariids, *Barkerina*, debris of molluscs and algae. 1731-H.21x.
25. Highly detritic limestone with abundant debris of dasycladaceans and codiaceans, molluscs and rare small foraminifers. 1733-H.17.5x.
26. Detritic, partly pseudoolitic limestone with *Orbitolina*, *Cuneolina*, miliolids, textulariids, debris of molluscs and echinoderms. 1735-H.21x.
27. Oolitic, pseudoolitic, detritic limestone with *Neotrocholina* (Tr), debris of molluscs. 791-R.21x.
28. As above with debris of dasycladaceans, codiaceans and textulariids. 1737-H.21x.
29. Detritic, pseudoolitic, "granular" limestone with textulariids and var. organic debris. 1740-H.21x.
30. Fine grained limestone with debris of algae, *Nezzazata* (N) and *Hensonella* (H). 1742-H.21x.
31. As above with *Acicularia* (A). 1746-H.21x.
32. Shaly limestone with textulariids, *Nezzazata*, miliolids, algal debris, molluscs. 1748-H.21x.

Photos 33—61. Unit LCrSIIc — Upper Aptian.

33. Shaly limestone with miliolids, textulariids, *Nautiloculina* (Na), debris of molluscs. 1749-H.21x.
34. Limestone with abundant *Orbitolina*. 611-M.21x.
35. Detritic, shaly limestone with abundant debris of dasycladaceans and codiaceans, molluscs and echinoderms. 1754-H.21x.
36. Shaly limestone with textulariids, miliolids, *Nezzazata*, debris of molluscs and echinoderms. 619-M.21x.
37. Detritic, shaly limestone with *Orbitolina*, debris of molluscs and echinoderms. 1753-H.21x.

38. Sandy limestone with iron oolites and debris of molluscs and echinoderms. 560-M.21x.
39. As above with elongated iron-oolites. 623-M.21x.
40. Shaly limestone with abundant *Orbitolina* and debris of molluscs and echinoderms. 623-M.21x.
41. As above with annelid tubes. 625-M.21x.
42. Shaly limestone with abundant *Orbitolina*. 626-M.21x.
43. Detritic, shaly limestone with abundant debris of echinoderms, dasycladaceans, molluscs. 627-M.21x.
44. Limestone with debris of molluscs and echinoderms. 570-M.21x.
45. Shaly limestone with *Choffatella* (C) and debris of molluscs and echinoids. 1606-H.17.5x.
46. Detritic limestone with iron-oolites. 630-M.21x.
47. Detritic limestone with *Orbitolina* and *Pseudocyclammina*. 1766-H.21x.
48. Limestone with abundant miliolids and debris of molluscs and echinoderms. 632-M.21x.
49. Fine-grained limestone with rare indet. foraminifers. 636-M.21x.
50. Fine grained limestone with *Pseudocyclammina* and debris of molluscs. 641-M.21x.
51. As above. 649-M.21x.
- 52-53. Fine grained limestone with *Orbitolina*, *Pseudocyclammina* (Ps) and var. organic debris. 575-M.21x. (So-called "Zumoffen" of Menara (Ramim)).
54. As above. 651-M.21x.
55. As above. 652-M.21x.
56. Detritic, partly crystalline limestone with miliolids, textulariids and debris of molluscs and echinoderms. 654-M.21x.
57. Oolitic, pseudoolitic, detritic limestone with debris of molluscs and echinoderms. 1433-R.17.5x. ("Zumoffen"-layers, s.str.).
- 58-59. As above with *Orbitolina* and bryozoans. 655-M.21x. ("Zumoffen"-layers, s.str.).
60. Detritic, oolitic, pseudoolitic limestone with miliolids, indet. agglutinated foraminifers and var. debris. 655-M.21x. ("Zumoffen"-layers, s.str.).
61. As above. 801-R.17.5x. ("Zumoffen"-layers, s.str.).

Photos 62-92. Unit LCrSIV — Albian (—Vraconian).

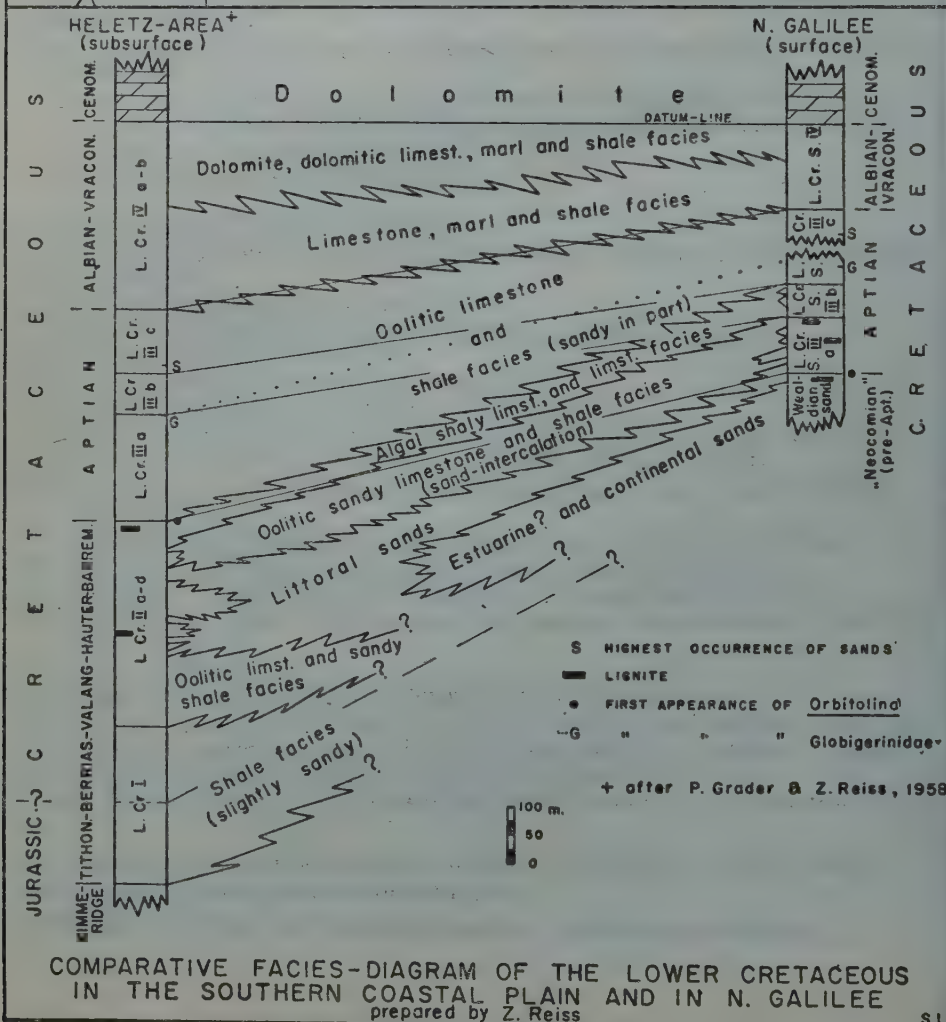
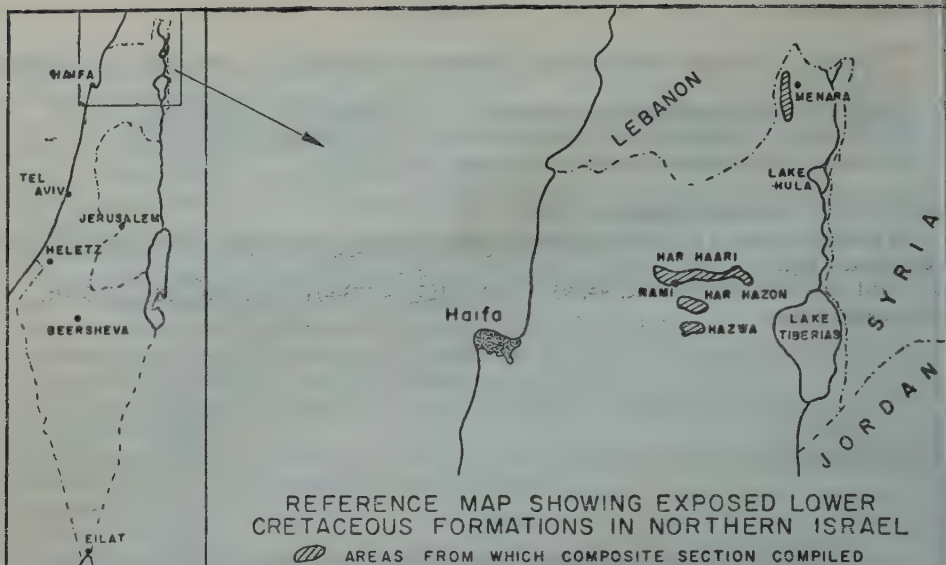
62. Finely detritic limestone with indet. orbitolinids, textulariids, debris of molluscs and echinoderms. 1436-R.17.5x.
63. As above with *Pseudocyclammina*. 1437-R.17.5x.
64. Limestone with textulariids, miliolids, *Cuneolina* (Cu), var. debris. 904-R.17.5x.
65. Limestone with *Orbitolina*. 1438-R.17.5x.
66. Limestone with *Praeglobotruncana* (Prg). 1467-R.44x.
67. Limestone with *Hedbergella* (Hd) and small debris. 1468-R.44x.
68. Detritic, partly crystalline limestone with miliolids and debris of molluscs. 908-R.17.5x.
69. As above with *Valvulammina* (?), "*Praecuneolina*" (Pr), miliolid, 580-M.21x.
70. Detritic, shaly limestone with *Cuneolina*, miliolids, *Nezzazata*, var. debris. 911-R.17.5x.
71. As above. 912-R.17.5x.
72. Partly crystalline limestone with textulariids, miliolids and var. debris. 1440-R.17.5x.
73. Fine grained limestone with *Hedbergella* and debris of molluscs. 957-R.44x.
74. Detritic limestone with miliolids and large agglutinated foraminifers. 959-R.17.5x.
75. Finely detritic limestone with miliolids, textulariids, *Cuneolina*, *Valvulammina* (?). 961-R.17.5x.
76. As above. 962-R.17.5x.
77. As above. 965-R.17.5x.
78. Sublithographic limestone with indet. foraminifers. 1626-M.21x.
79. Finely detritic limestone with orbitolinids, debris of echinoderms and molluscs. 966-R.17.5x.
80. Dolomite with rare molluscan debris. 1527-M.21x. (photos 80-92 from so-called "Vraconian").
81. Fine grained limestone with miliolids and debris of molluscs. 967-R.17.5x.
- 82-85. Partly dolomitic limestone with *Iraqia* (I) and debris of molluscs and echinoderms. 1451-R.21x.
86. Highly detritic limestone with textulariids, miliolids and fragments of molluscs. 969-R.17.5x.
87. Detritic limestone with molluscan debris. 970-R.17.5x.
88. Highly detritic limestone with fragments of molluscs and *Nezzazata*. 1051-R.21x.

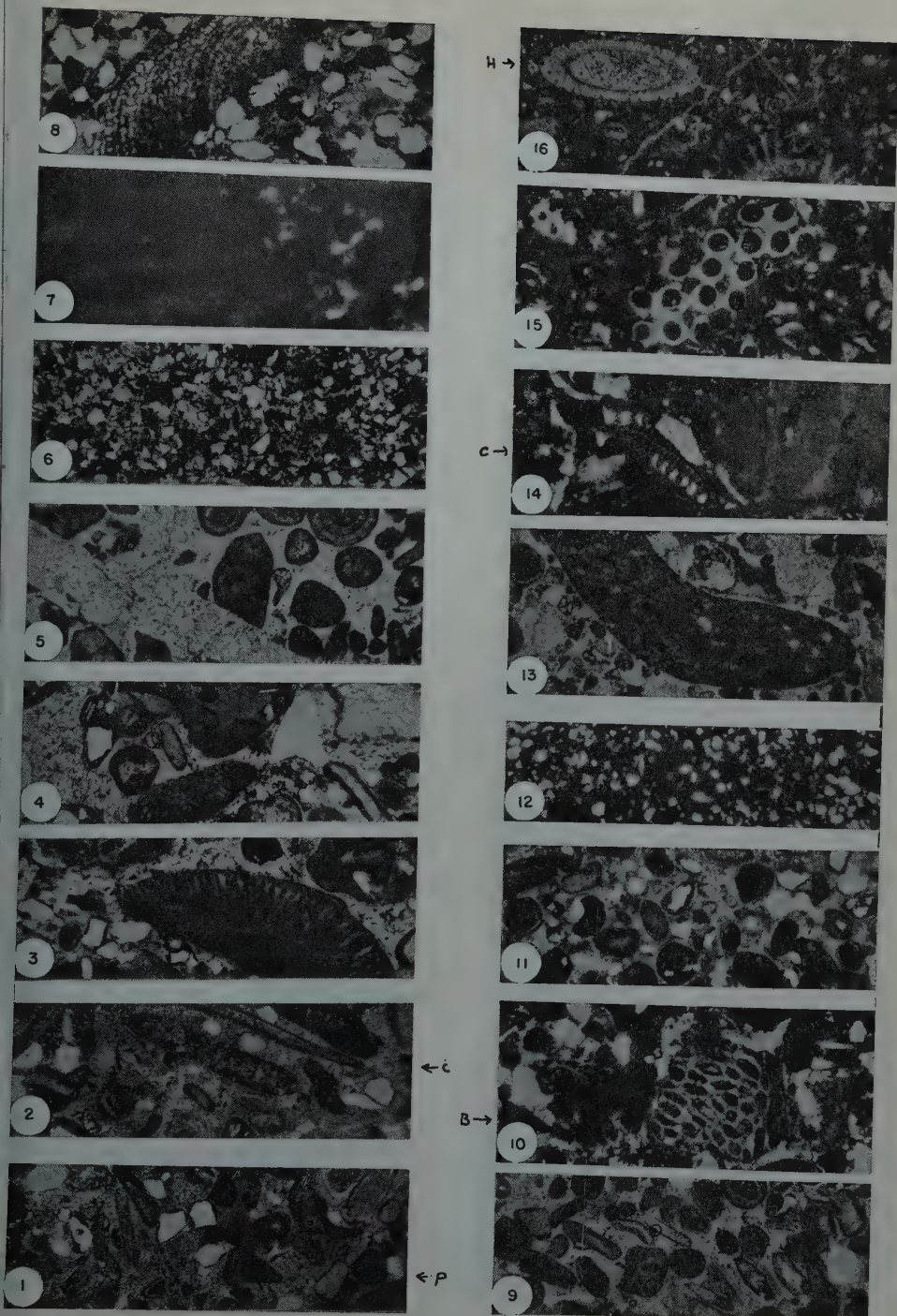
- 89. "Granular" limestone with miliolids, *Hedbergella* and debris of ostracodes and molluscs. 1502-R.17.5x.
- 90. Fine grained, sublithographic limestone with indet. foraminifers. 1503-R.21x.
- 91. Highly detritic limestone with abundant molluscan fragments. 1504-R.17.5x.
- 92. As above, with abundant debris of pelecypods. 1458-R.17.5x.

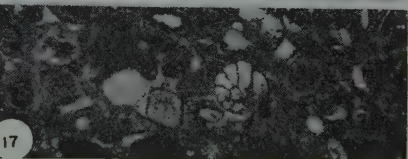
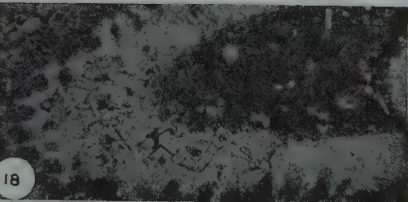
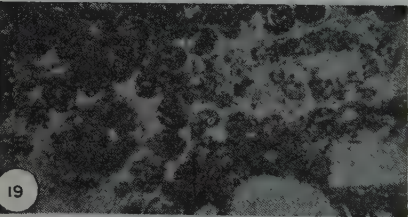
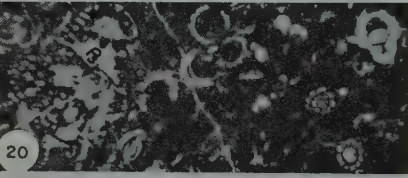
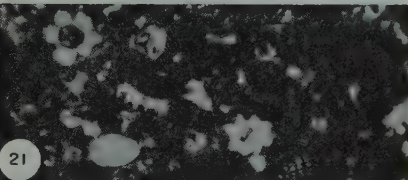
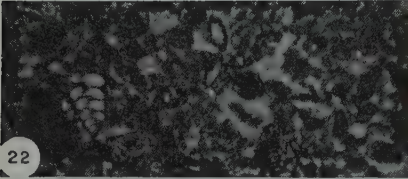
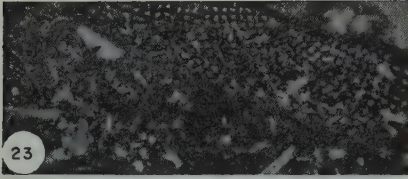
Photos 93-107. Hensonella cylindrica Elliott.

All specimens figured are from random sections of samples from Unit LCrSIIIb. Magnification of all photos 55x.

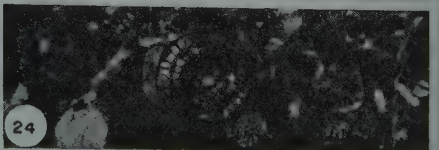
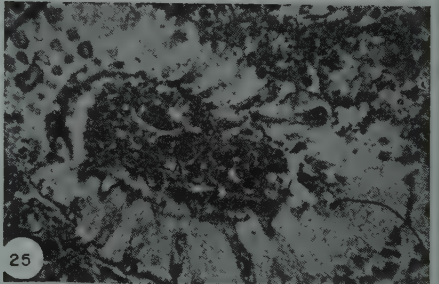
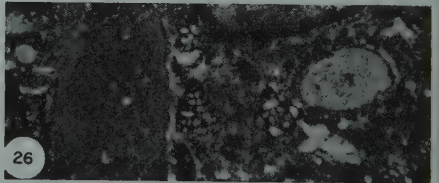
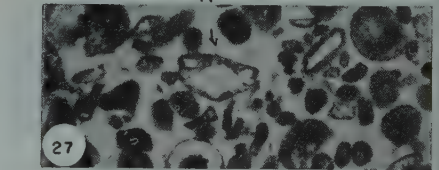
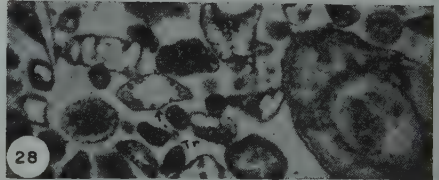
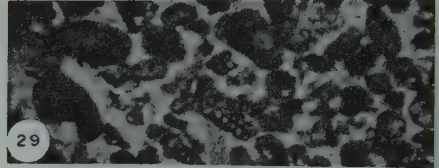
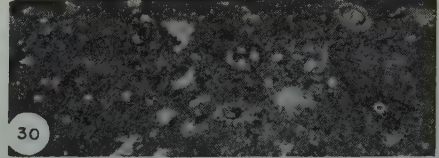
93, 99, 101, 103, 104, 105-788-R. 94, 95, 97, 100, 107 — 1730-H. 96,98, 102, 106 — 783-R.
96— crossed nicols.







H →
N →

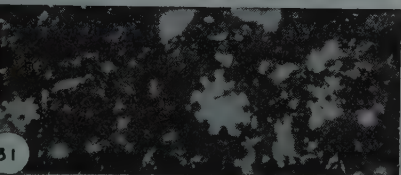
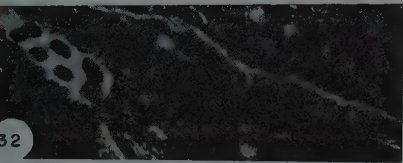
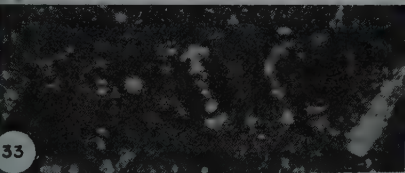
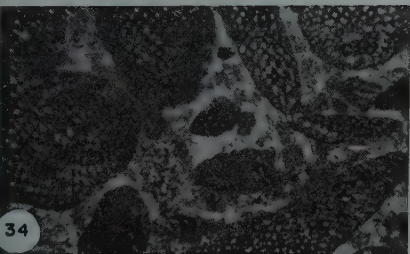
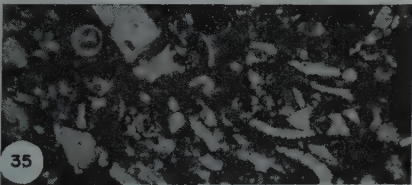
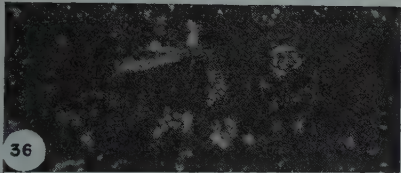
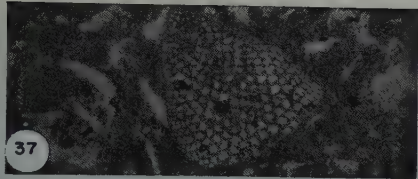


← P

← N

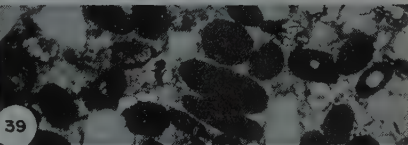
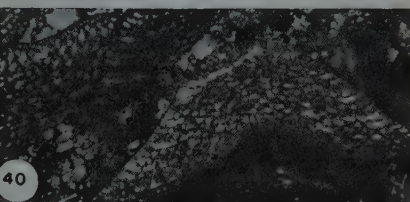
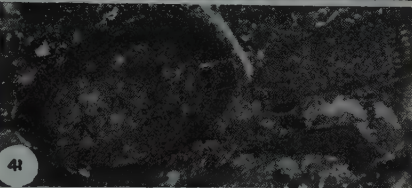
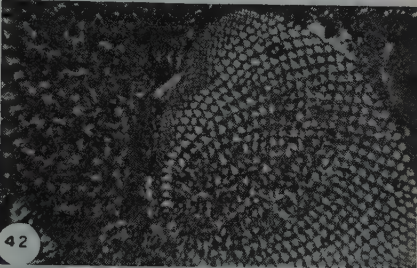
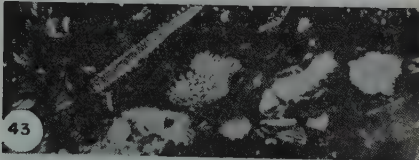
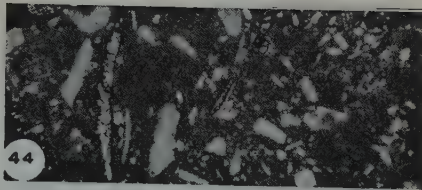
← H

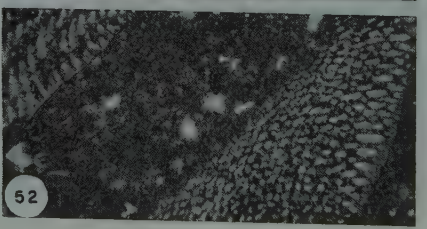
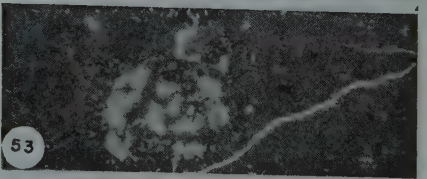
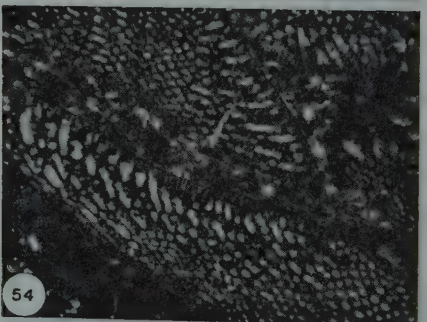
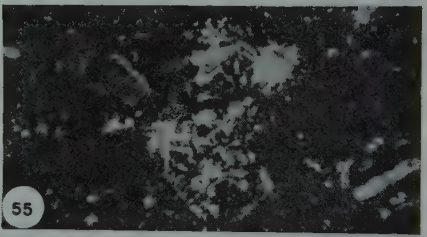
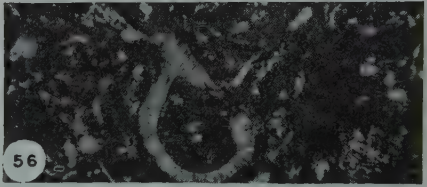
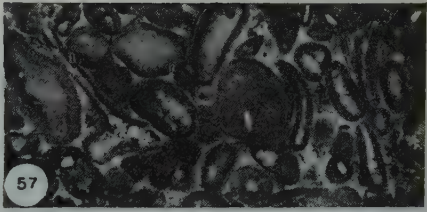
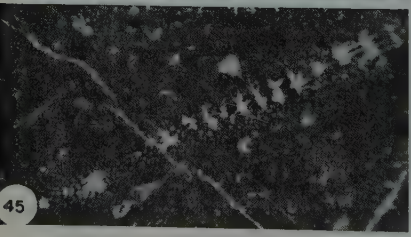
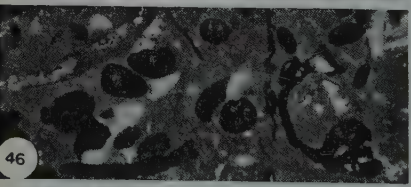
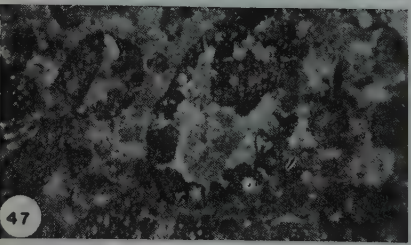
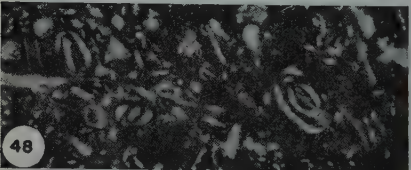
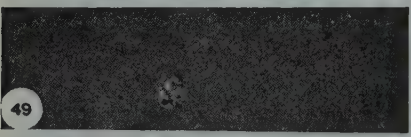
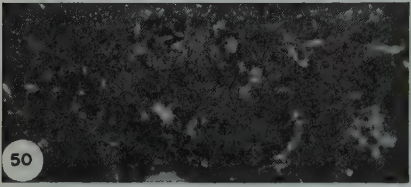
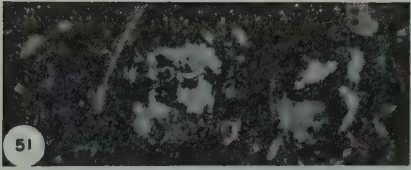
← N



← Na

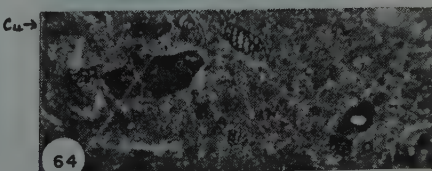
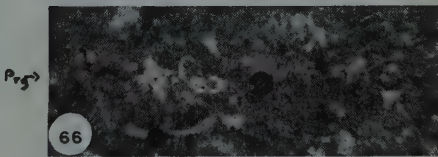
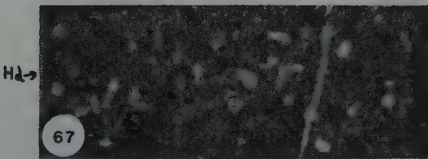
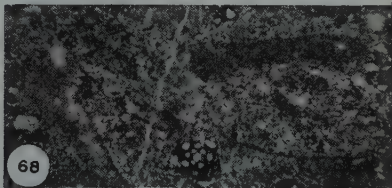
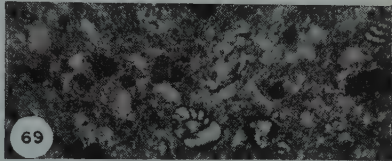
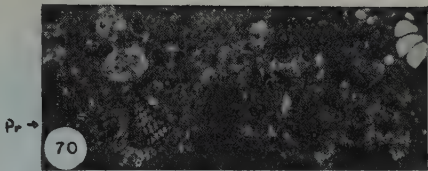
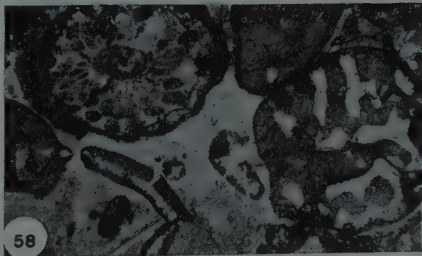
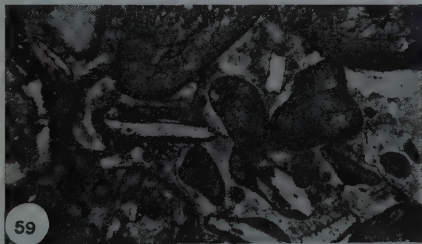
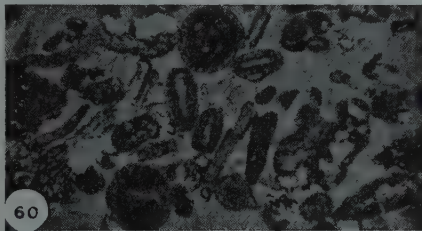
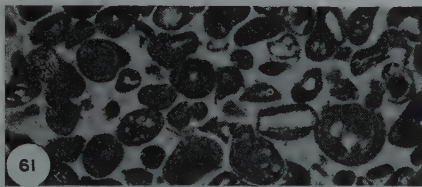
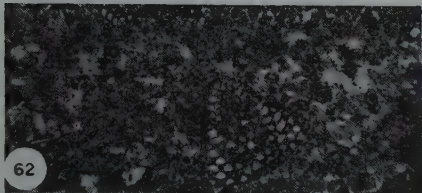
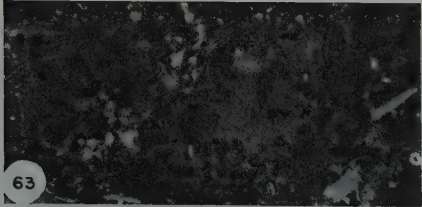
← A

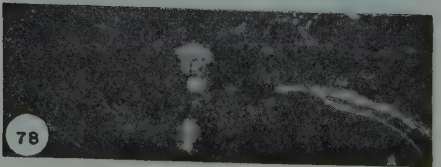
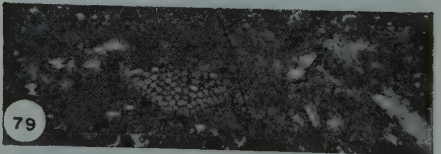
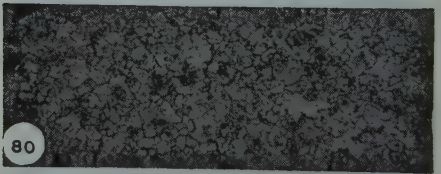
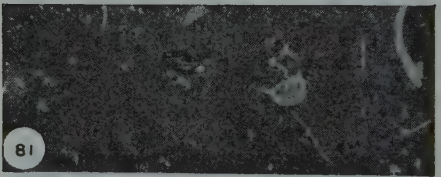
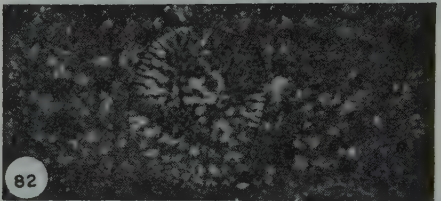
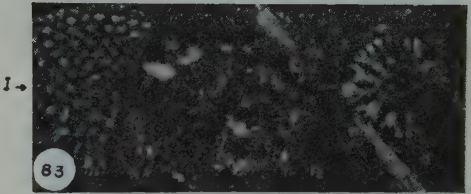
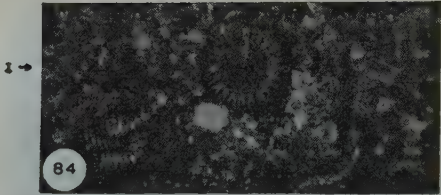
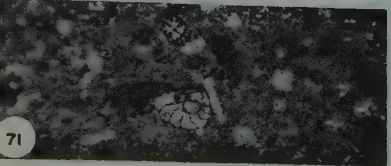
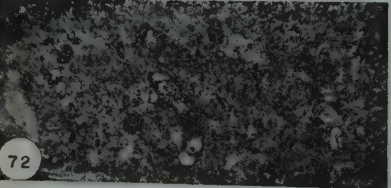
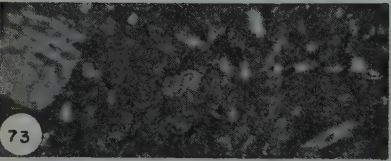
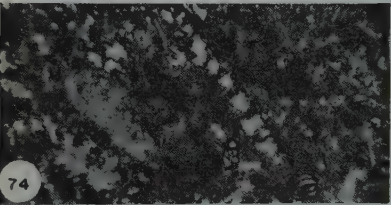
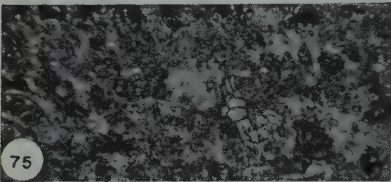
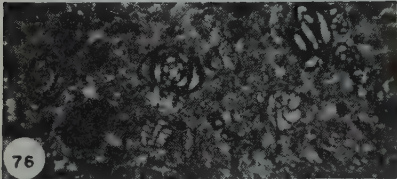
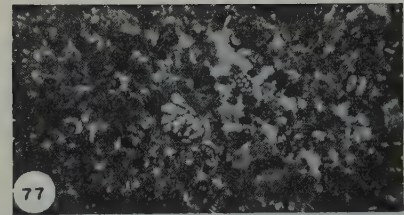


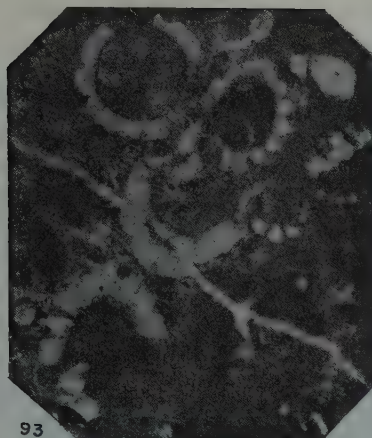


$P_2 \rightarrow$

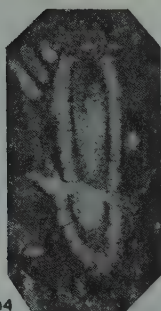
$\sim c$



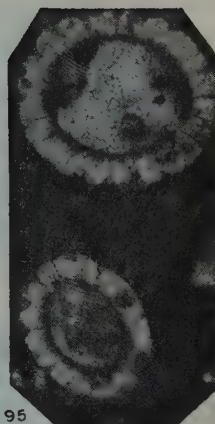




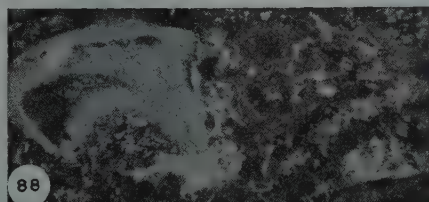
93



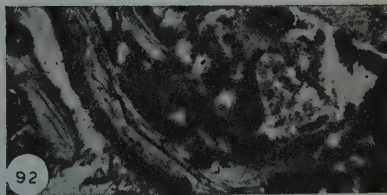
94



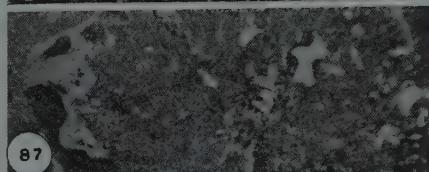
95



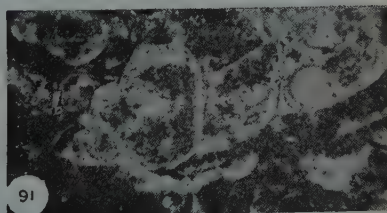
88



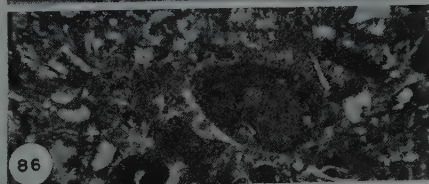
92



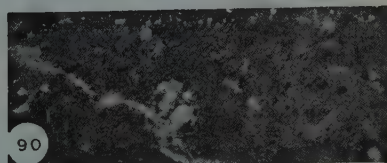
87



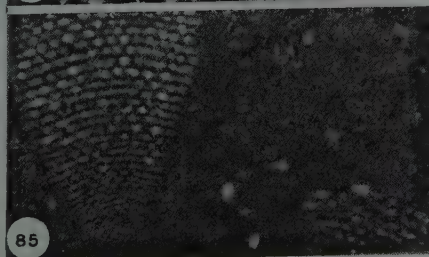
91



86

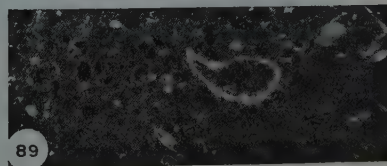


90

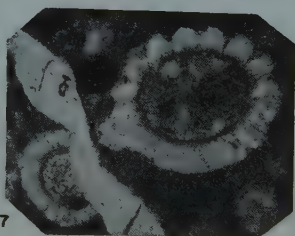
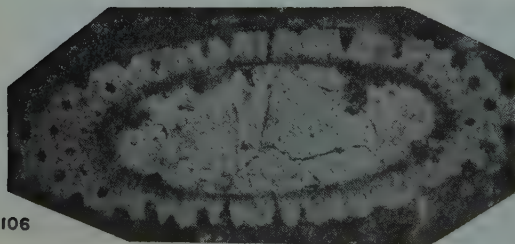
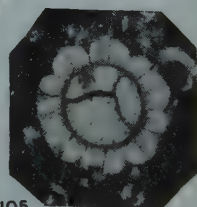
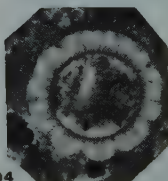
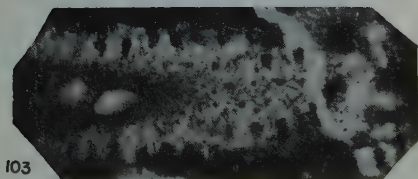
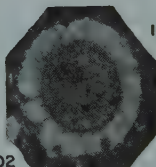
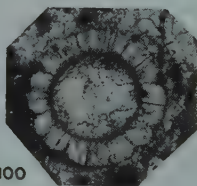
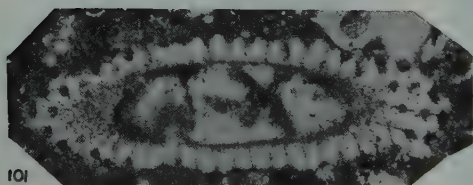
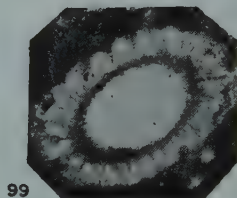
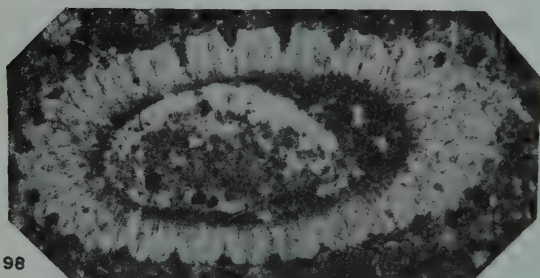
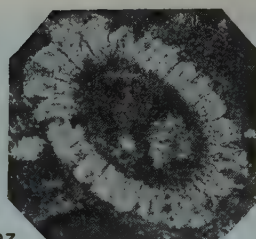
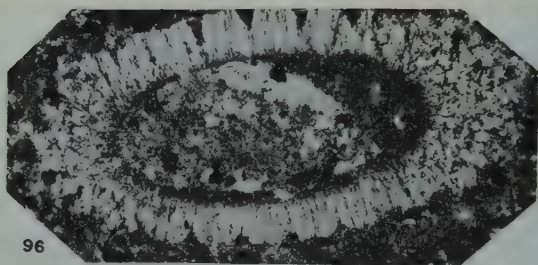


85

← I



89



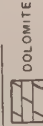
GENERALIZED COMPOSITE SECTION OF THE LOWER CRETACEOUS OF GALILEE*

STRATIGRAPHY				METERS (maximum thicknesses)	LITHOLOGIC COLUMN	POSITION OF FIGURED SAMPLES (figs. Nr.)
SYSTEM	PRESENT PAPER		OTHER AUTHORS			
	SERIES	STAGES	LITHOLOGICAL UNITS	STAGES	UNITS	
C R E T A C E O U S	UPPER CRETAC.	LOWER CENOMAN (PART)	UNNAMED	LOWER CENOMAN (PART)	LOWER DOLOMITE (PART)	
		Upper Vraconian		Upper Vraconian	dolom. - marl - series	80 - 86 - 92
	C R E T A C E O U S	Albian	L. Cr. S. IV	Lower Albian	limestone-marl series Kneimicerias layers	72 - 79
						68 - 71
		Upper	L. Cr. S. III c	Lower	Orbitolina - series	62 - 67
						57 - 61
	L O W E R C R E T A C E O U S	Albian	L. Cr. S. III b	Upper	Blanche (cliff "B")	47 - 56
						40 - 46
		Lower	L. Cr. S. III a	Lower Aptian	Oolitic lst. -sst. series (incl. "Mrejjatt-banc")	38 - 39
						33 - 37
		Lower	L. Cr. S. III a	Lower Aptian	Oolitic lst. -sst. series (incl. "Mrejjatt-banc")	30 - 32
						29 - 30
C R E T A C E O U S	UPPER CRETAC.	Lower Cenoman (part)	Unnamed	Lower Cenoman (part)	Lower Dolomite (part)	
		Upper Vraconian		Upper Vraconian	Lower Dolomite (part)	

* AFTER REPORTS BY AND INFORMATION FROM:
U. Golani, A. Nevo, A. Parnes, D. Neev, E. Rosenberg
U. Wurzbürger AND MICRO-PALEONTOLOGICAL WORK
BY THE AUTHOR.

I - Iraqia H - Hensonella

LEGEND.



DOLOMITE



DOLOMITIC
LIMESTONE



LIMESTONE



SHALY, MARLY & FINE
GRAINED LIMESTONES



SHALES, MARLS
& CLAYS



LIGNITE



OOLITIC



IRON-OOBITES
& CONCRETIONS



DETRITIC

WEATHERING PHENOMENA IN THE CRYSTALLINE OF THE SINAI IN THE LIGHT OF CURRENT NOTIONS

ISAAC SCHATNER

The Hebrew University of Jerusalem

ABSTRACT

The current conceptions about weathering tend more and more to discard insolation as the main promoter of the specific processes affecting crystalline rock-surfaces under desert conditions. Instead, the decisive role of hydration is stressed as well as that of the lithological structure, the latter being probably the most important factor conditioning spheroidal weathering and the "domic" exfoliation.

Observations carried out in 1956 in the crystalline high mountain area of the Sinai Peninsula prove conclusively the dependence of granular disintegration upon the availability of moisture, even in minute quantities but recurring at not too prolonged intervals. To an even greater extent this condition seems to be responsible for exfoliation in its various forms. Here too hydration is the dominant effecting process. True spheroidal weathering — unlike the formation of boulders by rounding-off at the corners and edges — appears however to be mainly conditioned by the existence of harder "cores" or nuclei within the granitoid bodies, surrounded by progressively less resistant zones. After a concentric scaling-off which in time markedly decreases in rate, there very frequently remains a thoroughly rounded boulder. It exhibits great resistance to further weathering, particularly because of an incrustation formed on the rock during the subsequent slowing-down of weathering, which some, times almost comes to a standstill. For largest-scale exfoliation by the spalling-off of big-thick, concentrically curved slabs, which greatly affects both the summits of the granitic mountains and the lowermost valley-slopes, unloading must be held responsible (hypogene exfoliation).

The specific form of alveolation termed "tafoni" is very often unrelated to the presence of joints. This and some other lines of evidence seem to indicate a distinct structural predisposition — the counterpart of that which conditions spheroidal weathering.

INTRODUCTION

Few subjects in present day geomorphology exhibit so many differences in fundamental concepts and such a lack of coordination between widely differing notions, as those dealing with the conditions and processes specific to the weathering of magmatic rocks. This applies particularly to the complicated phenomena designated as granular disintegration, scaling-off and exfoliation, as well as some types of alveolation. Most of the studies dealing directly or indirectly with these processes still employ concepts going back as far as the end of the last century. Few, if any reservations are made as to their validity, although this attitude been lately strongly impugned by an increasing number of field observations and by laboratory experiments. A mostly chronological review of the current notions (up to 1957) is given by Gentilli (1950), while a much more detailed and up to date one is implicitly

given in the comprehensive treatise of Wilhelmy (1958). So far these phenomena have been investigated in very few regions, and mostly dealt with only in the context of the macromorphology of the area under consideration. One of the regions where more extensive observations concerning desert weathering were made, was the Sinai Peninsula (Ball 1916, Hume 1925, Walther 1924) and the conclusions arrived at considerably influenced the general concepts on this subject in the first three decades of the present century. The current concepts, pertinent to this study of weathering phenomena in the Crystalline of Sinai and condensed to their essentials run as follows:

The theory of insolation

Up to the thirties of the present century granular disintegration, scaling-off, exfoliation and to some extent the formation of certain types of alveoli, particularly "tafoni" were thought to be the result of mechanical or physical weathering and specifically characteristic of dry desert conditions. It was assumed that they were primarily a result of insolation, which builds up on the bare rock surfaces minute but ever-recurring stresses due to high temperatures during the day and contractional stresses due to the sharp drop of temperature at night. Similar but far intenser effects were attributed to the wetting and subsequent cooling of the exposed rock surface following a downpour after a rainless period which might have lasted several years.

The preconditions underlying granular disintegration were assumed to be as follows: (a) The polyminerality of the crystalline rock, in which each constituting mineral has a different expansional and contractional coefficient. (b) The polychromacy of these constituents, with the result that the darker and more opaque minerals would by proportionately greater heat-absorption become more affected than the light-coloured ones (selective insolation). (c) The "disorder" in texture, i.e. the fact that the different minerals in a magmatic rock border each other at all possible facets and angles or are even intergrown. All this, together with the different coefficients of expansion of any mineral along its different axes was thought to produce considerable additional and cumulative stresses resulting in cracking and rupture of the surface and finally isolation of the individual minerals. Consequently the rock surface undergoes the process of complete detachment from the rock body (Vergrusung, arénisation) to form the coarse-grained sand detritus embedding the rock base or being carried away from it by various agencies.

Insolation was also regarded as the main cause underlying the scaling-off and exfoliation (including spheroidal weathering). For this the low conductivity of rock bodies was held responsible. As the temperature of only a few centimetres depth of the rock surface was raised sufficiently to set up the conjectural critical stresses, it was assumed as certain that between the intensely heated and expanding, cooled and contracting surface and the inner rock body there develop planes or zones of weakness parallel or sub-parallel to the insulated surface. As a consequence

of the progressive loosening of the surface, scaling-off of concentric curved spalls sets in, greatly aided by the cracks which criss-cross the surface.

The various forms of rock-split (Kernsprung) were also regarded as a result of insolation as well as some specific forms of alveolar weathering-out, although both decomposition and aeolic corrasion were assumed to participate in the genesis of the latter.

At about the thirties of the present century, insolation as the only or even the main cause of the processes enumerated above began to be questioned. Tarr (1915), Blackwelder (1953), and Griggs (1936) proved by laboratory experiments that heating and cooling of granites and associated rocks even within a higher range of temperatures than those endured by rocks in their natural environment do not in themselves produce the effects hitherto taken for granted. It was however pointed out by them and many others who disputed the role of insolation, that the time factor, involving innumerable repetitions of building up of stresses, could not adequately be brought to bear under laboratory conditions, nor could all the other indefinite factors now included in the term "rock fatigue".

Further doubts concerning the validity of insolation as the main factor in exfoliation arose with the observation that this process is perhaps even more effective in climatic zones fundamentally different from the arid ones and is inter alia the main cause for the slope-retreats and slope relieving of the peculiar mountain forms variously designated as "sugar-loaves", bell-shaped hills, cupolas (Helmberg) and others so characteristic of the Inselberge-landscapes of the savannah — and tropical-wet climates, where the diurnal range of rock-surface temperatures is considerably less than in arid conditions.

Another setback for the theory of insolation proved to be the fact that spheroidal weathering frequently occurs on rocks unexposed to the sun and may go on under a debris cover of 10 metres or more. Hence other conditioning factors and effecting processes were suggested as the main determining causes; first and foremost, latent primary structures within the rock responsible for the formation of specific directional joint-planes, and hydration, the chief weathering effecting process.

STRUCTURAL THEORIES

The conception that the internal structure of some types of magmatic rocks is the prime conditioning factor has found expression in two different theories, one known as the theory of hypogene exfoliation and a second which will be termed here "the theory of core structures".

The theory of hypogene exfoliation

This theory as put forward by Farmin (1937) holds as the basic premise, that with "unloading" by denudation, magmatic bodies hitherto overlain by and under enormous pressure from masses of other rocks undergo expansional adjustments to subaerial or near surface conditions. These adjustments involve the formation of potential or even latent joint-planes that later may come into being near the surface.

These joint planes must naturally reflect the subaerial surface configuration of the rock body. Hence they will be parallel and sub-parallel to the surface of an exposed block and will exhibit curvature conforming both to the primary shape of the magmatic block and to its exposed surface. When exposed to atmospheric agencies exfoliation will set in with the curved joints acting as primarily both directing and limiting zones. The theory of hypogene exfoliation is now generally accepted as the most probable explanation for the spalling-off of shells whose thickness may amount to many decimetres, and for the peculiar convex profile of the hill-forms mentioned above and their pronounced parallel retreating. Hypogene structures caused by unloading cannot however be regarded as a main conditioning factor of all the forms of exfoliation, particularly not of those involving spheroidal weathering as postulated by Farmin.

The theory of core structures

The "core hypothesis" is based on the assumption already put forward by Salomon (1926) that solidification in a magma does not proceed uniformly, but sets in earlier at some points than at others. It follows that there is formed within some kinds of magmatic rocks an arrangement of "nuclei" or cores of denser texture or of other properties relevant to their morphological behaviour when exposed to the atmospheric agencies. These round to oval-shaped cores are surrounded by zones of gradually weaker rock, separated from one another by curved planes, possibly of isothermal origin, which under subaerial to near surface conditions turn from potential or latent planes to actual ones, decisively conditioning the exfoliation and especially the kind termed spheroidal weathering. At present the "core hypothesis" seems to be gaining ground in current geomorphological thinking as the most adequate explanation of certain minor exfoliation and scaling-off phenomena (Chapman 1958, Ruxton and Berry 1957, Panzer 1954, Wilhelmy 1958).

HYDRATION

The probability that the complex chemico-physical processes included in the term "hydration" are the main cause of granular disintegration has already been assumed by Merrill (1895), Brenner (1896) and Dana (1896). Much later this process was also claimed to be mainly responsible for exfoliation, after the role of the peculiar joints within the magmatic rock bodies became evident.

Special importance was attributed by Mortensen (1950) to the wedge-work of salts (Salzsprengung). According to this, many salts crystallize out anhydrically, or almost so, in arid conditions, in the minute interstices and cracks of the rock surface. Even if they do contain some water of crystallization it becomes subject to evaporation. As soon as moisture becomes available it is rapidly absorbed in relatively large amounts by the salt minerals and causes an increase in their volume. The water also becomes a decisive stimulus in the crystallization of minerals in their first stages by re-initiation of their solution supply. This process — a variety of hydration — ever recurrent over long periods of time is now thought by many

to be mainly responsible for disintegration, and possibly also for scaling-off and associated phenomena in extremely arid regions (Kernwueste after Mortensen) and in regions where moisture is scanty although available from time to time in some form (rainfall, dew, fog) from year to year. It is also maintained, that the considerable rise in temperature connected with the rapid crystallization processes may be of some influence on disintegration.

CURRENT APPLICATIONS

The ways in which these concepts and notions find their application as working premises in current regional geomorphology are very symptomatic. A strong adherence to the insolation theory, modified and unmodified, is almost the rule and where the newer conceptions are applied, there is generally a tendency to link them in some way to the insolation theory as an important co-factor. Very characteristic is the absence of any distinction between boulders rounded by the weathering-off of their corners and edges and those produced by spheroidal weathering, and the scanty use of the theory of hypogene structures as a prime condition for exfoliation. Lautensach (1950) attributes spalling-off of thick convex shells in Korea and in the Iberian Peninsula (Dwa-Cfa and Csa-Csb, respectively, after the Koeppen system) to seasonal differences in temperature; he does the same for all the minor scaling-off phenomena. Klaer (1956) explains the sheeting-off taking place on slope-surfaces of the crystalline mountains in Corsica as a consequence of the large diurnal differences in temperature. The same explanation is applied by him to the tafoni cavities. According to Chapman and Greenfield (1949) the origin of the rounded boulders lies in the development of joint-planes along which blocks are separated from each other and eventually detached from the main rock body. The boulders however are supposed to have been originally angular blocks bordered by joints intersecting each other at right angles. Their corners and edges are subject to the most intensive weathering, being the meeting-point or meeting-lines of two or three joint faces. Consequently they are blunted-off and the block gradually attains the form of a rounded boulder which then disintegrates by spalling-off or in time completely crumbles into grus. Whether the former or the latter becomes the main process of disintegration depends, according to Chapman and Greenfield (1949, p. 417), only upon the general "cohesive strength between the mineral constituents of the rocks".

The "Salzsprengung", generally acknowledged as a very plausible and important factor has not yet been properly investigated as an agent conditioning weathering processes in deserts other than those of South America — dealt with by Mortensen (1950) — and of Central Sahara. (Meckelein 1959)

WEATHERING PHENOMENA IN THE CRYSTALLINE OF THE SINAI PENINSULA

In 1956 in the course of a ten days' stay at the Monastery of Sainte Catherine with the expedition of the Hebrew University, the adjacent area was investigated especially with regard to its weathering phenomena. The investigation was then

extended — although in a more cursory fashion — to Wadi Ba'aba and Wadi Mokateb the noted "Valley of rock-inscriptions". In the first-mentioned valley large-scale exfoliation in the granitic masses and tafoni in the sandstones is outstandingly developed; in the second the effect of weathering upon very old inscriptions was the main objective. All these phenomena, however, are also present in the area surrounding the monastery and here they were more thoroughly examined.

The area and its basic physiography

The monastery at the head of the ed-Deir valley and the adjacent plain e-Raha lies about 1500 metres above sea-level and forms the base-level of the Gebel Musa Massif whose peak attains a height of 2285 m. About 6 km SW the highest mountain of Sinai, Gebel Catherine (2637 m), terminates the area more thoroughly examined.

Both massifs are very effective precipitation intakers and greatly influence the moisture conditions of their local base-levels. The lithological conditions prevailing in the area under closer consideration are extremely diversified as is generally true in all the Crystalline of the peninsula. Granites make up most of the surface rock with a strong preponderance of the well known coarse-grained, "pink" Sinai granite. The red granites, of finer grain-grading, cover much smaller areas, but are morphologically of greatest importance owing to their relative homogeneity and greater resistance to weathering. In the vicinity of the monastery dikes are not very frequent, especially in comparison with the Wadi Feiran to the west and some other adjacent "dike countries".

The Sinai High Mountains with Mount Saint Catherine as their topographical centre form a climatic province of their own within the Sinai Peninsula. As a corollary to this, weathering phenomena to be observed here do not at all or at least not in a similar intensity occur in other more arid parts of the peninsula, even where the lithological conditions are very much alike. It is not only the relatively high amount of precipitation which the huge and high massifs receive, but also the important fact stressed by Awad (1951) that a considerable part of the precipitation comes down in the form of snow. This implies longer surface contact with moisture, delayed run-off and far more favourable infiltration possibilities than under regular desert conditions where rains are the predominant form of precipitation.

There are no long-range measurements of precipitation in High Sinai — those available were recorded in the observatory of Gebel Catherine and cover a period of only 3 years: 1935–1937 (ref. 17). According to these measurements the mean yearly precipitation was 62mm. The average number of days per year of precipitation, of such great importance especially in an arid region, was as follows: About 11 days with an amount less than 0.1mm and 10 days with precipitation exceeding 1.0 mm per diem, implying as usual heavy downpours within very short times measured in minutes. Consequently, there exists considerable run-off channelling on the slopes of the High Massifs, although the generally very shallow channels are only partly products of erosion, preconditioned as they are either by joints or by weathered-out



Figure 1

Joint conditioned sub-surface channeling in intensely disintegrating coarse-grained granite (slope base of Gebel Musa).

dikes mostly of basic rocks or by both. Where joint-sequences determine the course of the channels, the latter very frequently form short sub-surface passages, but only in the coarse-grained granite (Figure 1). Weathering-out seems primarily responsible for these sub-surface channel-parts, with corrosive erosion playing only a subsidiary role. There do not exist any data on dew in this region, but only some indirect evidence; the intensity of weathering, the widely distributed duri-crusts covering virtually any surface of some rock-types — indicate relatively heavy and frequent dew fall.

Far more conspicuous is the presence of relatively abundant and persistent ground-moisture and particularly of ground-water which feeds several springs and wells both in the vicinity of the monastery and in the adjacent valleys, particularly that of Wadi Feiran, rendering the latter the biggest oasis of the mountaineous Sinai. Another widely-distributed indicator is the surprisingly abundant bush vegetation not only on the water-retaining alluvial fill in the valleys but also in the e-Raha plain and on the lower slopes of mountains. In the sub-summit region from 2000m upwards, vegetational cover again becomes relatively considerable. All this implies not only larger amounts of moisture, but also longer periods of their availability and explains why both the High Massifs themselves and their base-plains and valley-grounds exhibit weathering phenomena not to be found elsewhere in Sinai, neither with regard to intensity nor with regard to the presence of almost all possible forms specific to desert environment, except those found in the extremely arid areas, and mainly due to salt weathering.

Granular disintegration

In the area under consideration granular disintegration is encountered in every place where the "pink" Sinai granite with its large crystals of feldspar and abundant biotite-content forms the rock-surface. There is however a marked difference in the intensity of disintegration depending on the following conditions:

- (a) Free standing rock-bodies exhibit the most intensive granular disintegration surfaces.
- (b) The nearer the rock surface is to the valley-floor or to that of some of the broader plains at the foot of the mountains, the more intensive is the disintegration and conversely.

For this the following causes seem to be responsible:

The greater availability of moisture nearer the valley floors. Here the moisture is conserved for longer periods because of the lesser exposure of the slope-bases and the adjacent ground to winds that promote evaporation. Here also the quantity of moisture supplied by run-off is greater due to slope-wash concentration and stays longer in the detritus cover than on steep, relatively smooth upper slopes where run-off is very rapid. Dew formation too seems highly favoured on lower ground, one of the main causes being temperature inversion.

- (c) It can be observed everywhere that granular disintegration proceeds far more rapidly and affects rocks to greater depth on blocks and slopes *not* exposed to the strongest and longest insolation. The reverse seems to be the rule. The most intensive disintegration is found on block and slope surfaces facing North and West, the dominant directions of the rain-bringing winds, whereas the surfaces facing South are only rarely affected by disintegration of similar intensity.
- (d) Blocks and slope-parts that are shaded, generally exhibit more intensive granular disintegration than those lacking shade or shaded for shorter periods of the day.
- (e) Where boulders and slope-faces are embedded in grus, the surfaces in contact with the detritus are generally more affected by disintegration than those above the grus matrix. The higher the surface above the detritus, the smaller the disintegration and vice versa. Investigations of the lower portions of the rock buried by detritus clearly indicate that disintegration continues in these portions at a similar undiminished rate and intensity or even somewhat more rapidly.
- (f) Low boulders are subject to most intensive disintegration. The dependence of weathering on moisture is illustrated by the fact that the granular disintegration very strongly affects those edges of the boulder that are in contact with the ground and thus generally unexposed to insolation (Figure 2). The most intensive disintegration, however, goes on in boulders which are subject at the same time to spheroidal weathering. Whereas on other rock-bodies the depth to which disintegration affects the rock amounts to a few centimetres and gradually decreases, in the boulders affected by spheroidal weathering the weathering-zone usually attains a greater depth. Moreover, the process of "storied" disintegration occurs, naturally i.e. granulation proceeding from each concentric exfoliation plane,



Figure 2

Intensely disintegrating granite boulder of "loaf" shape horizontally and vertically sub-jointed. (Slope facing the monastery from the NW)

so that each spalling-off segment, which may even attain a thickness of as much as 10cm, usually still contains in its middle portion rock-substance little or not at all affected by disintegration.

- (g) Both the rock surface, which underwent most thorough and deep-reaching disintegration, and the granular detritus accumulated at the base of the rock affected and partly embedding it, are composed of relatively few individual isolated crystals. It is only rarely that individual crystals can be picked up "by hand", as claimed by Leonard (1927). Usually they still form small aggregates, which crumble easily under the least pressure. Their colour is very often not that of the fresh unaffected rock, but a duller greyish hue acquired either by weathering or by a microscopically thin dust-film impregnating them.

Almost no granular disintegration in the strict sense of the term can be observed on the surfaces of the red granite. On the contrary, these surfaces are mostly very smooth and conspicuously varnished by incrustation. Nabatean and other petroglyphs dating back more than 1000 years, cut in some of the rock-faces of red granite, have remained fresh and almost unaffected by weathering. (Figure 6)

Exfoliation

Three forms of exfoliation — in the widest sense of the word — can be distinguished in the area under consideration:

- (a) *Large-scale exfoliation, frequently referred to as "domic" exfoliation.* It involves spalls amounting to several square metres in surface-area and several decimetres in thickness. Their shape very frequently approaches that of an elongated

trapezoid with slightly curved sides converging upward. As far as could be observed, domic exfoliation affects first and foremost slopes built up of harder and more homogeneous rock. It was nowhere to be found on slopes of the coarse-grained "pink" granite, nor where dikes were somewhat more numerous.

Large-scale spalling-off can be observed in two height zones, separated from each other by the whole height of the slope. Many summits are subject to intensive spalling-off and exhibit a typical cupola-form with convex slopes flattening out towards the summit and steepening downslope as in the summit of Sheiq Nebi Saleh, about 12km north of Gebel Musa. Heavy exfoliation involving large spalls occurs also on the lowermost slopes which rise immediately above the valley-bottoms. These spalls are very conspicuous along the Wadi Ba'aba where giant spall-slabs in all stages of detachment from the slope-face clothe the slope-base for some kilometres (Figure 3).

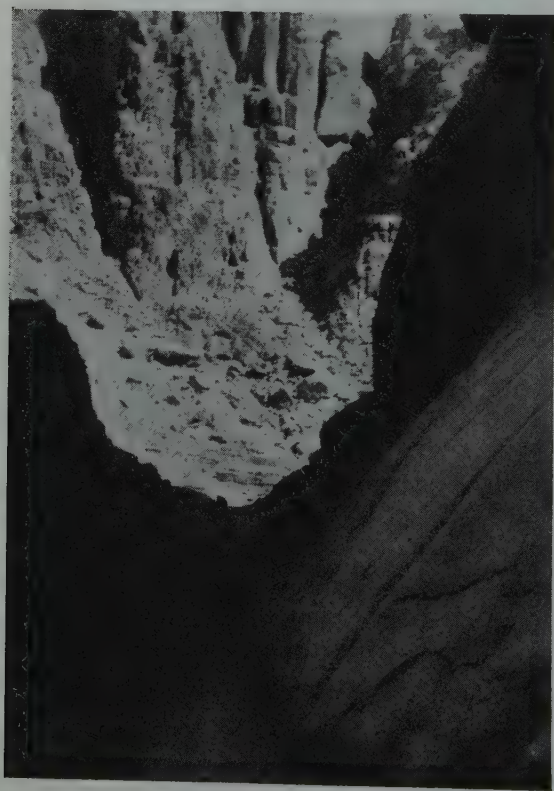


Figure 3
Large scale spalling-off at the northern slope base of Wadi Ba'aba



Figure 4
Spheroidal weathering in coarse-grained granite.

The location of the zones where domitic exfoliation is most strongly developed again demonstrates the part played by increased moisture availability.

(b) *Concentric boulder exfoliation most strikingly and characteristically developed in spheroidal weathering.* This kind of exfoliation is, analogous to the granular disintegration, most frequent and intensive on the lowermost slopes and on isolated blocks strewn over the widenings of the valleys. The external conditions which to all appearance promote spheroidal weathering are much the same as those promoting granular disintegration.

(a) Boulders facing the luv-side are subject to most intensive concentric exfoliation.

(b) It seems that here too the less the blocks are exposed to insolation the more developed is their concentric scaling-off. The positive influence of shade is fairly clear.

(c) On slope-faces and blocks partly or entirely buried under detritus, exfoliation appears to go on just as fast as on the uncovered surface of the rock. In some places it can be seen that the buried part of the rock is more affected by exfoliation than the part in free contact with the air. There can be no explanation for this fact other than that the detritus preserves moisture for longer periods and this, when taken up by the rock, promotes exfoliation there.

(d) In broader valley-floors and in the intramountainous plains (e-Raha etc.) many boulders can be observed which by their shape combined with remnants of exfoliation-shells indicate that they were subject to concentric exfoliation (Figure 5).



Figure 5
Exfoliating core-boulder.

Between those given to spheroidal weathering while still forming part of the slope-face and these free-lying boulders, the chief difference is that the latter are (1) generally bigger than the blocks undergoing spheroidal weathering; (2) they generally consist of more compact rock-material, possibly even of somewhat different petrographic constitution, whereas spheroidal weathering goes on only in coarse-grained granite. It may be assumed that the former represent end-products of exfoliation; harder cores of considerable volume, whose surface subsequently is subject to only minor scaling-off. As against this it seems very probable that even the more compact parts of boulders undergoing spheroidal weathering may eventually in a relatively short time disintegrate completely or leave only small residual bodies, whose resistance to further weathering is equal to that of the big core-boulders.

(3) Scaling-off or more correctly sheeting-off of small, thin pieces of rock surface is noticeable chiefly in rock material that is harder and of finer grain than the "pink" granite. (Figure 6). This kind of scaling-off seems to affect mainly altered rock surfaces including incrustated ones. It is also a characteristic and probably the most important process affecting the inner sides of the tafoni. Here too, great independence from insolation could be observed and much evidence of hydration as the main operating process.

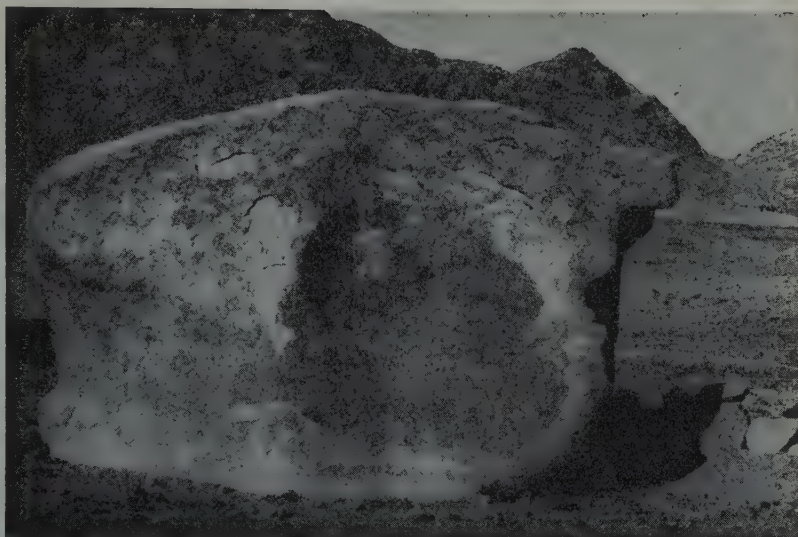


Figure 6

Core boulder, heavily incrustated, sheeting off, with initial concavities whose surfaces are covered by very ancient rock-cut inscriptions. (SE corner of the e-Raha plain)

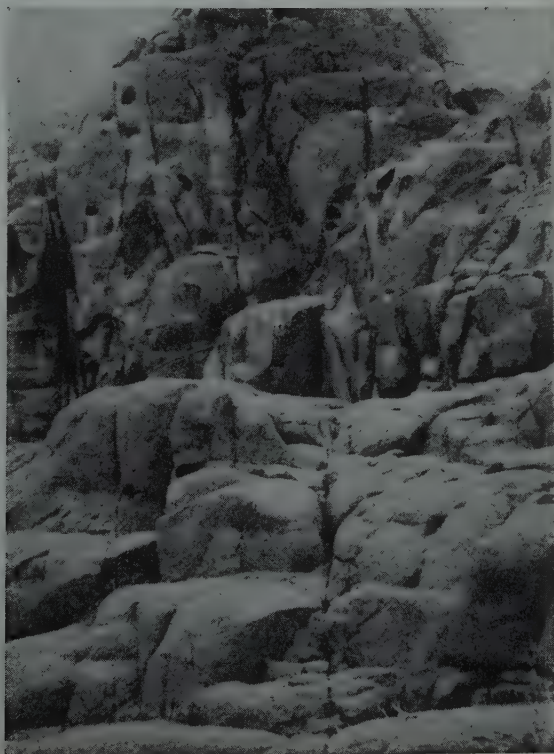


Figure 7

Tafoni formation in the strongly jointed summit region of Gebel Musa.

Jointing

Jointing is extremely well developed everywhere in the Crystalline of Sinai and plays an important and very conspicuous part especially in the evolution of the slopes. The intensity and spacing of the joints depend primarily on the nature of the rock. In the coarse-grained granites the spacing both of the vertical and of the horizontal joint -planes is very close. The distance ratio between the vertical and the horizontal joints generally amounts to 1:0.5–0.6 or even less, i.e. the vertical joint-planes "quarrying-out" a block are at least double the length of the horizontal ones (Figure 7). In other kinds of rock, where the crystals are smaller, the jointing becomes generally more widely spaced. There exists another important difference. The joints in the coarse grained granite open out wider after a relatively short time and penetrate into the rock-body deeper than occurs with other rocks of magmatic origin. (Figure 7). Very characteristic is the influence of dikes upon the jointing. Where "positive" dikes exist, i.e. dikes less susceptible to weathering than the intruded rock, the jointing decreases in frequency and becomes widely spaced, more or less in proportion to the spacing and width of the dikes. That is to say: the nearer the dikes run to each other, the wider spaced are the joints in the rock-face bordered by the dikes and vice versa. Where dikes exist, the direction of the joints, especially of the vertical ones, generally conforms fairly well to that of the "negative" ones, i.e. those formed mostly by basic intrusions and turned by weathering and erosion into channel-like forms rilling the slopes.

Of special interest are the secondary joints. Everywhere in the coarse-grained granite there appear joints diagonally cutting or meeting the vertical ones and running obliquely to the horizontal joints. (Figure 1). Many lines of evidence seem to indicate that these joints develop much later than the main joints, i.e. the vertical and horizontal ones.

Many sub-joints, parallel to the vertical ones are to be seen everywhere in the coarse-grained granite, already taking on the form of elongated boulders with completely blunted corners and separated one from another by older, wide open joints. There can be no doubt that also these sub-joints developed some considerable time after the opening and widening of the former. The secondary joints are mostly very narrow and open only to a limited depth; a third to a half of that of the primary joints. Of particular interest are sub-joints developing sub-parallel to the upper surface of the boulders, halving them as it were and thus giving them a loaf-like appearance (Figure 2). These joints develop on the up-slope part of the boulders, which is also the part most affected by disintegration, however, they do not usually continue towards the lower end of the boulder, but very often peter out midway or in the last third of the boulder. Sub-joints of the sort described could be observed only in boulders given to very intensive granular disintegration.

Where spheroidal weathering develops, the joints become indistinct, less straight and more widely spaced (Figure 7). Very many slope-faces exhibit close-spaced joint-planes above and below the zone of spheroidically weathering-out blocks,

whose extent is generally much greater than the space between the joints mentioned above. This again confirms the assumption that spheroidal weathering develops only where some kind of a harder core exists and not on a simple boulder with blunted-off corners.

The wider spacing of the joints of the rock-faces where spheroidal weathering is developed and the generally curved direction of the joints also seem to indicate that the joint-grid of these parts of the granite developed in some concordance to the spacing of the hard cores, which generally appears to be much wider than that of the joints in the granite lacking the above-mentioned structure.

Rock-splits (Kernsprung)

Rock-splits or cracks are a widely distributed micro-feature of the Crystalline of Sinai. Two main forms can be distinguished:

- a. Splits that occur in relatively large blocks and subdivide them into two or more unequal segments.
- b. Parallel and almost equally spaced cracks which almost invariably affect small boulders of inconsiderable height above the ground. A common characteristic of each form is that it either never occurs in the coarse-grained granite or cannot be here distinguished from joint-planes. They share another characteristic in that all blocks of any size are usually heavily incrustated on their outer surfaces.

Between the two forms of split-cracks there exist some other distinct differences.

A. The split-cracks which occur in the larger blocks are very unevenly spaced. B. Both the line of the crack visible on the surface of the block and the inner crack-surface, curve up and down and at times the former even zigzags in sharp minute angles. The crack surface within the rock is not flat but conchoidally curved up and down. C. The crack faces are generally sub-parallel to the base, but not to the upper surface of the split block (Figure 8).

In contrast, the split cracks occurring in the smaller blocks resting on the ground with broad bases exhibit an extremely regular pattern: a. The splits are generally almost equi-distant. b. They are almost perfectly parallel to each other. c. Their edges are sharp and straight. d. The inside faces, created by the splitting, are almost perfectly flat. e. Some of the cracks are closed by mineralisation. Most frequently the cracks run at an almost right angle to the base face of the blocks.

Rock-splits could be observed only in free-standing blocks fully exposed to insolation or at least in blocks in very loose contact with any other larger rock body. This leaves insolation, and the rock-fatigue created by it, as a most plausible explanation of their genesis.

Splitting-offs of lens-shaped rock-segments on free-standing thoroughly rounded boulders proved very intriguing. Here a marked affinity to curved joint-planes is very suggestive. The further development of both split-off segments and the surfaces created by the split-crack is characteristic of exfoliation, and a common cause and formation may be assumed.

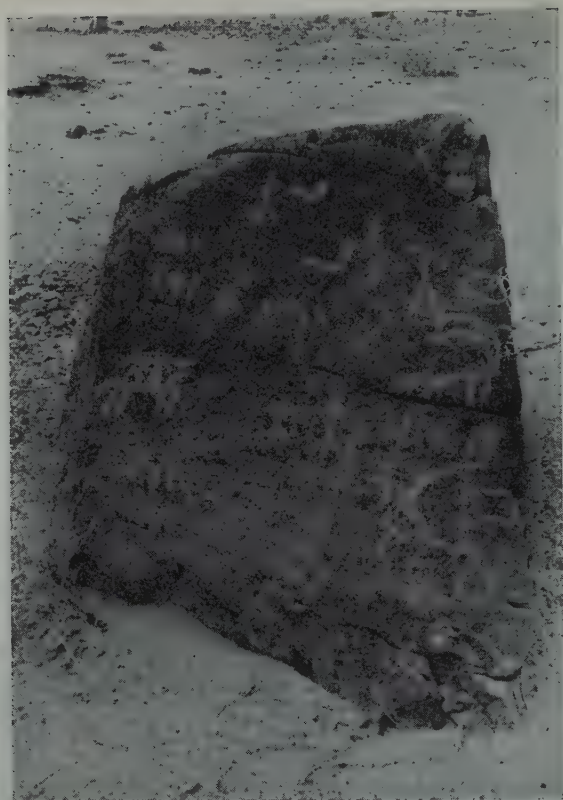


Figure 8

Split-cracking in red granite block covered with ancient rock cut inscriptions. (SE corner of the e-Raha plain).

Alveolation

Alveolation ranging from minute holes (Broeckelloeher) to good-sized cavernous forms — tafoni — is only present in the High Sinai and not in the more arid mountainous parts of the peninsula, except for the areas covered by sandstones, both the “primaire grès” (Awad) and the Nubian sandstones. In the latter these forms are very common, although very different in shape and apparently also in origin from those developed in the granitoids (Figure 9).

That the alveoli, especially the bigger ones, are dependent for their formation upon moisture, seems very probable in view of their location and distribution. They are far more numerous on the luv-sides, and correspondingly rare or absent both in the lower and more arid mountainous regions of the Sinai Peninsula and in parts of the High Sinai where for various reasons moisture is insufficient. Thus,

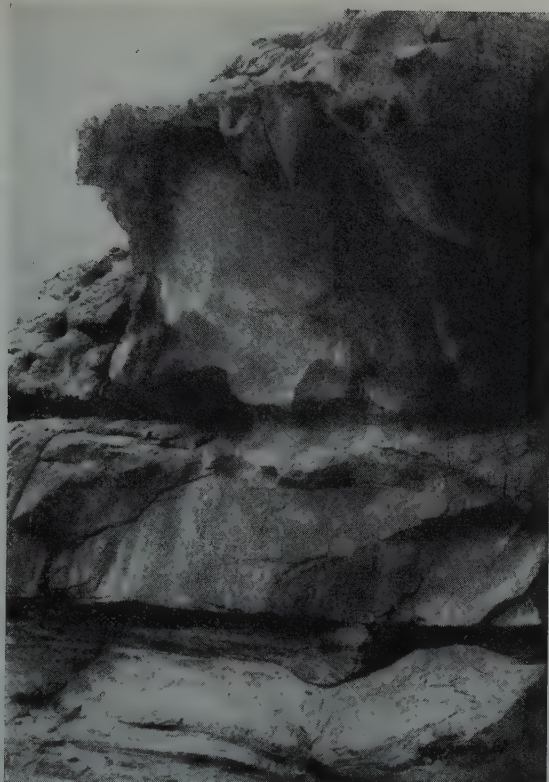


Figure 9

Tafoni in the "primaire grès" on the west side of Wadi Mokateb. At the base, well preserved rock-cut inscriptions.

characteristically the lower slopes of the valleys, both those formed in granite and those formed in sandstone are pockmarked by innumerable small cavities. Bigger ones prevail in the summit region of the High Sinai, in so far as this is built up of granite. Tafoni become here the predominant micro-morphological feature (Figure 7).

It is generally assumed that alveoli, especially the larger type, originate from and are dependent upon joints or at least upon cracks. Actually, there are many hole-formations arranged along major and minor joints and these doubtless represent joint-widenings affected by solution or some other kind of weathering-out at weak spots or at the intersection of joints and cracks. But against this, holes of all sizes, especially bigger ones, can everywhere be observed, having no connection with any visible joint-face and even quite far from any joint-plane. Sometimes this occurs even where joint-planes are very near each other. Here the non-relation between joint-planes and cavities is absolutely manifest (Figure 7).

Hence it may be asked, whether a similar conditioning (in the opposite sense)

does not exist for this kind of phenomena. That is to say that as a counter-part to hard cores there may exist some regular patterns within the granite, i.e. small rock parts with lessened cohesion, representing rock-material interposed between series of hard cores or existing within a granite undifferentiated into cores but nevertheless containing parts of lesser density or homogeneity.

The former suggestion seems confirmed by some direct observations: a. There are many tafoni which to all appearance were initiated by detaching and rolling-down of a core boulder. Not only do the shape and size of these tafoni correspond exactly to the size and curvature of the boulders most frequently found nearby, but in many cases such boulders still exist right down under the cavities which, they most probably created by detaching themselves and rolling down.

b. Another not less conclusive although more indirect indication is supplied by the very form of some bigger core-boulders. Here on two or more sides shallow concavities develop very frequently exhibiting in form great similarity to the typical tafoni in their initial stage (Figure 6). On some boulders the process leading to these concave forms is clearly observable (Figure 10). On the convex surface of the boulder

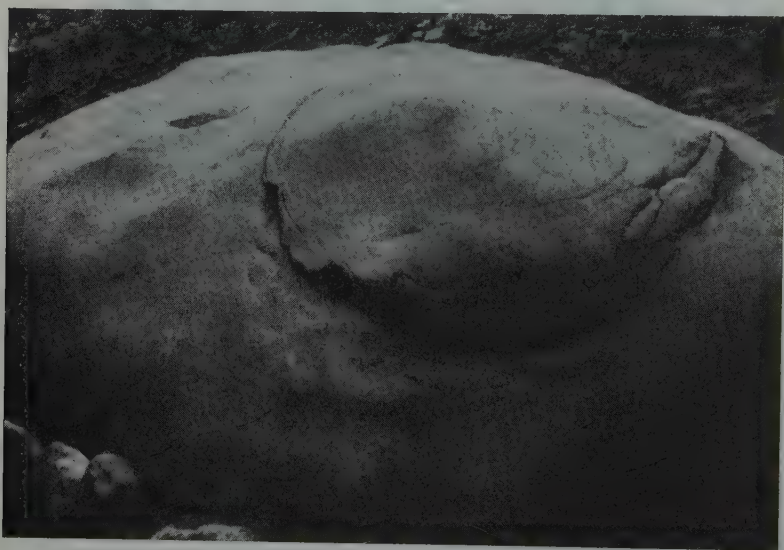


Figure 10

Development of a concave surface in a core boulder by splitting off (?) of a lens-shaped segment. (Vicinity of St. Catherine Monastery).

a curved crack develops, separating and in time detaching a lens-shaped segment from the rock-body. The separated piece undergoes relatively rapid weathering by scaling-off and surface cracking, whereas the concave plane under the lens becomes incrustated and thus almost immunized at least against more rapid rock-decay. On all these concave surfaces, as well as in the tafoni proper, weathering goes on, but

extremely slowly. This can be seen by the almost perfect state of preservation of inscriptions cut in them, some of which date back more than a thousand years (Figure 6). The weathering-out of the concavities and the eventual total disintegration of the separated part leaves a concave scar which, protected as it is by incrustation, nevertheless continues to grow in volume and in depth by small-scale sheeting, which also affects the crust. Very important is the fact that the scaled-off sheets are *excentric* with regard to the boulder body, thus almost exactly counterparting the processes leading to the formation of the rounded core-blocks.

The same process is to be observed within true tafoni-forms which, in contrast to the cavities in the sandstones of Sinai with their rectangular forms exhibit mostly oval ones. No support could be found anywhere for the explanation lately put forward by Klaer (1956) that the temperature differences within the tafoni are responsible for the scaling-off of the thin sheets and hence for the growth of the cavities. The tafoni are not subject to such great and rapid changes in temperature as are the rock-surfaces directly exposed to the rays of the sun, nor are they subject to such rapid cooling. Here too, hydration is possibly more effective, owing to the stagnation of the air within the cavities and consequent condensation by cooling at night. This moisture formation as well as water infiltrating from above, must be held responsible for the minute flaking-off.

REFERENCES

1. AWAD, H., 1951, *La montagne du Sinai Central*, Publ. de la Société Royale de Géographie d'Egypte, Le Caire.
2. BALL, J., 1916, *Geography and Geology of West Central Sinai*, Ministry of Finance. Egypt, Cairo.
3. BLACKWELDER, E., 1953, The insolation hypothesis of rock weathering, *Am. Jour. Sc.*, **26**, 97-113.
4. BRANNER, J.C., 1896, Decomposition of rocks in Brasil, *Bull. Geol. Soc. Am.*, **7**, 255-314.
5. CHAPMAN, C.A., 1958, Control of jointing by topography, *Jour. Geol.*, **66**, 552-58.
6. CHAPMAN, R.W. AND GREENFIELD, M.A., 1949, Spheroidal weathering of igneous rocks, *Am. Jour. Sc.*, **247**, 407-429.
7. DANA, J.D., 1896, *Manual of Geology*, 4th ed., Philadelphia, John Wiley, Philadelphia.
8. FARMIN, R., 1937, Hypogene exfoliation in rock masses, *Jour. Geol.*, **45**, 625-635.
9. GENTILI, J., 1950, Rainfall as factor in the weathering of granite, *C.R. Congr. Int. Geogr.*, Lisbonne 1949, II, Lisbonne, 263-269.
10. GRIGGS, D.T., 1936, The factor of fatigue in rock exfoliation, *Jour. Geol.*, **44**, 783-796.
11. HUME, F.W., 1925, *Geology of Egypt*, Vol. I, Cairo.
12. KLAER, W., 1956, Verwitterungsformen im Granit auf Korsika, *Pet. Geogr. Mitt. Ergh.*, **261**, Gotha, Ministry of Finance and Survey, Cairo.
13. LAUTENSACH, H., 1950, Granitische Abtragungsformen auf der Iberischen Halbinsel und in Korea, ein Vergleich, *C.R. Congr. Int. Geogr.*, Lisbonne 1949, II, Lisbonne, 270-296.
14. LEONARD, R.J., 1927, Pedestal rocks resulting from disintegration, *Jour. Geol.*, **35**, 469-474.
15. MERRILL, G.P., 1895, Disintegration of the granitic rocks of the district of Columbia, *Bull. Geol. Soc. Am.*, **6**, 321-333.
16. MECKELIN, W., 1959, Forschungen in der zentralen Sahara, Braunschweig, Westermann Verl. Braunschweig.
17. *Meteorological reports for the years 1935, 1936, 1937*, The Ministry of Public Works, Phys. Dept., Cairo 1941, 1942, 1944.

18. MORTENSEN, H., 1950, Das Gesetz der Wuestenbildung, *Universitas*, **5**, 801-814.
19. PANZER, W., 1954, Verwitterungs- und Abtragungsformen im Granit von Hongkong, *Mortensen Festschrift*, Bremen.
20. RONDEAU, A., 1958, Les "Boules" du granite, *Zschr. f. Geomorph.*, **2**, 211-224
21. RUXTON, B.P. AND BERRY, L., Weathering of granite and associated features in Hong Kong, *Bull. Geol. Soc. Am.*, **68**, 1263-1292.
22. SALOMON, W., 1926, Kugelfoermige Absonderungen, *Sitzber. Heidelberger Akad. d. Wiss. Math. — Nat. Kl.* 11. Abh., Berlin-Leipzig, 1-7.
23. TARR, W.A., 1915, A study of some heating tests and the light they throw on the disintegration of granite, *Econ. Geol.*, **10**, 348-367.
24. WALTHER, J., 1924, *Das Gesetz der Wuestenbildung*, 4. Aufl. Leipzig, Quelle und Meyer, Leipzig.
25. WILHELMY, H., 1958, *Klimamorphologie der Massengesteine*, Braunschweig, Westermann Verl. Braunschweig.

NEW DATA ON THE ARTESIAN AQUIFERS OF THE SOUTHERN DEAD SEA BASIN AND THEIR GEOLOGICAL EVOLUTION.

Z.L. SHIFTAN

Geological Survey of Israel

ABSTRACT

A number of new water wells drilled along the western fault escarpment of the Dead Sea Rift have resulted in additional proof of the importance of the Nubian Sandstone as an aquifer in Southern Israel. The water is under artesian pressure. It is slightly saline. The concentration and chemical character of the water of this aquifer are modified by dilution with fresh water or by addition of salt, on passage from the Nubian Sandstone into dolomites of the mountain formations or into the Lisan formation of the Dead Sea Basin. The origin of this water is probably connected with the early stages of the Samra-Lissan Lake.

INTRODUCTION

The occurrence of an artesian aquifer in the southern Dead Sea Basin and its relation to other, — also artesian, — aquifers found near the western fault escarpment were described in an earlier paper (Shiftan 1958). Since that time additional information has become available, through the drilling of a number of deep water wells at the foot of the mountains bordering the Dead Sea Valley in the West. Most of the earlier conclusions regarding the occurrence of underground water, the character of the salinity and the hydrological conditions have been confirmed, but some of them have now to be revised, and a more complete picture of the underground water regime and its geological evolution can be obtained.

In particular, the importance of the so called "Nubian Sandstone" (this term being used here for the mainly Lower Cretaceous sandstone sequence, also known as Kurnb Sandstone, see ref. 7), as an underground water reservoir has been proved by two of the new wells, in addition to the oil prospecting well (Mazal No. 1) described earlier (Shiftan 1958). The potential importance of the Nubian Sandstone as an aquifer in Israel was mentioned by Picard (1953), and underground water was known since 1952, to exist in this formation, under phreatic conditions, in the Southern Arava. The Sdom region, however, is the first in Israel where water from the Nubian Sandstone is actually exploited directly, and also indirectly, i.e., from other aquifers replenished mostly from the Nubian Sandstone. The 3000 m³/hr. available today are used by the Dead Sea Works for washing the evaporation pans and for other industrial purposes.

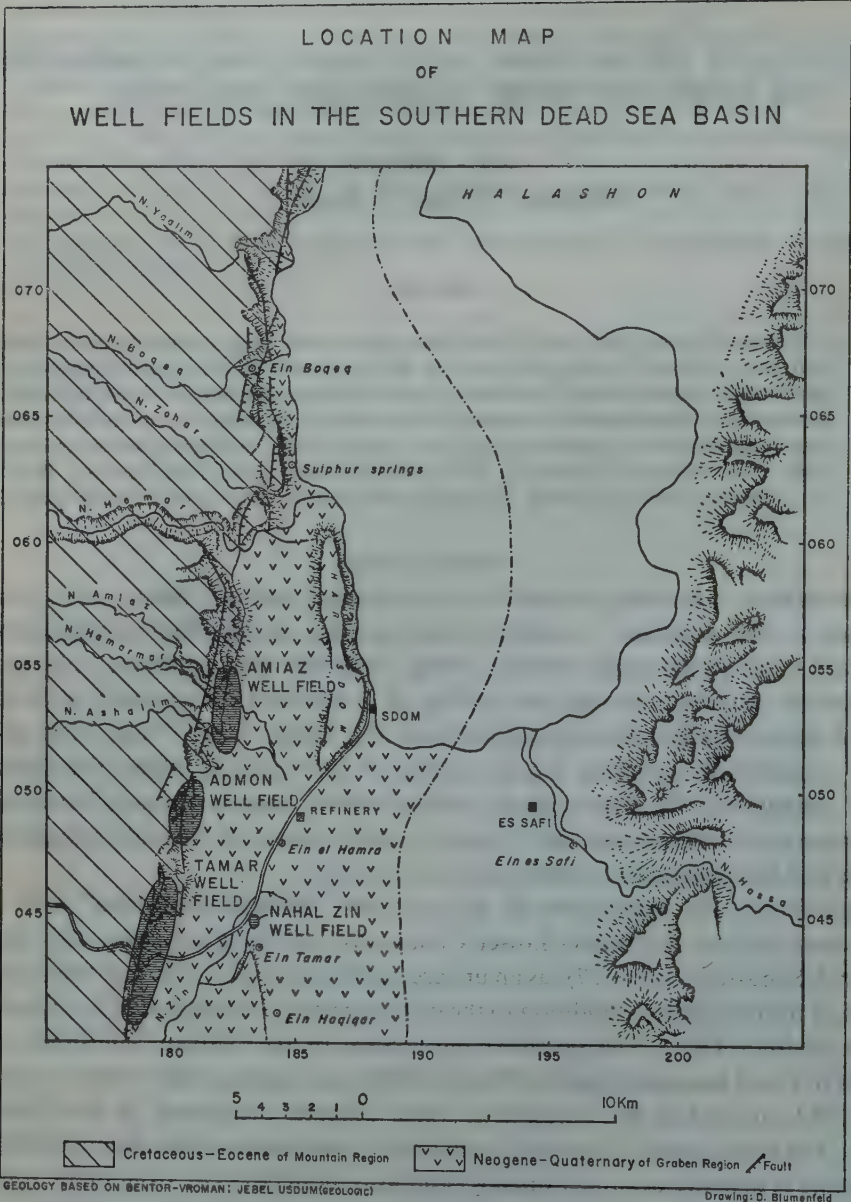


Figure 1

GEOLOGICAL AND HYDROLOGICAL DATA FROM THE NEW WELLS

All the new wells have been drilled very close to the fault escarpment bordering the Dead Sea Rift on the West. Ten wells have been completed and three are still being drilled. The wells are located in three fields (Figure 1):

1. The Tamar well field
2. The Admon well field
3. The Ami'az well field.

An attempt to correlate the geological logs of these wells with the sections by Bentor and Vroman (1960) is made in Figure 2. Not in all cases has a satisfactory correlation been obtained, probably because of the special geological conditions in the fault zone, changes in facies and thickness of formations between distant areas and possibly also due to the limited reliability of the drill samples. All wells are located on, or very near, outcrops of various Cenomanian formations.

The Tamar well field

This field is situated approximately 10 km south-southwest of the potash plant of the Dead Sea Works, where the Sdom highway passes from the Negev mountains into the Dead Sea Valley. It comprises 7 wells:

1. Mazal No. 1 (the oil prospecting well described in an earlier paper (Shiftan 1958))
2. Tamar No. 1
3. Tamar No. 3 (see ref. 6)
4. Tamar No. 4
5. Tamar No. 5
6. Tamar No. 6 (not yet completed)
7. Tamar No. 7 (not yet completed)

After water was struck in the oil prospecting well Mazal No. 1, an attempt was made to obtain a supply of underground water by drilling a well in the same geological situation, at a slightly lower elevation, near the highway, in order to make full use of the artesian pressure. This well, drilled by Water Planning Inc. had to be abandoned because of a strong inflow of asphalt from fissures into the well at a depth of 28–38 m which was continually clogging the drilling tools (Shiftan 1958). Later, a new well was brought down at the same location by the Dead Sea Works, which also drilled all the other new wells in the area. This well, named Tamar No. 1*, reached a depth of 246m, after overcoming the difficulties caused by asphalt seepages at 64–68m depth. Notwithstanding the mainly dolomitic character of the section bailing tests proved that no water in quantity could be supplied by this well. The clogging of fissures by asphalt was assumed to be the reason.

* Although the location for a well named Tamar No. 2 has been fixed no well has been drilled there so far.

The next well, Tamar No. 3, was located at the foot of the cliff forming the main fault escarpment south of the Sdom highway, in order to find out whether the occurrence of asphalt in the fissures of the dolomite is confined to the Mazal fault block, or is a regional feature. Water was struck here in the lower beds of the dolomite of unit c5, at a depth of 33m. No asphalt was encountered. The water table dropped slightly while drilling progressed, and came to rest finally at 28.6m depth, corresponding to -255m M.S.L. The total depth of the well is 76m. While pumping 300m³/hr. the drawdown increased steadily to 9.05m. At the same time a slight increase in salinity occurred, from 733mg Cl/1 to 800mg Cl/1. When the rate of pumping was reduced to 250m³/hr. the drawdown was 7.62m, and on further reduction of pumping to 200 m³/hr. it became 5.50m. The temperature of the water was 38°C.

The next two wells drilled in the Tamar field, Tamar No. 4 and No. 5, proved that even under extremely similar structural conditions a given layer may show rather different degrees of fissuring. Tamar No. 4 was drilled some 300m south of Tamar No. 3, also at the foot of the main fault escarpment. Here, however, no water in quantity was found in the dolomite of unit c5, and the well was deepened into the dolomite of unit c3, to a total depth of 200m.

The first water appeared at a depth of 45m, rising to 38.80m (= -255.80 M.S.L.). A slight additional rise of the water table occurred at 156m depth, after passing a 3m thick clay bed. At 176m depth, the water table rose to 37.50m (= -254.50 M.S.L.). The pumping test resulted in 150 m³/hr. with a drawdown of 4.20m, 250m³/hr. and 290 m³/hr. with a 7.50 and 9.60m drawdown respectively. A very slight drop was noted in the resting water table of Tamar No. 3, but when the rate of pumping was stepped up to 290 m³/hr. a slight rise (!) in the original level of Tamar No. 3 was recorded.

Tamar No. 5, situated approximately 800m south of Tamar No. 4, failed to produce satisfactory yields even when deepened into the dolomite unit c3. The 130m³/hr. pumped from the (upper) dolomite unit c5 were considered unsatisfactory. There was no notable increase in yield within the (lower) dolomite unit c3, but water started flowing from the well when (Nubian) sandstones were struck at a depth of 275-280m. The well was deepened to its final depth by a rotary rig (10").

The initial rate of flow was 280m³/hr. dropping after some time to 210m³/hr. and then remaining steady. On shutting off this flow, a pressure of 5-5.5 atmospheres was measured, bringing the calculated hydrostatic level of this confined aquifer to -185m M.S.L. The temperature of the water was 42°C.

While drilling this well, the (upper) dolomite c5 aquifer was carefully separated from the Nubian Sandstone aquifer. When the 10" casing was cut at 90m depth, after completion of drilling operations, the artesian flow from the sandstone was absorbed by the dolomite aquifer, bringing about a 11m rise in the water level. With the installation of the pump this connection was cut by the insertion of rubber rings, and the artesian flow returned in full. The water level in the dolomite went

down again to the original level. With the present installation* it is possible to use either the artesian flow alone, or to pump both aquifers by lifting the pump slightly above the separating rubber rings.

At present, two more wells are being drilled, Tamar No. 6 and No. 7. Tamar No. 6 is located in a ravine west of Mazal No. 1, and is to be another attempt to investigate the possibilities of practical exploitation of the water found in the Mazal oil well. Although some asphalt was met here, as in Tamar No. 1, bailing tests indicate that there is reason to expect successful results.**

Tamar No. 7, situated north of the Mazal block aims at investigating the hydrogeological conditions in this structurally more complicated section.

The hydrostatic levels of the Tamar well field, for the three separate aquifers, are compared in Table I.

TABLE I

Hydrostatic levels of the three aquifers in the Tamar well field, (abs. elevation in meters, M.S.L.)

aquifer		Mazal 1	Tamar 1	Tamar 3	Tamar 4	Tamar 5	Tamar 6	Tamar 7
dolomite	c5	—	- 362*	- 255	- 258	- 267	- 279	- 287
"	c3	- 273	—	—	- 255	- 261	- 269	- 270
Nub. Sst.	1k	- 185	—	—	—	- 185	—	—

* static water

2. The Admon well field.

After the successful completion of the first Tamar wells, testing of underground water conditions in other sections along the main fault escarpment started. The first area selected was the so called "Red Sand Wadi" (Nahal Admon), named after the red colour of the rocks of the Hatseva formation cropping out near the cliff on the downthrown side of the fault. Two wells have been completed there.

Admon No. 1 is 143m deep. Water was struck first at a depth of 46m, rising to 39m from the surface (-279m M.S.L.). From 102.50m downwards, practically all the cuttings disappeared, indicating extremely strong fissuring of the rock. On reaching 102m depth, water started to flow from the well, but this flow ceased after a few hours, and the water level came to rest at 3.45m from the surface (-243.45m M.S.L.). At the depth of 112.50m a bailing test was made. After bailing out 200m³, well rounded fluvatile gravels were found in the well. When 540m³/hr. were pumped, the water level dropped steadily during 8 hours, to 20m from the surface. When pumping was discontinued, the level returned to 4.80m. This test lasted 15 days.

* This installation was designed and constructed by I. Alnir, consulting engineer in charge of drilling operations for the Dead Sea Works Ltd.

** Note added in proof: Since then 250m³/hr have been pumped with a drawdown of approximately 1.20m from the c5 aquifer, and artesian flow started at 140m depth (c3).

Continuing the pumping test, $420\text{m}^3/\text{hr.}$, were pumped around the clock, bringing the level gradually down to 27m, with a daily drop of 25–30cm during the last days. 8 days after the test, the level had returned to 4.43m from the surface. The temperature of the water was 34°C .

Admon No. 2 is situated in an analogous geological position some 800m north of Admon No. 1. After drilling with a percussion rig to a depth of 244m, the well was deepened by a rotary rig (10") to 295m. Apart from Tamar No. 5 and Mazal No. 1 it is the only well so far to have reached the Nubian Sandstone in the Sdom region proper.

Water was first struck at 90m depth, and the water level rose gradually. Water started flowing from the well at 260m depth, and a strong and constant flow of $180\text{m}^3/\text{hr.}$ was found at 290m depth.

The Ami'az well field

In the continuation of the main fault escarpment north of the Admon field and under similar structural and stratigraphic conditions, two more wells have been drilled and a third one is being drilled. This well field is situated near Naqb-el-Am'az (Nahal Ami'az).

Ami'az No. 1 met with a perched aquifer, — probably still in the c5-dolomite, — at an elevation of -282m M.S.L. The water was unusually fresh, but no practically exploitable yield could be proved. A second aquifer was found at 60m depth, (-307m M.S.L.), and the water level remained steady at this depth until the well was completed at 105m. in blue clay (probably c4). $250\text{m}^3/\text{hr.}$ were pumped with a drawdown of 30cm only. The static level was found, however, 30cm lower after one week of pumping.

Ami'az No. 2, situated 1km north of Ami'az No. 1 went down to a total depth of 174m, possibly just touching in the last 5m the uppermost beds of c1–c2. The water level was found at 62m depth, and remained practically unchanged (-307m S.L.). A cave, 3m high, was encountered between 92 and 95m depth (in c4?). $450\text{m}^3/\text{hr.}$ were pumped during a test, with a drawdown of approximately 1m.

Ami'az No. 3 is still being drilled. At the present depth of 279m no sufficient supply has been struck yet. The water level was encountered at 97m depth, rising to 76m (-316m M.S.L.). With further progress of drilling the water level continued to rise gradually and reached 70m when the well was 221m deep (-310m S.L.). At this depth, in sandy shales of unit c1, a sudden rise occurred to 64m (-304m M.S.L.).*

Comparison of static levels and yields from the various aquifers

As shown in Table I there is good agreement between the static level of the Nubian Sandstone aquifer of Mazal No. 1 and Tamar No. 5, in spite of the fault line separating the two wells. The pressure at Admon No. 2 brings the hydrostatic head to -156m M.S.L. , approximately 30m higher than in Tamar No. 5.

* Note added in proof: A further rise was observed in the Nubian Sandstone at 279m depth.

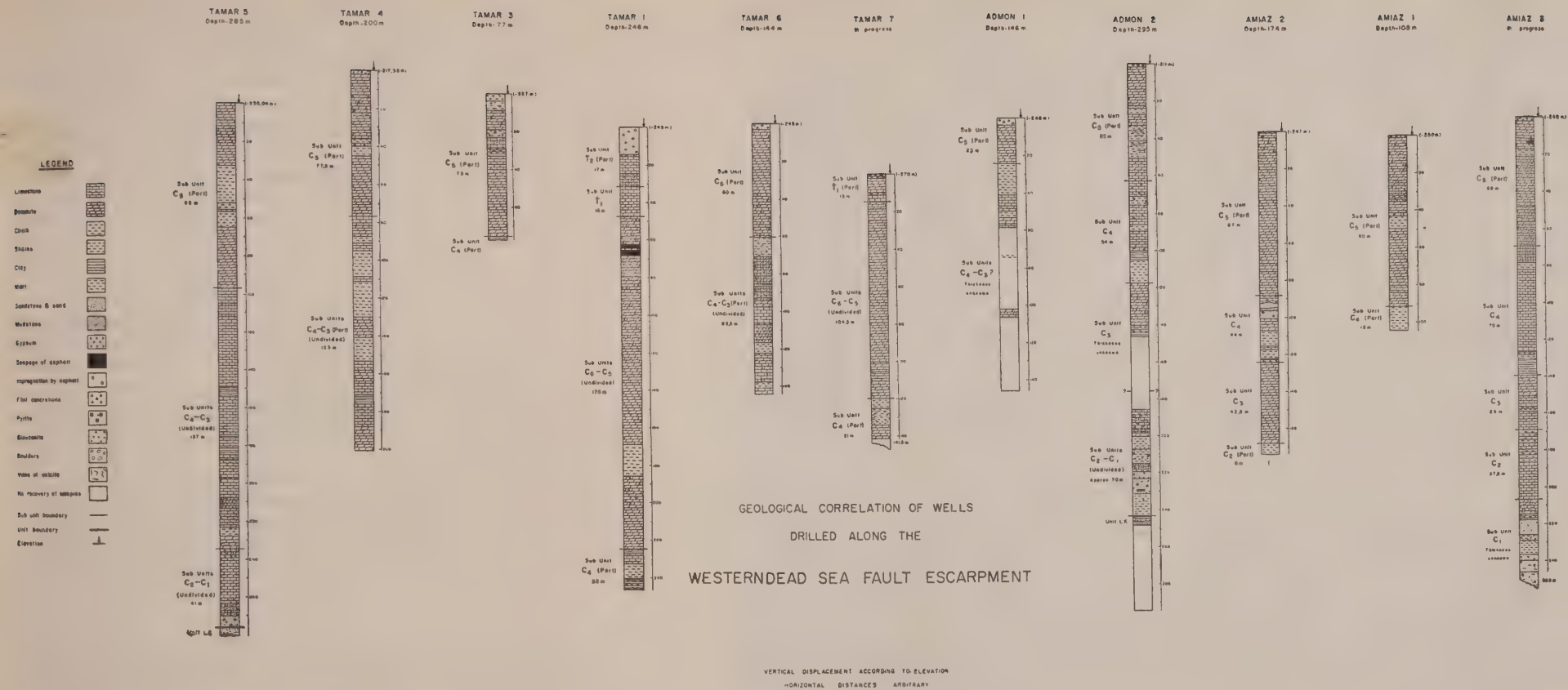


Figure 2

INDEX

1	2	3	4	5	6	7	8	9	10	11	12	13	14	15	16	17	18	19	20	21	22	23	24	25	26	27	28	29	30	31	32	33	34	35	36	37	38	39	40	41	42	43	44	45	46	47	48	49	50	51	52	53	54	55	56	57	58	59	60	61	62	63	64	65	66	67	68	69	70	71	72	73	74	75	76	77	78	79	80	81	82	83	84	85	86	87	88	89	90	91	92	93	94	95	96	97	98	99	100
---	---	---	---	---	---	---	---	---	----	----	----	----	----	----	----	----	----	----	----	----	----	----	----	----	----	----	----	----	----	----	----	----	----	----	----	----	----	----	----	----	----	----	----	----	----	----	----	----	----	----	----	----	----	----	----	----	----	----	----	----	----	----	----	----	----	----	----	----	----	----	----	----	----	----	----	----	----	----	----	----	----	----	----	----	----	----	----	----	----	----	----	----	----	----	----	----	----	----	-----

For the c3 (lower) dolomite aquifer the static head is practically the same in Mazal No. 1, Tamar No. 6 and Tamar No. 7, and slightly higher in Tamar No. 4 and No. 5. Comparing these levels with the corresponding levels in the c5 (upper) dolomite aquifer, it appears that the original zone of best connection between the Nubian Sandstone and the dolomite aquifers lies around the well Tamar No. 3. The original pressure conditions have changed since, because of the exploitation of the water.

Considerable differences in the water level were measured in the Admon field. These may, to some extent, be due to a temporary seepage of artesian water from the Nubian Sandstone into the higher horizons while Admon No. 2 was drilled. In the Ami'az wells water levels correspond well.

In the c5 (upper) dolomite aquifer, the water level is higher in the main mountain block (Tamar No. 3) than in the downfaulted Mazal block (Tamar No. 1).

HYDROLOGICAL INTERPRETATION

Two principal conclusions can be arrived at on the basis of these data:

- (1) The highest hydrostatic level is found in the Nubian Sandstone aquifer. It is therefore justified to assume a replenishment of the two dolomite aquifers by the Nubian Sandstone, either through open fissures in fault zones or by lateral contact along faults, or by slow upward percolation through the strata. Deepening of all wells into the Nubian Sandstone would probably produce artesian flow in most of them.
- (2) The location of a well in a fault zone is no guarantee for finding enough open fissures in any particular dolomite rock unit. Definite Karstic phenomena have been found in some wells (Admon No. 1, Ami'az No. 2). Despite Karstic conditions, yields from the various dolomite units in the Tamar wells Nos. 3, 4 and 5 differ considerably, although structural conditions are identical.

SALINITY

The results of the chemical analyses of the water samples, taken during drilling operations and pumping of the new wells, are given in Table II. An older analysis, from a shallow well in Nahal Zohar, and the analysis of the water from the Nubian Sandstone from Mazal No. 1 are included for reference. Data are given in the original form, as received from the chemical laboratory of the Mekoroth Water Company. Inconsistencies concerning sums of ions and percentages result from the fact that only major ions are represented in the table.

Comparing these analyses with the previously published ones (Shiftan 1958) from the Nahal Zin wells, the Metsada exploration holes, the samples from Mazal No. 1 and some of the springs, a more complete picture of the chemical characteristics of the water from the various aquifers can now be obtained, which leads to conclusions concerning the hydrologic regime and its evolution.

TABLE II

GROUNDWATER ANALYSES FROM WELLS AT THE WESTERN DEAD SEA FAULT ESCARPMENT																									
WELL	Depth in m	AQUIFER	Tot Soln	CHLORIDE			SULPHATE			NITRATE			BICARBONATE			CALCIUM			MAGNESIUM			SODIUM			Sum of cations
				mg/l	F°	%	mg/l	F°	%	mg/l	F°	%	mg/l	F°	%	mg/l	F°	%	mg/l	F°	%	mg/l	F°	%	
TAMAR 1	228	C ₅ -C ₆ DOLOMITE	2540	1127	98.14	73	385.8	40.13	18.9	3.0	0.29		225.6	18.5	8.5	137.0	39.22	18.0	111.0	45.03	21.2	615.1	33.43	61.0	218.6
TAMAR 3	51	C ₅ DOLOMITE	1590	666.5	94.08	56.5	465.3	48.45	28.9	0.88	0.07		296.7	24.5	14.6	186.5	46.67	27.8	79.8	32.83	19.5	385.0	8.00	5.9	167.40
TAMAR 5	72	C ₆ DOLOMITE	2825	1116	187.5	65.0	305	62.08	25.8				274.3	22.5	9.3	242.2	60.49	25.0	142.2	56.81	24.2	567.2	123.4	60.9	242.4
TAMAR 5	234	C ₅ DOLOMITE	2445	914.8	281.2	62.5	521.8	54.37	26.5	0.0	0.4		286.5	23.5	11.4	208.3	51.5	24.8	111.0	44.5	21.5	507.8	110.5	53.2	207.73
TAMAR 5	280	NUBIAN SANDSTONE	1840	626.7 8x+1.5	88.74 0.09	57.2	391.8	40.62	26.6				286.5	23.5	15.35	163.0	40.7	26.6	60.1	28.8	17.6	385.5 8x+9.66	74.9	1.6	153.48
ADMON 1	50	C ₆ DOLOMITE	3800	1425.4	201.1	63.5	781.8	81.47	25.7	2.7	0.12		414.8	34.0	10.8	325.7	81.35	25.7	81.8	33.65	10.6	928.7	202.19	63.6	317.15
ADMON 1	107	C ₅ DOLOMITE	2870	1063.7	150.1	62.8	823.7	83.8	27.4	4.2	0.34		268.6	23.75	9.9	272.2	84.23	22.7	85.1	35.02	13.6	691.7	190.57	63.0	239.8
ADMON 1	143	C ₅ DOLOMITE	2900	1042.5 8x+2.8	149.9 0.18	62.9	613.2	63.89	26.7	0.8	0.06		335.5	27.5	11.5	214.0	53.44	22.4	85.8	35.31	14.7	681.8	148.4	62.0	239.8
ADMON 2	120	C ₆ DOLOMITE	2950	1081.4	152.6	62.0	642.0	66.89	27.2				329.2	27.0	11.0	177.1	44.23	18.0	103.9	42.77	17.4	734.7	153.9	64.9	246.9
ADMON 2	232	C ₅ DOLOMITE	4000	1499.8	211.6	63.5	312.0	95.0	28.6				304.8	25.0	7.5	274.6	68.56	20.6	120.0	49.42	14.8	983.5	214.1	64.2	332.1
ADMON 2	275	NUBIAN SANDSTONE	5300	2304.7	325.9	73.5	876.0	91.33	20.8				317.0	26.0	5.88	271.8	87.87	19.3	102.4	42.13	9.5	1832.7	335.6	75.1	443.6
AMIAZ 1	32	C ₅ DOLOMITE, PERCHED AQUIFER	395	83.1	12.01	37.8	107.0	11.5	35.0	10.6	0.86		91.4	7.5	23.6	44.9	11.2	35.3	21.4	8.8	27.7	54.2	11.8	37.0	31.8
AMIAZ 1	70	C ₅ DOLOMITE	1355	468.6	56.06	53.9	312.8	32.59	26.6	3.5	0.29		104.6	13.5	10.9	80.9	22.11	18.0	80.8	30.8	25.1	320.6	69.84	57.0	122.7
NAHAL ZOHAR	14	C ₅ DOLOMITE (7)	2535	1135	160.1	73.6	424.7	44.2	20.2				184.6	13.5	6.2	197.3	49.3	22.6	111.1	45.7	21.0	564.7	122.8	56.4	217.8
MAZAL 1	597	NUBIAN SANDSTONE Artesian confined Aquifer	3805	1400.0	197.7	63.0	915.3	95.4	30.5				253.0	20.7	6.5	272.7	68.1	21.8	66.6	27.4	8.70	1003.0	218.3	69.5	313.3

mg/l

milligram/liter

F°

franch degrees = 5x milliequivalent

%

percentage of total anions or cations

Carnielio, Drawing section

Geological Survey, Irbid

mg/l milligram/liter

F° French degrees = 5x milliequivalent

% percentage of total anions or cations

Carmelit, Drawing section
Biosci. Geol. Survey, Israel

Table 2

1747

Total salinity

Only the sample from the perched aquifer of Ami'az No. 1 (32m depth) can be described as fresh water. Another sample from the same well (70m depth) and the water from the Boqeiq spring already show higher salinities.

Apart from these small and practically not very important aquifers, the water of best quality was found in the Nubian Sandstone of the well Tamar No. 5 (1840 mg/l). The salinity of this water is much lower than that found in the water from the same formation in Mazal No. 1, Admon No. 2 and in the Nahal Zin wells.

While assuming previously the feeding of the Nahal Zin aquifer from the aquifers of the Tamar-Mazal mountain border, a difficulty arose from the fact that the salinity in the Nahal Zin aquifer is in many cases lower than the salinity of the water found in the c3-and c5- aquifers of Mazal No. 1. A dilution by fresh water infiltrating from surface runoff in the bed of the Nahal Zin was assumed to explain this situation. With the discovery of the low-salinity water in the Nubian Sandstone aquifer, this assumption becomes unnecessary.

The hitherto available samples are listed in order of their total salinity in appendix 2. Most of them show salinities ranging from 1500 to 3000mg/l.

Variations in salinity within the Nubian Sandstone aquifer

Comparing salinities for the Nubian Sandstone aquifer alone, an increase is found as one proceeds from the southernmost well, Tamar No. 5, northwards to Mazal No. 1 and Admon No. 2. The comparatively low salinity at Tamar can be explained by a more vigorous groundwater flow caused by the proximity of the Nubian Sand-

stone outcrops of Makhtesh Hathira and Tsafit Valley, — both areas of present or past infiltration— and by the good hydrological connection in this part of the main fault escarpment between this aquifer and the Lisan aquifer.

In the Admon region, on the other hand, the distance to the Nubian Sandstone outcrops is larger, and rather impervious beds of the Hatseva formation adjoin the main fault escarpment. The higher salinity in Mazal No. 1 is explained by its partial tectonic- and consequently hydrological isolation from the main mountain block, impeding the participation of the deeper aquifer in the active subsurface drainage regime of today.

Changes of salinity with depth

While salinity decreases with depth in Tamar No. 5, the opposite occurs in Mazal No. 1 and Admon No. 2 (Table 3). Any attempt to explain this apparent inconsistency has to allow for the possibility of penetration of water from the Nubian Sandstone aquifer into the dolomite aquifers, because of the higher hydrostatic pressure of the Nubian Sandstone aquifer.

TABLE III

depth (m)	Changes of salinity (mg/l) with depth		
	Tamar No. 5	Mazal No. 1	Admon No. 2
72.....	2825 (c5)		
120.....			2930 (c3)
190.....		2680 (c3)	
234.....	2445 (c3)		
252.....			4000 (c3)
275.....			5300 (N.S.)
280.....	1840 (N.S.)		
292.....		3590 (c3)	
597.....		3805 (N.S.)	

The lower salinities in the dolomite aquifers of Admon are easily explained by dilution of the upward migrating Nubian Sandstone water by fresh water infiltrating directly into the dolomite aquifers. The intake areas would be the northern plunging parts of the main northern-central Negev anticlines, Hatsera and Hathira. The fact that such infiltration does exist is shown by the fresh, — and comparatively fresh — perched water horizons occurring at Ami'az, Boqeiq, and farther north. Additional proof is provided by the ion ratios (see below p. 282).

The annual recharge must be much smaller for the Tamar region, having as potential intake areas the eastern flank of the Hathira anticline, already in definite rain-shadow, and the upper Nahal Zin with the northern, plunging termination of the Ramon anticline. There is certainly less rainfall over these areas than over the highlands adjoining the Ami'az Admon region to the West and South-West. If, therefore, dilution of Nubian Sandstone water does occur in the dolomite aquifers

of Tamar, it must be rather limited. It is, in fact, masked completely by actual addition of salts (see p. 282).

The lower salinities of the dolomite aquifers in Mazal No. 1 — adjoining the Tamar field, — can, of course, not be explained by direct infiltration from the scantier rainfall, but by the close hydrological contact of the dolomite aquifer of this block with the dolomite aquifer of the main mountain block (see Shiftan 1958 figure 3), while the water from the Nubian Sandstone remains more stagnant, and therefore more saline. This, too, is corroborated by the chemical similarity of the respective samples (see below p. 282).

Chemical character, ion ratios

Table II and Figure 3 show the general chemical character of the various samples. They are all — apart from the one sample from the perched aquifer (30m depth) of Ami'az — of the chloride-sulfate type. As far as the ratios between the major ions are concerned, many of the samples resemble the type described by Schoeller (1955) as "eaux hyperchlorurées et eaux thalassochlorurées". They differ, however, from these samples in one important detail; their much lower concentration.

The samples from the Nubian Sandstone aquifers of Tamar No. 5 and Admon No. 2 are rather similar in chemical character (Figure 3b). The relationship between the major ions is expressed by:

$$rNa > rCa > rMg \quad (rMg/rCa = 0.6), \quad rCl > rSO_4 > rHCO_3.$$

Chlorine slightly exceeds sodium in Tamar No. 5, indicating a slight positive base exchange, while there is a very slight excess of sodium over chlorine in Admon No. 2.

The Nubian Sandstone water from Mazal No. 1 is different, showing a slight excess of sodium over chlorine, and a relatively higher calcium and sulfate content. This points to addition of calcium sulfate to the original water and a negative base exchange. The same chemical characteristics are still more clearly observed in the Metsada oil prospecting well, where the aquifer lies deeper and the water is even more stagnant than in the Mazal block.

The chemical character of the original Nubian Sandstone water, as represented by the samples from Tamar No. 5 and Admon No. 2, is modified while the water passes into other strata forming "secondary aquifers."

In the dolomite aquifers of the Tamar well field, the most important change in chemical character accompanying the increase in salinity is addition of magnesium chloride and sodium chloride. The ion ratios of the salts making up the difference between the salt content of the Nubian Sandstone water and the c5 dolomite water are similar to those found in the highly saline water from the seismic shot holes near the Dead Sea Works' potash plant (confined Lisan aquifer) (figure 3c). Thus, the higher salinity in the upper aquifer of Tamar No. 5 can be explained either by a 20% concentration and addition of sodium chloride and magnesium chloride, or by

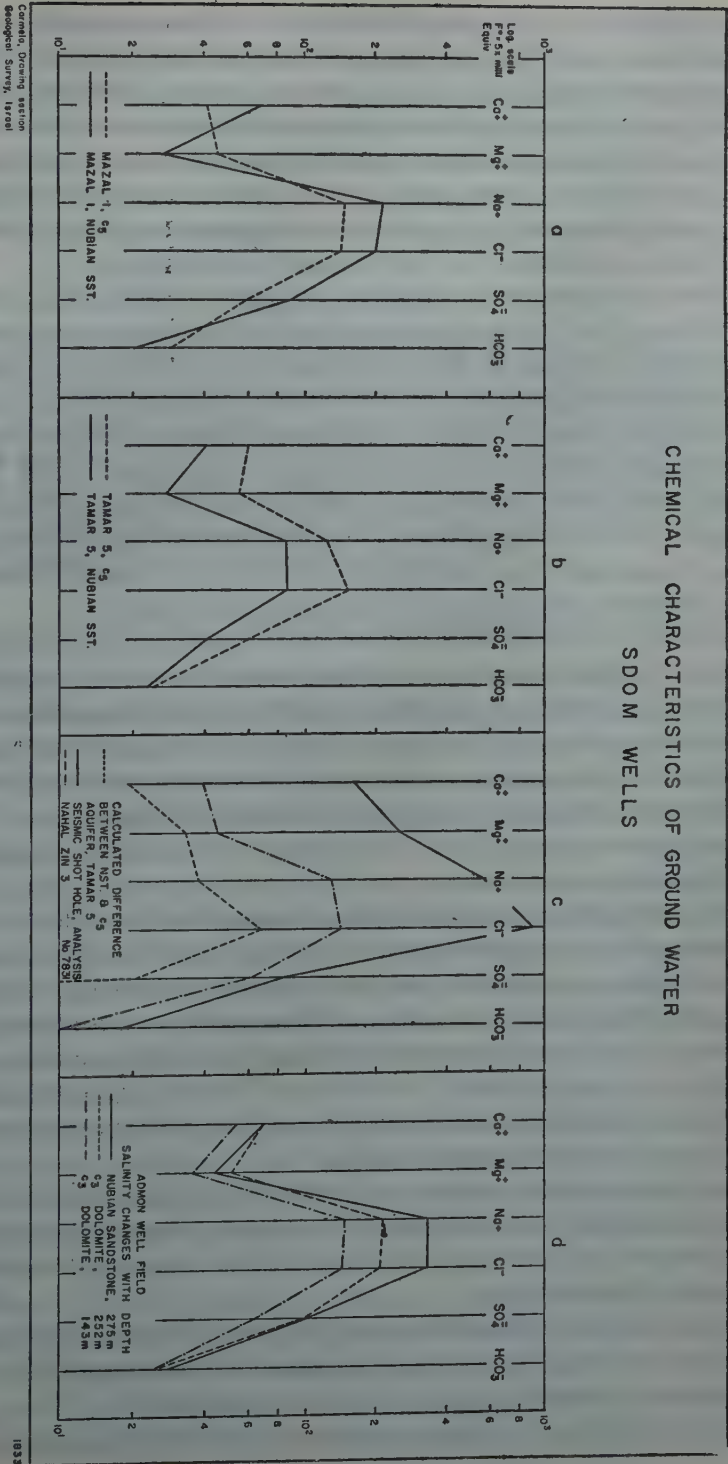


Figure 3

addition of these salts and some calcium sulfate, without concentration. The origin of the additional salts from the Lisan salt flats is clearly indicated. The extensive underground water seepages in the area between the potash plant and the Nahal Zin well field form widespread salt incrustations and efflorescences. The salts from this area reach the Tamar mountain border by dust storms, and the limited rainfall brings them into the shallower ground water, without being able to flush them out. Another possibility would be a widespread impregnation of the Lisan sediments with such salts, and diffusion by direct contact in the fault zone.

A relative enrichment with magnesium chloride is found also in the dolomite aquifer of Mazal No. 1, as compared with the Nubian Sandstone aquifer in the same well (Figure 3a). This may be due to the influx of water from the dolomite aquifer of the main mountain block (Tamar well field), as explained above. In this sample, a slight reduction of sulfate and a corresponding increase in bicarbonate is noticed.

In the Admon area, the water sample from the uppermost aquifer (50m) shows an increased amount of calcium together with a reduction in magnesium and a very slight negative base exchange (Table II). The increased salinity of this sample is probably due to local conditions and the static nature of the water in layers of limited porosity (limestone intercalation between shales and clays).

The water from 107m depth in Admon No. 1 is chemically almost identical with water from the dolomite aquifer of the Mazal block. The sample from 143m depth is also similar, but a slightly lower sulfate and higher bicarbonate content may indicate a slight reduction of sulfate. The sample from the same aquifer at Admon No. 2, 120m depth is of the same character, and differs only in a reduced calcium and a higher magnesium content, probably due to exchange processes.

The sample from Admon No. 2, 252m depth, shows a strong admixture of water of the Nubian Sandstone type.

In order to explain the character of the samples from the dolomite aquifers in the Admon well field by modification of Nubian Sandstone water of the Nubian Sandstone water occurring there, one has to assume dilution by water of low total salinity, containing mainly magnesium, calcium, sulfate and bicarbonate. Addition of such water from the limestone-dolomite formations with intercalations of gypsiferous marls recharged by rainfall over the north-eastern Negev highlands, fits well the conclusions arrived above concerning the salinity trend and the general hydrogeological situation of the Admon region.

If there is any addition of eolic-cyclic salt originating in the Dead Sea Basin, this effect is completely masked here by the addition of comparatively fresh sulfate-carbonate water. The low salinity of the water from the perched aquifer at Ami'az corroborates this conclusion.

The rather unique character of the water from Ami'az No. 1, 70m depth, may be due to addition of magnesium chloride to water in which magnesium had previously been exchanged for sodium (contact with Lisan sediments?).

The main modification the Nubian Sandstone-water undergoes when passing through

the Lisan formation is addition of sodium chloride, magnesium chloride, and some calcium sulfate. While in the original Nubian Sandstone-water sodium more or less equals chlorine, or is slightly higher, and calcium always exceeds magnesium, the result of the changes is waters in which chloride is always higher than sodium, and magnesium exceeds calcium (Figure 3c). The progressive changes are well illustrated by comparing the ion relations of the Nubian Sandstone-water from Tamar 5 with the water from Nahal Zin No. 3 and from the seismic shot-hole near the Potash Plant.

Hydrogen sulfide

Although a strong smell of hydrogen sulfide is noted in almost all wells, and pyrite is found in many rock samples, no indications of far reaching sulfate reduction phenomena such as high bicarbonate content together with low sulfate content are found in the samples of water from the wells on the fault line. Some samples with very slight indications of reduction phenomena were mentioned above. The possibility that much of this gas is derived from the oxidation of pyrites, or from the bituminous material occurring in the rocks, should be considered.

THE ORIGIN OF THE SALINITY AND THE UNDERGROUND WATER REGIME

The principal conclusion to be drawn from the data supplied by drilling in the zone of the western fault escarpment of the Dead Sea Rift concerns the practical importance of the Nubian Sandstone as an aquifer in Southern Israel. While in the North of the country the Lower Cretaceous is to a large extent developed in argillaceous shaly facies with limestone intercalations, and is inferior as an aquifer to the mainly dolomitic-calcareous Cenomanian formations, the more sandy facies of the Lower Cretaceous strata in Southern Israel may make them one of the main underground water reservoirs in this part of the country. It should also be borne in mind that, as the sandy facies in the Lower Cretaceous becomes predominant in the South, the total thickness of the Cenomanian formation decreases. At the same time, the thickness of the dolomite members as compared with the total thickness of the Cenomanian, decreases and consequently the importance of this formation as a groundwater reservoir diminishes.

The water of the Nubian Sandstone aquifer represents a strongly diluted brine of the hyperchloric-thalassochloric type. This water saturates, with total salinity increasing from the Tamar region northwards, the upper layers — and probably also deeper ones, — of this sandstone. The origin of this water requires the following geological conditions:

- (a) formation of highly concentrated brines of the hyperchloric-thalassochloric type, and possibly also salt deposits, in the rift valley,
- (b) ample exposure of Nubian Sandstone along the border of the rift,
- (c) change of the hydrologic regime by climatic and/or tectonic accidents, bringing about a strong influx of fresh water into the depression; this fresh water dilutes

- the brines and forms a lake with a level reaching well up to the border of the rift valley; at this stage, the sandstones become saturated with the diluted brine.
- (d) sedimentation in this lake seals off the sandstone outcrops with impervious sediments, trapping the brines.

These conditions might well correspond to the beginning of the Upper-Foothill Samra-Lisan cycle of sedimentation (Bentor and Vroman 1960). The general discharge of underground water was controlled, at that time, by the probably highest levels of the Samra — early Lisan Lake. The many travertine deposits on the escarpment mark the base level of ground water discharge under these conditions. The active ground water regime could not affect at that time the Nubian Sandstone aquifer because of the strong hydrostatic counterpressure of the lake, and the progressive sealing off by impervious sediments. Only with the regression of the Lisan Lake, and the gradual lowering of the lake level and the basis of underground drainage, a point was reached where the hydrostatic pressure in the Nubian Sandstone was sufficient to allow for the beginning of discharge of water into overlying and adjoining strata, mainly along fault lines. Tectonic processes may have had their part in the activation of this new regime.

At present, this process, together with dilution by direct infiltration of rain water and admixture of more recent saline water or salts, is still going on. The considerable hydrologic resistance of the "secondary" Lisan aquifers has kept artesian pressure in the fault zone high. The underground water seepages and springs of the lower parts of the Southern Dead Sea basin represent, therefore, the outflow of the water from the Nubian Sandstone, adjusting its hydrostatic level slowly, against considerable hydrologic resistance, to the present position of the basis of drainage.

The water of the Nubian Sandstone aquifer is, therefore, fossil water dating from Late Foothill — Samra — Early Lisan times (Late Pliocene-Early Pleistocene).

It should be mentioned, that the occurrence of travertine overlying Nubian Sandstone in Makhtesh Hatsera also fits well into this conception. As long as the lake level was higher than the hydrostatic pressure in the Nubian Sandstone aquifer, no discharge in the Dead Sea region was possible. Some limited infiltration, however, occurred in the Makhteshim. As Nahal Tsafit was probably not yet eroded at that time down to the sandstone, the lowest exposure was in Makhtesh Hatsera, and overflow springs may have appeared there. With the lowering of the lake level, and the beginning of discharge in the Dead Sea basin, these springs disappeared.

One is tempted to correlate the difference between the present day water level in Makhtesh Hatsera, as found in wells, and the elevation of the travertine, with the amount of water that has been withdrawn from the Nubian Sandstone since outflow began. Too little, however, is known at present about hydrological conditions in Makhtesh Hatsera to allow for such far reaching conclusions.

APPENDIX NO. 1

*Lithological description of the cuttings from the**Tomar Admon and Amiaz Wells*

TAMAR NO. 1

0-11.5	No sample available
11.5-14.5	Boulders
14.5-15.5	Boulders and some limestone cuttings
15.5-16.5	Limestone, gray crystalline
16.5-24.0	Limestone, grayish, crystalline, Meleke-like
24.0-32.7	Dolomite, gray granular with some asphalt
32.7-47.0	Limestone, gray chalky
47.0-59.0	Dolomite, light coloured with spots of asphalt
59.0-62.8	Dolomite, fine grained with some asphalt
62.8-64.0	Asphalt, liquid
64.0-65.2	Dolomite, gray, hard, crystalline with some asphalt
65.2-68.5	Asphalt, liquid
68.5-74.5	Dolomite, gray, hard
74.5-79.5	Dolomite, gray crystalline
79.5-86.0	As above with some asphalt
86.0-92.5	Dolomite, dark, gray, crystalline
92.5-100.0	As above with some asphalt
100.0-112.0	Dolomite, light gray, crystalline
112.0-117.5	As above
117.5-130.0	Dolomite, dark gray, crystalline
130.0-137.0	As above
137.0-146.0	As above
146.0-157.0	Dolomite dark brown, crystalline
157.0-168.0	As above
168.0-185.5	Marl, yellow-grayish, soft
185.5-192.0	Dolomite, brown, crystalline
192.0-200.0	As above
200-202	As above — more light coloured
202.0-210.0	Dolomite, brown, crystalline
210.0-224.0	As above

TAMAR NO. 3

0-4.0	Mixed alluvial sediments
4.0-9.0	Chalk, white, soft and some boulders
9.0-14.5	Dolomite, grayish, hard, crystalline
14.5-19.0	As above
19.0-23.0	Chalk, white, soft with some flint
23.0-28.5	Limestone, light gray and some gray marl
28.5-33.0	Clay, calcareous gray
33.0-40.0	Limestone, argillaceous, grayish
40.0-46.0	Dolomite, calcareous, light coloured, crystalline
46.0-48.0	Dolomite, calcareous, gray
48.0-75.0	Dolomite, dark gray, hard, crystalline
75.0-76.0	Clay, shaly, dark gray
76.0-77.0	As above

TAMAR NO. 4

0-12.0	Marl, light coloured and boulders
12.0-13.0	Dolomite, light brown and crystalline
13.0-22.0	Dolomite, light brown and crystalline with limestone and flint
22.0-29.5	Dolomite, light brown and gray
29.5-36.0	As above
36.0-38.2	Marl, greenish
38.2-40	Dolomite, gray, crystalline, with some pyrite
40-45	Limestone, argillaceous, yellow, soft
45.0-50.5	Dolomite, greenish, light coloured
50.5-59.0	Dolomite, light coloured and calcareous
59.0-77.0	Dolomite, light brown and granular
77.0-82.0	Limestone, light coloured
82.0-87.5	Dolomite, dark gray and light brown sandy dolomite
87.5-91.0	Marl, greenish
91.0-95.0	Limestone, light coloured, crystalline
95.0-109.0	Marl, greenish
109.0-111.5	Limestone, gray
111.5-130.0	Marl, light coloured
130.0-141.0	Dolomite, light brown with white flint
141.0-153.5	Marl, greenish
153.5-156.0	No samples available — possibly limestone
156.0-158.0	Limestone, gray
158.0-163.5	Dolomite, white and banded
163.5-165.0	Limestone, gray
165.0-171.0	Limestone, dark gray and detritic
171.0-176.3	Clay, gray
176.5-184.0	Limestone, gray, crystalline
184.0-188.0	As above
188.0-200.0	Dolomite, light soft with impregnation of asphalt

TAMAR NO. 5

0-11.0	Dolomite, gray, coarse grained
11.0-15.0	Dolomite, buff, mixed with marl
15.0-30.0	Dolomite, gray, coarse grained
30.0-32.5	Dolomite, dark gray, coarse grained
32.5-52.5	Marl, light gray, chalky
52.5-68.0	Dolomite, gray, with some gray limestone and flint
65.0-78.0	Dolomite, dark gray
78.0-97.0	As above
97.0-100.0	Limestone, white yellowish, soft
100.0-105.0	Limestone, white, crystalline
105.0-112.0	Limestone, gray, argillaceous and pyritic
112.0-149.0	Limestone, gray, crystalline
149.0-154.5	Clay, calcareous, soft, gray
154.5-159	Limestone, light gray, hard
159-162	Limestone, grayish, chalky with crystals of calcite and pyrite
162-169	As above
169-176	Limestone, grayish, hard with some green clay
176-177	Marl, greenish, chalky
177-187	Limestone, gray, argillaceous and pyritic
187-188	Clay, grayish, shaly
188-198	Limestone, white, fine grained impregnated by asphalt, and light-coloured limestone and some clay.

198-207	Limestone, white, hard fine grained impregnated by asphalt, and organogenic limestone with some clay
207-212	Dolomite, light coloured, hard, porous
212-223	Limestone, light coloured, impregnated by asphalt
223-228	Marl, greenish
228-234	Dolomite, gray, hard, fine grained
234-239	Limestone, light gray, fine grained with some veins of calcite
239-261	As above, with dark oolites, sand and glauconite
261-269	Limestone, light gray, fine grained, bituminous, pyritic with some clay, glauconite and flint
269-276	Sandstone, gray to dark gray, fine grained, silty, with glauconite and flint-concretions
276-280	Sandstone, gray, medium grained with glauconite and some flint

TAMAR NO. 6

0-3	Boulders
3-37	Dolomite, gray, hard, crystalline
37-50	Dolomite as above, with some asphalt
50-60	Dolomite, brown-gray, hard, porous
60-70.7	Chalk, gray, argillaceous
70.7-94.5	Dolomite, calcareous, gray, hard, crystalline, impregnated with asphalt
94.5-106	Limestone, light yellow, fine grained with asphalt, some faunal remains
106-106.5	Marl, green and soft
106.5-116.5	Dolomite, chalky, gray, fine grained
116.5-121.5	Marl, light green, soft
121.5-129	Dolomite, dark gray, hard, coarse grained
129-137.5	Limestone, gray, crystalline with some asphalt
137.5-141.5	Marl, bituminous, dark green, soft
141.5-143.7	Limestone, gray to yellow, crystalline

TAMAR NO. 7

1-3	Boulders
3-10	Dolomite, gray, hard
10-11.5	Marl, variegated, soft, friable
11.5-15.0	Limestone, bright coloured, hard
15.0-70.0	Dolomite, gray, hard, crystalline
70-79	Dolomite, gray-black, hard, coarse grained
79-100.5	Dolomite, gray, hard, crystalline
100.5-120	Dolomite, light gray, soft, friable
120-125.5	Marl, gray
125.5-134	Marl, argillaceous, gray
134-141	Dolomite, bituminous, dark, hard

ADMON NO. 1

0-4	Boulders
4-11	Dolomite, brown gray, hard
11-20	Dolomite, light yellow, soft
20-23.5	Dolomite, white, soft
23.5-27	Marl, yellow, soft
27-40	Marl, bituminous, gray, soft
40-46	Shales, calcareous, gray
46-49	Dolomite, gray, hard, crystalline
49-52	Marl, gray, soft

52-56	Dolomite, gray, hard, crystalline
56-58	Limestone, gray, fine grained
58-75	No samples available
75	Marl, bituminous, gray
75-106	No samples available
106	Dolomite, gray, hard, crystalline
106-146	No samples available

ADMON NO. 2

0-2	Boulders
2-22	Dolomite, gray, hard crystalline
22-24	Limestone, argillaceous, light coloured
24-27.5	Marl, yellow, soft
25.7-33	Dolomite, gray, hard
33-41	Marl somewhat calcareous, yellow
41-50.5	Marl, calcareous, yellowish with intercalations of limestone
50.5-62.5	Limestone, gray and some dolomite
62.5-76	Shales, calcareous, gray, pyritic
76-86	Clay, calcareous, gray, pyritic
86-89	Clay, calcareous, yellow
89-98	Limestone, dolomite, yellowish
98-100	Limestone, shaly, pyritic, gray
100-105	Clay, shaly
105-117	Marl, bituminous, gray
117-125	Dolomite, bituminous, gray
125-134	Dolomite, gray, hard, spotted, with asphalt
134-140	Dolomite, gray, hard
140-145	Marl, yellowish
145-185	No samples available
185-192	Limestone, gray, crystalline, fissured
192-195	Limestone, gray, with some pyrite
195-197	Limestone, argillaceous with some glauconite
197-200	Sandstone, gray with some glauconite
200-213	Marl, gray, greenish with some glauconite and pyrite
213-218	Limestone, argillaceous, gray pyritic with some glauconite
218-230	Sandstone, variegated with intercalations of limestone and some pyrite and glauconite
230-242	Marl, blue gray, pyritic
242-247.5	Clay, blue with some white limestone
247.5-295	No samples available

AMIAZ NO. 1

0-24	Dolomite, brown, hard, crystalline and black flint
24-31	Dolomite, calcareous, brown, hard and white flint
31-34	Dolomite, brown, hard crystalline with some marl
34-41.5	Chalk, white, soft, friable
41.5-43	Dolomite, brown, hard, crystalline and some flint
43-50	Marl, greenish, soft
50-60.5	Dolomite, light gray
60.5-80	Dolomite, brown, hard, porous crystalline
80-92	As above
92-105	Clay and marl, bluish, soft

AMIAZ NO. 2

0-1	Boulders
1-11.5	Dolomite, light brown, hard and some flint
11.5-44	Dolomite, gray brown, hard, coarse grained
44-62	Dolomite, light gray, crystalline, coarse grained
62-71	Dolomite, gray brown, hard, crystalline
71-75	Dolomite, reddish brown, crystalline
75-88	Dolomite, dark gray, crystalline
88-89	Clay, and marl, dark, soft
89-92	Dolomite, blackish, crystalline with flint
92-95	Cave
95-100.5	Mudstone, dark gray-black
100.5-107	Dolomite, gray, hard
107-115	Marl, gray
115-117	Dolomite, gray, hard
117-124	Marl, gray
124-168	Dolomite, gray, porous, crystalline
168-174	Marl, bluish gray

AMIAZ NO. 3

0-3	Boulders
3-17	Dolomite, brown, hard, crystalline
17-21	Marl, light yellow
21-32	Dolomite, brown, crystalline and yellow marl
32-48	Dolomite, brown, hard, crystalline
48-69	Dolomite, brown, crystalline and yellow , marl
69-78	Limestone, light coloured with gypsum and marl
78-82	Marl, light yellow
82-92	Limestone, shaly, bituminous
92-125	Limestone, black gray, with faunal remains
125-127	Chalk, white, gray, friable
127-129	Marl, bluish-gray
129-138	Clay, blue, soft
138-149	Dolomite, brown, hard, crystalline
149-155	Limestone, light gray, hard
155-167	Limestone, light gray, hard
167-174	Marl, gray
174-178	Limestone, gray hard
178-185	Marl and clay, gray
185-205	Limestone, gray, hard, medium grained
205-206	Sand, white with some glauconite
206-213	Dolomite, gray and some sand and glauconite
213-216	Clay with some pyrite and glauconite
216-219	White sand
219-220	Clay and sandstone with glauconite
220-224	Sandstone, gray, fine grained with glauconite
224-227	Pyritic shales, sandy, gray and some glauconite
227-235	Shales, gray
235-236	Sandstone, gray with pyrite
236-238	Sandstone, gray, with pyrite
238-244	Shales, calcareous, sandy, gray with pyrite
244-246	Sandstone, gray, with pyrite and glauconite

APPENDIX NO. 2

Groundwater samples from the Dead Sea Basin, in order of their total salinity (mg/l)

Sample	salinity	aquifer
Ami'az No. 1,32m	395	c5
Ami'az No. 1,70m	1355	c5
Boqeiq spring	1680	c5
Tamar No. 5,280m	1840	N.S.
Naqb Mezell, Tahal 23m	1915	t
Tamar No. 3,51m	1990	c5
Naqb Mezell, Tahal (?)	2015	t
Nahal Zin No. 3,18m	2350	q2
Tamar No. 5,534m	2445	c3
Nahal Zin No. 1,35m	2490	q2
Ein Tamar	2520	q2
Nahal Zohar, 18m	2535	t
Tamar No. 1, 228m	2540	c3
Nahal Zin No. 3, 70m	2540	q2
Nahal Zin No. 1, ?	2600	q2
Nahal Zin No. 3, 70m	2610	q2
Nahal Zin No. 1 (?)	2665	q2
Mazal No. 1, 190m	2680	c3
Mazal No. 1, 190m	2685	c3
Ein Haqiqar	2750	q2
Tamar No. 5, 72m	2825	c5
Ein Haqiqar	2835	q2
Admon No. 1, 107m	2870	c3
Admon No. 1, 143m	2900	c3
Mazal No. 2, 96m	2900	q2
Admon No. 2, 120m	2930	c3
Mazal No. 2, 120m	2930	q2
Mazal No. 1, 292m	3590	c3
Nahal Zin No. 3, 70m	3660	q2
Admon No. 1, 50m	3800	c5
Mazal No. 1, 597m	3805	N.S.
Mazal No. 1, 594m	3995	N.S.
Admon No. 2, 252m	4000	c3
Nahal Zin No. 4, (?)	4835	q2
Admon No. 2, 275m	5300	N.S.
Metsada No. 1, 636m	5580	N.S.
Metsada No. 1 "	6470	N.S.
Shot hole, km 103	6940	q2
Nahal Zin No. 2,	8700	q2
Shot hole km 103	11,350	q2
" " " "	11,740	q2
Metsada Plain, struct. hole	15,350	n
Hamei Zohar	50,400	?
Hamei Zohar	68,950	
Dead Sea Water	272,480	

ACKNOWLEDGEMENTS

The author wishes to express his gratitude to the Mekoroth Water Company for the permission to use and publish part of the chemical analyses of water samples, to E. Rosenthal of the Hydrogeology Division, Geological Survey of Israel, for examining and describing the well logs and drawing the correlation table, and, to Y. Bendor, Director of the Survey, for the reading of the typescript and many helpful suggestions.

REFERENCES

1. BENDOR, Y.K. AND VROMAN, A., 1954, The Geological Map of the Negev, 1:100,000, Sheet 16: Mount Sdom, with explanatory text, first edition, *Geological Survey of Israel, Jerusalem*.
2. BENDOR, Y.K. AND VROMAN, A., 1960, The Geological Map of the Negev, 1:100,000, Sheet 16: Mount Sdom, with explanatory text, second (revised) edition, *Geological Survey of Israel, Jerusalem*.
3. PICARD, L., 1953, Outline on Groundwater Geology in Arid Regions, *Desert Research, Proc. Int. Symp. Israel Res. Council. Spec. Publ. No. 2*, pp. 583-591.
4. PICARD, L., 1953a, The history of Groundwater Exploration in Israel, *Desert Research, Proc. Int. Symp. Israel Res. Council. Spec. Publ. No. 2, Geol. Inst. Israel, Publ. No. 4*.
5. SCHOELLER, H., 1955, Géochimie des eaux souterraines, *Rev. de l'Institut Français du Pétrole et Annales des Combustibles liquides, (Paris)*.
6. SHIFTAN, Z.L., 1958, An artesian aquifer of the Southern Dead Sea Basin, *Bull. Res. Council of Israel, 7G, 27*.
7. BENDOR, Y.K. et al, 1960, Lexique Stratigraphique International, Vol. III Fasc. 10c2, Israel, Centre Nationale de Recherches Scientifiques, Paris.

NODULES CUPRIFERES DU NEGUEV MERIDIONAL (ISRAEL)

A. SLATKINE

Technion — Israel Institute of Technology, Haifa

Le cuivre a été exploité depuis une très haute antiquité, dans la vallée désertique de l'Arava, qui s'étend du sud de la Mer Morte au Golfe d'Eilat. Les données archéologiques (Glueck 1952) indiquent que l'activité minière fut la plus intense à l'âge du fer et tout spécialement sous le règne du Roi Salomon. Le centre minier le plus important de l'Arava à cette époque, se trouvait au Wadi Menayieh, l'actuel Timna, à une vingtaine de km environ au nord du port actuel d'Eilat. Dans la région de Timna le cuivre apparaît dans quatre horizons distincts (Bentor 1956-1960): 1° Le "Lower Shales" (Georgian). — 2° Le "Upper Shales" — (Georgian). — 3° Le "Lower Variegated Sandstone" (Paléozoïque). — 4° Le "White Nubian Sandstone" (Mésozoïque ?). Le "Upper Shales" renferme l'important gisement de Timna, développé par sondages au cours de la dernière décennie, et qui est actuellement en pleine production. Le minerai qui est situé entièrement sous le niveau actuel de la vallée contient exclusivement des minéraux oxydes: principalement du chrysocolle, accompagné de malachite, d'atacamite, de diopside et de tenorite. Aucun sulfure n'a été décelé. Ce gisement serait d'origine lagunaire et syngénétique (Bentor 1956).

Le "Lower Variegated Sandstone" est un grès grossier, coloré, recouvrant le "Upper Shales". A 30-40m au-dessus du contact avec le "Upper Shales" il contient du cuivre sous forme d'imprégnations lenticulaires de chrysocolle et de turquoise (Bentor op. c.). L'horizon du "White Nubian Sandstone" renferme les nodules cuprifères qui font l'objet du présent travail. Actuellement ces nodules ne présentent pas d'intérêt économique. Mais à l'époque biblique ils constituaient un minerai riche, facilement récupérable tant in situ que dans les alluvions, tandis que l'horizon du "Upper Shales", qui affleurerait au niveau du sol ne présentait qu'une minéralisation diffuse et trop pauvre pour la technique métallurgique de l'époque. Les nodules du "White Nubian Sandstone" furent donc intensément exploités tandis que le gisement paléozoïque fut totalement négligé, à l'inverse des conditions actuelles. La présente étude apporte quelques précisions concernant la minéralogie et la genèse de ces nodules. Il comporte l'examen microscopique en sections minces et en sections polies d'une vingtaine de spécimens recueillis dans la région de Timna et celle du Nahal Shchoret à une quinzaine de km plus au sud.

Nous remercions le Dr. L. Heller du Service Géologique d'Israël, qui a déterminé un des échantillons aux rayons X, ainsi que le Prof. O. Schnepf du Technion, Haifa, qui a effectué une analyse spectrochimique.

NODULES DU "WHITE NUBIAN SANDSTONE"

Le caractère distinctif de la minéralisation du "White Nubian Sandstone" est la présence de sulfures de cuivre et de plantes fossiles cuprifères (Bentor op. c.). Dans les trois horizons inférieurs les sulfures font défaut. Les nodules sont dispersés sporadiquement dans un grès blanc friable, pauvre en matière argileuse ou organique. Leurs dimensions ne dépassent pas une dizaine de cm. La forme est grossièrement lenticulaire, mais parfois reproduit intégralement des formes végétales: branche (Figure 1), tige ou fruits (Figure 2).

Caractères microscopiques

Le trait dominant est la présence ou l'absence d'une structure végétale.

Les nodules à structure végétale sont les plus nombreux. La structure végétale est parfois bien conservée (Figure 3), mais le plus souvent elle apparaît sous forme de vestiges fragmentaires de tissus cellulaires. La Figure 3 représente une partie de la section d'une tige où les différents détails d'une structure ligneuse concentrique apparaissent dans leur position originelle. Une autre texture, beaucoup moins évidente d'une origine végétale apparaît dans certains nodules à formes ovoïdes: aucun vestige de texture cellulaire n'est présent mais l'altération de la chalcosine procède suivant un canevas qui suggère une origine organique (Figure 6). En général dans ces nodules les éléments détritiques sont très abondants. Il s'agit probablement de fruits, partiellement substitués par la matière minérale et dans leur plus grande part remplis par du quartz détritique. A la périphérie des nodules on trouve en général une zone irrégulière de quartz détritique cimenté par des minéraux cuprifères ou ferrifères. Cette zone peut s'étendre assez profondément vers le centre du nodule, mais la fréquence des grains de quartz décroît invariablement et fortement de la périphérie vers le centre.

Minéralogie

Les minéraux comprennent des composés cuprifères, des oxydes de fer, des éléments détritiques et des minéraux occasionnels.

Minéraux cuprifères

La présence de *cuivre natif* est exceptionnelle. Une petite plage de quelques mm² a été trouvée au centre d'un nodule à texture ligneuse cellulaire, associée à de la chalcosine, de la cuprite et une matière carbonacée qui n'a pas été déterminée.

La *chalcosine* est toujours présente sous forme massive, ou en vestiges soulignant généralement une texture, ou comme ciment entre les grains de quartz. Les observations en lumière réfléchie indiquent la variété orthorhombique de basse température. Elle contient toujours de la *covelline*, souvent abondante le long des clivages. L'analyse spectrochimique d'un fragment de chalcosine extrait d'un nodule montre la composition suivante:

Conc. sup. à	0,1 %	:	Cu,Ca,Mg,Si,Zn
Conc. voisine de	0,1 %	:	Mn,Pb,Ti
Conc. inf. à	0,1 %	:	Ag,Co,Ni,Ru (Anal. O. Schnepf)

Après Cu le principal constituant est Zn. L'examen optique et l'analyse aux rayons X ne montrant pas de minéral spécifique du zinc, nous supposons que cet élément se trouve comme hôte dans la chalcosine.

La *cuprite* n'est pas fréquente. Elle apparaît dans quelques échantillons, associée à la chalcosine à laquelle elle communique un reflet rougeâtre.

La *malachite* est un des minéraux les plus abondants. Elle constitue presque la totalité de certains échantillons. Elle est en général grenue et souvent le grain, hérité de la chalcosine, montre une nette relation spatiale avec une texture cellulaire primitive, sans par ailleurs que la forme intégrale des cellules soit nécessairement conservée, comme c'est le cas dans les vestiges limoniteux (Figure 12). Une variété fibreuse, de formation ultérieure, forme le remplissage de fissures. Des vestiges de texture cellulaire sont parfois décelables (Figure 9 et 10), mais en général la cristallisation de la malachite a effacé toute texture organique. La malachite est en général le terme direct de l'altération de la chalcosine; cependant par places, au contact chalcosine-malachite, s'intercale une mince bande d'un minéral semblable à la malachite, mais à faible biréfringence et donnant une teinte de polarisation bleue anormale. Il s'agit peut-être d'un sulfate instable. L'examen aux rayons X n'a pas donné de résultat probant.

L'*azurite* se trouve occasionnellement, associée à la malachite, à la périphérie des nodules.

L'*atacamite* a été déterminée aux rayons X. Les déterminations optiques ne sont pas probantes.

Le *chrysocolle* se trouve dans les passes détritiques où il se forme aux dépens du quartz. En général, il est rapidement remplacé par la malachite.

Le *diopase* est occasionnel. Il se trouve en petits cristaux pénétrant le quartz, au contact de la chalcosine, ou comme remplissage de fissures.

Oxydes de fer

Nous groupons ici sous le terme général de *limonite*, les mélanges de goethite et d'hématite, que l'on trouve toujours associés dans tous les nodules où subsiste une texture ligneuse cellulaire. En fait les détails les plus fins de ces tissus n'apparaissent nettement que lorsqu'ils sont conservés par la limonite (Figures 4, 7, 10, 12). La limonite peut remplacer également des tissus végétaux dépourvus de structure, par exemple le cœur de branches ou de tiges (Figure 3). De la limonite plus récente se trouve comme remplissage de fissures ou sous forme de rosettes (Figure 13).

Minéraux détritiques

Du quartz en grains anguleux ou arrondis, se trouve en quantité variable dans tous

les échantillons, généralement dans une zone périphérique. Le ciment intergranulaire consiste le plus fréquemment en malachite, plus rarement en chalcosine, chrysocolle, hématite ou opale. Lorsque le ciment est cuprifère les grains de quartz sont généralement attaqués à la périphérie et à l'intérieur, le long de fissures (Figure 11). Le quartz peut être remplacé par la chalcosine, la malachite ou le chrysocolle, partiellement ou même totalement, ne laissant que de vagues contours. La raréfaction progressive des grains de quartz à partir de la périphérie vers le centre est probablement dû à un processus de substitution par la chalcosine. La *calcédoine* détritique se rencontre occasionnellement. L'*opale* est très rare. Elle a été trouvée dans un seul échantillon, comme ciment entre les grains de quartz.

Minéraux occasionnels

De la kaolinite, du gypse et de la calcite se trouvent parfois comme ciment entre les grains de quartz ou comme remplissage de fissures.

Les nodules sans structures végétale sont des grès cimentés par de la chalcosine et ses produits d'altération: malachite principalement et chrysocolle.

ORIGINE DES NODULES

La présence du cuivre dans le "White Nubian Sandstone" a été attribuée à l'action de végétaux en décomposition sur des solutions cuprifères provenant du lessivage des imprégnations cuprifères du "Lower Variegated Sandstone" (Bentor op. c.). D'autre part, des végétaux fossiles et des concrétions cuprifères analogues à ceu du Néguev se trouvent dans les gisements dits des "Red Beds" en différentes régions des U.S.A. Ils ont été étudiés par plusieurs auteurs dont Richards (1915), Fath (1915), Papenfus (1931), Fisher (1937), Butler (1938), Wiese (1957) et Brummer (1958). En général, les nodules des "Red Beds" contiennent de la pyrite ou de la marcassite ainsi que des débris végétaux carbonifiés, de sorte que la relation entre ces minéraux et la chalcosine n'est pas difficile à établir. La précipitation de la chalcosine est attribuée à l'action réductrice de la pyrite ou de la matière organique sur des solutions cuprifères sulfuriques.

Aucun des échantillons que nous avons étudiés ne contient de la pyrite et un seul renferme quelques parcelles de matière organique, par ailleurs de détermination douteuse et associée à un minéral qui n'apparaît qu'exceptionnellement: le cuivre natif. Cependant, les débris de bois fossiles qui se trouvent dans le "White Nubian Sandstone" sont toujours limonitisés et contiennent fréquemment, en surface, des cristaux et des agregats cristallins de limonite pseudomorphe d'après la pyrite. Ces cristaux prouvent sans aucun doute que le minéral qui se substitua initialement à la matière végétale fut de la pyrite. Il est naturel d'appliquer cette conclusion aux nodules cuprifères. Nous émettons de plus l'hypothèse que la limonite qui constitue le ciment des concrétions gréseuses, dépourvues de texture végétale, provient aussi de l'altération d'une pyrite originelle. Dans les nodules du Néguev les données microscopiques établissent clairement que la cuprification est postérieure à la ferri-

fication. Dans les tissus cellulaires les relations texturales montrent que la chalcosine a remplacé une partie ou la totalité des cellules après leur pyritisation. Les vestiges limonitiques représentent les fractions oxydées des tissus pyritisés qui n'ont pas été remplacés par la chalcosine. La précipitation de la chalcosine s'explique ainsi facilement par la réaction bien connue de la pyrite sur les solutions cuprifères acides en milieu dépourvu d'oxygène. Dans les nodules où les résidus limonitiques manquent et la texture ligneuse n'est pas évidente la cause de la précipitation de la chalcosine est douteuse. L'effet réducteur peut être attribué théoriquement à la matière végétale ou à une activité bactérienne mais ce ne sont, ici, que des hypothèses spéculatives. Le fait que les végétaux étaient déjà pyritisés, et souvent envahis par du sable, laisse supposer qu'ils avaient acquis un certain degré de compaction, par carbonisation par exemple, et ne laisse que peu de place à l'hypothèse d'une action réductrice directe de la matière organique en putréfaction. Dans la majorité des cas l'action réductrice doit être attribuée à la pyrite.

On peut supposer d'après les formes bien conservées de certains des nodules cuprifères (Figures 1 et 2) qu'ils n'ont pas ou guères subi de transport après la cuprification. Ils auraient donc été cuprifiés à leur emplacement actuel ou aux environs immédiat. Ceci implique, étant donné la distribution extrêmement sporadique des nodules, et le manque de relations avec des fractures (qui auraient pu servir d'accès à des solutions cuprifères relativement concentrées) un degré extrême de dilution des solutions contenant le cuivre en migration. Que des bois fossiles pyritisés puissent concentrer certains éléments, dans un état d'extrême dilution est prouvé par la présence sur certains débris de bois fossiles limonitisés, trouvés dans le même horizon, de minéraux plombifères bien cristallisés tels que la wulfenite, l'anglésite*, la cérusite* et la plattnerite*. Le plomb n'est connu dans la région que sous forme de traces dans les minerais cuprifères des horizons paléozoïques et a dû migrer dans un état de dilution encore plus poussé que le cuivre.

La formation de la limonite, de la malachite et autres minéraux oxydés est due à des processus d'altération atmosphériques, qui indiquent un abaissement du niveau hydrostatique. La présence des carbonates (et incidemment de la plattnerite, qui d'après Garrels (1960) est un excellent indicateur de milieu oxydant alcalin) caractérisent un milieu alcalin.

CONCLUSIONS

La plupart des nodules cuprifères du "White Nubian Sandstone" sont des plantes fossiles. Les tissus de ces plantes ont été substitués initialement par de la pyrite, (qui peut être d'origine biochimique). Les formes intactes des structures ligneuses laissent supposer que la matière végétale, au moins dans certains des tissus les plus résistants, n'a subi ni écrasement, ni putréfaction. Les végétaux pyritisés ont ultérieurement été remplacés totalement ou en partie par de la chalcosine, précipitée à partir de solutions acides diluées, suivant un processus de réduction bien connu. Les concrétions cuprifères d'origine non végétale se sont formés probablement par

* Détermines par Dr. L. Heller

un processus identique. Il n'y a pas d'indication que de la chalcosine aie été précipitée directement par de la matière organique en décomposition; mais il est possible que dans certains cas de la chalcosine aie été précipitée directement par de la matière organique déjà carbonifiée. Un abaissement ultérieur du niveau hydrostatique a provoqué l'oxydation partielle ou totale des minéraux cuprifères et ferrifères. Dans l'état de nos connaissances actuelles la source du cuivre doit être attribuée au lessivage des niveaux cuprifères plus anciens.

Une autre donnée qui ressort des observations microscopiques est le degré d'instabilité que peut atteindre le quartz en présence de composés cuprifères. Les exemples de remplacement du quartz par la malachite, le chrysocolle ou la chalcosine sont très fréquents. Ce processus, observé ici à petite échelle, pourrait être appliqué à l'interprétation de concentrations cuprifères plus étendues dans les sédiments gréseux des niveaux paléozoïques de la région.

LITTÉRATURE CITEE.

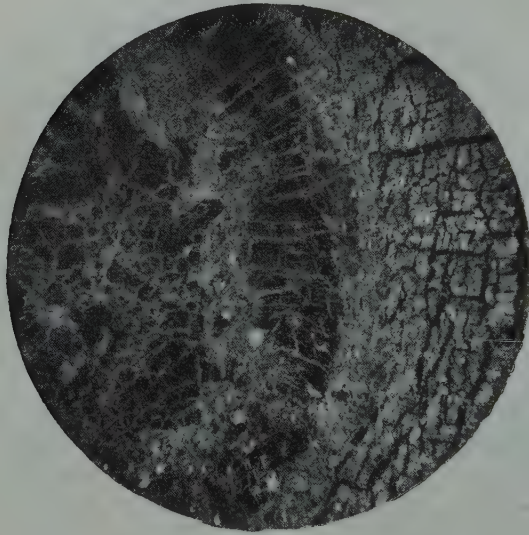
1. BENTOR, Y.K. (edit.), 1960, *Lexique Histographique Internationale*.
2. BENTOR, Y.K., 1956, Origin of the mineral deposits of the Negev, Jerusalem, *Isr. Geol. Surv.*, unpubl. rep.
3. BRUMMER, J.J., 1958, Supergene copper-uranium deposits in Northern Nova Scotia, *Econ. Geol.*, **53**, 309.
4. BUTLER, R.D., 1938, A "Red Beds" type copper occurrence, Wyoming Co. Pennsylvania, *Econ. Geol.*, **33**, 625.
5. FATH, A.E., 1915, Copper deposits in the "Red Beds" of South-Western Oklahoma, *Econ. Geol.*, **10**, 140.
6. FISHER, R.P., 1937, Sedimentary deposits of copper, vanadium-uranium and silver in South-Western United States, *Econ. Geol.*, **32**, 906.
7. GARRELS, R.M., 1960, *Mineral equilibria at low temperature and pressure*, N.Y. Harper.
8. GLUECK, N., 1952, The other side of the Jordan, *Am. Sch. of Oriental Res.*, New Haven, Conn.
9. PAPENFUS, E.B., 1931, "Red Beds" copper deposits in Nova Scotia and New Brunswick, *Econ. Geol.*, **26**, 314.
10. RICHARDS, L., 1915, Copper deposits in the "Red Beds" of Texas, *Econ. Geol.*, **10**, 634.
11. WIESE, JR., R.G., 1957, an occurrence of mineralized organic material in Nova Scotia, *Econ. Geol.*, **52**, 78.



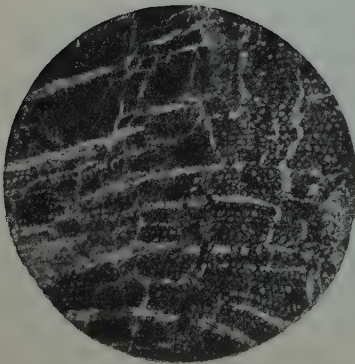
1



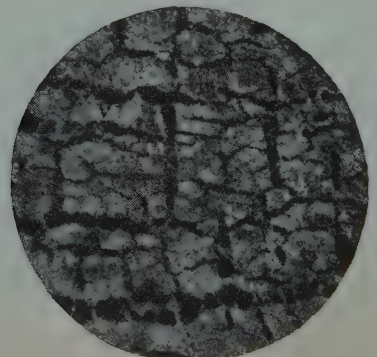
2



3



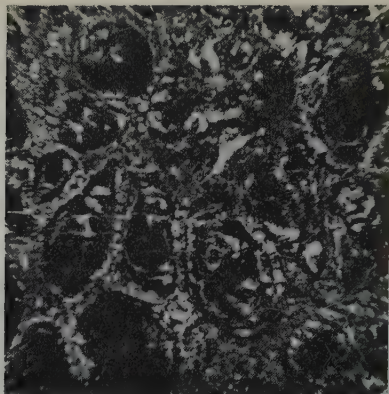
4



5

- Fig. 1 et 2.** Végétaux fossiles cuprifés. Fig. 1. montre un fragment de branche transformé presque entièrement en malachite. Fig. 2 représente un fruit présumé. La mince crête longitudinale marquerait la suture des deux coques. Grandeur naturelle.
- Fig. 3.** Fragment de la section d'une tige montrant différentes textures juxtaposées ou superposées. A gauche: partie centrale de la tige formée de limonite (sombre) et malachite (clair); la limonite dérivé de pyrite ayant remplacé un tissu ligneux sans structure, et ayant été remplacée partiellement par de la chalcosine. Au centre bande limonitique ayant préservé une fine texture ligneuse cellulaire. A droite texture réticulée soulignée par de la chalcosine résiduelle (noir) dans le malachite (clair). Section mince. 16: 1.
- Fig. 4.** Même section. Détails de la texture cellulaire dans la bande centrale. Parois des cellules: limonite dérivant de pyrite; intérieur des cellules: malachite dérivant de chalcosine. La substitution des tissus végétaux s'est effectuée sélectivement. Superposée à la texture cellulaire une texture réticulée plus grossière. Section mince. 40:1.
- Fig. 5.** Même section. Détails de la texture réticulée:chalcosine (noir) dans malachite (clair). Dans la malachite on distingue encore les traces de la texture cellulaire. Section mince. 40:1.

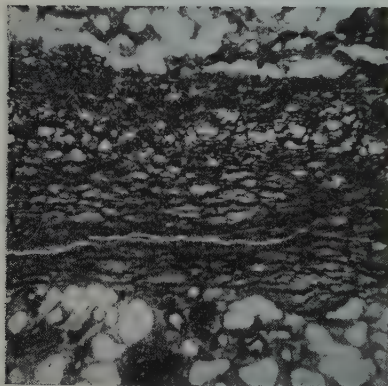
6



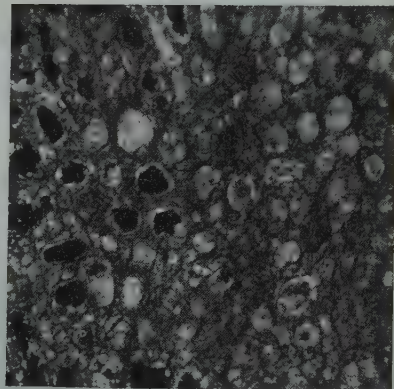
7



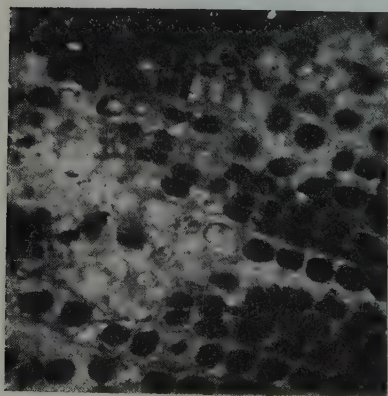
8



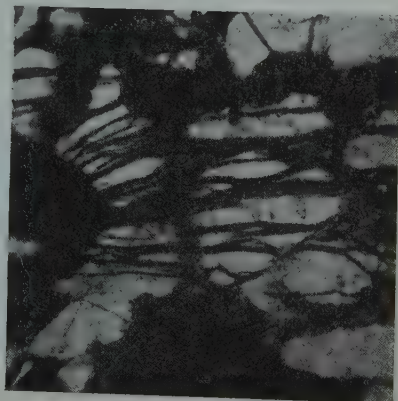
9



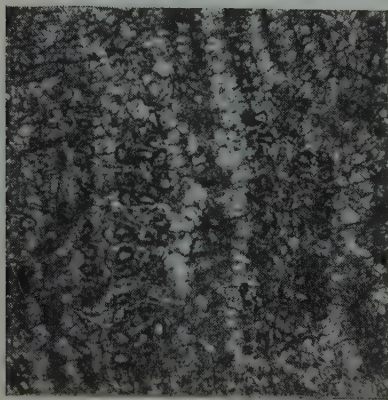
10



11



12



13



- Fig. 6. Altération de la chalcosine (noir) en malachite (clair) suivant une texture qui paraît héritée de formes végétales. La grosseur des grains croît fortement à partir du centre vers la périphérie. Section mince. 20:1.
- Fig. 7. Au centre bande de chalcosine (sombre) s'altérant en malachite suivant une texture qui rappelle un tissu végétal écrasé. A la périphérie grains de quartz détritiques cimentés par de la malachite. Section mince. 21:1.
- Fig. 8. Texture ligneuse cellulaire. Cellules de limonite (noir) dans malachite où subsistent des traces de la texture primitive. Section mince. 80:1.
- Fig. 9. Vestiges de texture cellulaire dans malachite. Parois des cellules en limonite; l'intérieur en malachite. A noter la texture grenue de la malachite héritée de la chalcosine et correspondant en grosseur à la dimension des cellules. Section mince. 80:1.
- Fig. 10. Texture ligneuse cellulaire. Alternance de bandes de limonite et de malachite. Les fins détails de la texture cellulaires sont bien conservés dans les passes de limonite. Section mince. 21:1.
- Fig. 11. Texture ligneuse cellulaire. Vestiges de chalcosine (noir) dans malachite où la texture est encore bien visible. Section mince. 80:1.
- Fig. 12. Grains de quartz détritiques (clair) partiellement remplacés par de la malachite (sombre). Section mince. 80:1.
- Fig. 13. Limonite secondaire en rosettes dans malachite. Section mince. 180:1.

IRAQ-EL-BAROUD, NOUVELLE GROTTÉ PRÉHISTORIQUE AU MONT CARMEL

M. STEKELIS

Laboratoire d'Archéologie Préhistorique, l'Université Hébraïque de Jérusalem

ABSTRACT

L'auteur expose les résultats des fouilles dans la grotte d'Iraq el-Baroud an Mont Carmel. Dans cette grotte ont été mis en évidence des niveaux du Néolithique (tahounien), du Mésolithique ancien (Kebarien) et du Paléolithique Supérieur.

L'Oued Misliyah est un des nombreux petits vallons du Mont Carmel. Il est situé à 16 km environ au Nord de Mugharet-el-Wad, bien connue des préhistoriens pour ses remarquables grottes préhistoriques, admirablement fouillées par Miss D. A. E. Garrod.

L'Oued Misliyah est très pittoresque et d'une beauté sauvage. A un kilomètre et demi de son embouchure, entre le confluent du vallon Bir Fadil et Misliyah, sur sa rive droite, se cachent deux grottes connues sous le nom d'Iraq-el-Baroud et citées par le Comte von Mülinen (1908):

“Folgt man dem Bachbette des wādi missilli, das nur eine wilde Schlucht darstellt, so gelangt man, nachdem von Süden das Wādi Bir Fadil eingemündet, nach einer halben Stunde zu der Felswand a'rāq el bārūd mit zwei im Winter von Fellāhen bewohnten Höshlen. Sie hat ihren Namen von der dichten Schicht salpeterhaltigen Ziegendüngers, der den Höhlenboden Bedeckt und von Fellāhen zur Bereitung von Pulver (Bārūd) benutzt wird. Die grössere Höhle sitzt tief in den Fels hinein fort und zerfällt in grössere und kleinere saalartige Abteilungen, welche teilweise Tropfsteinbildung aufweisen.”

LE SITE DES FOUILLES

Description générale

Ce n'est qu'en 1941 que j'ai essayé de les retrouver. La plus grande des deux grottes s'ouvre vers le Sud-Ouest du coteau. (fig. 1). Elle possède deux entrées; par la première, on pénètre dans une grande salle de 20 m de large sur 30 m de long. Très bien éclairée et aérée, cette salle paraît être la seule à avoir été habitée. Au fond de la salle, se trouve un passage vers une deuxième salle obscure (25 m × 20 m) de laquelle un couloir obscur mène à d'autres chambres. Mais celles-ci n'ont pas été explorées à cause d'un éboulement qui a complètement bouché le passage. Près de la paroi Est de la grande salle, plusieurs blocs énormes qui se sont détachés de la voûte rendent dangereux le passage dans un autre couloir.

La deuxième entrée était complètement masquée par des arbres. Une partie de la

Received July 10, 1960

voûte, qui devait être assez mince, s'effondra et recouvrit le talus; plusieurs autres blocs tombés au pied du talus, le recouvrirent entièrement. Plus tard, un mur de terre sèche fut élevé par des bergers arabes pour fermer cette entrée.

Avant de commencer les fouilles proprement dites, le sol de la grotte, retourné jusqu'à 20 cm de profondeur, a été nettoyé. La terre a été ramassée et tamisée. Des centaines de silex taillés, éclats, lames et nuclei, furent ainsi recueillis.

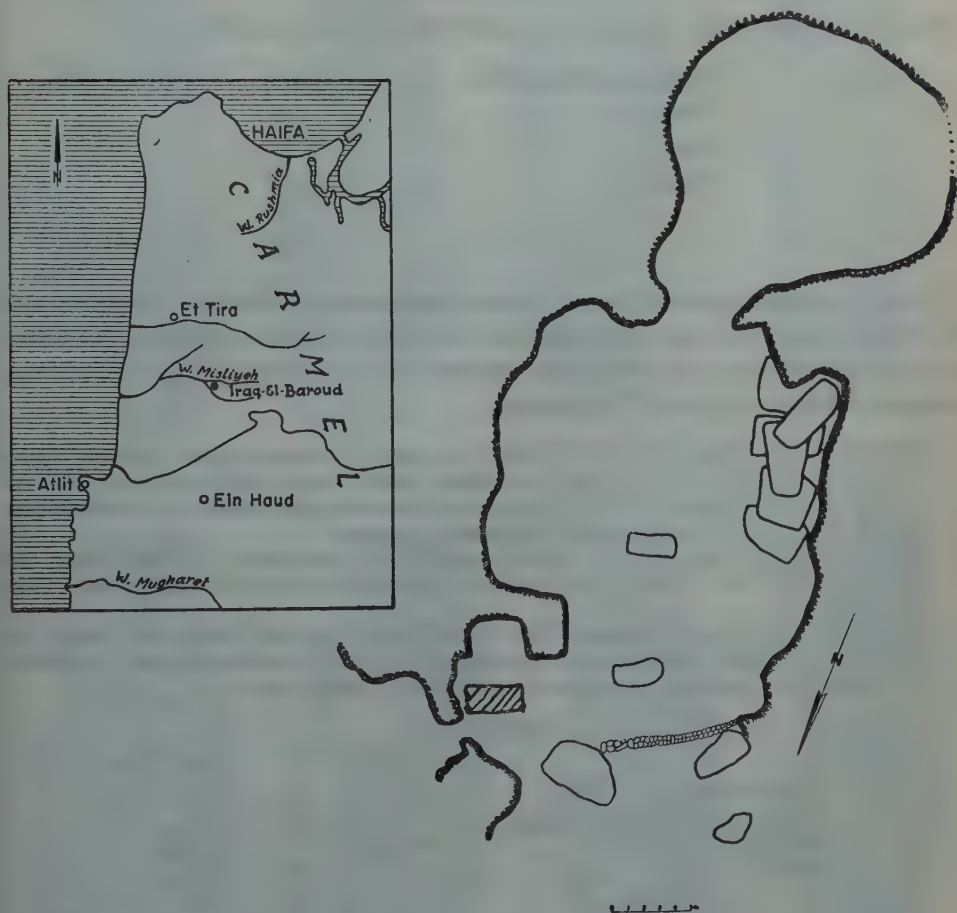


Figure 1
Plan de la grotte.

La stratigraphie

Près de la paroi ouest, le sol, dur, était intact. Une tranchée de 4 m de longueur sur 2 m de large a été creusée perpendiculairement à la paroi. La coupe s'étale ainsi, de haut en bas:

- | | | |
|----------------|---------------|---|
| A ₁ | 0 à 0.10 m | terre grisâtre assez dure. — "TAHOUNIEN" |
| A ₂ | 0.10 à 0.30 m | terre argileuse brunâtre, mélangée à de la pierraille, et silex taillés. — "KEBARIEN" |

B	0.30 à 0.60 m	terre argileuse, brunâtre, tendre, contenant pierrailles, os brisés et silex taillés du "Paléolithique supérieur"
C	0.60 à 1.10 m	terre argileuse brune, compacte, mélangée à des petites pierres, des éclats ayant subi l'action du feu, des os brûlés ou calcinés. — "AURIGNACIEN MOYEN"
D	1.10 à 1.20 m	A ce niveau les fouilles ont été arrêtées.

MATÉRIEL LITHIQUE

Niveau A₁

Dans cette couche, assez mince, peu de silex taillés furent recueillis:

Éclats non retouchés	12
Hachettes	3
Pics	1
Nuclei	4
	<hr/>
	20

Parmi les éclats, quatre seulement portent des traces d'utilisation. Les nuclei, à un plan de frappe, ont une forme allongée. La figure 2 montre les trois hachettes et le pic trouvés dans ce niveau. Les hachettes et le pic ont des bords aux arêtes coupantes et sont du type dit Tahounien.

1. Hachettes en silex brun (8.5×3.5×1.7 cm). Les deux faces sont taillées à grands éclats. Le biseau a été obtenu par "un coup de tranchet latéral" donné sur chacune des deux faces.
2. Hachette en silex brun (8.5×3.1×1.2 cm.). Les deux faces sont taillées. La hachette est pourvue d'un biseau et porte encore des traces de gangue.
3. Hachette en silex brun (7.5×3.6×2 cm). Les deux faces sont taillées à grands éclats. Le biseau a été fait d'un "coup de tranchet latéral" donné sur une face, tandis que l'autre a été retouchée.
4. Pic recouvert d'une patine blanche (9.3×3.7×1.2 cm). Les deux faces sont taillées. Il présente une extrémité appointée par une série de petits éclats enlevés sur l'une des faces. Cette pièce a été trouvée à la surface du sol, dans la grande salle.

Niveau A₂

		Pourcentage
Grattoirs simples	13	5.9
Grattoirs nucléiformes et rabots	49	22.2
Raclettes	3	1.3
Burins: d'angle	7	3.18
bec-de-flûte	9	4
plan	5	2.27
busqué	2	0.9
à troncature	3	1.36
atypique	5	2.27
Lames: retouchées	54	24.5
écaillées	2	0.9
de faucilles	4	1.8
Encoches	3	1.36
Pointe Emireh	1	0.4
Microlithes	70	31.8
Total	<hr/> 230	<hr/> 100.0



Figure 2
No. 1—3 Hachettes, 4 Pic

Nuclei	26
Éclats avortés	18
Éclats bruts	83
Éclats à crête	35
Éclats	71
Lames	184
Lamelles	207
Tablettes de rafraîchissement	26

230 outils ont été trouvés dans cette couche. Comme à tous les autres niveaux, l'outillage lithique est fait sur du silex turonien de bonne qualité, que les occupants des grottes trouvaient sur le plateau du Mont Carmel.

Grattoirs: Ils représentent 5.6% de tout l'outillage. Ils sont simplement préparés sur des lames courtes ou des éclats. Cinq grattoirs sont faits sur des éclats d'épannelage et portent leur cortex (fig. 3. No. 15). Un des grattoirs, fait sur un petit éclat, est unguiforme (fig. 3. No. 3): un autre des grattoirs, fait sur une petite lame, est double (fig. 3. No. 1). Les grattoirs nucléiformes et à rabots sont en nombre considérable, ils représentent 21.3% de tout l'outillage.

Raclettes: Très rares (1.3%). Elles sont faites sur de petites lames (fig. 3 No. 2).

Burins: (13.2%). Plusieurs types de burins: à troncature oblique (Nos. 8, 10, 14); burins plans (No. 11); Burin "busqué" (No. 16, 12); en bec-de-flûte (No. 13). Il est intéressant de signaler que tous les burins sont faits sur des éclats d'épannelage et portent encore leur cortex. Le No. 14 est un burin sur éclat avorté.

Lames de faucille: Ce sont des lames quadrangulaires à retouches dites "Helouan" du type Natoufien. (fig. 3 No. 6, 7) Il faut aussi signaler deux lames écaillées et (fig. 3 No. 17) un éclat à encoche.

Pointe d'Emireh. (fig. 3. No. 4) petite pointe dont la base a subi un amincissement par une retouche sur les deux faces.

Retouchoir: Un rognon de silex de 62 cm, qui a probablement servi de retouchoir, montre des traces d'utilisation à ses deux bouts

Les nuclei: 26 nuclei de différentes tailles atteignant jusqu'à 7 cm: 5 nuclei prismatiques à deux plans de frappe; 4 globuleux; 1 pyramidal et les autres (16) n'ont pas de forme définie.

Les déchets de taille sont nombreux: 35 lames à crête et 83 tablettes de rafraîchissement.

Lames et éclats: les lames brutes (184) sont plus nombreuses que les éclats (71).

Les éclats ne présentent que rarement des retouches d'utilisation.

Lamelles: 140 lamelles non retouchées ont été ramassées. Elles sont minces, allongées droites ou incurvées soit à droite soit à gauche, souvent terminées en pointe acérée.

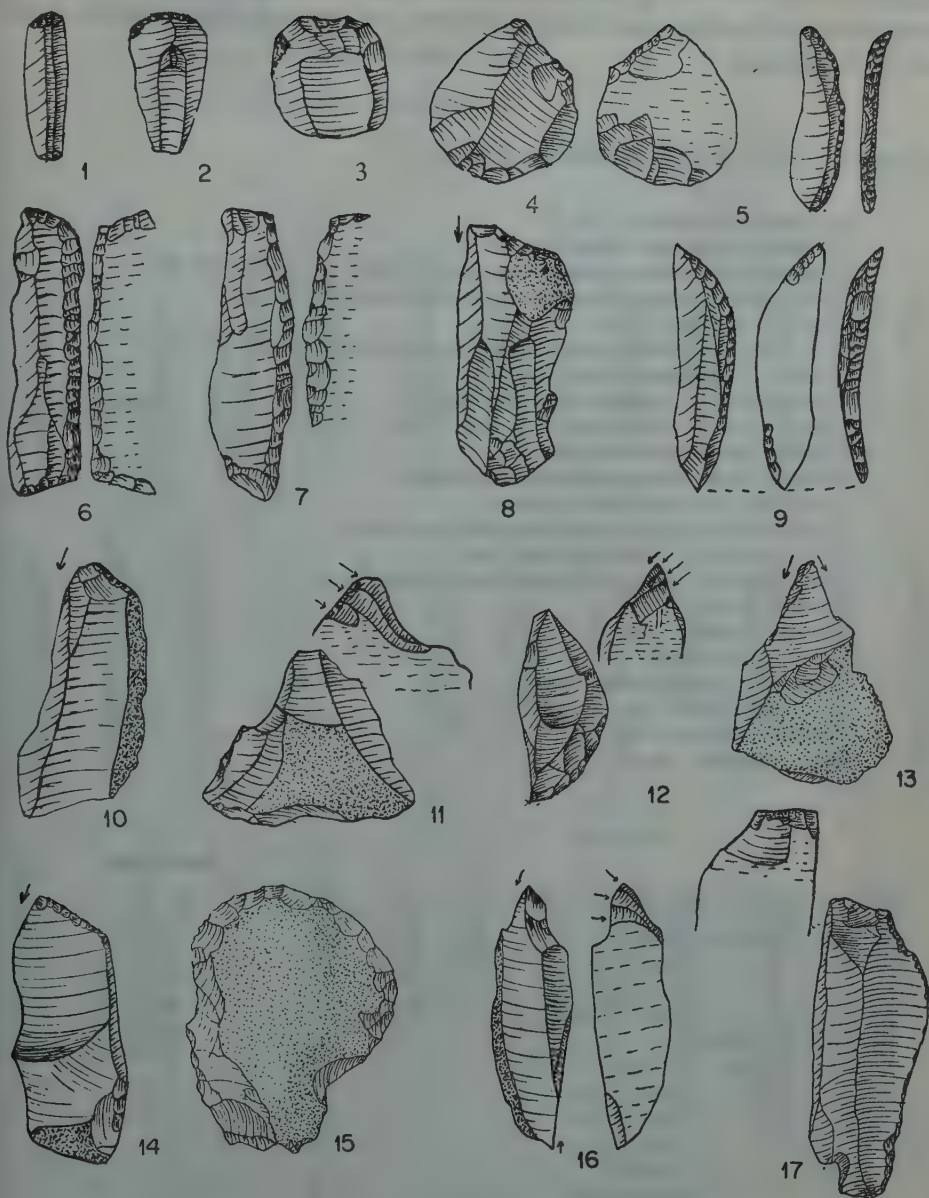


Figure 3.

Niveau A2: Burins à troncature—8, 10, 14; Burin "busqué"—12, 16; Burin plan—11; bec-de-flûte—13; Lames de faucille—6, 7; Raclette—2; Lamelles à dos—5, 9. Pointe d'Emireh—4;

Quelques unes présentent, le long de leur grand axe, une courbure prononcée sur le plan vertical. Les lamelles non retouchées étaient destinées à la fabrication de divers outils microlithiques.

Microlithes: 3.7% de tout l'outillage. (fig. 4)

Lamelles à dos rabattu 1—4, 25	8
Lamelles à troncature oblique. no. 5—8	6
Lamelles à troncature oblique et à base arrondie par des retouches No 30	2
Lamelles à troncature oblique dont le dos et la base sont arrondis par des retouches No 9	4
Lamelles à troncature oblique à dos et à retouches inverses Nos 11, 12	3
Lamelles à troncature concave et à dos	2
Lamelles à dos et à retouches inverses No 22	3
Lamelles courbes retouchées vers la base No 24	3
Lamelles droites retouchées vers la base	4
Lamelles à base tronquée et à encoche latérale	2
Lamelles à deux tranchants retouchés	2
Lamelles à tranchant retouché par retouches inverses	2
Lamelles courbes à fines retouches No 22	8
Lamelles à tranchant partiellement retouché Nos 23, 28	2
Lamelles à crête	1
Lamelle "Kebara" Nos 13—16, 31	6
Lamelle à cran distal	1
Lamelles à coches alternes No 35	1
Segment de cercle Nos 29, 30	4
Micro-Châtelperron No 20	2
Micro-Gravette No 33	2

Niveau B

		Pourcentage
Pointes "Châtelperron"	43	24.5
Grattoirs: simples	23	13.0
carénés	5	2.8
à museau	1	0.5
nucleiformes	1	0.5
Raclettes	5	2.8
Burins: d'angle	10	5.7
à troncature	7	4.0
bec-de-flûte	8	4.5
plan	6	3.0
"busqué"	4	2.0
polyédrique	1	0.5
atypique	6	3.0
Lames: retouchées	27	15.4
tronquées	10	5.7
écaillées	3	1.7
Lamelles retouchées	10	5.7
Encoches	5	2.8
Total	175	100

Lamelles de burin	16
Nuclei	38
Lames à crête	26
Tablettes de rafraîchissement des nuclei	59
Éclats bruts	137
Éclats et lames sans retouche	79



Figure 4.
L'Outillage microlithique.

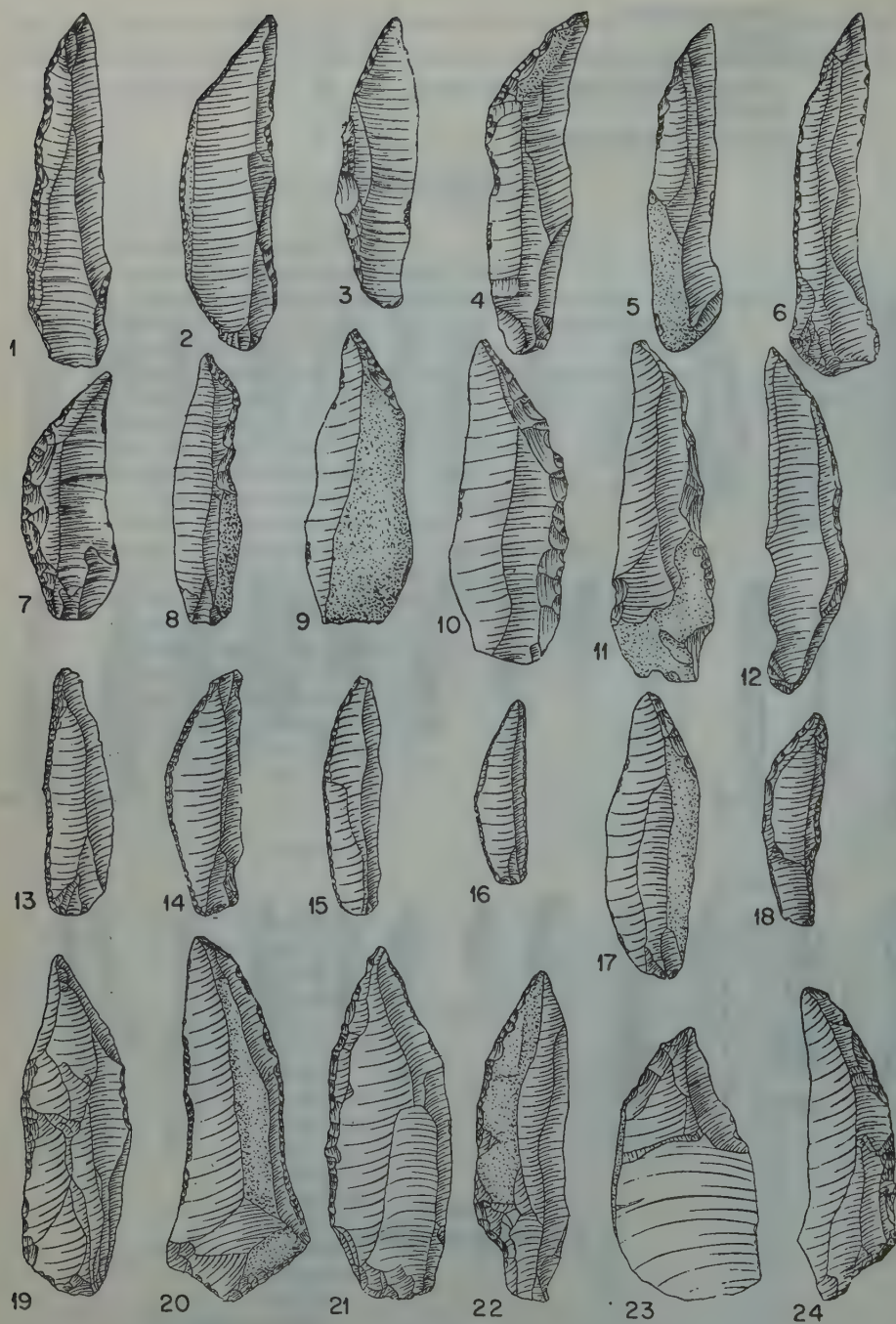


Figure 5.

Pointes de „Châtelperron”: fig. 5 (24.5%). C'est une belle série de pointes sur lames à dos courbe rappelant les pointes de Châtelperron des gisements français. Leur longueur varie entre 4cm. et 7cm. 33 de ces pièces sont déjetées à gauche. Les retouches partent de la face d'éclatement. Nous n'avons trouvé aucune pièce à bord abattu par retouches partant des deux faces. Les tranchants ne portent que rarement des retouches et assez peu de traces d'usure. Deux lames, (Nos. 22 et 24) ont à leur extrémité proximale une encoche à retouches abruptes partant de la face d'éclatement et formant une sorte de pédoncule basal servant probablement à les emmancher.

Lames tronquées: (5.7%). La plupart proviennent d'éclats d'épannelage et portent encore leur cortex. La retouche porte rien que sur la troncature. (fig. 5 No 9, 17, 23).

Lames retouchées: (15.4%). Les lames sont à retouches continues ou partielles sur l'un ou sur les deux bords. No. 20: une base tronquée et deux encoches proximales.

Grattoirs: (fig. 7) Les grattoirs simples dominent. Ils représentent 13% de l'outillage. Ils proviennent parfois d'éclats d'épannelage. Les parties actives sont généralement convexes, rarement concaves, No 11, ou rectilignes. Ils sont très rarement retouchés sur les bords. Les Nos. 1 et 8 sont des grattoirs sur éclats ayant un front denticulé. Le No. 2 est en "éventail" et les Nos. 3 et 4 sont unguiformes, à bout plus ou moins rectiligne. Les Nos. 6 et 7 sont à bout convexe tandis que le No. 5 est à bout rectiligne mais à encoche latérale. Le No. 8 est un grattoir fait sur un épais éclat d'épannelage, le front est surélevé, mais par l'absence des retouches lamellaires on ne peut pas le classer parmi les "grattoirs carénés".

Enfin le No. 11 est un grattoir double à bout concavo-convexe dont un front porte un coup-de-burin.

Des grattoirs carénés et à museau font timidement leur apparition. (fig. 7 No 9,10) Les raclettes se maintiennent encore.

Les burins (fig. 6): représentent 20.4% de l'outillage. Les burins d'angle sont les plus nombreux (5.7%). Un d'entre eux est double. (No 1) 4.5% des burins sont en bec de flûte. Les burins d'angle à troncature (Nos 3, 4, 9, 15, 17, 18) (4%) et busqués sont fréquents (4%). 3% de burins plans, dont un double. (Nos 2, 16) Les burins polyédriques sont très rares. Et enfin, il faut signaler des burins atypiques (3%).

Les lamelles: retouchées représentent 5.7%. On peut distinguer parmi elles des lamelles à dos rabattu et à fines retouches sur l'autre bord, puis des lamelles partiellement retouchées, soit sur les deux bords, soit sur un seul, ainsi qu'une lamelle fine à cran proximal. (Nos 10-13)

"Pointe de la Gravette": une belle pointe à dos rabattu se rapproche du type dit de la Gravette. (No 14)

Divers: Il faut signaler en outre des lames à encoches (2.8%) ainsi que des lames écaillées (1.7%).

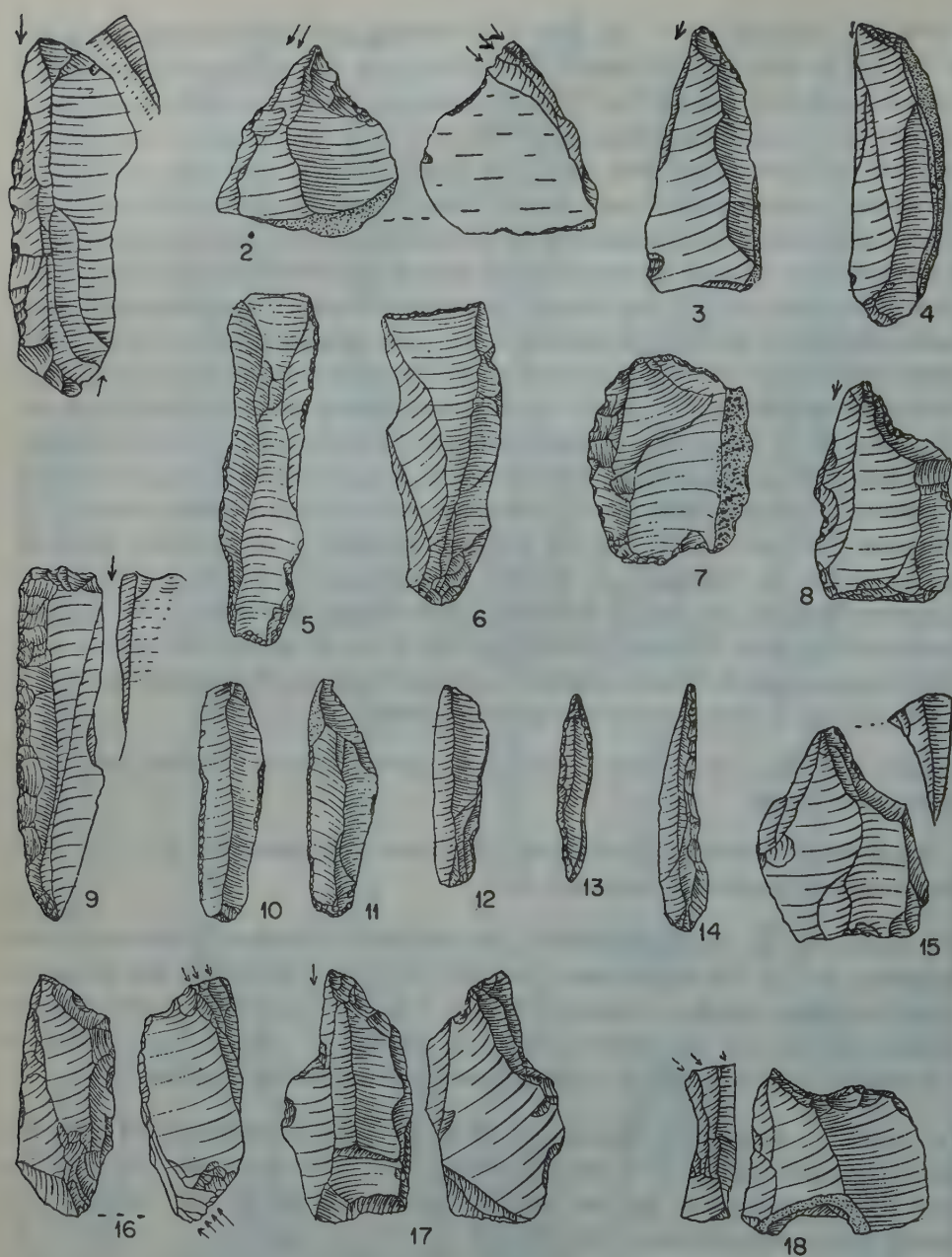


Figure 6.

1—Burin d'angle double; 2, 16. Burin à troncature; 10—14 lamelles retouchées; 5. Lame retouchée 6, 7—grattoir simple.

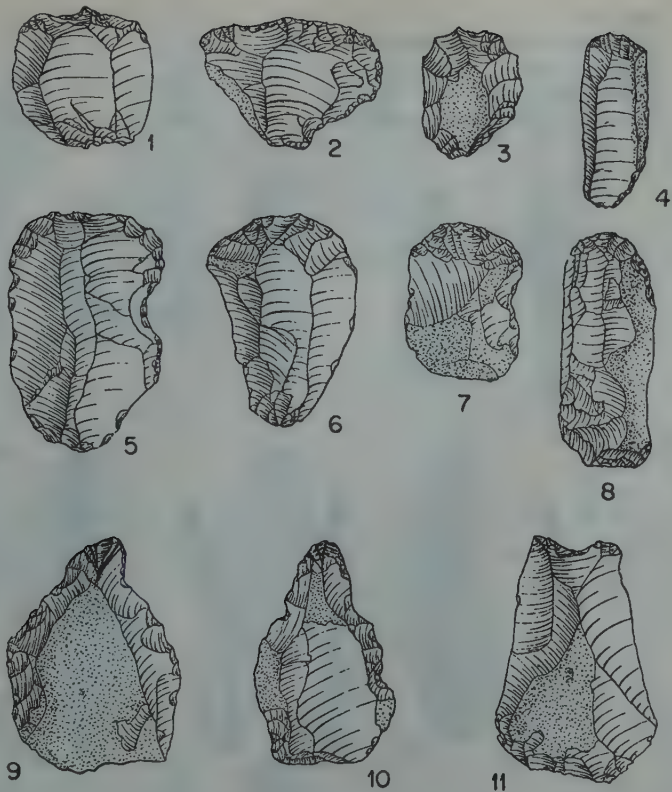


Figure 7.
Grattoirs simples; grattoirs à museau (9, 10)

Les nuclei, au nombre de 38, sont soit prismatiques, soit globuleux. Les déchets de taille comportent 59 tablettes de rafraîchissement, 26 lames, 137 éclats bruts et lames non retouchées et 16 lamelles de burins.

Niveau C		Pourcentage
Grattoirs: simples	15	12.0
carénés	8	5.4
nucléiformes et rabots	20	13.7
Raclettes	1	0.6
Pointes: Font-Yves	15	12.0
variées	2	1.3
Burins: plans	2	1.3
atypiques	16	10.2
Lames retouchées	68	46.0
Total		147
		100.0

Nuclei	16
Tablettes de rafraîchissement	40
Lames à crête	40
Éclats bruts	15
Lames et éclats sans retouche	90



Figure 8.

5. Pointe de Font-Yves; 1, 2; 6—8 Lamelles retouchées; 3. grattoir sur lamelle; 4. grattoir à museau.

Grattoirs: Les grattoirs simples sur lames ou éclats sont ici des instruments relativement abondants (12%). (fig. 9. Nos 1, 2, 9). Parmi les grattoirs il faut mentionner un à bord denticulé (fig. 9. No 4). Les rabots et grattoirs nucléiformes font ici leur apparition (13.7%), tandis que le nombre des grattoirs carénés est très faible (5%). Parmi ces derniers, il faut mentionner un grattoir pseudo-caréné sur une lame mince jusqu'au niveau du front qui est épais et à retouches abruptes. (fig. 9. No 6). Les grattoirs carénés typiques (fig. 9. Nos 3, 7, 8) sont faits sur des éclats dont le front porte des retouches lamellaires régulières.

Burins: La plupart des burins sont atypiques (10.2%). Les burins d'angle ou en bec-de-flûte n'apparaissent pas à ce niveau. Nous avons à signaler seulement deux burins plans (fig. 9. No 5). En outre, il faut signaler une pièce exceptionnelle. Les deux moitiés de cette pièce ont été trouvées à deux niveaux différents, une moitié au niveau B et l'autre au niveau C. Les deux morceaux se raccordent. Rassemblés, ils représentent une lame à retouches sur un bord, ayant à son bout un burin

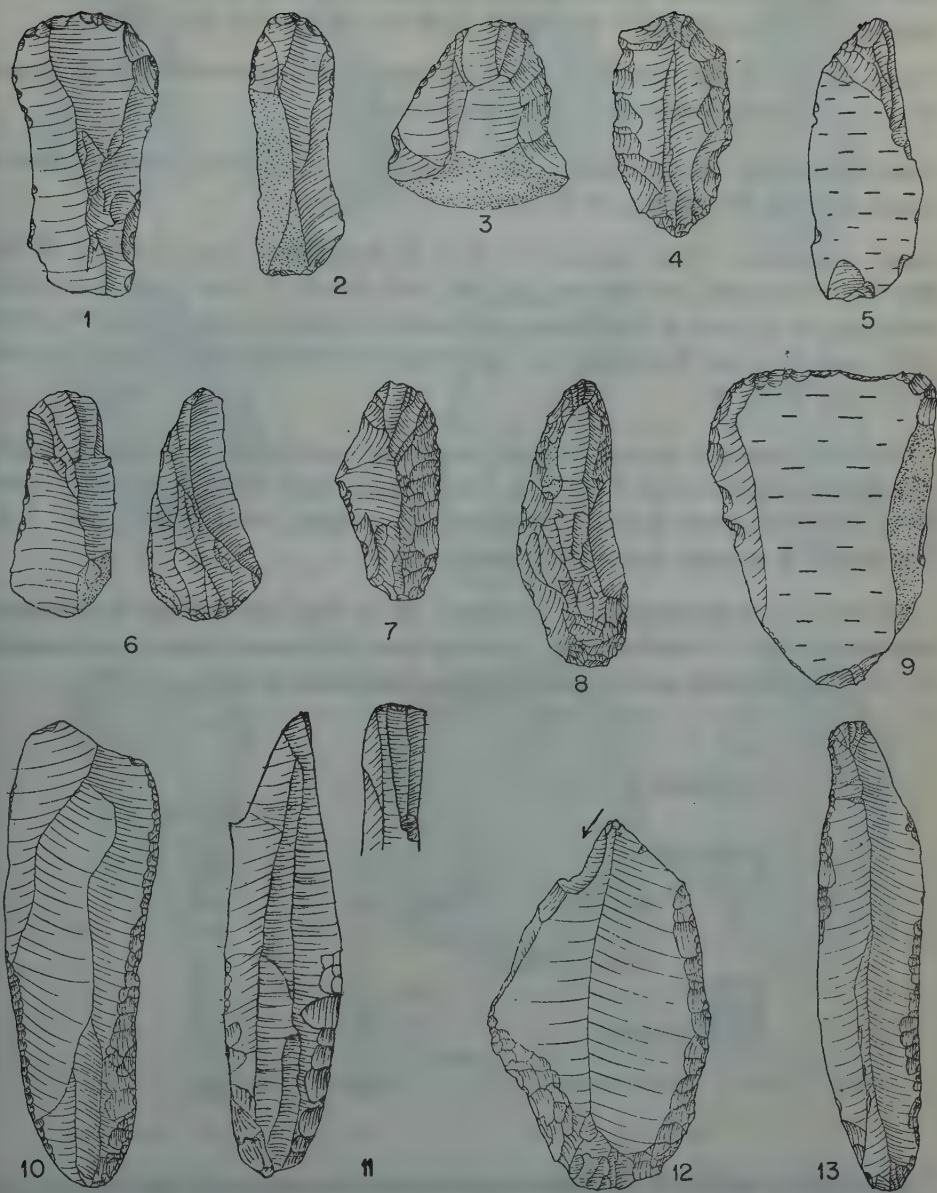


Figure 9.

Niveau C. "Aurignacien moyen": 1, 2, 9 — grattoirs simples; 4 — grattoir denticulé; 3, 6, 7, 8 — grattoirs carénés; 5 — burin plan; 12 — grattoire burin; 10, 13 — lames retouchées; 11 — burin polyédrique.

polyédrique. Il est très probable que cet outil était employé comme ciseau et avait été brisé au cours du travail. Il faut penser également que cette pièce est un indicateur important de la rapidité avec laquelle la terre s'est accumulée dans la grotte.

Pointes de Font-Yves: (12%). Au total, 15 pointes ont été trouvées. Nous faisons figurer ici une belle pointe de ce type. (fig. 8 No 5)

Outils composites: Il faut signaler une lame dont l'un des bouts est un grattoir et l'autre un burin d'angle (fig. 9 No 12).

Lames retouchées: Elles représentent 45% de l'outillage. Nous donnons ici une belle lame retouchée partiellement sur les deux bords et une autre à retouches continues, sur un bord et partiellement retouchée sur l'autre. (fig. 9, Nos 10, 13). Et enfin, nous donnons également une petite lame à retouches continues sur les deux bords. (fig. 8 No 9)

Les lamelles ne sont pas nombreuses, une dizaine seulement. Elles sont retouchées soit sur les deux bords (fig. 8 Nos 6, 1, 7) soit sur un seul. Enfin, nous avons trouvé deux lamelles pointues finement retouchées sur les deux bords (fig. 8. No. 2, 8). Une lamelle à encoche (retouches inverses).

Les nuclei sont pyramidaux ou globuleux, 16 au total. 40 tablettes de rafraîchissement du nuclei, 15 lames à crête, 64 éclats bruts, 90 lames et éclats non retouchés et 7 lamelles de burins ont été recueillis parmi les déchets de taille.

Niveau D

		Pourcentage
Pointe Emireh	1	1.8
Grattoirs: simples	9	16.0
carénés	10	18.0
à museau	6	10.9
nucléiformes	8	14.0
Racloirs	3	5.0
Burins	4	7.0
Lames retouchées	10	18.0
	51	90.7

Les grattoirs carénés et en museau caractérisent ce niveau (fig. 10). Ils sont taillés soit sur des éclats courts et épais, soit sur de petits blocs portant encore leur cortex. Tous portent les caractéristiques retouches lamellaires. Parmi les grattoirs carénés, on peut signaler (fig. 10 No. 8) un caréné déjeté, un autre pseudocaréné (par l'absence de retouches lamellaires) et un grattoir préparé sur un éclat d'épannelage, enfin, un burin d'angle sur troncature (fig. 10 No 6).

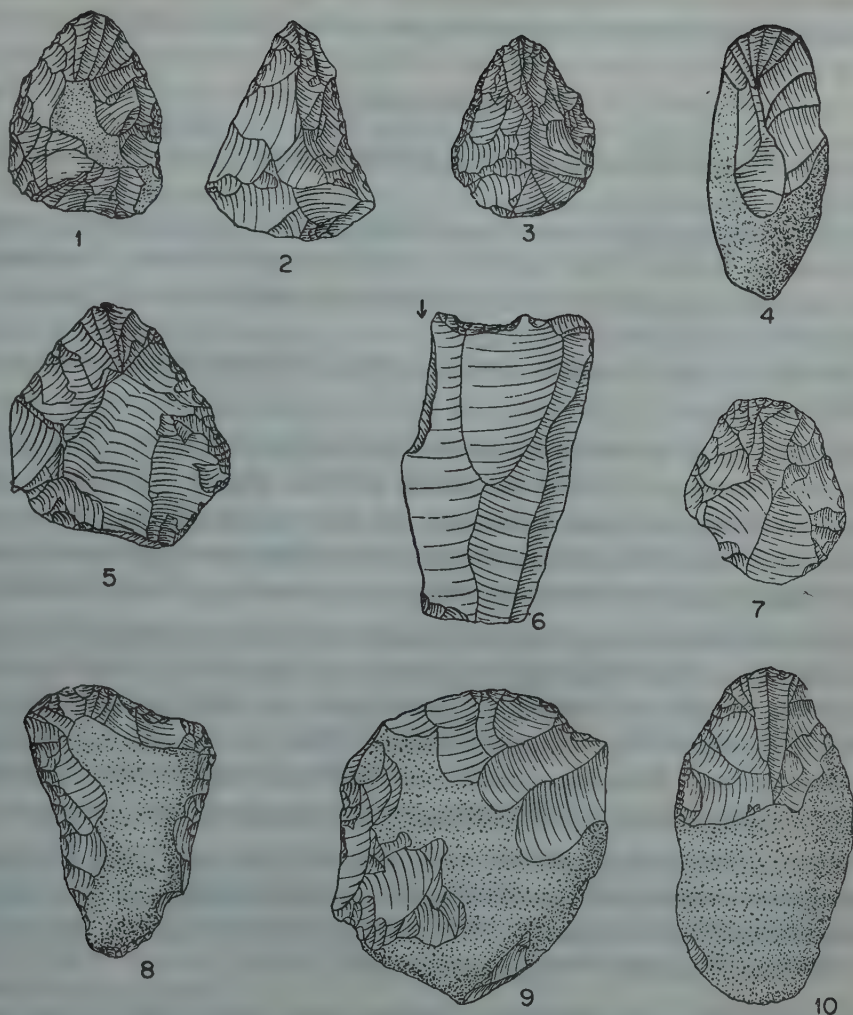


Figure 10

Niveau D. 1 — 3 grattoirs à museau; 4, 7, 10 — grattoirs carénés; 8 grattoir déjeté.

Il faut mentionner un type d'outil assez rare dans cet ensemble. C'est une petite lame pointue à retouches très fines sur un bord, ayant un cran proximal bien retouché.

En général, ce niveau a livré une industrie peu abondante. Nous avons recueilli au total 51 outils proprement dits, et 13 nuclei ainsi qu'une dizaine d'éclats bruts. Nous avons dû arrêter nos fouilles à ce niveau en raison de l'étroitesse du sondage.

La faune découverte dans la grotte d'Iraq-el-Baroud a été confiée au Professeur

G. Haas de l'Université Hébraïque. Malheureusement, un incendie qui eut lieu dans les bâtiments de l'Université au Mont Scopus, a détruit tout le matériel.

CONCLUSIONS

Le matériel lithique livré par la couche A₁ est très pauvre. Il peut être très proche du Tahounien.

L'industrie lithique de la couche A₂ semble être très proche de celle de la couche C de la grotte de Kebara: Cette industrie à microlithes qui s'intercale, dans la grotte de Kebara, entre le Natoufien et le Paléolithique supérieur, a été baptisée par Mlle Garrod, le *Kebarien*.

L'ensemble lithique découvert dans la grotte d'el-Baroud reste pour nous une énigme.

D'un côté, par les lamelles à dos rabattu, les triangles scalènes, les grattoirs et les burins caractéristiques, cet ensemble semble avoir un rapport typologique avec le *kebarien*. D'un autre côté, par la présence des armatures de faucille portant sur le tranchant le poli de l'usage et l'absence totale d'un outillage osseux et de micro-burins, nous ne pouvons nous permettre de rattacher cette couche à celle du *Kebarien*.

On pourrait certainement, si l'on veut, penser à une phase plus évoluée du *kebarien*. Mais étant donné nos faibles connaissances sur ce dernier et son rôle encore peu clair dans le paléolithique supérieur, et encore moins son influence sur le Natoufien, nous préférons, pour le moment, la prudence. Plutôt que de rattacher l'ensemble d'El-Baroud à un "Kebarien évolué", nous préférons attendre que de nouvelles découvertes dans les grottes de Palestine, nous livrent de nouveaux documents.

L'industrie lithique découverte dans les couches B, C et D, de la grotte d'El-Baroud se rattachent à un ensemble culturel unique du paléolithique supérieur et est peut-être comparable à celle des niveaux D₁ et D₂ de la grotte d'El-Ouad, au mont Carmel, que Mlle Garrod qualifie d'"Aurignacien moyen".

Mais mes études sur le paléolithique supérieur de la grotte de Qafzeh, ainsi que les récentes fouilles dans la grotte de Kebara m'ont donné la possibilité d'étudier à fond les différentes phases du Paléolithique supérieur de ces grottes et de constater de nouveaux faits insuffisamment mis en lumière lors des fouilles menées dans les grottes du Carmel (fouilles Garrod) et dans les grottes du Désert de Judée (fouilles R. Neuville).

Prenant en considération ces nouvelles constatations d'ordre stratigraphique et typologique, la subdivision du Paléolithique supérieur de Palestine en six phases successives, comme elle a été proposée autrefois par R. Neuville, soulève aujourd'hui, certaines difficultés.

D'abord, la phase I de Neuville, caractérisée par la présence de la pointe dite d'Emireh comme "fossile directeur" de cette phase, doit être abandonnée. En effet,

l'aminçissement de la base par une retouche qui est la caractéristique des pointes d'Emireh, est une technique spéciale qui apparaît non seulement sur les petites pointes triangulaires d'Emireh, mais aussi sur des éclats et sur des lames retouchées ou non retouchées. L'origine de cette technique est dans le Levalloiso-Moustérien de la grotte de Qafzeh. Cette technique apparaît sporadiquement dans le Paléolithique supérieur de même que dans le Mésolithique et quelquefois dans le Néolithique de Palestine. Ces faits, d'ordre typologique, mettent en doute la première phase du Paléolithique supérieur de Palestine, qui, sans la pointe d'Emireh, serait identique à la IIème phase de Neuville.

La II-ème phase a été découverte dans la grotte d'Erq-el-Ahmar, couches F-E. Il paraît que la couche F de cette grotte était séparée par une couche stérile du niveau levalloisien. L'ensemble lithique caractéristique de la phase II comporte des pointes droites retouchées, des grattoirs plats à faible museau et des grattoirs sur bout de lames. Comme nous l'avons déjà dit plus haut, cette phase ne diffère de la phase I (grotte d'El-Tabban) que par l'absence de la pointe d'Emireh.

La subdivision du paléolithique supérieur de Neuville en six phases (I-VI) a été établie par lui d'après ses propres fouilles dans les grottes du Désert de Judée. Cette subdivision soulève maintenant certains problèmes d'ordre stratigraphique: Nous savons que dans aucune des grottes préhistoriques du Désert de Judée, les six phases n'ont été découvertes dans une séquence stratigraphique. La phase I a été mise à jour dans la grotte d'El-Tabban, les phases II, III et IV dans la grotte d'Erq-el-Ahmar, et les phases V et VI dans la grotte d'El-Khiam. Il est suffisamment clair que la séquence est relative et non pas absolue.

En ce qui concerne la séquence des phases II, III et IV d'Erq-el-Ahmar, il paraît que la phase III n'a pas immédiatement suivi la phase II, et la phase IV n'est pas venue tout de suite après la phase III. Les industries lithiques découvertes dans les couches E et C ont livré un matériel relativement très pauvre et peu caractéristique. C'est pourquoi on peut supposer que ladite grotte ne fut pas habitée pendant la formation de ces couches.

En outre, cette subdivision se complique du fait que la technique de la préparation du plan de frappe qui subsista dans les quatre premières phases, disparaît dans les deux dernières.

Nous voyons donc que le Paléolithique supérieur de Palestine et sa stratigraphie sont plus compliqués qu'on ne l'avait supposé jusqu'ici et que sa subdivision en phases doit être réétudiée à la lumière des faits nouveaux mis à jour par les récentes fouilles exécutées dans ce pays. Nous ne pouvons pas, dans le cadre de cette étude, entrer dans les détails de cette subdivision et la discuter. Le Paléolithique supérieur de Palestine et même du Proche Orient, doit être considéré d'un point de vue très large, comme une mosaïque dont les éléments sont plus ou moins nombreux et plus ou moins différents.

Quant à l'outillage du Paléolithique supérieur découvert dans la grotte d'el-Baroud, bien que dépourvu de la technique de préparation du plan de frappe, il semble être très proche de l'ensemble de la couche D des grottes du Carmel.

REFERENCES

1. VON MÜLINEN, 1908, Beiträge zur Kenntnis des Karmels, *Deutsche Palästina Ver. Zeitschr.*, 81-82.
2. STEKELIS, M., 1942, Preliminary report on soundings in prehistoric caves in Palestine, *Am. School. Orient. Research Bull.*, 86, 2-14 (also in 1941 *Palestine Antiquities Dept. Bull.*, 11, 115-118)

ON THE RED SEA RIFT PROBLEM

A. J. VROMAN

Mapping Division, Geological Survey of Israel

ABSTRACT

Reasoning and experiments show that the parallelity between the coasts of the Red Sea does not prove that Africa and Arabia drifted apart, but is the consequence of the laws of normal faulting in tensional rift-valleys. The Jordan-Dead Sea Rift, standing obliquely to the regional tension pattern, has a small component of lateral movement. Crescentic border-faults are explained as inherited from a fault-system older than the Rift Valley.

INTRODUCTION

The parallelism of the Red Sea coast lines of Western Arabia and Africa is such a salient feature that nearly all the authors from Lartet (1869) to Quennell (1956), who worked in the area, were impressed by it, and many of them published remarks on its cause. By rotating the map of Arabia through a few degrees in a clockwise direction (Figures 1a, 1b) it becomes indeed apparent that both coasts of the Red Sea



Figures 1a, 1b

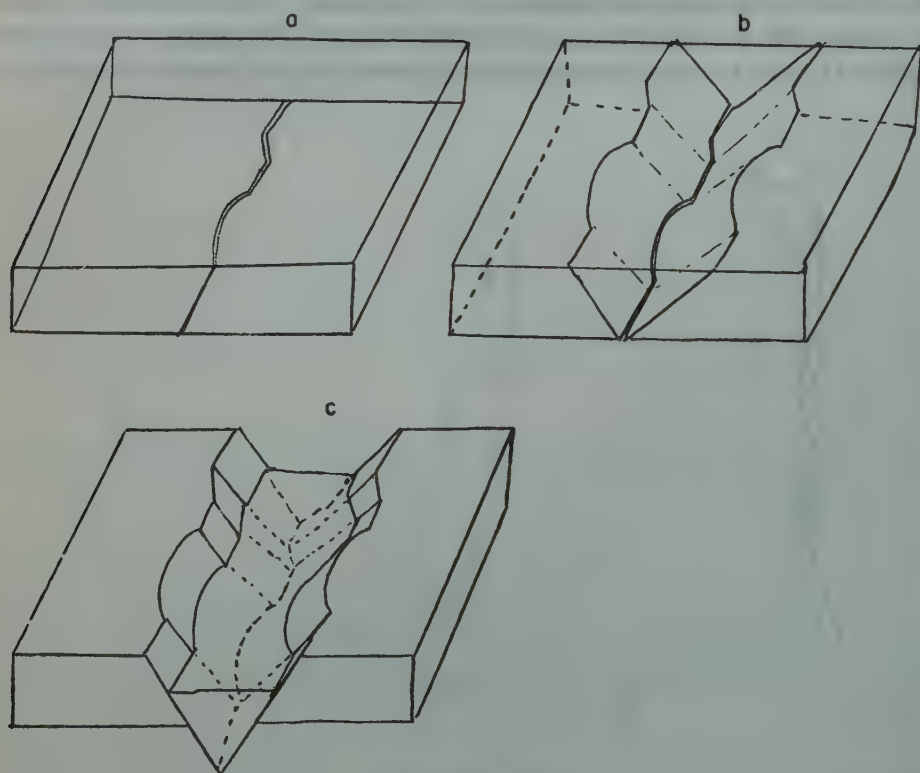
Received December, 1960

are as closely parallel as the two banks of a meandering river. Such a striking feature certainly needs explanation and should not be regarded, as some authors (Henon 1956) did, as a mere coincidence.

The most obvious explanation for the parallelism of the coast lines is the assumption that the two coasts were originally in contact and have since drifted apart, a suggestion made by several authors. It will, however, be shown in this paper that another cause is much more probable: clay experiments and theoretical considerations have shown that the opposite walls of every normal rift valley not only can, but should be parallel, provided rocks are reasonably homogeneous and tension is similar over the whole affected area.

I. RIFT VALLEY THEORY AND EXPERIMENTS

Rift valleys as large as the Red Sea have doubtlessly a deep-seated origin. Let the irregular line in Figure 2a represent the first crack at the bottom of a sial block, where tension started. Clay experiments and the laws of applied mechanics show that, if tension continues, two sets of normal faults will grow upward, until they reach the surface. This is a conjugate set of shear-faulting caused by the simple strain of



Figures 2a, 2b, 2c

tension. The fault-faces dip towards each other at an angle of 60 to 70° or less, and thus cut off a wedge-shaped block of the sial crust. Continued tension leads to the sagging down of this block and the formation of a normal rift valley (Figures 2b, 2c). As both shear-zones start from all the points of the initial irregular crack at depth, the two lines along which the shear-planes intersect the surface will both be parallel to the first crack and consequently, parallel to each other. When the bottom of such a rift valley is covered by the sea the wrong conclusion can easily be drawn, namely, that the two coasts once touched each other and have since drifted apart.

The classical graben experiment was carried out by H. Cloos (1939): by pulling a *straight*-edged board from below a cake of clay at very low speed, (E. Cloos 1955), a wedge of clay slowly sinks and a *straight*-walled rift valley (with some secondary step faults) is formed (Figure 3). As the first crack always coincides with the edge

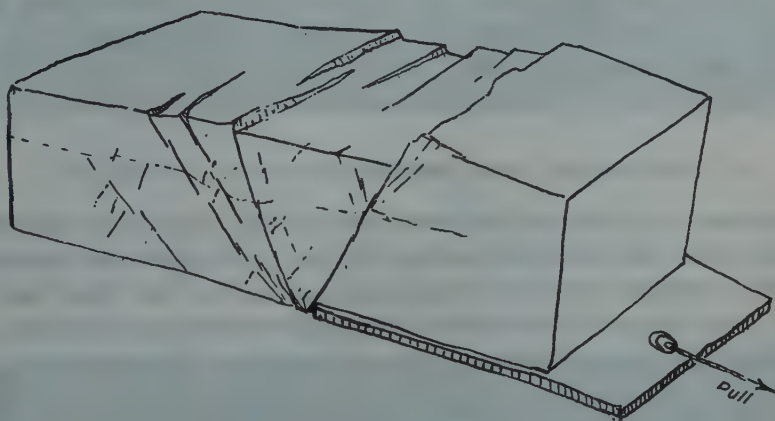


Figure 3

of the board the shape of the rift-borders necessarily reflects the shape of the board-edge. The present author, with the assistance of A. Nevo, has modified the original experiment, by pulling a *curved*-edged board from below the clay. The ensuing stages of the faulting process were strikingly similar to those pictured in Figure 2. A rift valley was formed with parallel, but curved, borders, the curves being parallel to those at the edge of the board (Photos 1-4).

The experiment revealed an additional feature, not shown on Figure 2 but known to exist along the bottom of the Red Sea; along the entire bottom of the rift-valley, but especially around the bulges of the curved border faults, minor step-faults are formed in the clay. The floor of the Red Sea itself shows similar structures. Soundings indicate (Nesteroff 1952, Tazieff 1952) that "we have here obviously the picture of a rift-valley, the central strips of which sank deeper than the outer ones", (author's translation from Nesteroff's paper).

Nesteroff (1955) and Henson (1956-57) draw from these facts the convincing

conclusion that the Red Sea has been formed by the subsidence of a wedge through tensional forces with little — if any — additional drift.

Furthermore, the drift-theory encounters another difficulty; that of the time at which the Red Sea came into existence.

When a sea or ocean is formed by drift, i.e. split open by the separation of two continental blocks, the sediments laid down on the floor can never be older than the event of separation. As the adherents of the drift-theory date the birth of the Red Sea floor from early Cretaceous time, sediments — either continental or marine — older than Cretaceous must be absent from the rift-floor.

Older rocks are exposed in one major region in the rift-floor: the triangle of the Danakil Hills (N. Ethiopia, Figure 1b). Here several small cores of the old Precambrian basement are surrounded by a large mantle of Jurassic and Triassic sediments. On the basis of the drift-theory the Red Sea must therefore be of Pre-Triassic, if not of Precambrian age.

II. THE DEAD SEA BASIN AND ITS RELATION TO THE RED SEA

Many adherents of the idea of continental drift link the origin of the Red Sea with that of the Dead Sea–Jordan rift valley. Figures 1a, 1b show how the sliding of the Arabian peninsula north-eastward, along the “rail” of the Dead Sea–Jordan rift-line, opened the cleft of the Red Sea. They regard therefore the Dead Sea–Jordan rift as a long strike-slip fault with a displacement of about 100 kilometres.

Figures 4a, 4b are an enlargement of the north-corner of Figures 1a, 1b. They feature the idea of A.M. Quennell (1958) on the origin of the Dead Sea Basin which he regards as a “gap” in the Jordan rift-valley. Quennell (1956–57) believes that this “gap” is caused by a strong curve, or rather an en échelon arrangement, in the original strike-slip line, and that by the strike-slip movement the two sides of the curve moved away from each other. Accordingly, the Dead Sea Basin is similar in structure to the cleft of the Red Sea, and its length should be about the same as the width of the Red Sea.

Objections against this theory are many-fold, and only some of them are mentioned here. First, the objections against the mechanism of drift for the origin of the Red Sea also apply to the Dead Sea Basin. As the Red Sea is a normal rift-valley, the widening movement will be only a fraction of that which would be caused by drift, i.e., a few kilometres at most, this is far too short a distance to form the “gap” of the Dead Sea Basin. Second, if the Red Sea is of Pre-Triassic age, as it must be in the drift theory, the Dead Sea Basin — formed by the same process — must be equally old. The off-set of the iso-facies lines of the Jurassic and Triassic formations across the Dead Sea-rift — which has been cited as one of the main arguments in

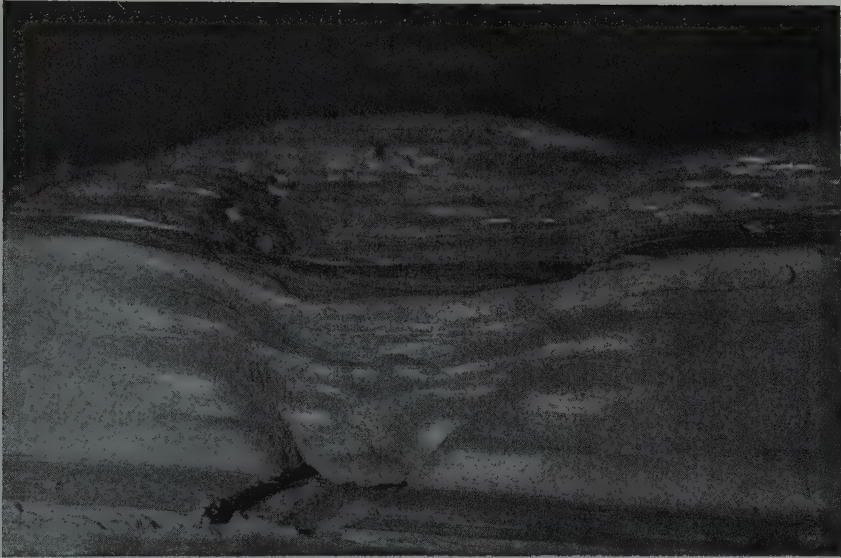


Photo 1

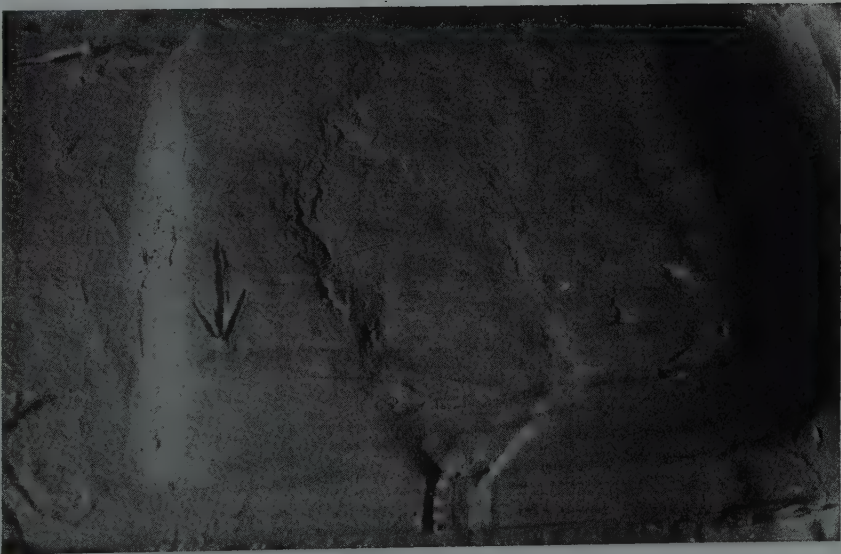


Photo 2

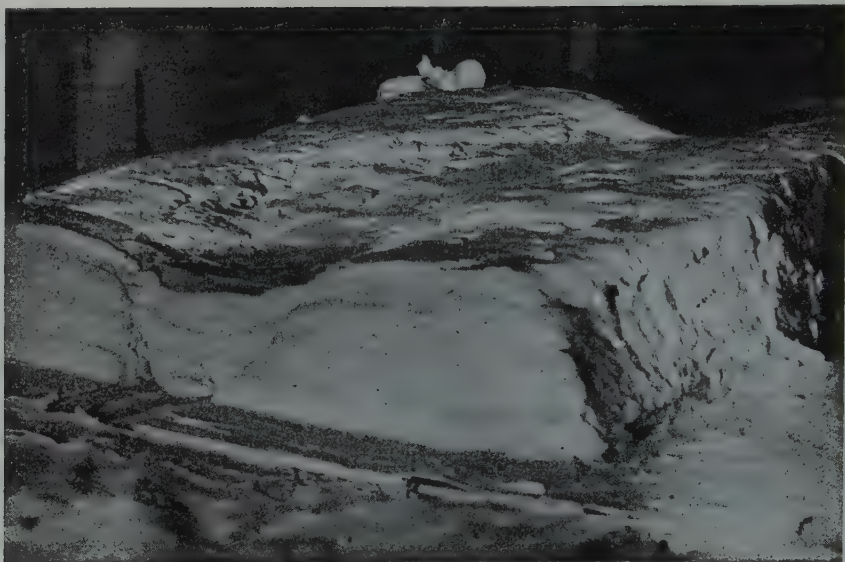


Photo 3

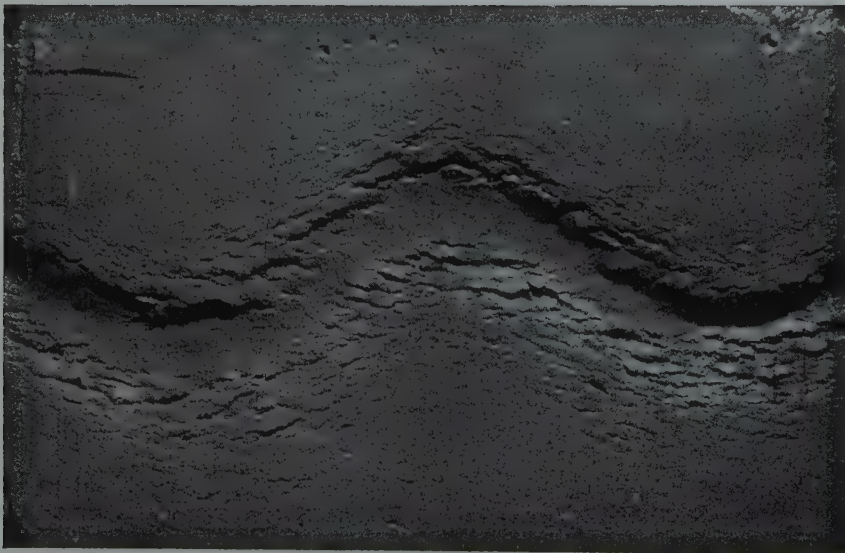


Photo 4

favour of the strike-slip theory of the Dead Sea-Jordan rift — would then be a feature younger than the rift-movement and can no more be regarded as being the result of a horizontal movement along the Dead Sea-Jordan line.

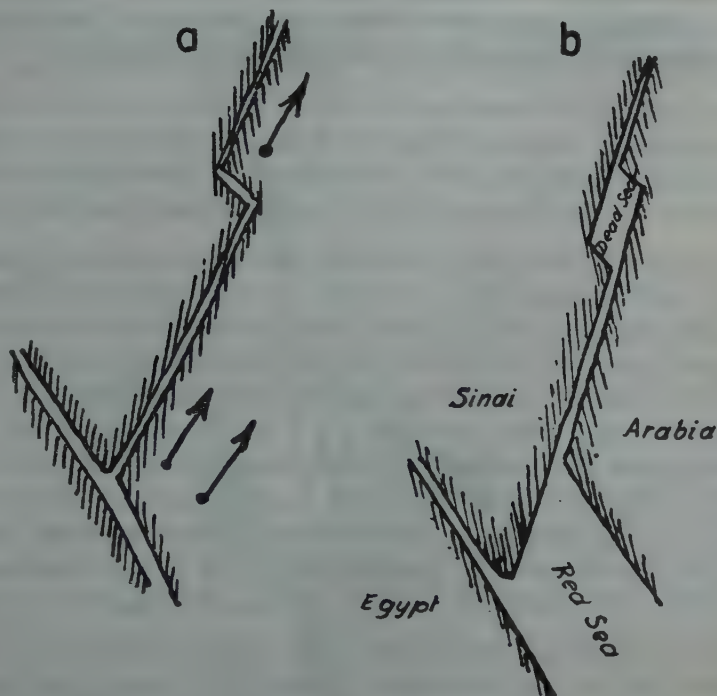


Figure 4

Another objection arises from the contrasting gravity picture of both areas. The Red Sea shows a very strong positive gravity anomaly and according to Quennell's conception a similar feature should be expected for the Dead Sea. In fact, the Dead Sea shows one of the strongest known negative anomalies; it would be beside the point, to enlarge here on the possible reason for this contrast.

III. RELATIONSHIP BETWEEN DIRECTION OF TENSION AND EXTENSION OF RIFT VALLEYS

A true rift-valley cannot be reproduced experimentally by a strike-slip movement alone; the presence of a tensional component is essential. Nature shows the same: even the giant transcurrent St. Andreas fault has no resemblance to any of the known rift-valleys and at best a few straight and shallow furrows can be observed.

The presence of a strike-slip component will, of course, not prevent the formation of a rift-valley. The Suez-Red Sea rift stands at 40 degrees to the Aquaba-Jordan rift,

and therefore, if the pattern of forces is uniform, at least one of these rift-valleys must stand oblique to the pulling forces.

The general case of tension oblique to the rim of a block has been investigated by H. Cloos in a clay-experiment (cast No. 13, University of Cincinnati). The main outline of the rift-valley remains parallel to the rim of the block, whereas the individual faults — cutting the graben-border into typical piano-keys ("touches de piano") — run approximately at right angles to the dilatating force (Figure 5).

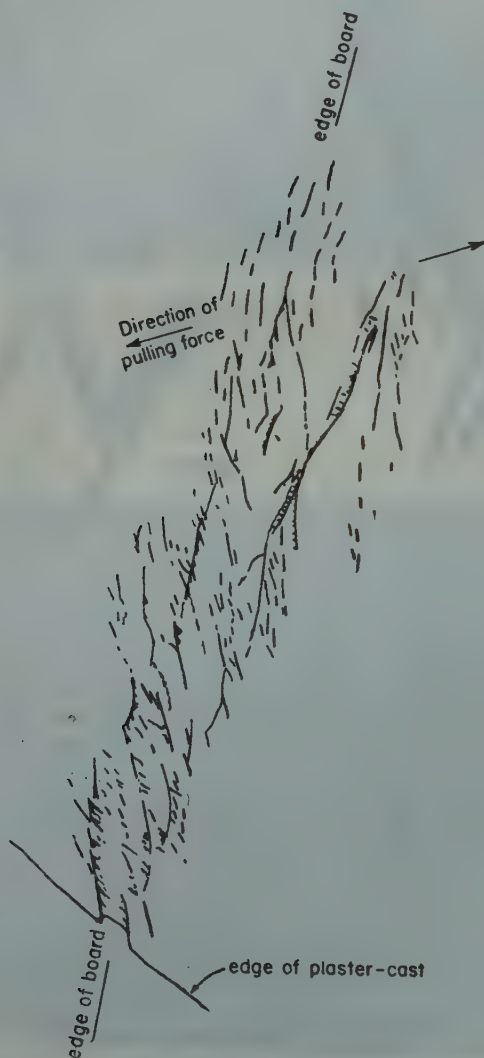


Figure 5

It is indeed remarkable that the Eilat – Dead Sea rift along the east side of the Sinai triangle exhibits a fault pattern very reminiscent of that shown in Figure 5: the individual faults trend generally due N., i.e., oblique to the main NNE-SSW trend of the rift valley (Figure 6). The Red Sea rift valley, on the other hand, has a fault pattern indicative of tension directed at a right angle to the first curved crack.

This whole part of the Middle East, i.e., the region between the Nile and the Gulf of Suez, Central Sinai, Southern Syria, Eastern Jordan and Northern Saudi-Arabia, is sliced by a dense pattern of NW-SE directed tension faults and lines of volcanic eruptions; the NNE-SSW running Eilat–Dead Sea–Jordan rift is an isolated feature at odds with the general NW-SE orientation of the fault pattern (Figure 7), is a strong indication that the Jordan–Dead Sea rift stands in part oblique to the regional tension.

The strike-slip component along rift-faults should attain its maximum, where the graben-faults trend parallel to the direction of the tensional force. This situation obtains in Syria and the Lebanon (upper part of Figure 7): the rift-valley, called here Bakaa Plain, turns in this area from N-S to N 30° E, i.e., into a direction at right angles to the N 120° E trending eruption lines of Syria. The west fault of the Bakaa Valley, the “Yammouneh-fault”, (L. Dubertret 1955) shows accordingly many features of a true strike-slip fault; east of its southern end several bachi-anticlines — caused by the rotational strain — are cut off by the rift fault (e.g. the Saghbine-anticline), and its northern extremity cuts through the length of the Lebanon-anticline, the eastern half of which, Jebel Akroum, has been shifted a few kilometres to the north in relation to the western half (Jeb. Kammouha) (L. Dubertret 1955).

But nowhere along the entire length of the Dead Sea–Jordan rift are there any indications of large-scale longitudinal displacements, and certainly not a slip of 100 kilometres.

IV. CRESCENTIC FAULTS

Curved faults border the western side of the Jordan Valley near the Sea of Galilee; L. Picard once called them “crescentic faults”, and regarded them as normal features of a rift valley. The genetic relationship between crescentic faults and rift valleys is, however, open to doubt. These faults are limited to well defined zones, where special conditions seem to prevail. Moreover, as is well shown in Figure 8, these curved faults are not confined to the vicinity of the rift valley, but appear over the whole of Galilee: Mount Carmel, Mount Tabor and Mount Meron are all bordered along their eastern-sides by such crescentic — or better, “sygmoidal” — faults.

A glance on the map (Figure 9) shows, that in Egypt a similar zone of sygmoidal faults stretches from the Bitter Lake westward to Cairo. From the structural point of view, this region has much in common with the Galilee: Again, two main kinds of

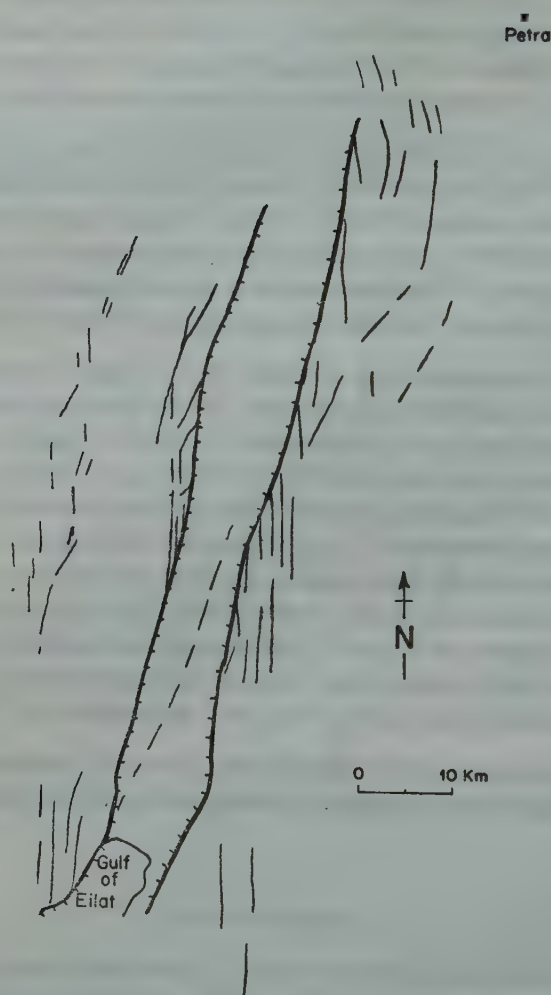


Figure 6

faults are present, one sigmoidal type trending roughly NW-SE, and a second type with an E-W orientation; those of the latter type are sometimes split into a series of small WNW-ESE-directed en échelon faults.

Notwithstanding the large throws of the sigmoidal faults along the border of the rift-valley, it is thus unlikely that they are inherent in the rift structure. More probably the double pattern of E-W and sigmoidal NW-SE faults belongs to an older and different tectonic phase and has in part been "assimilated" by the rift-



Figure 7



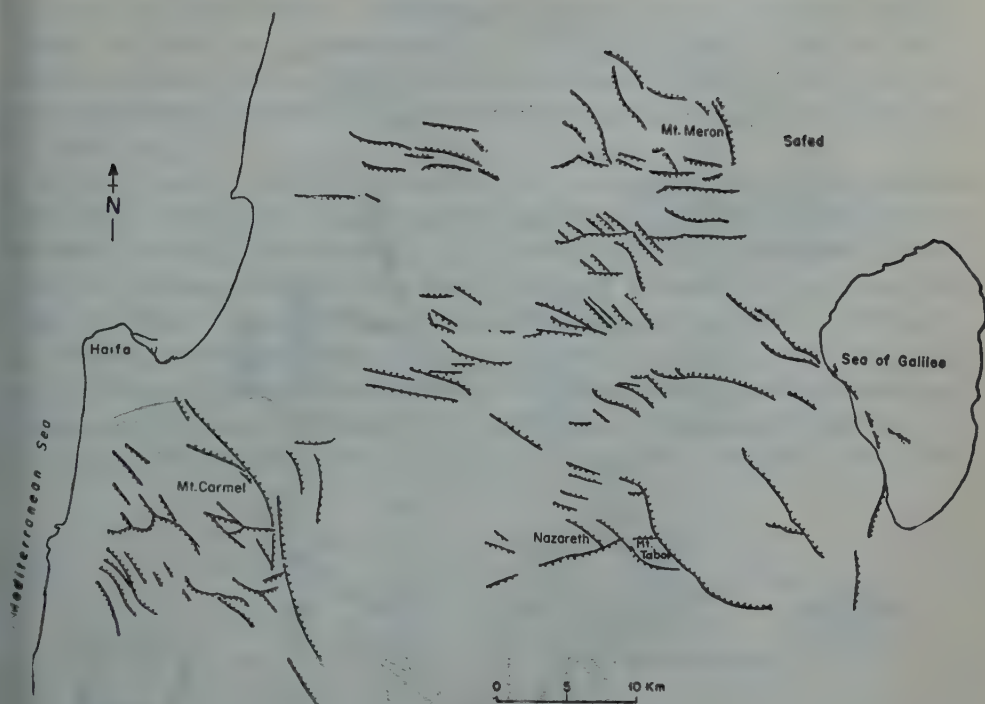


Figure 8

valley. The question thus arises as to the kind of mechanism which has produced this older pattern.

Clay-experiments show that an identical pattern of faults is produced by a pure strike-slip movement. The set up of such an experiment first carried out by W. Riedel (1929), is the same as in the "classical" rift-valley experiment; a clay-cake rests with one side on a stationary table-top, whereas the other half rests on a movable straight-edged sheet (Figure 10). Instead of pulling this sheet away at a right angle to its edge, the pulling-force is now exerted in a direction *parallel* to it. The result is the formation of two sets of shear-faults, one set consisting of a row of densely set en échelon faults, cutting the line of movement at about 15° , and a second set, slightly stronger than the first one, cutting the line of movement at about 70° .

As shown in Figure 10, however, the clay covering the plate and the clay covering the table are pushed into opposite directions. Because of this inversion of the sense of movement across the edge of the plate, the second set of shear-faults is jerked into an "S" shape.

This double pattern of shear-faults (the straight en échelon set and the "S" or "sygmoidal" set) appears three times on Figure 9: there are three E-W lines about

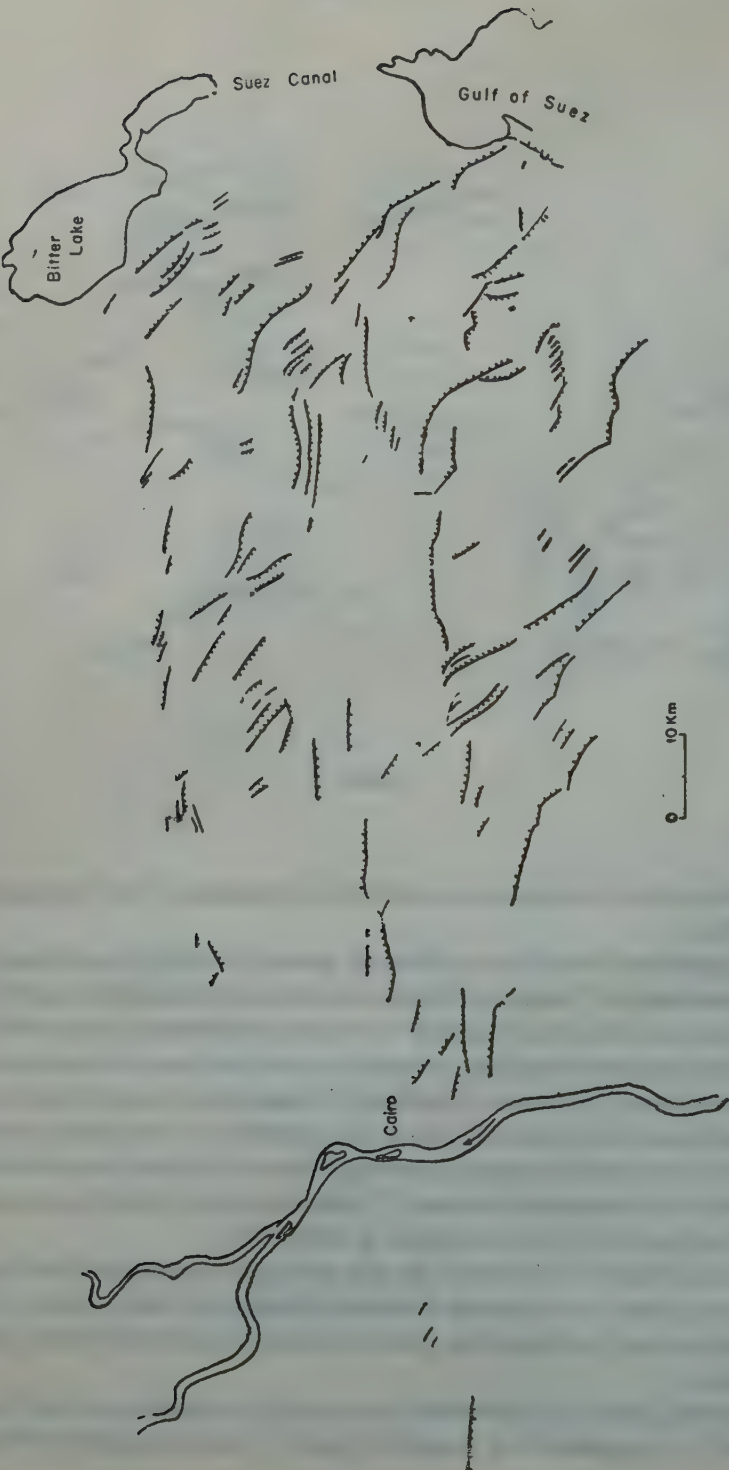


Figure 9

15 kilometers apart, partially composed of en échelon faults, crossed by the NW-SE directed "sygmoidal" faults. Comparing this picture with the experiment shown in Figure 10, it may be concluded that it is caused by the relative movement of four blocks, separated from each other by E-W directed deep-seated faults; in every case the northern block slipped eastward along the north-edge of the next block to the south.

Figure 8 shows a similar — though less clear — example. Figure 7, a generalized map of the fault pattern of the entire region, the main E-W directed strike-slip zones are marked by double arrows. All of them — with the exception of the border-faults of the Bekaa Valley — have the same sense of movement, as they should have since all of them — again with the exception of the younger Bekaa faults — are associated with the same folding phase which brought about the "Syrian fold-trend", (folds of Sinai-Negev-Judea-Galilee-Lebanon). This folding-phase (starting in the Upper Cretaceous) antedates the "tafrogetic" subsidence of the rift valley (starting in the Tertiary). The crescentic faults bordering the west side of the Jordan- and Suez-

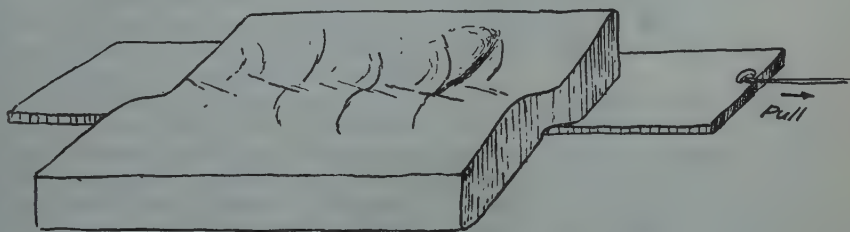


Figure 10

rift (Figures 8 and 9) are therefore parts of older "sygmoidal" faults which have been rejuvenated by the later tafrogenetic movements and which the border-faults of the rift valley have accordingly assimilated into their own fault-system.

ACKNOWLEDGEMENTS

The author is indebted to Prof. E. Cloos (J. Hopkins Univ.) who taught him the technique of experimental tectonics used by him and his late brother, to A. Nebo (Oranim Seminary, Israel) who succeeded to carry out the first experiments in this country under the authors guidance, and to the members of the Mapping, Division of the Geological Survey of Israel (J. Arkin, M. Braun and I. Yishaki) for their experiments.

REFERENCES

1. CLOOS, H., 1939, Hebung Spaltung Vulkanismus, *Geol. Rundschau*, **30**, 405-527.
2. CLOOS, E., 1955, Experimental analysis of fractional patterns, *Bull. Geol. Soc. Am.*, **66**, 241-256.
3. DUBERTRET, L., 1955, Carte Géologique du Liban au 1/200,000, *Rep. Liban. Minist. des travaux public*.

4. LARTET, L., 1869-72, Essai sur la géologie de la Palestine etc., 13, footnote.
5. NESTEROFF, W. D., 1955, Quelques résultats géologiques de la campagne de la Calypso, Mer Rouge, *Deep Sea research quarterly*, 2, 274-283.
6. QUENNELL, A. M., 1958, The structural and geomorphic evolution of the Dead Sea rift, *Quat. Journal Geol. Soc.*, C, 1-27.
7. QUENNELL, A. M., 1956, Tectonics of the Dead Sea rift, *XXth Intern. Geol. Congress, Mexico*, (not printed).
8. RIEDEL, W., 1929, Zur Mechanik geologischer Brucherscheinungen, *Centr. bl. Min. etc.*, Abt. B, 354-68.
9. TAZIEFF, H., 1952, Une récente campagne océanographique en Mer Rouge (note préliminaire), *Bull. Soc. Belge de Géol.*, 61, fasc. 1.

REVIEW AND COMMENTS

SOILS OF ISRAEL AND THEIR CLASSIFICATION

1. **SOILS OF ISRAEL. CLASSIFICATION OF THE SOILS OF ISRAEL**, By S. RAVIKOVITCH. Faculty of Agric., Hebrew Univ., Rehovoth, July 1960, 89 pp. Hebrew, 19 pp. English summary, tables, photos.
2. **PROPOSAL FOR THE CLASSIFICATION OF ISRAEL SOILS**, By J. DAN AND HANA KOYUMDJISKY, Spec. Publ. 24, Agric. Research Station, Beit Dagan, October 1959, 141 pp. Hebrew, 24 pp. English summary, tables. Mimeog.

Two significant publications dealing with the soils of Israel and their classification have appeared recently (in Hebrew, with English summaries). Since the writer has published in this bulletin¹ a morphological and taxonomic comparison of the soils of Israel with soils from other countries, which included a review of the classifications used by various workers in Israel, it would seem appropriate to review and discuss these new publications in order to bring the inquiry up to date.

Both new publications have in common the fact that they present a much more detailed classification than has been previously used in Israel. Assuming that this extension is based on observed and studied soils, they thus enlarge considerably our knowledge of the variability of our soil landscapes. The nomenclature and systematic approach in deriving the various subdivisions differ, however, in each publication and deserve detailed scrutiny.

Ravikovitch uses 6 groups as the primary subdivision, chosen on the basis of parent material or climate. These are then subdivided into 20 types representing the major genetic soil units, as determined by their major chemical and morphological properties. Variations in parent material, topographic or hydromorphic conditions and degree of leaching are used as criteria for subdivision into 85 sub-types, while mainly chemical criteria serve as a basis for further subdivision into 309 varieties, with additional sub-varieties based on texture variations. The 3 types of saline soils (solonchak, solonetz, solod), subdivided by Ravikovitch into 9 sub-types and 21 varieties, are kept separate from the general classification; the presence of soluble salts being also considered as a criterion at the level of sub-types and lower levels.

Dan and Koyumdjisky use 5 orders, divided into 13 sub-orders, which are chosen on the basis of the principal factor of soil formation as the major level of division. These are divided into 22 great soil groups and 51 sub-groups as determined by the major features of the soil profile and by soil forming factors other than the dominant. Finally 170 types are recognized on the basis of variation in the soil profile characteristics.

Since we are usually able to make morphological comparisons with soils from other countries¹ at the level of the major genetic soil types, the criteria for choosing them ought to follow as far as possible generally accepted and international standards. Seen from this standpoint there are no great differences between the soils recognized as major genetic units by both systems, except that important new suggestions for correlation with well known great soil groups are made by Dan and Koyumdjisky. No great changes in the recognized units are introduced at this level by Ravikovitch.

However, as no sufficiently exact general criteria exist for the grouping and subdivision of these world soil groups, each proposed classification can choose and define its own criteria for this purpose. To be called intrinsically sound a classification must withstand the scrutiny of a logical examination and prove itself suitable in the field during actual mapping; something which is not easily achieved.

Dan and Koyumdjisky call their system appropriately "A proposal for the classification of Israel soils". Though Ravikovitch by implication gives the impression of a fully defined and definite classification system, it too cannot be regarded as more than a valuable progress report as long as it has not been thoroughly tested in the field.

The major and most important part of Ravikovitch's publication is an essay of about 13,000

words listing and describing the characteristics of the soil types of Israel, and we shall discuss it first. This description is supported by tables listing in numerical form the common range of the various chemical and physical properties, and is enhanced by a large number of photographs of typical landscapes and soil profiles. It would appear from the list of references which lists mainly papers by Ravikovitch and co-workers, including many unpublished reports, that the major aim of the essay was to summarize the large number of chemical data which have been carefully assembled by Ravikovitch and co-workers over the last 30 years. Reference to all papers, including those of other workers, is made in the text in a somewhat offhand and unusual way; by appending them to the last sentence of each major section.

There is no doubt that the large number of data on which the tables are based are of major significance to the knowledge of our soils. Unfortunately, however, their presentation merely as ranges, without additional information as to the number of analyses made, their average values or distribution, detracts much from their significance. The ranges listed are generally rather wide and overlapping so as to make it often impossible to discover any dissimilarities between the properties of several groups.

Ravikovitch doesn't utilize the tabulated data in any interpretative way, but merely repeats them in different words. Thus, while the content of K_2O and P_2O_5 is listed in percentages (of total soil), expressions very high, high or low are used in the description without ever indicating the significance of this grouping or what it is based on. Similarly the numerical range of C/N ratios is listed in the tables and quoted in the description as high, medium or low without any reference to the meaning of these values. The range of cation exchange capacities and saturation percentages of the various cations are listed in the tables and in the text, but unfortunately no indication is given as to the change of these properties with depth in the profile, which would be most indicative of the soil's dynamics. The tables also list the ranges of the total content of SiO_2 and $Al_2O_3 + Fe_2O_3$ and the SiO_2/R_2O_3 of the colloidal fractions, pH, $CaCO_3$ and soluble salt content. The description includes in addition some determinations of heavy minerals (by A. Vroman) and clay minerals, again without evaluating these data and without any attempt at a genetic interpretation or comparison between the groups.

The tables are completed by listing the texture, clay and aggregate content of the soils, and in some instances field capacity and wilting point moisture (by Y. Rubin) are added. The description in the text is introduced by a brief morphological description which mentions the main horizons and parent material of the soil and its usual depth, and is rounded out by mentioning its regional distribution and usual agricultural utilization.

It is difficult to see for whom these descriptions are intended. While the general reader will find a mass of detailed but generally unrelated data, which he will be unable to interpret, the research worker and soil specialist will regret that he cannot consult the valuable original data on which the tables and text are based. He would have preferred to have the actual data for several typical soil profiles which might be used for comparison with other data and serve for supplemental interpretations of origin or quality. While soil genesis is briefly discussed in an introductory chapter on general lines, the major problems of soil genesis in our environment are skirted.

With regard to the classification system used by Ravikovitch, the major stress laid on parent material, as exemplified by the use of names such as basalt soils, loess soils, but also as criteria for subdivision at several levels, causes obvious difficulties. The undesirability of rock names or parent materials for naming a soil has been pointed out previously¹. Numerous divisions into subtypes or varieties are based on variations in parent material, but one is left to wonder to what extent this has changed the soil processes, properties or utilization. Two of the six primary groups are called alluvial and aeolian soils, and we are therefore forced already from the outset to make the difficult distinction from what material a soil has developed. Thus the various genetically related Mediterranean steppe and desert steppe soils, as the *brown soils of semiarid regions* and the *loess-like soils*, are separated primarily on the basis of the assumed parent material. On the other hand the *brown-red sandy soils (hamra)*, also formed from aeolian material, are grouped with the climatically defined red earths.

The inclusion of soils formed under hydromorphic conditions as a subtype of the genetic soil type is useful and should be advantageous during mapping of soil associations. On the other hand the use of illuviation as a criterion for differentiation at the low level of varieties is certainly surpris-

g, and probably due to a large extent to the emphasis on parent material in determining the type and subtype. The stress at the more detailed level of varieties on chemical characteristics which require laboratory determinations might cause difficulties in the application of the system to field mapping.

Summarizing, it would seem that Ravikovitch's system is mainly technical and empirical, with predominantly petrographic and chemical characteristics chosen as criteria for differentiation, and which does not sufficiently stress the relationship between the determinative properties, pedogenic processes and the environmental factors which have directed them.

Dan and Koyumdjisky precede their proposal by a review of the principles of soil classification, with reference to a large number of systems proposed or used in various countries. They have adapted for their use a functional system similar to that of Zakharov (1927), which emphasizes that one or two of the soil forming factors dominate in their influence on soil development and determine its major characteristics. In another connection the author² has pointed out that not only do such functional systems oversimplify the relation between the soil forming factors and the observed soil characteristics, but that they are also theoretically at fault by implying an equilibrium state between the conditioning factors and soil properties and by disregarding the everlasting lag in adjustment to a changing environment. In order to understand the multitude of combinations in soil properties it is necessary to consider all the factors and the complete evolutionary history of a given landscape. Criteria for grouping the observed morphological properties should therefore be based on our knowledge of the soil processes and genetic trends rather than merely on the present conditioning factors. This seems especially relevant in Israel, where a large part of the soils is polygenetic, having developed under changing environmental conditions.

Dan and Koyumdjisky give a fairly detailed morphological description and evaluation of the discussed soils, down to the level of subgroups, but without any analytical data. An important and most welcome feature of their work is a set of tables which a) aims to demonstrate the interrelation of the soils with the soil forming factors: climate, parent material, topography (ground water) and time (degree of development), and b) attempts to correlate their system with a number of classifications used both here and abroad.

Their list of great soil groups includes *grumusols*, which they consider to encompass the heavy alluvial and basaltic soils, and of which they distinguish several subgroups. Somewhat more problematical appears their equation of the *nazaz* soils with *planosols*, and of the coastal red sands (*hamra*) with *non-calcic brown* or *reddish chestnut* soils. The characteristic well developed steppe and desert-steppe soils of the semiarid Northern Negev do not seem to have been considered in sufficient detail, while the undeveloped alluvial and aeolian soils have been divided into a number of subgroups. However, the endeavour of the authors to show genetic relationship between the various groups and their attempt in correlation with other classifications makes the system easily amendable, including so the consideration of soil processes along the principles outlined above. I understand (personal communication) that both *burozem* and *serozem* soils have been duly included in a corrected version of the system.

Both classifications before us are at present somewhat unwieldy in use because of the profusion of very long connotative-descriptive names. No doubt that as a more generally accepted classification will be worked out, it will become necessary to introduce new and short soil names for each group and subgroup, as has been done recently in the new U.S. National Soil Classification System³. In conclusion, we must again welcome the appearance of both publications, which bear witness to the interest and significance attached to our soils and the progress that has been made in knowing them and recognizing their different characteristics and qualities. At the same time they again indicate a great need for the unification and standardization of all systems used*.

DAN H. YAALON
Department of Geology
The Hebrew University of Jerusalem

* At present both S. Ravikovitch and J. Dan, together with other specialists, are cooperating with the writer on a committee with the aim of arriving at an agreed system of soil classification for Israel.

REFERENCES

1. YAALON, D.H., 1959, Classification and nomenclature of soils in Israel, *Bull. Res. Counc. of Israel*, **8G**, 91-118.
2. YAALON, D.H., 1960, *Trans. 7th Int. Cong. Soil Sci., Comm. 5*.
3. SMITH, G.D. ET AL., 1960, Soil classification — a comprehensive system (7th approximation) *U.S. Soil Cons. Serv.*, 265 pp.



יוצא לאור ע"י

מוסד ויצמן לפרסומים במדעי הטבע ובטכנולוגיה בישראל
המועצה המדעית לישראל - משרד החנוך והתרבות - האוניברסיטה העברית בירושלים

Published by

THE WEIZMANN SCIENCE PRESS OF ISRAEL
Research Council of Israel, Ministry of Education and Culture
The Hebrew University of Jerusalem, Technion-Israel Institute of Technology
The Weizmann Institute of Science, Bialik Institute

Printed in Israel

Raphael Haim Hacohen Press Ltd. Jerusalem